Technische Universität München
Fakultät für Elektrotechnik und Informationstechnik
Lehrstuhl für Erneuerbare und Nachhaltige Energiesysteme

Flexibility in Power Systems - Requirements, Modeling, and Evaluation

Dipl.-Ing. Matthias Huber

Vollständiger Abdruck der von der Fakultät für Elektrotechnik und Informationstechnik der Technischen Universität München zur Erlangung des akademischen Grades eines

Doktor-Ingenieurs (Dr.-Ing. Univ.)

genehmigten Dissertation.

Vorsitzende: Prof. Dr.-Ing. Sandra Hirche

Prüfer der Dissertation:

1. Prof. Dr. rer. nat. Thomas Hamacher
2. Prof. Ross Baldick, PhD (schriftliche Beurteilung)
   Prof. Dr.-Ing. Rolf Witzmann (mündliche Prüfung)

Die Dissertation wurde am 25.08.2016 bei der Technischen Universität München eingereicht und durch die Fakultät für Elektrotechnik und Informationstechnik am 03.04.2017 angenommen.

Abstract

Many of the world's power systems are currently transforming towards systems with high shares of renewable energy sources like wind and solar power. As these technologies generate electricity depending on weather conditions, the residual system constituted by thermal generation, storage, and transmission must be able to cope with the occurring fluctuations. Its timely reaction to changes in output from renewable sources, whether foreseen or unforeseen, requires the residual system to be flexible. In this thesis, the quantitative flexibility requirements for power systems with different degrees of variable generation are assessed in a first part. Results highlight the importance of the mix of wind and solar power independent of the country being considered: systems with high shares of solar power impose especially high flexibility compensation by other sources. Results also indicate a significant reduction of flexibility requirements by increasing system sizes, which can be realized by powerful transmission grids. Mathematically, the operational behavior of a power system can be modeled as the unit commitment and economic dispatch problem. It aims at optimizing production costs while considering technical and economical constraints. In the second part of this thesis, an innovative and superior model for describing start-up costs in the unit commitment model is developed based on the current state-of-the-art formulations. This new approach includes the power plant temperature as an additional variable, which leads to improved computational efficiency and accuracy. As this new approach resembles real physical behavior closer, other technological features like limited heat-up speed or start-up speed dependent wear-and-tear costs can be introduced with only little additional computational burden. The overall model implementation includes a linear load flow modeling, which allows including flexible transmission elements such as phase shift transformers and direct current lines. In the third part of this thesis, the developed model is employed to evaluate different options for increasing the flexibility of a power system: flexible thermal generation, transmission extension, transmission flexibility, and storage. A dataset is developed containing information on all thermal power plants, renewable generation, storage, and transmission lines for a European power system reduced to 268 regions. All options are evaluated regarding their operational costs, their requirement to curtail renewable generation, and their effect on CO_2 emissions. Two different systems are considered: a model of Germany alone where all technical details are included and a model of the entire European power system with reduced model complexity. Results indicate the importance of enhanced thermal power plants as well as storage for the German system. For the entire European case, transmission is the most important measure for efficient integration of variable renewable energy sources.

Zusammenfassung

In vielen Regionen der Welt werden derzeit die Stromversorgungssysteme transformiert und dabei große Anteile an Wind- und Solarstrom integriert. Das residuale System aus konventionellen Kraftwerken, Speichern und Netzen muss daher in der Lage sein, die wetterbedingten Schwankungen in der Erzeugung auszugleichen. Diese Anforderung erfordert vom residualen Stromsystem einen hohen Grad an Flexibilität. Im ersten Teil dieser Arbeit werden die Anforderungen an die Flexibilität bei verschiedenen Ausbaugraden von fluktuierenden Erzeugern mit statistischen Mitteln bestimmt. Die Ergebnisse zeigen die Wichtigkeit der Anteile von Wind- und Solarstrom im Erzeugungsmix: Besonders Systeme mit einem hohen Anteil an Solarstrom erfordern einen hohen Grad an Flexibilität. Des Weiteren zeigen die Ergebnisse, dass die Flexibilitätsanforderungen in sehr großflächigen Systemen mit einem gut ausgebauten Stromnetz erheblich geringer sind. Das Betriebsverhalten des Stromsystems kann mittels der Kraftwerkseinsatzplanung mathematisch beschrieben werden. Der Betrieb erfolgt mit dem Ziel der Kostenminimierung unter Berücksichtigung der technischen Restriktionen des Systems. Im zweiten Teil der Arbeit wird aufbauend auf dem Stand der Technik ein innovatives und verbessertes Verfahren zur Berücksichtigung der Startkosten in der Kraftwerkseinsatzplanung vorgestellt. Dieser neue Ansatz beinhaltet die Einführung der Kraftwerkstemperatur als zusätzliche Modellvariable, wodurch sich die Recheneffizienz und -genauigkeit verbessert. Zudem bildet das Modell so die physikalischen Eigenschaften der Kraftwerke realistischer ab. Dadurch können auch weitere technische Details wie beschränkte Startgeschwindigkeit oder Startkosten in Abhängigkeit der gewählten Startgeschwindigkeit ohne großen Aufwand modelliert werden. Das erstellte Rechenmodell enthält neben der Kraftwerkseinsatzplanung auch die Optimierung des Speichereinsatzes sowie eine lineare Lastflussmodellierung, welche auch die Abbildung von flexiblen Netzelementen wie Phasenschiebern und Gleichstromverbindungen ermöglicht. Im dritten Teil der Arbeit wird das entwickelte Modell eingesetzt, um verschiedene Optionen der Flexibilitätserhöhung in einem realistischen Stromsystem zu testen. Hierzu wird ein Datensatz der thermischen Kraftwerke, erneuerbaren Erzeugung, Speicher und Netze für ein auf 268 Knoten reduziertes europäisches Stromsystem erstellt. Die verschiedenen Optionen werden dann anhand der Betriebskosten, der abzuregelnden erneuerbaren Energien sowie der resultieren CO_2-Emissionen bewertet. Die Ergebnisse zeigen insbesondere für Deutschland die positiven Auswirkungen von erhöhter Flexibilität im thermischen Kraftwerkspark sowie von Speicherausbau. Bei Betrachtung des gesamten europäischen Systems erzielen Netzausbaumaßnahmen die größten Effekte, womit diese als wichtigster Baustein zur Integration von erneuerbaren Energien im europäischen Kontext identifiziert werden können.

Acknowledgments

The work of this thesis was carried out between 2011 and 2016 at the Technical University of Munich, the TUM CREATE Centre for Electromobility in Singapore, and the University of Texas at Austin. I want to use this opportunity to express my gratitude to several people who strongly supported me throughout the course of this thesis.

First of all, I want to thank my supervisor Professor Thomas Hamacher who gave me the chance to work at his chair(s) and to conduct this PhD thesis. The fruitful discussions, ranging from technical parts of the research to their political and philosophical dimension, inspired many of my ideas. His incredible ability to motivate people definitely helped to bring some of these ideas to results and to overcome doubts and hesitations. I am very grateful to him for granting me the necessary freedom, giving me the chances to work interdisciplinarily, and for encouraging me to go abroad, which significantly broadened my scientific horizon.

Also, I am indebted to Professor Ross Baldick for giving me the chance to spend several months with his research group at UT Austin and for his ongoing support (among other things, his willingness to examine this thesis). I very much enjoyed the intensive and in-depth discussions and group meetings with him. Working with him also greatly improved my knowledge about optimization procedures in power system planning.

Next, I would like to thank Professor Rolf Witzmann who graciously and on short notice agreed to be part of the examination board and to fill in for the oral examination.

An important part of this thesis was conducted in cooperative work with the Research Unit Applied Geometry and Discrete Mathematics of Professor Peter Gritzmann, namely together with my co-authors Matthias Silbernagl and René Brandenberg, to all of whom I would like to extend my deepest gratitude. Only with their outstanding expertise in discrete optimization, their ingenious ideas, and their drive for perfection through many sleepless nights was it possible to obtain major results of this thesis.

With regard to the joy of working across institutes, I am also grateful to Professor Wolfgang Utschick for his support and his contagious passion for exciting research questions.

Without naming individuals, many thanks also go to all of my colleagues at each of the institutions I spent time in the last years. My research greatly profited from the shared project work and the countless brainstorming sessions. I cherish the memorable times we spent far from academics and the friendly atmosphere that made the many hours we did spend in the office so enjoyable.

I extend my heartfelt thanks to my mother, Gertraud, for her love and support throughout the years, my father, Richard, for bringing my attention to energy problems and renewable technology, and my sister, Christina, for always helping me out when I found life getting complicated.

I want to express my sincere and deep gratitude to my wife, Sina, for her incredible patience support during all the ups and downs throughout the course of this thesis. Her undying optimism always brought me back on track and, at least in some moments, spread over improving my own mood and motivation. Finally, I want to thank my son, Johann, for reminding me of more important things and for the sleepless nights that finally motivated me to bring the thesis to an end.

Contents

Chapter 1

Introduction

> And God said, Let there be light: and there was light.
>
> Genesis 1:3

Modern society has long adapted to the notion of constant energy availability. Both, the industry and residential sectors run on the precontext of having electrical power available whenever needed. In the hydro-thermal power systems of the 20th century, this varying demand could be met by planning power generation accordingly. When there was said to be light, there was light.

However, this light came at a cost. The dependability of traditional power sources such as coal, oil, and gas was found to have drawbacks regarding world climate as well as finiteness and distribution of these resources. Hence, the 21st century has brought one of the largest changes in power systems planning and operation. Many countries increasingly started integrating alternative energy sources such as wind and solar power into their grids. This poses a fundamental challenge to the constant availability of power. With varying supply from wind and sun, power systems of the present and future will need to be profoundly more flexible in meeting the needs of modern societies. This thesis is concerned with exploring this flexibility and investigates how planning in a modern power system can be improved to ensure that there will always be light when it is needed.

This first chapter of the thesis presents the motivation and goals of this dissertation. Section 1.1 gives a short introduction and motivation to the topic in a historic context. Section 1.2 provides an overview of the objectives and lists the major contributions of this thesis. Afterwards, Section 1.3 shortly outlines the thesis. Finally, Section 1.4 provides a list of all articles that were published within the course of this dissertation.

1.1 Motivation

Today, the power systems of many countries are in a phase of transition. New technologies that generate electricity from wind and solar energy are introduced into former

hydro-thermal power systems. This yields great chances for many countries and global society as a whole since renewable energy sources promise sustainability and independence. At the same time, as the generation from those variable renewable energy (VRE) forms are highly fluctuating and uncertain in their production, new challenges for power system operation arise. The system balance has to be kept in every moment although the electricity output from this new sources changes very fast and can only be predicted with uncertainty. Fluctuations have to be balanced by the residual power system of remaining controllable generators and storage. The ability to perform this balancing act by adapting to changing and unexpected situations can be called power system flexibility.

Europe, especially Germany, is on the forefront of this new trend. Considerable amounts of renewable energy generation have already been introduced to the power system. Fig. 1.1 depicts the development of photovoltaic (PV) and wind generation capacity installations for Germany and worldwide. In both cases, growth is tremendous and clearly indicates the paradigm shift towards those sources. This yields the requirement to analyze and prepare for the challenges ahead.

This thesis is concerned with the challenges that power systems will face from those installations in their operation and the necessary flexibility that must provided. It includes a statistical analysis of the variability from the new sources, an extensive discussion and further development of modeling techniques, and finally, an application of the developed model methodology in numerical simulations evaluating different measures to enhance system flexibility. Both the statistical analysis and the numerical model computations are conducted in the German and European context.

This first section puts the current challenge with the integration of VREs into a historic perspective of power system development. An overview is given of how balancing was handled and which flexibility measures where used in the early years of electrification, in the present situation, and in a prospective future power system.

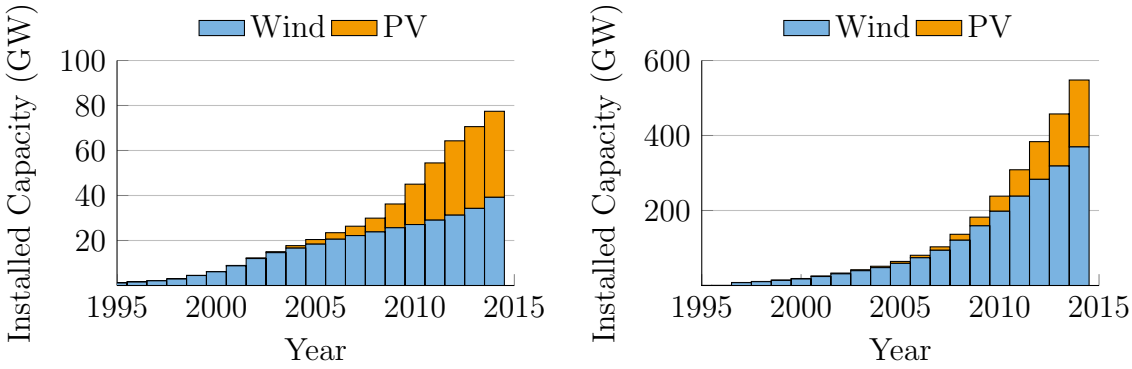

Figure 1.1: Development of wind and PV capacities in Germany (left) [32] and globally (right) [23, 70]. The overall installed electricity generating capacities are at around 200 GW in Germany [33] and at roughly 6800 GW globally [41]

1.1.1 Supply and Demand Balancing in the Beginning of Electrification

Flexibility has always been a prominent topic in power systems design and is not an entirely new challenge, neither from a technical nor from an economical point of view. In the beginning of electrification, balancing fluctuations and low utilization rates of power plants were a major concern and many efforts were undertaken to increase utilization rates of power plants [123]. Ideas for increasing the utilization of power plants were diverse. The main suggestion was combining different loads by adding load from motor power to the formerly lighting power-only load [114, 123]. Concepts for incentivizing flexible loads in the form of warm water heaters were also already discussed as early as in the 1920s [13]; a discussion that is currently resurfacing after almost 100 years. Furthermore, connecting multiple power plants in an electric grid allowed defining different types of plants from a base load to a peak load plant that was used for balancing purposes. In several locations, for instance in the city of London, batteries were installed. They stored electricity in times with low demand and released the energy at times with high demand [163]. As soon as grids were installed and several power plants were used to supply load in one system, dispatching the power plants in an economic and reliable way came high on the agenda. Operation on a two-shift basis was introduced for turbines in London [173], which shifted former base load plants to a scheme of daily start-up and shut-down processes. Many experiments were conducted to establish quick start-up procedures. Special attention was given to measuring metal temperatures of different power plant parts. This measurement allowed to plan and execute start-up more efficiently after brief and longer periods of shut-down. To summarize, from almost the beginning of electrification, several measures for balancing variable load were employed:

- Demand side management
- Grid extension
- Battery storage
- Management and increasing flexibility of thermal power plants

Interestingly, those measures are still seen as the key factors in the current transition towards the integration of high shares of renewable energies.

1.1.2 The Current Situation - A System in Transition

In the decades after the start of electrification, an increasing number of people gained access to electricity across the western world. Many power plants were set up and transmission grids were heavily extended. The power systems in Europe or the United States of America (USA) began to have countless components including lines, generators, and transformers that had to be operated safely. At the end of the 20th century, this made people call those systems “the most complex machines in the world” [129]. Still, those systems operated reliably. The systems include an automatic balancing mechanism, called automatic generation control (AGC), that reacts to mismatches

in supply and demand. Furthermore, systems incorporate stability mechanism for voltage control and many other parameters. Today, the foundations for transition are still those large interconnected systems that allow balancing fluctuations of load and major tripping of power plants and transmission lines. While these systems have worked reasonably well for decades, the beginning of the 21st century has brought changes yielding new challenges. First, power systems are being liberalized. This allows for decentralized decision-making. Yet, it also leads to increased complexity in coordination of investments and operation. The second and main challenge for current power systems arises from the integration of renewable energy sources. The latter is also the focus of in this thesis. Introduced to address current global headline issues such as climate change, finiteness of fossil fuels, opposition to nuclear power, and pursuit of self-reliance, renewable energy sources have been added to the existing, complex systems. Nevertheless, their introduction now also requires restructuring and further improvement of balancing strategies that has not been satisfactorily dealt with yet.

1.1.3 Look Ahead - Old Challenges with New Complexity

The future of power systems seems to be foreshadowed by its current transition. Especially the integration of variable renewable energies seems to extend globally. The capacities of such facilities have been increasing dramatically over the last years and plans for further extensions exist in many countries [75]. Fig. 1.1 shows the installed capacities of wind and solar power in Germany exposing their tremendous increase over the last years. Despite this shift towards renewable energies, experts believe the system will most likely be a hybrid system with the remaining thermal-hydro conventional system and the newly integrated variable renewable energies. Furthermore, storage and grids might be extended. Within this frame for future development, the old issue of optimizing the design and operation of the system with regards to economic and technical concerns becomes increasingly complex.

In traditional power systems, the major source of variation came from load varying throughout the day. With the introduction of variable renewable generation, this situation changes dramatically as renewable sources are variable and uncertain in their nature as well as location-dependent.

Especially wind and solar generation fluctuate throughout days and weeks and cannot be accurately predicted. Fig. 1.2 illustrates the high variations that future net load (=load minus generation from wind and solar) will face. This will pose additional challenges to the power system:

- The controllable part of the power system has to be able to balance the upcoming fluctuations and the resulting ramps on different timescales.

- The variation in load and the variable generation will show deviations from their predictions. This leads to an uncertainty in the operational planning that has to be handled.

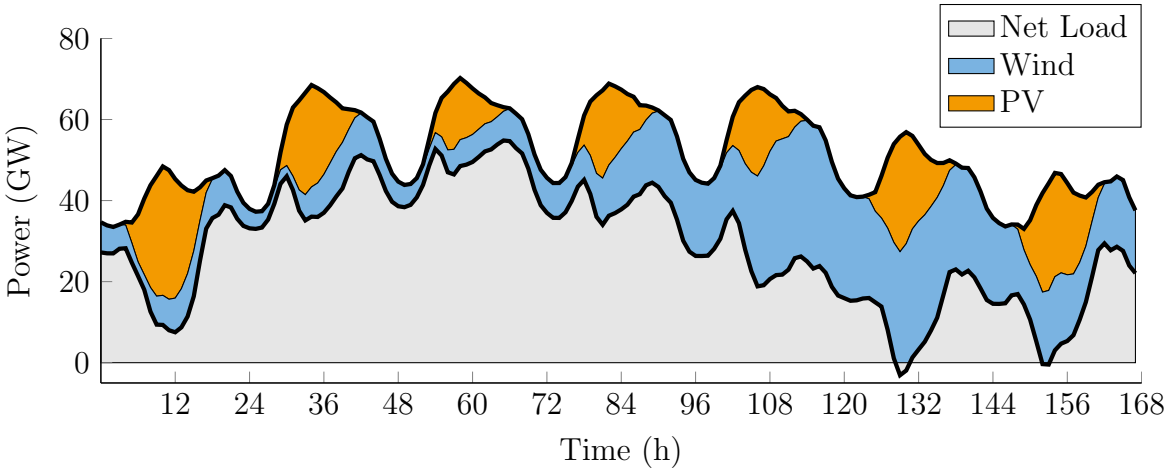

Figure 1.2: Illustration of net load ramps in a power system with high shares of wind and solar power

Regarding the temporal challenge, power systems planning will have to face situations of extreme steep ramping events. As an example, one of the most critical times of day has been shown to be the early evening: sun and consequently electricity generation from PV is declining while demand is rising at the same time. Californian System Operators called this effect the "duck curve" [35]. Fig. 1.3 illustrates the situation for Germany and Italy and demonstrates the challenge system operators will face. The figure illustrates load, net load (NL), and PV generation for a Sunday and a subsequent Monday. While in Germany, demand is only rising on weekend evenings, the effect is pronounced strongly for both days in Italy: Net load rises from around 10 GW to 45 GW within hours in the scenario with highest PV installations of 45 GW. This steep increase is an example of a load ramp that has to be provided by an output increase of on-line generators and the start-up of additional generators.

Another major challenge in the integration of renewable energy sources is a new spatial divergence of generation and load. A system of nuclear and fossil power plants leads to spatial convergence of generation and demand since power plants could be built close to load centers. As wind and solar generation are heavily dependent on the location, the introduction of VREs requires long distance transportation of electricity. A similar situation was experienced at the beginning of electrification with the installation of hydro power plants. Some countries still rely on large shares of distant hydro power plants (e.g. Brazil) and their experience in transmission planning might be helpful for planning systems with high shares of wind and solar generation.

All in all, the challenges that have to be faced in future power system operation are similar to the challenge in the beginning of the electrification: balancing enormous uncertain fluctuations in the system across time and space. However, the system of the 21st century has grown considerably more complex and reliability standards have substantially increased.

Remarkably, the measures discussed to overcome the challenge are still similar to the

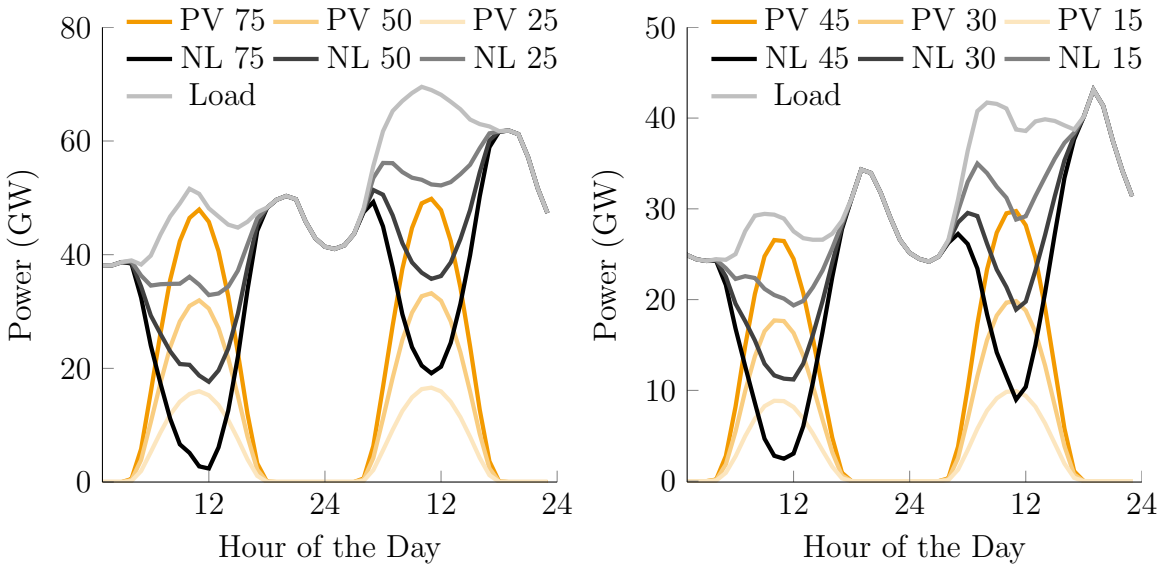

Figure 1.3: Duck curves (dark gray, NL=net load) for Germany (left) and Italy (right) for different installed PV capacities (orange, PV in GW)

ones suggested more than a century ago: transmission grids need to be further extended in order to balance generation of VREs at different sites. Furthermore, discussions revolve around storage plants to store power from renewable sources and demand side management (DSM) including changing demand to other hours of the days. Finally, the important questions of the flexibility of fossil power plants arise anew: How fast can on-line plants react? How long does start-up take and how much does it cost?

The statistical analysis, model development, and model evaluation within this thesis ought to shed a light on the challenges of future complex and high-stakes power systems and to examine which of the measures are best suited to tackle these challenges.

1.2 Objectives and Contributions

The research of this thesis is centered around the challenges of efficiently integrating large amounts of variable renewable energy sources in former hydro-thermal power systems. The major challenge in renewable integration is the variability that has to be balanced by the residual system. The thesis is divided into three parts around this question. In the first part, the flexibility requirements are determined by statistical analysis of time series of future wind and PV generation and net load. In the second part, an appropriate modeling framework of flexible components in power systems is developed based on the unit commitment (UC) problem. The components modeled are the flexible power plants, storage, as well as demand side management. Additionally, load flow constraints based on a linearized DC flow approach are included. A special focus and innovative approach is described for the modeling of thermal power plants, as this can be seen as a methodological focus of this thesis. The integration of uncertainty is a further aspect in the modeling framework. It is discussed in a following chapter. In the third part, flexible concepts of fossil power plants are evaluated in scenarios of

the future European power system, which is modeled based on publicly available data. Scenarios investigate the effects of increased power plant flexibility, grid extensions, grid flexibility, and storage. Finally, the different options to better deal with the fluctuating sources are evaluated and compared.

The main contributions can be summarized to the following bullet points:

- Flexibility requirements in future power systems with large shares of renewable generation are quantified by statistical analysis (joint work with Desislava Dimkova and Thomas Hamacher).
- The state-of-the-art modeling for the unit commitment (UC) problem is improved by the introduction of power plant temperatures as a new variable. This new approach improves both the computational efficiency of the UC modeling and the accuracy of power plant representation (joint work with Matthias Silbernagl and René Brandenberg).
- Based on the temperature model, new ideas for evaluating the flexibility of fossil power plants are presented and partly implemented and tested (joint work with Matthias Silbernagl).
- Different modeling approaches for regarding power flows in UC models are presented, compared, and evaluated. The implemented model allows to model flexible components in the grid like high voltage direct current (HVDC) lines or phase shift transformers (PSTs).
- Options to consider uncertainty (which arises from wind and PV generation forecasts) are described, categorized, and evaluated. The effects of uncertainty on the flexibility requirements and the value of flexible elements in power systems is estimated.
- A dataset is developed that represents the European power system with 268 nodes. The model serves as structural test case in this thesis and is a basis for future power system studies at Technical University of Munich (TUM).
- The computational burden of different levels of details for the large-scale power system with 268 nodes, 510 lines, and 2860 power plants (of which 1252 are controllable) is investigated.
- Different concepts for enhancing the flexibility in the system are evaluated in extensive numerical studies for the German and European power system.
- Conclusions for future planning and operation of power systems with high shares of variable renewable energies are derived and presented.

1.3 Outline

The thesis can be split into three main parts:

- **PART I: Definitions and Quantification of Flexibility in Power Systems**
  - **Chapter 2** gives an overview of power system operation and planning and discusses the term flexibility in this context.
  - **Chapter 3** presents a statistical analysis of future variability caused by the integration of VREs.
- **PART II: Power Systems Modeling**
  - **Chapter 4** presents the developed modeling framework.
  - **Chapter 5** describes possible approaches for considering uncertainty in UC models.
- **PART III: Evaluation of Flexibility Measures**
  - **Chapter 6** presents the dataset that was developed.
  - **Chapter 7** presents the results of extensive numerical studies evaluating different options for increasing system flexibility.
- **Chapter 8** concludes the thesis.

1.4 Publications

Parts of the thesis have already been published as papers or are rewritings of published papers. Part I and Part II are based on articles already published by the author as prepublication, while the results in the numerical simulations of Part III are introduced within this thesis for the first time. Minor differences in the datasets of the three parts are due to further development of the main dataset over the course of this dissertation. Yet, comparisons and conclusions across parts are still possible. The main dataset that is a result of this thesis is described and used in Part III. The publications that are relevant and (partially) included in the different chapters are provided below.

Publications relevant to Part I:

- M. Huber, D. Dimkova, T. Hamacher. Integration of Wind and Solar Power in Europe: Assessment of Flexibility Requirements, *Energy* 69, 236-246, 2014. [105]

Publications relevant to Part II:

- R. Brandenberg, M. Huber, M. Silbernagl. The Summed Start-up Costs in a Unit Commitment Problem, *EURO Journal on Computational Optimization*, 2016 [25].

- M. Silbernagl, M. Huber, R. Brandenberg. Improving Accuracy and Efficiency of Start-up Cost Formulations in MIP Unit Commitment by Modeling Power Plant Temperatures, *IEEE Transactions on Power Systems*, Volume 31, Issue 4, 2015. [185]

- M. Huber, M. Silbernagl. Modeling Start-up Times in Unit Commitment by Limiting Temperature Increase and Heating, *12th International Conference on the European Energy Market (EEM)*, Lisbon, May 2015. [111]

- M. Huber, A. Trippe, P. Kuhn and T. Hamacher. Effects of Large Scale EV and PV Integration on Power Supply Systems in the Context of Singapore, *3rd IEEE PES International Conference and Exhibition on Innovative Smart Grid Technologies (ISGT Europe)*, Berlin, October 2012. [112]

Publications relevant to Part III:

- M. Huber, T. Hamacher, C. Ziems and H. Weber. Combining LP and MIP Approaches to Model the Impacts of Renewable Energy Generation on Individual Thermal Power Plant Operation, *IEEE Power and Energy Society General Meeting (PES GM)*, Vancouver, BC, July 2013. [108]

- T. Hamacher, T. Hartmann, K. Siala, M. Huber, P. Kuhn, L. Stolle. Gesicherte Stromversorgung in Bayern, *Study for the Bavarian Ministry of Economic Affairs and Media, Energy and Technology*, 2016. [86]

Other publications that where conducted within the course of this dissertation:

- P. Kuhn, M. Huber, J. Dorfner, T. Hamacher. Challenges and Opportunities of Power Systems from Smart Homes to Super-Grids, *Ambio* 45, pages 50-62, 2016. [126]

- M. Huber, C. Weissbart. On the Optimal Mix of Wind and Solar Generation in the Future Chinese Power System, *Energy* 90, 235-243. [113]

- M. Huber, A. Roger, T. Hamacher. Optimizing Long-term Investments for a Sustainable Development of the ASEAN Power System, *Energy* 88, 180-193. [109]

- J. Stich, M. Mannhart, T. Zipperle, T. Massier, M. Huber, T. Hamacher. Modelling a Low-Carbon Power System for Indonesia, Malaysia and Singapore, *33rd IEW International Energy Workshop*, Beijing, 2014. [191]

- M. Huber, F. Sanger, T. Hamacher. Coordinating Smart Homes in Microgrids: A Quantification of Benefits, *4th IEEE PES International Conference and Exhibition on Innovative Smart Grid Technologies (ISGT Europe)*, Copenhagen, October 2013. [107]

- H. Mangesius, S. Hirche, M. Huber, T. Hamacher. A framework to Quantify Technical Flexibility in Power Systems Based on Reliability Certificates, *IEEE PES International Conference and Exhibition on Innovative Smart Grid Technologies (ISGT Europe)*, Copenhagen, October 2013. [143]

- B. G. Neudecker, P. Wimmer, M. Huber, T. Hamacher. Energy Economic Assessment of Range Extension Technologies for BEVs in 2020, *Conference on Future Automotive Technology Focus Electromobility* München, March, 2013. [82]

- M. Huber, F. Sänger, T. Hamacher. Das „ Post-EEG “ - Potenzial von Photovoltaik im privaten Strom- und Wärmesektor, *Energiewirtschaftliche Tagesfragen*, 09/2013 [110]

- T. Hamacher, M. Huber, J. Dorfner, K. Schaber, A. M. Bradshaw. Nuclear Fusion and Renewable Energy Forms: Are they Compatible? *Fusion Engineering and Design* 88, Issues 6-8, pages 657-660, 2013. [87]

- M. Huber, J. Dorfner, T. Hamacher. Electricity System Optimization in the EUMENA Region, *Project Report for the Dii GmbH*, 2012. [106]

Part I

Definitions and Quantification of Flexibility in Power Systems

Chapter 2

Power System Operation and Planning

This chapter briefly describes the basics of current power system operation from a technical and control perspective. Further, an overview of the current electricity markets is provided and the methods to approximate market operation within this thesis are introduced.

2.1 Physical Framework of Power Systems

While few system and policy studies emphasize the fact, the operation of electric power systems is determined by the fundamental laws of physics. Each power system is a network of generators and loads where, in each instant, supply and demand have to be balanced. The transmission and distribution of electricity from generators to consumers follows Kirchhoff's and Ohm's laws. Hence, in its design and operation, a stable system operation requires several system parameters to be kept within boundaries during steady state and during disturbances. Three major stability criteria can be identified: balancing active power which is measured by frequency stability, keeping voltage differences within boundaries (voltage stability), and keeping the phase angle differences below a stability limit (phase angle stability) [129]. The three criteria can be briefly described as follows:

- **Frequency Stability**: Current power systems work with rotating generators and motors which run at a constant frequency of 50 Hz or 60 Hz (e.g. Europe predominantly 50 Hz, US predominantly 60 Hz). Whenever the frequency deviates from this nominal set point, control measures have to be employed to counter the imbalances (see Section 2.5.3).

- **Voltage Stability**: Voltage at each node in the network is another critical system variable. Whenever electricity is transported over long lines or whilst appliances are consuming power, voltage drops at those nodes according to Ohm's law. Voltage stability requires the voltage differences between all nodes of a network to be within a certain limit in the steady state and after disturbances. In alternate

current (AC) systems, voltage stability is a complex issue that requires control of both active and reactive flows. For detailed information on this matter, the reader is referred to standard literature, e.g. the textbook of Prabha Kundur [129].

- **Rotor Angle Stability**: Generators and motors in AC systems are rotating with a given frequency (see frequency stability above) and the power transfer from one node to another depends on the difference in their phase angles. Up to a certain phase angle difference, more power is transported with a higher angle difference which leads to a self-stabilization mechanism: Whenever output at the sending node increases, the phase angle difference is increased and more power is transported. This effect can be seen as a restoring force as it allows additionally generated power to be transported when required. Beginning with an angle difference of 90°, an increasing difference will lead to a lower power transport - a further increase of power feed-in at the sending node can thus lead to a desynchronization and instability in the system. Again, the reader is referred to Kundur [129] for a detailed technical description.

While this thesis is mainly concerned with the provision and balancing of active power achieving frequency stability, planners of the large-scale integration of renewable energy sources must remember that system requirements go beyond active power balances.

2.2 Classification of Balancing Tasks

To attain the three stability criteria, power systems are balanced in different temporal and spatial dimensions that can be distinguished and categorized. A simplified illustration of the key tasks of power systems planning and operation is given in Fig. 2.1. While the figure is not an all-embracing description of this process, it helps classifying the part of balancing that is considered in this thesis: The focus of this thesis lies in the operational time range of seconds to days, which includes all tasks highlighted in blue in the figure. It is ultimately concerned with balancing active power and managing frequency stability.

Three key tasks are executed in the blue operational timescale: unit commitment (UC), economic dispatch (ED), and the provision of ancillary services. In the UC task, decisions are made about each power plant's on-line status in the upcoming hours determining start-up or shut-down. The time horizon for these decisions ranges from several hours to several days ahead in time. In the ED phase, the exact amount of power production for each plant is determined, a step than can be completed very close to actual operation. Ancillary services are then required to balance the mismatch from scheduled generation to actual load. A cascading control system that includes frequency stabilization by speed control (primary control) and frequency restoration by the AGC, consisting e.g. of secondary and tertiary control, is in place. Different definitions exist of whether speed control is part of AGC or not. Many scholars (e.g. Kundur [129] or Jokić [117]) define speed control separately from AGC. While speed control is activated in a decentralized way at each power plant, the AGC is activated

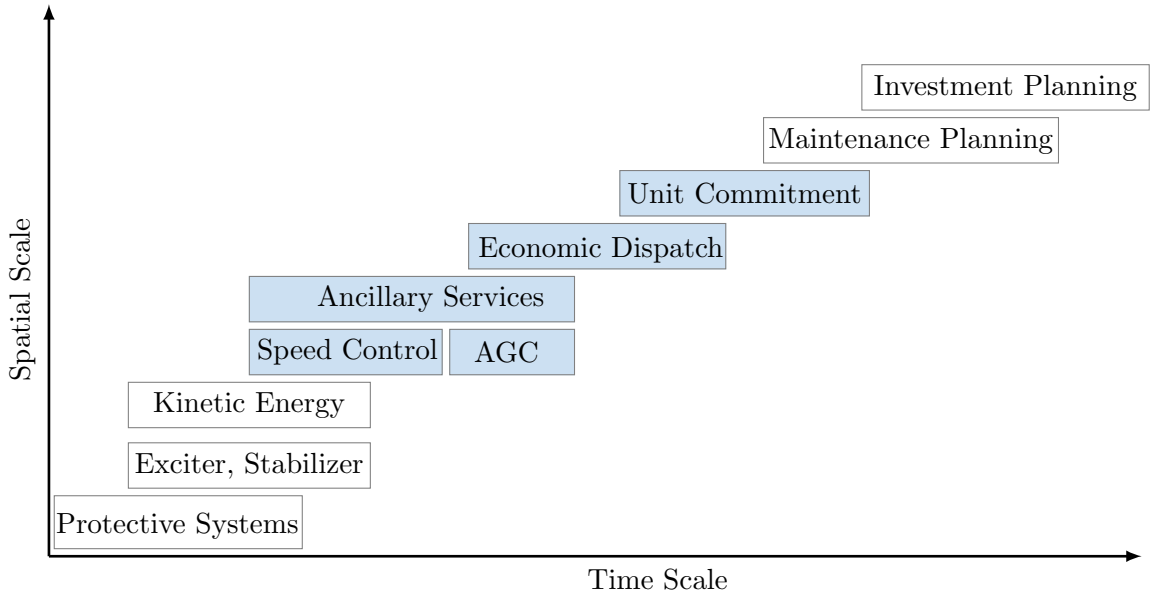

Figure 2.1: Temporal and spatial scales of key tasks in the planning and operation process of power systems. This thesis focuses on blue tasks in the operational time range. Illustration adapted and adjusted from Jokić [117]

.

centrally in reaction to system measurements. In a historic context, speed control was implemented very early when frequency restoration was still performed manually at especially assigned plants. Later, AGC enabled sharing the balancing tasks among generators and improving system efficiency. For this thesis, AGC includes secondary and tertiary control while speed control is a separate part of the ancillary services.

Beyond this operational timescale, there are also tasks in power systems planning and operation that are executed with both a shorter and a longer horizon. On the very short timescale of power system operations, protective systems may prevent larger damages or outages by isolating faults. This can, for example, include the protection of lines from overheating by the usage of simple overcurrent relays [129, p. 904 ff].

Another task on a very short timescale is the control of exciters. Exciters produce the magnetic field in generators, which is required for transforming rotating energy to electricity. As the generator output voltage is proportional to the magnetic field, the control of exciters is thus an important feature and task for voltage control and stability [129]. Control schemes should be able to quickly react to any changes or disturbances in the system in order to guarantee stability during a change of the system steady state (transient stability).

On the very short timescale of seconds, the pure kinetic energy of the rotating masses in the system is a stabilizer in itself by providing inertia when frequency drops or increases. A drop in frequency might be caused by a generator outage. It entails a slowdown of rotating masses and, thus, an extraction of kinetic energy from the system. The heavier these rotating masses are, the more time is available for the ancillary services to react to frequency changes.

With a longer time horizon of month to years, the maintenance and investment planning takes place. Maintenance planning includes revision of power plants or parts of the grid, which are not available during those times. Maintenance planning can be seen as an optimization problem as, for instance, electricity prices are expected to be lower during some month of the year due to seasonal effects of load and renewable generation. Power plants should be maintained during times with lower prices and where opportunity costs for the utility are lowest. For a system operator or integrated utility, maintenance should be scheduled in a cost optimal way while enough capacity has to be available throughout the year.

In the longest time horizon considered, investment planning is executed. Utilities or governments have to adequately plan their infrastructure, i.e. power plants and transmission grids, for the upcoming years and decades. Investment decisions are crucial and underinvestment can have severe consequences as (partial) blackouts might occur. The actual actors responsible for different parts of the infrastructure vary from country to country. In the case of Germany, power plants are owned by private utilities that also decide on their investment plans individually. The grid is operated by Transmission System Operators (TSO), a highly regulated company. This company must operate the power grid in order to fulfill transmission and stability according to market outcomes.

For most tasks, a valid correlation between temporal and spatial scales can be observed: the smaller the timescale, the smaller the spatial scale. Control actions that are executed within milliseconds are mostly performed directly at components of power plants while planning for transmission investments is done on the spatial scale of the entire system. Still, the categorization of tasks in the temporal scale of Fig. 2.1 is a simplified approximation and interpretation.

The scope of this thesis is the development and application of models that are applied to study balancing processes in the operational timescale including unit commitment, economic dispatch, and scheduling of ancillary services. By evaluating different options for improving the operational behavior of the system, the model results at those operational scales can give insights on investment planning.

2.3 Electricity Markets

Since electricity markets were liberalized in many countries, the operation of power systems is coordinated by markets in most of the western countries. Liberalization has been encouraged in the US since 1978 by the passage of the Public Utility Regulatory Policies Act and in Europe, starting in England and Wales, since 1989 [9]. Before the liberalization of the electricity markets, the blue-colored tasks of Fig. 2.1 where conducted by state-owned or state-regulated utilities, which were vertically integrated institutions that were in charge of generation as well as transmission. This vertical integration was broken up with the liberalization. Transmission, generation, and distribution are not operated by one entity anymore but multiple actors can enter and take part in different tasks. The concrete design of markets for different aspects of power supply, however, differs greatly from country to country in both the basic

structure and the traded products.

For the case of Europe, these organizational differences are a major obstacle on the way towards a common European market and a more efficient utilization of the continent spanning power grid. Especially the integration of renewable energy sources would benefit greatly from an improved cooperation amongst the different market places in Europe. An initiative with the goal of fostering the exchange between market regions is the Price Coupling of Regions (PCR) project. An achievement of the project is the development of EUPHEMIA (Pan-European Hybrid Electricity Market Integration Algorithm), a single price coupling algorithm which is used since 2014 [164].

The large-scale integration of variable renewable energy sources (VRE) into existing power systems also yielded large changes in electricity supply and markets since VRE sources mostly have marginal costs of zero. This led to dramatic changes in price formation at the markets. Fig. 2.2 depicts the effects on market prices by the introduction of VREs: renewables produce a shift of the supply curve which leads to a reduction of prices. This so-called merit order effect was estimated to be at 2.3 €/MWh per 1 GWh of reduction in residual load in Germany for the years 2007-2009 [178]. This value depends on many factors and several studies were conducted and found different values. Still, the value gives an idea about the quantitative effect on electricity markets.

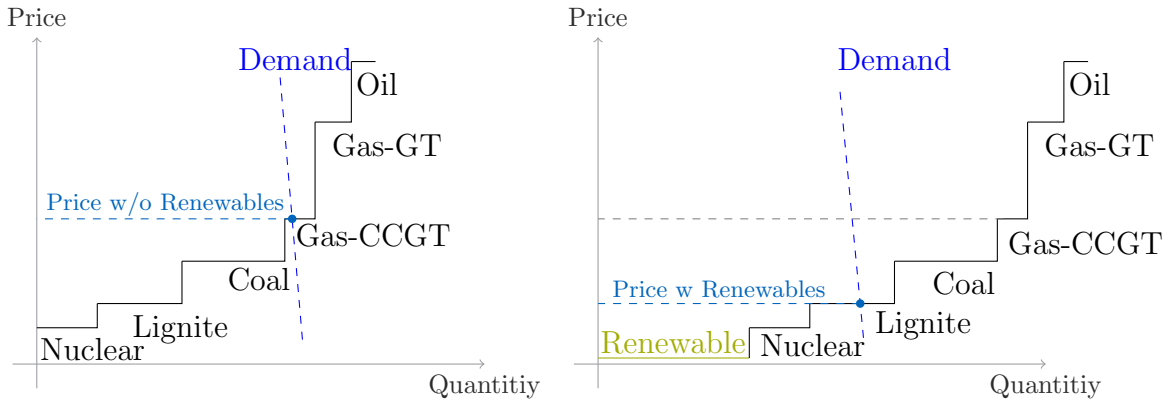

Figure 2.2: Reduction of market prices by the introduction of renewable energies with zero marginal costs

The liberalization and the introduction of VREs are the major aspects of current power system transformation. Modeling power system operation requires understanding the underlying markets as driving force for decision-making. Different aspects of electricity markets and their consequences for model development are discussed in the following.

Types of bids Two basic regimes can be distinguished: systems with complex bidding functions and systems with simple price quantity bids [45]. In the first type of systems, there typically is an independent system operator (ISO) that conducts all operational steps from a security-constrained unit commitment to all types of transmission operation. This type of market is referred to as a centralized market by Baldick et al. [9] and an integrated system by Wilson [210]. A suggestion for naming such markets types could

be "unit commitment market" in order to emphasize the fact of centralized UC decision. The ISO can receive complex bids that include start-up costs or ramping costs. This kind of system is applied in many of the US power systems, e.g. ISO New England, New York, or PJM [9]. A question that arises in such systems is how to incentivize the generators to exactly follow the schedules according to the UC and ED of the ISO. Often, non-transparent side or up-lift payments to compensate for start-up costs are required. Approaches to minimize such payments have recently been tackled by Hua and Baldick [104].

In Europe however, systems with simple price-quantity pairs are commonly installed. In Germany, for instance, the European Energy Exchange (EEX) collects all bids from generators and then, considers the bids according to prices until the complete demand can be supplied. All generators receive the same price in a so-called uniform pricing in contrast to pay-as-bid markets which is implemented, for instance, in the reserve auctions in Germany [155]. With those "simple" bids, more of the planning is conducted in a decentralized way. This type of market is therefore referred to as a "decentralized market" by Baldick et al. [9]. As major parts of market coordination is still done in a centralized platform, naming this type "partly decentralized" might be even more accurate. Each power producing company performs UC modeling with expectations on prices. This kind of UC problem is also called the "self-scheduling" of a thermal producer [186]. Decentralized optimization by utilities can be interpreted as solving the dual of the ISO's central optimization problem [210]. The results of both approaches might be very similar but not necessary the same due to the duality gap of the integer problem. Recent studies however suggest that the duality gap in UC is quite small [104].

Geography Another aspect to characterize different market designs is the geographical organization of the market. The basic distinction can be drawn between nodal markets and zonal markets: in nodal markets, a price is found for each node of the system whereas in zonal markets only one price is set for the whole area considered. In the European system, mostly zonal markets are implemented and generators can bid no matter where they are placed geographically within a market zone [99]. The size of the market zones in Europe mostly comprises one or several countries, e.g. Germany/Austria and France constitute two separate market zones. The advantage of zonal prices against nodal prices can be seen in a uniform price for consumers within an entire country. A major disadvantage of this market system lies in possible market outcomes that are not feasible due to grid restrictions. The impact of market zone sizes and required re-dispatch was, for example, studied by Van den Bergh et al. [19]. Furthermore, investment in new generators might be inefficient, as local scarcity is not considered. Whenever market outcomes are not feasible due to grid constraints, operators have to re-dispatch power plants, e.g. a power plant in the north is shut down while a power plant in the south of the system has to start up. With the introduction of large amounts of VRE in Germany, the single zone market has become problematic as more and more re-dispatch is required. As a consequence, geographical market components are currently discussed [57].

Time schedules and products Markets have to secure the matching of supply and demand in each point of time ranging from milliseconds to hours as shown in Fig 2.1. The different timescales result in various market products. In most systems, there is a separate market for energy and for different types of reserves. The concrete products are manifold and especially energy products are traded with varying time ranges.

In the case of Germany, markets for primary, secondary, and tertiary reserves exist in addition to a market for energy. Markets for capacities are discussed but have not yet been implemented. Other regions, e.g. New England, implemented such capacity markets, where generators are paid for being installed and being able to provide electricity in times of scarcity [46].

Energy is traded with different products and at different places. Bilateral trading is possible in most markets on the over-the-counter (OTC) market, and different auctions take place at exchanges like the European Power Exchange (EPEX) spot market which includes a day-ahead market and an intraday market. While the day-ahead market is cleared one day before actual dispatch, the intraday market allows for corrective actions up to an hour before dispatch [141].

Depending on the specific power systems, different definitions and specifications of reserves exist [176]. In the following, the definitions are considered as they are used in Germany, where three different reserve types are traded: primary reserve, which is activated automatically as soon as frequency deviates by more than 10 mHz, secondary reserve, which is activated whenever frequency deviations last for more than 30 seconds, and tertiary (minute) reserve, which can replace secondary reserves if required [155]. Currently, reserve is procurred in auctions with a pay-as-bid format but discussions about changing to a uniform pricing are ongoing [155].

2.4 Unit Commitment and Economic Dispatch

This section describes the Unit Commitment (UC) process, which is used to assign an on/off status to each power plant and the economic dispatch (ED) process that defines the steady state operating point for the power plants that are on-line. Mostly, energy for discrete time spans are scheduled, i.e. energy production is assigned to each unit that has to be provided over a defined period of time, e.g. one hour.

2.4.1 An Optimization Problem

Depending on the market structure, the UC and ED can either be solved by an ISO with the goal of meeting electricity demand at lowest costs or by a utility that maximizes profit and finds optimal bidding strategies. In both cases, the UC and ED problem can be seen as an optimization problem that needs to be solved. Solutions can be found with different algorithmic approaches (see Chapter 4), but basic technical limitations have to be considered in all cases: power plants can either be on-line or off-line which makes the problem an integer optimization problem. Additionally, power plants are constrained in their ramping (including start-up and shut-down), amongst others. Furthermore, UC

problems can include the operation of storage with additional constraints or constraints concerning the transmission system. Solving the UC problem is difficult since the on/off decision has to be made for all power plants in the system and for each step in the planning period. The number of possible combinations is exponentially growing by the number of time steps and the number of power plants considered. Currently, the commonly employed approach to solve UC problems is mixed-integer programming (MIP) which allows to find solutions with a criterion for the degree of optimality. A detailed description of the MIP modeling can be found in Chapter 4 which also includes the improvements to current state-of-the-art formulations introduced with this dissertation.

2.4.2 Energy-Based Scheduling

UC modeling – as applied in this thesis – schedules energy for each modeled hour. This reflects current market design where energy is traded per hour (or 15-minute intervals in several cases). Scheduling and trading with energy blocks has a major disadvantage: it leads to mismatches of power supply and demand. Fig. 2.3 shows an exemplary load and the scheduled energy blocks respectively. On the left, hourly scheduling is applied and deviations between energy blocks and load are severe. The gap between the energy block and the load has to be balanced by the ancillary services as described below. In reality, power plants do not follow this exact schedule of constant hourly power output jumping to the next output after precisely one hour. Instead, plants must be smoothly regulated to reach the respective desired levels. However, operators are allowed to plan with those jumps and hourly frequency deviations occur as described studies e.g. by Weissbach and Welfonder [207]. The authors of this study find that reducing trading periods could significantly reduce the required reserves. Fig. 2.3 on the right illustrates the effect of reducing the size of energy blocks to 30 minutes. The deviations become less and the scheduled supply matches the load with higher precision.

As power plants are operated in terms of power and not in terms of energy output, the interpretation of energy scheduling is a problem that modelers face when setting up a UC model. This is true, for instance, for the start-up ramps, which give maximal percentage of power output change after synchronization. In energy schedules, the parameter can be interpreted as the maximal energy that a power plant can provide in the first hour after start-up. In a consideration of power output, the power plant could reach 100% of its power output within the first hour of operation while the energy production during that hour will be less. As a consequence, pure technical parameters have to be adjusted for energy scheduling.

As an alternative to energy scheduling, Morales-España et al. [151] propose the ramp-based scheduling approach, which might improve market operations significantly. Regulators are already discussing ideas that point towards the introduction of special ramping products, see e.g. [61]. The idea of the ramp-based approach is to schedule linear ramps instead of energy blocks. Here, power plants must provide electricity according a predefined curve. This allows a more realistic consideration of power consumption

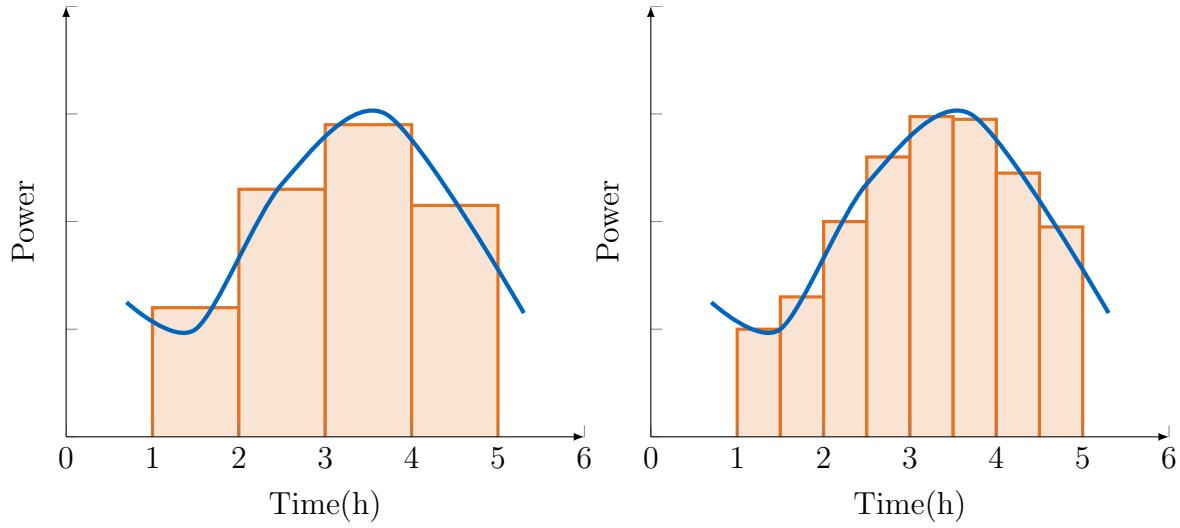

Figure 2.3: Deviations from load with hourly (left) and with 30 min (right) energy scheduling. The blue lines are the power demand while the orange bars are the scheduled energy blocks.

and might reduce reserve requirements. The major disadvantage of the ramp-based approach is the pricing and exact definition of traded products. An alternative solution to tackle the problem would be trading energy products in shorter periods, e.g. 5-minute blocks. As computational possibilities increase, the latter solution might be favored by operators. In unit commitment type markets, an option could be to compute day-ahead commitment decisions in an hourly resolution followed by a real-time market with marginal prices updated every 5 minutes.

2.5 Sub-hourly Balancing: The Ancillary Services

This section describes the approach for balancing the mismatch between generation and demand in the sub-hourly scale, which results from energy scheduling and from forecast inaccuracy.

2.5.1 Stability Problems While Dealing With Certainty

Even in systems with perfect forecasts of load and VRE generation, sub-hourly balancing is required as energy bids are discrete in time. Fig 2.3 above illustrates the difference in actual load and scheduled energy blocks that must be balanced by frequency control schemes. Hirth at al. [96] showed that there was an average imbalance of up to 1.5 GW in the German system in 2012 which was mainly caused by hourly schedule changes.

2.5.2 Stability Problems Caused by Uncertainty

Another reason for the employment of the control system is forecast uncertainty. In many power systems, the market operation is based on two different stages: the first stage is a day-ahead market where decisions about the UC for the following day are

taken. This is the case in many power systems, especially those being operated by an ISO. In the second stage, the intraday market, an exact matching of load and demand is organized by using multiple market products. Many power plants require a long time horizon for planning their operation, e.g. a cold start of a coal power plant takes up to 12 hours [183]. During the whole planning procedure, forecasts on the net load must be made and planning can be adjusted accordingly. When forecasts change several hours ahead of the actual event, rescheduling in the intraday market might be an effective measure. Whenever rescheduling is not possible anymore, the mismatch of generation and demand has to be balanced by the control system.

The integration of VREs into the system increases the challenges for accurate forecasts. While the forecast accuracy increases, absolute forecast errors might still increase because of rising capacities. Lenzi et al. estimate an increase of secondary/tertiary reserve requirements from currently around 4 GW up to 20 GW (roughly 20% of the yearly peak load) with heavy VRE integration in Germany [136]. Alternative options, such as adjusting the reserves with higher VRE capacities, and a further discussion on whether requirements will actually increase are discussed in Chapter 5 of this thesis.

2.5.3 Technical Solutions for System Stability - The Control System

The control system in many power systems is based on frequency stabilization. All power generating units and also consumers, like motors, are rotating at near-constant speed of 50 Hz (60 Hz in several systems). This frequency is uniform throughout the entire network and therefore, it is a perfect global control signal. Whenever generation is higher than load, the excess energy will speed up the rotating masses of generators and motors. Detecting the increased frequency leads to a control loop that reduces output of several/all generators until the frequency returns to 50 Hz. The same is true for an underproduction, where the energy "gap" is taken from the rotating system and frequency drops. Frequency regulation is often executed with several different types of control, i.e. primary, secondary, and tertiary control.

Whenever an imbalance of load and generation occurs, a frequency deviation is the consequence. At first, speed control is activated automatically. The participating generators have a so-called "droop control", which changes output as illustrated in Fig. 2.4. In this example, frequency increases from f_0 to f_1. This means generation is higher than load and rotating generators speed up. As soon as the frequency increase is detected by decentralized controllers at the power plants, output is reduced according to the (linear) droop curve.

Speed control stabilizes the frequency. However, it does so at a higher/lower level than the 50 Hz. In the example of Fig. 2.4, frequency is increased from f_0 to f_1. Thus, the AGC system, consisting of secondary and tertiary control, is activated subsequently to bring frequency back to the nominal value. The principle is a classical integral controller [129]. Further, the difference in scheduled flows versus actual power flows between control areas is corrected. Power flow deviations result from the primary

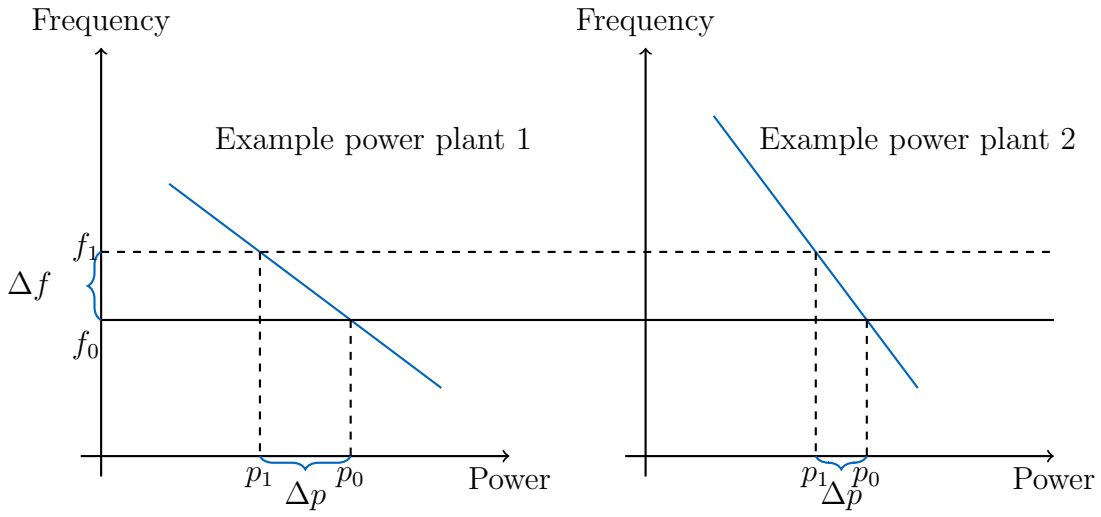

Figure 2.4: Droop control of two different power plants. At the same frequency deviation, the power plant on the left is providing more primary reserves than power plant on the right.

control being activated across the complete network while secondary reserve is activated afterwards in the control area of fault to counter the imbalances locally.

2.5.4 Scheduling Ancillary Services

In order to be able to provide reserves when required, power plants have to schedule reserve bands. Returning to the example illustration in Fig. 2.4, the power plants have to be operated above their minimum power output with enough buffer to ramp-down according to the droop curve. For upward reserves, the power plant must be operated below maximum power output. Assigning the reserve bands to the power plants is a task that can be included in the UC problem formulation. For upward reserves, it might be better to run more expensive power plants at lower levels, while for downward reserves, cheaper plants operating at full power could be employed.

2.6 The Concept of Power System Flexibility

Reacting to a mismatch in generation and load - foreseen or unforeseen - has always been an essential part of power systems operation. While the task had always required flexibility of at least several generators, power system flexibility is high on the agenda of academic discussion again today due to the challenges regarding large-scale integration of VREs. Many articles have been published in recent years on the topic, ranging from formal definitions to numerical investigations on requirements and capabilities. This section gives an overview of the research on the topic and how “power system flexibility” is defined in this thesis.

2.6.1 Approaches in Literature

The topic and the term "flexibility" and "flexibilty requirements" came into discussion (again) very shortly in articles focusing on finding metrics for flexibility in power systems [130, 131, 140, 143, 202]. The latter, Ulbig and Andersson [202], formulate a flexibility trinity of ramp rate, power, and energy. Another first attempt to categorize flexibility requirements was conducted by King et al. [121], who propose a qualitative framework for measuring a system's flexibility needs in terms of three metrics: ramp magnitude, ramp frequency and response time. The metric that was developed by Lannoye et al [130] focuses on the ramp capability of the system in certain set points. The theory was extended with network constraints by Horn [102] and the basic idea of this approach is explained here. In the scheduling process, power plants are assigned setpoints. According to their maximal ramp rates, power plants have a certain ability to change the setpoint within a defined time horizon, which is similar to the provision of reserves. The special measure is now to include line flow limitations in an optimization framework that finds the available flexibility, i.e. the ability to change the setpoints. The ideas of this flexibility metric which include line constraints are, to a certain degree, included in a UC approach that includes ramp and capacity reserves which was developed by Morales-España et al. [147] and which is described in Section 5.6. Instead of analyzing the system's ability ex-post, requirements are set in the scheduling process in a way that enough ramping capability is available at all times.

Another approach worth mentioning is the work of Bucher et al. [30], where a framework for defining regional flexibility requirements is described. This framework allows to define accurate reserve procurement requirements for system operators. Optimized reserve procurement can increase system efficiency and system stability. In the same direction, but with a temporal focus, Nosair and Bouffard [157] term a flexibility requirement envelope, which defines requirements on ramping, storage, and capacity over a future time interval. Ulbig [201] defines operational flexibility in power systems by stating: "Operational flexibility is the technical ability of a power system unit to modulate electrical power feed-in to the grid and/or power feed-out from the grid over time." Ma et al. [140] consider a power system to be flexible if it can cope with uncertainty and variability in demand and generation to maintain system reliability at reasonable additional costs. Insufficient flexibility may limit the share of variable renewable generation a power system can accommodate. It is thus of major importance to understand and quantify upcoming flexibility requirements in order to optimally prepare the system. In this thesis, the flexibility requirements of VREs arising from its variability are quantified.

2.6.2 Defining Flexibility for this Thesis

The discussion above shows that various definitions and ideas about the term flexibility in a power system context exist. The major aspect is that flexibility is considered to be the ability of the system to react to changes (foreseen or unforeseen) in the residual load. A very comprehensive definition as being used in this thesis is given by:

The flexibility of a System is the ability of the system to adapt to external changes, while maintaining satisfactory system performance [152].

While the definition originates in transportation science, it perfectly describes the term in the context of this thesis. The external changes can be either expected changes including deterministic variability or unexpected changes comprising outages and imperfect forecasts. Power systems have to be able to cope with both.

For this thesis, the main restriction to a general definition comes from the timescales considered. The focus of the thesis is to model and analyze all operational aspects in the range from UC decisions to the scheduling of ancillary services (see blue-colored tasks in Fig. 2.1). In accordance with the definition, flexibility in this thesis is described as the system's ability to react to changes in the range of one hour to one day. Short-term flexibility is also considered by scheduling of reserves. However, actual output changes are only considered on an hourly base in the modeling framework. This focus on the hourly timescale is consistent for all parts of the thesis. In the first part, a time series analysis focuses on the resulting challenges in that scale. The modeling approach described in the second part is mostly independent of timescales. Yet, so far, most of UC models are applied to hourly planning of the next day. The same is true for the numerical studies presented in the third part, where different flexibility measures are analyzed with regard to their effectiveness in balancing variability from increased VRE generation. Different aspects of system flexibility are relevant for these scales. In the UC stage, the power plants' ability to switch on and off quickly and their start-up/shut-down time are of high relevance. Further, the minimum power output at which a plant can operate is relevant for planning more efficient schedules with fewer start-ups. The ability of storage to shift energy from times with VRE production to times with lack of energy can reduce curtailment and prevent start-up of power plants for very short times. In the ED task, major concerns are the quick changes of output from one hour to the next that does not include start-ups. Finally, the reserve scheduling allows the system to react to unforeseen events and deviations of load resulting from energy schedules (compare Fig. 2.3).

2.6.3 Technological Options for Providing System Flexibility

In order to overcome the challenges imposed by the increased variability, there are several sources that are possible providers of the necessary flexibility in the system on the timescales of minutes to several hours or days. Flexible power plants, storage, integrated DSM, and an enhanced transmission grid can provide the power system with flexibility [89, 115]. Those are briefly described in the following section without going into deep technological details.

Flexible generation The first possibility to counterbalance fluctuations is a flexible and controllable generation. There are several options for flexible generation that include all types of fossil fuel power plants, nuclear plants, biomass plants, as well as hydro generation to some extent. The focus of this work lies on the flexibilization of large

centralized fossil fuel-fired plants that will remain a major constituent of most power systems for the next decades in Europe [69]. Three different types can be distinguished:

- Steam turbines: include coal, lignite, (old) oil and gas, and nuclear power plants. The major characteristic of those plants is an external combustion process that evaporates water and heats steam, which is then put through turbines.
- Gas turbines: are mostly natural gas and sometimes oil-fired power plants. The fuel is burnt with compressed air and the expanding gas then drives the turbine.
- Combined cycles: are a combination of a gas turbine and a steam turbine. The exhaust gas of the gas turbine is used to heat the steam for the steam turbine leading to higher efficiencies.

Options to increase their flexibility are manifold and concern different parameters and different parts of the power plant. The two different cycles have different major limitations and challenges for improvement. While the operational range of gas turbines requires a high minimum power output due to the internal combustion process and resulting carbon monoxide emissions at lower power outputs, the ramping and start-up capabilities are much better than those of steam cycles. The latter are quite slow due to limitations of temperature increase/decrease in the steam cycle. Still, reducing minimum power output to very low values seems to be possible because of external combustion [92].

For gas turbines, the most important factor for further improvement lies in enlarging the operating range. Ideas for reducing the minimum output can be a bypassing of compressed air for increased fuel-to-air ratio or by preheating of air [213]. Operational range can also be extended to values above the rated power by injection of water or steam [189].

For steam turbines, increased ramp and start-up capabilities appear both essential and challenging. Ideas to increase ramp rates include sliding pressure values in order to be able to match steam and metal temperatures also during fast output changes [92]. An effective measure to reduce start-up times of steam power plants is to employ steam cooling of the outer casing, which allows reducing thickness of the casing and, in turn, allows for faster temperature changes. This measure is reported to allow for a reduction of start-up times to up to 50% [92]. Ideas to keep units warm, installing thermal storage, or usage of improved material that withstands the thermal stress during heat-up are also being discussed [92].

The aim of this thesis is to test different parameter variations and evaluate their effect on the system. The technical details of how the parameter improvements are realized are not considered. Yet, results indicate the importance of improvements in specific areas.

Storage Another option to provide flexibility in the system is storage. Storage can include pumped hydro in a form that already exists across Europe. Extension of those

plants is possible to some extent but potentials are limited. Other options include compressed air storage, hydrogen, or batteries. While hydrogen promises to be the most interesting option for seasonal storage, batteries could be appropriate for solving short and medium term balancing problems. Biggest challenges and weaknesses for storage are insufficient efficiency in the case of hydrogen-based systems and high costs in the case of battery systems. Especially for the latter, progress is observed and first applications to power system balancing are tested on large-scale systems as well as on small-scale smart homes [81]. The research of this thesis focuses on the effect of storage on the operational timescale. However, storage might also be required for long-term balancing to counter seasonal effects. As a further reading on effects of storage in this context, the interested reader is referred to e.g. Kuhn [125] or Kühne [127].

Flexible demand Flexible demand is a further option that might help to integrate VRE sources and has been discussed heavily in literature for some time. The basic idea is to either shift electricity consumption to other points in time or to increase/decrease consumption at certain times without any compensation at other times. Technological options to perform such tasks are manifold. The simplest and oldest idea for such load levelers are electric heaters [13]. Other ideas frequently discussed are electric vehicles that can shift their charging according to availability of generation from VRE. The same can be done with electricity consumption in households, e.g. washing machines, or in commercial buildings, e.g. cooling devices or even elevators. In industry, there are ideas to shift part of production to time with lower prices [193]. Within this thesis, an idea of how to include flexible demand in a UC problem is described at the example of controllable charging of electric vehicles.

Grid flexibility Power systems are coupled, networked systems. When regarding the possibility to adapt for changes in the system state, a consideration of the network structure and the resulting constraints is required (as mentioned and described e.g. by Horn [102], see Section 3.1). There are technical options to influence the power flow. These include direct current (DC) lines that are not determined by line reactances but can be controlled directly. Depending on the situation in the grid, DC lines can transport more or less energy and thereby enable increased efficiency in the remaining AC grid. Another option to reach a similar effect can be achieved by phase shift transformers (PSTs), that allow to change the angle between two nodes in a network. Electricity flow can therewith be bypassed from overloaded lines and the overall grid transport capacity is increased, see e.g. [18, 84, 203].

Transmission extension A well-connected grid helps to diminish the variability and therefore can significantly reduce the flexibility requirement in the system. Grid extensions can be executed in form of AC lines but also in form of DC lines that have further advantages through their controllability. Improved VRE integration through grid extension has been studied and positive effects are remarkable for Europe (e.g. see [85, 106]) and globally (see e.g. [1, 38].

2.7 Consequences for Power System Modeling and Flexibility Evaluation

The goal of modeling power systems within this thesis is to evaluate flexibility improvements that allow for a more efficient integration of VRE sources. This requires considering as many technical and organizational aspects of the above mentioned as possible. However, computational power and system complexity requires modelers to reduce the system to relevant aspects. When regarding system flexibility as the main topic of this thesis, the question to be answered is how to best formulate the respective models. As described above, timescales at which flexibility requirements can be assessed range from milliseconds to years. The focus of this thesis is the range of hour-to-hour flexibility including the sub-hourly balancing. Models at that timescale can include the UC decisions and the scheduling in form of ED as well as the constraints for reserve provision. Further, network flows and flexible components in the grid as well as storage must be included to evaluate measures at this timescale.

Concerning the organizational representation of the system, the question arises whether the model reflects market outcomes as they are achieved in real-world operations. The discussion above explained that market design always gains at achieving cost-optimal provision of electricity to consumers. Therefore, the modeling with a UC optimization mimics a system with perfectly designed markets. Currently, the European electricity market is organized in country-based price zones and exchange between countries is possible based on net transfer capacities (NTCs). However, tendencies towards a flow-based market coupling can be observed since this would be required for an efficient common European market place [15]. In the thesis, such a flow-based market coupling with 268 zones is assumed. The high number of zones reflects the tendencies towards smaller market zones (e.g. splitting of the Germany/Austria zone, discussions on two German zones, etc. [57]) and are driven by the disperse physics of VRE sources.

Chapter 3

Flexibility Requirements

This chapter presents joint work with Desislava Dimkova and Thomas Hamacher [105]. We provide an extensive statistical analysis of occurring ramps in future power systems. The geographical focus of this chapter is Germany and Europe and timescales considered are 1-12 hours which is the most important time frame for operational planning.

3.1 Literature Overview

At first, some literature overview of research conducted on the topic is provided. The literature list is long and besides discussing appropriate metrics for flexibility (see Chapter 2.6), some research has been done on describing the flexibility requirements of national power systems, for example, requirements in Ireland were analyzed by Lannoye et al. [132]. In case studies, by upscaling real wind power data for several European and US regions, Holttinen et al. [101] show that high penetration of wind power can increase the magnitude of extreme net load ramps and change their time of occurrence. The above-mentioned studies focus on the impacts of large wind shares on power systems. The variability of photovoltaics (PV) has been studied mostly for individual sites by Mills and Wiser [145]. Therein, the flexibility requirements of large-scale penetration of both wind and PV are investigated and a comparative perspective is adopted. The authors find that an extension of interconnections and a geographical spread of generation drastically reduce variability.

The temporal dimension of ramp requirements is characterized in [121] by means of a so-called ramp envelope which bounds the magnitude of ramps over a given timescale with a certain probability. Lannoye et al. [132] discuss the importance of the considered time horizon and analyze changes in wind power production in Ireland on timescales ranging from 15 minutes to 9 hours. In a study by the German Association for Electrical, Electronic & Information Technologies (VDE) [65], flexibility requirements for the German power system are analyzed in scenarios about the future development of PV and wind installations. The study covers different timescales ranging from 1 to 20 hours and shows that ramp rates in Germany will increase strongly in the next years. The outlined studies show the importance of the topic as well as the additional research that is required and addressed in this chapter of this thesis.

Additional requirements from uncertainty As described in Section 2.5.2, uncertain forecasts are a further challenge for the integration of large shares of VREs. Whenever those predictions are incorrect, reactive actions have to be taken in the intraday market or by employing reserves, both increasing system costs. In order to technically handle those corrective actions within a day or even within hours in the timescale of minutes, additional flexibility is required in the system.

Concerning the quantity of uncertainty introduced, two trends are observed: On the one hand, the increasing capacity is leading to a situation where forecast errors become more severe in terms of absolute power mismatch. On the other hand, the accuracy of forecasts is steadily improving in relative terms which leads to reduced flexibility requirements. Current reserve markets might reflect the latter effect as the reserve sizes are not increasing in many European countries [28] but even decreasing in Germany [96] so far. Hirth and Ziegenhagen [96] report a reduction of reserve requirements by 15% since 2008 while wind and solar generation has tripled in the same time. The two opposing trends could even out for the next years; however the improvements in forecast accuracy might converge at some points and further improvements might be difficult. Brouwer et al. [28] gives a literature overview of current forecast errors and finds a Root-mean-square error (RMSE) forecast error for wind day planning in the range of 4.5%-6.5% for Germany, around 9% for Ireland and West Denmark and 5-15% for US sites. The values for PV are reported to be higher in Germany with 13%, and lower in the US, e.g. 3.1% to 4% for California. The same study also founds (by literature review as well), that reserve requirements of power systems with VREs will increase as soon as penetration rates are higher than 20% of annual production. Further research is required in order to really quantify those effects in system models.

The adoption of the power system to those uncertain events and an adequate operational planning is discussed in Chapter 5. A simple approach based on changing forecasts is then also implemented for test cases and flexibility evaluation in Chapter 7. The major focus of the thesis lies in dealing with the challenges from variability, and the following statistical analysis as well as most of the simulations conducted focus on those aspects.

Novelty of contribution In this Chapter, flexibility requirements at timescales from 1 to 12 hours for power systems with projected high shares of wind and PV are analyzed. Compared to previous work, the analysis is extended to 27 European countries (the European Union members, with the exception of the isolated power systems of Malta and Cyprus, together with Norway and Switzerland) and statistically highlights basic properties that are common to most systems depending on the percentage of VRE in the system and the wind/PV mix. Results show that the wind/PV mix is equally important for the ramp requirements as it was shown to be for system costs [48] and the minimal mismatch between renewable generation and load [91, 182]. Still, the share of wind/PV and their mix do not explain all the variability in the system; differences between countries remain. In order to understand and explain those differences, additional system parameters are investigated: the geographical system size as well as the wind and solar resource potential in terms of full load hours (FLH). By that, methods

described above are extended and a first move to a generalized characterization of future flexibility requirements in power systems is undertaken.

The results provide a deeper understanding of the occurring ramp rates in many power systems. They allow for designing the variable system in such a way as to minimize problems in the controllable system or, if this is not possible, to foresee upcoming requirements and adapt the controllable system in an adequate way.

3.2 Database and Scenario Generation

3.2.1 Database Description

The analysis is carried out using modeled time series of onshore wind and solar PV power production for the period 2001–2011 in 27 countries in Europe. The time series are based on NASA reanalysis data [177], which consists of hourly values of wind speed and solar irradiance at a spatial resolution of 0.5° E/W and 0.66° N/S for the whole world. The weather data for each spatial grid cell was converted by Janker [116] into wind and PV power production time series. The analysis explicitly excludes offshore wind power in order to employ a unified framework for comparing countries and regions respecting the fact that not all countries have the possibility to install offshore power. In addition, historical offshore data is only rarely available, thus validation is difficult.

From the time series for wind and solar power in the grid cells, a weighted average is built to obtain aggregated power production at the regional and country level. The weighting factor for each cell is proportional to the resource potential in terms of wind speeds or solar radiation (energy density) – more capacity is assumed to be installed on sites with higher energy density as this is cost-efficient. The weights are generated separately for wind and PV and for each modeled country or region as follows: the grid cell with the lowest density is assigned a weight of zero and the one with the highest density is assigned the difference between the maximum and the minimum energy density values of all cells in the respective country. A linear interpolation between those two weighting factors is applied to obtain weights for the grid cells with wind speeds or solar radiation in between. Finally, the weighted average electricity generation of all cells in each hour is normalized with respect to installed capacity, i.e. it is converted into hourly wind and PV capacity factors (CFs) in the interval $[0, 1]$ [116]. Fig. 3.1 shows the average annual full load hours of the thus obtained wind and PV power generation in the analyzed countries.

For the investigations in this Chapter, the most important factors are the power ramps, or gradients, occurring over different time horizons. A power ramp $\Delta_h P$ is defined as the change of power in a given time interval of h hours:

$$\Delta_h P(t) = P(t) - P(t-h) \tag{3.1}$$

where $t = \{h+1, ..., 8760\}$, $P(t)$ is the wind or PV power production in a spatial unit (country or region) at time t. In order to validate the simulated power output profiles, the frequency distributions of hourly ramps of simulated wind and PV power

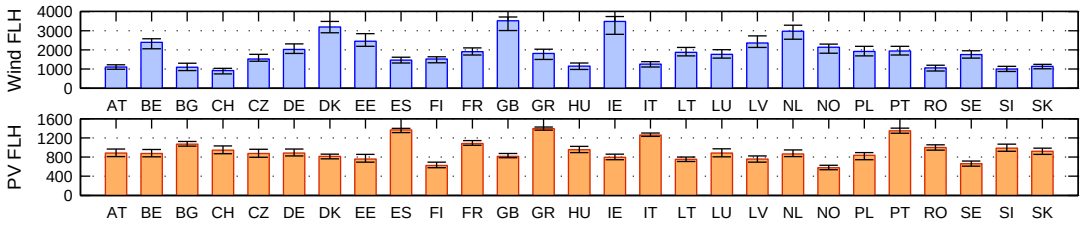

Figure 3.1: Average onshore wind and solar PV full load hours per year over the period 2001–2011 as well as their range

are compared with respective data from the transmission system operators (TSO) in Germany [79] and also with actual wind feed-in data for Ireland [58]. As Fig. 3.2 shows, the model data reproduces very closely the actual ramp behavior both for wind and solar power output.

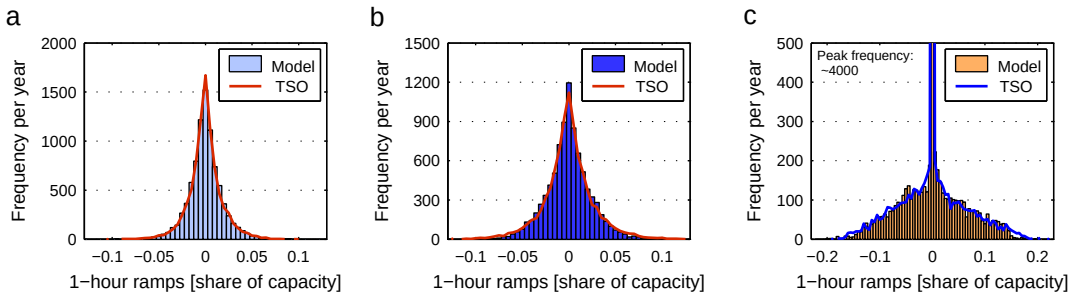

Figure 3.2: Frequency distributions of hourly ramps of simulated and actual production: (a) Wind 2011, Germany, (b) Wind 2010, Ireland, and (c) PV 2011, Germany. Wind and PV power is normalized with respect to installed capacity.

3.2.2 Scenarios for Wind and PV Generation and Resulting Net Load

Scenarios for future net load, i.e. load minus generation from variable renewables, particularly onshore wind and solar PV, are generated based on the data described above. Net load ramps are chosen as a measure of the flexibility requirements of power systems since every change in net load has to be balanced by flexible resources such as dispatchable power plants, storage or responsive loads in order to maintain system stability.

Hourly load profiles for the analyzed countries come from the European Network of Transmission System Operators (ENTSO-E) [62]. Load data for the year 2011 is used in all scenarios to isolate the impact of wind and PV on the variability of net load. A small number of hourly load ramps which lie more than five standard deviations below or above the mean in the original load ramp series are considered outliers and smoothed out in the time series (0.007% of all data points). Annual electricity consumption is assumed to remain at the level reached in 2007.

Electricity generation from wind and PV is calculated by multiplying the hourly capacity factors, obtained from the weather data, with the installed wind and PV capacities which

are varied in scenarios. The VRE capacities are a function of the total contribution of wind and PV to annual electricity consumption α and the share of PV in the wind/PV energy mix β. The definitions for α and β are adopted from other studies focusing on the capacity or storage requirements in power systems with high shares of PV and wind power (e.g. [90, 182, 190] use similar methods) and are given by:

$$\alpha = \frac{\sum_{t=1}^{t=8760} P_{\mathrm{W}}(t) + \sum_{t=1}^{t=8760} P_{\mathrm{PV}}(t)}{\sum_{t=1}^{t=8760} D(t)}, \tag{3.2}$$

$$\beta = \frac{\sum_{t=1}^{t=8760} P_{\mathrm{PV}}(t)}{\sum_{t=1}^{t=8760} P_{\mathrm{W}}(t) + \sum_{t=1}^{t=8760} P_{\mathrm{PV}}(t)}, \tag{3.3}$$

where P_{W} and P_{PV} are the hourly power outputs of wind and PV at time t and $D(t)$ is the electricity demand.

In each country, the net load $\mathrm{NL}(t)$ can be computed as load minus generation from wind and PV by

$$\mathrm{NL}(t) = D(t) - P_{\mathrm{W}}(t) - P_{\mathrm{PV}}(t), \tag{3.4}$$

and the ramps of the net load accordingly by

$$\Delta_h \mathrm{NL}(t) = \Delta_h D(t) - \Delta_h P_{\mathrm{W}}(t) - \Delta_h P_{\mathrm{PV}}(t). \tag{3.5}$$

For the computation of scenarios, the power generation from wind and PV should be described in terms of the varied parameters α and β, the predefined hourly capacity factors $\{\mathrm{CF_W}, \mathrm{CF_{PV}}\} \in [0, 1]$, and the electricity demand $D(t)$. The overall energy that is produced throughout a year by either wind or PV can be defined to

$$\sum_{t=1}^{t=8760} P_{\mathrm{W}}(t) = \alpha(1-\beta) \cdot \sum_{t=1}^{t=8760} D(t) \quad \text{and} \quad \sum_{t=1}^{t=8760} P_{\mathrm{PV}}(t) = \alpha \cdot \beta \cdot \sum_{t=1}^{t=8760} D(t), \tag{3.6}$$

and the share of energy that is produced in each hour is defined by

$$\frac{\mathrm{CF_{PV}}(t)}{\sum_{t=1}^{t=8760} \mathrm{CF_{PV}}(t)} \quad \text{and} \quad \frac{\mathrm{CF_W}(t)}{\sum_{t=1}^{t=8760} \mathrm{CF_W}(t)}. \tag{3.7}$$

The annual sum of the capacity factors equals the full load hours for the respective technology. Finally, the ramp rates of net load $\Delta_h \mathrm{NL}(t)$ are a linear combination of the ramp rates of load, wind, and solar power which can be defined by

$$\Delta_h \mathrm{NL}(t) = \Delta_h D(t) - \frac{\alpha(1-\beta)\sum_{t=1}^{t=8760} D(t)}{\sum_{t=1}^{t=8760} \mathrm{CF_W}(t)} \Delta_h \mathrm{CF_W}(t) - \frac{\alpha\beta\sum_{t=1}^{t=8760} D(t)}{\sum_{t=1}^{t=8760} \mathrm{CF_{PV}}(t)} \Delta_h \mathrm{CF_{PV}}(t). \tag{3.8}$$

The occurring ramps are all computed relatively to the peak load in each country to allow for comparisons across regions. Peak load is interpreted as an indicator of system

size because conventional power plant fleets are traditionally sized to meet the annual demand peak with a reserve margin for accommodating outages and extreme load events.

Thus, the system flexibility requirements posed by VREs are determined in the model by the following factors:

- the VRE penetration level α and the wind/PV mix β as choice variables resulting from policy and investment decisions;
- the ramp behavior of load and the inherent ramp properties of wind and PV power. These properties are determined by geographical location, generator placement, and system size, and will be described by means of frequency and temporal ramp distributions in Section 3.3;
- the correlation between the load and the VRE gradients as well as between wind and PV ramps. Load and VRE ramping up or down at the same time counterbalance one another, whereas wind and PV power ramps in the same direction add up to increase the system balancing requirements.

The combined energy penetration of wind and PV (α) that is considered is 10%, 30%, 50% and 70% of annual electricity demand. As there are other renewable energy technologies such as hydropower, biomass and geothermal that can be deployed in addition, a share of 70% of wind and PV can be interpreted as a fully renewable power system. At each penetration level, the share of PV β is set to 20%, 40% and 60%.

After showing the effects of different levels of VRE penetration, a focus of the research will be the 50% scenario. A 50% wind/PV share is discussed as an intermediate target in 2030 on Europe's way towards a fully renewable power system [95]. A further argument for having a closer look at that scenario is that research showed that renewable integration becomes especially challenging in terms of ramps at that share.

In the scenarios, excess energy is not cut off; the residual load can thus rise from negative to the maximum load leading to ramps with a magnitude of more than one. A ramp of one means that all controllable resources, except the capacity reserves, are required to provide full load in the specific time frame.

An aggregated European net load is calculated from the country time series as follows: a VRE penetration target α and a wind/PV mix β are selected for Europe as a whole and this α/β combination is assigned to each country making up the European power system. Unrestricted electricity transport is assumed between the countries.

It should be noted that the analysis focuses on flexibility requirements in certain scenarios about future development of wind and PV power capacities. Changes in the net load caused by DSM or storage are not modeled as they are already seen as a countermeasure for the variability of renewables, i.e. as part of the flexibility of the residual system.

3.2.3 Limitations of Net Load Modeling

The model captures very well the variability of the system at current levels of wind and PV penetration in the validation countries. Still, the remaining question is whether the scenarios for net load are scalable for future projections of variable generation or whether there are upcoming effects that would change the outcome. The following effects are identified to have influence on the ramping requirements from further integration of variable generation, i.e. wind and solar:

- Variability of wind may decrease as more turbines get installed but there may be a saturation effect [101].
- Climate change might lead to more extreme weather events. Still, it is unclear if this has any effects on ramping requirements [172].
- Improved wind turbines could be deployed. The effects are not predictable, however, as the enormous ramping requirements challenge the system, wind turbine producers might have incentives to develop turbines with "flatter" power curves.
- Load might change as well: people's work and leisure rhythm, a structural change of the economies and upcoming flexible load and power autonomy of household and industry can also have influence on flexibility requirements in the public power system [74].

To summarize, there are several changes in the behavior of wind and solar generation on the horizon, but most are likely to have low influence or their effects are not quantifiable at present. Overall, the flexibility requirements will be lower than suggested in this paper as new technologies and an optimized placement of generators could reduce variability.

3.3 The Wind/PV Mix as Determining Factor for System Flexibility Requirements

Results in this section identify the total share of wind and PV in electricity consumption α combined with the share of PV in the VRE mix β as determining factors for ramp requirements in future power systems. First, the ramp properties of the individual time series are introduced: load, wind and PV. Then one-hour ramp events of net load are shown in scenarios in order to quantify the ramp requirements from hour to hour resulting from the combined effects of the load and VRE time series. Finally, an analysis of longer ramps of duration from 2 to 12 hours is conducted, as this is critical due to start-up times of conventional power plants [65].

3.3.1 Ramp Properties of Wind and PV Generation in Europe

Fig. 3.2 illustrates the basic shape of the frequency distributions of onshore wind and solar PV power fluctuations. Wind power is characterized by high frequency and low

magnitude ramps concentrated around the center of the distribution. The largest ramps occurring are in the range of 6–10% of installed capacity per hour in medium-sized and large European countries, and 11–18% per hour in geographically small countries. About half of all hourly solar power ramps are equal or close to zero because of zero production at night but the distribution has long and heavy tails with ramps reaching 18–25% of capacity per hour in most analyzed countries and up to 12–14% in the Nordic countries. The distribution of load gradients is skewed towards upward ramps, typically reaching extremes of 10–15% of peak load per hour in the analyzed European countries.

On the basis of the frequency and temporal distributions of variable generation ramps, the countries in Europe can be grouped into clusters which have similar wind and PV flexibility requirements in terms of ramp magnitude and frequency: North, Center and South. The load, wind and PV time series have a distinct ramp behavior whose daily and seasonal pattern is shown in Fig. 3.3 for three different European countries representing those clusters (North: Ireland, Center: Germany, South: Italy).

The first row depicts the hourly gradients of consumer load in each country. On a daily basis, the largest load ramps are the morning rise with a duration of 2–3 hours and a less prominent evening ramp up when lights and appliances are switched on at the same time. While some differences exist, the same basic load ramp structure appears in all European countries. Wind and solar power both follow a diurnal cycle. The middle row of Fig. 3.3 shows that although wind power generation is very volatile, it tends to decrease around sunrise and sunset, after which it tends to increase again. This pattern is most prominent in Germany and also other countries in Europe's center whereas countries in Scandinavia and the Southern peninsulas rarely experience large wind power ramps. In terms of frequency of large ramps, wind fluctuations pose the highest flexibility requirements in small Northern countries such as Ireland and Denmark. Regarding PV fluctuations, the frequency of large ramps clearly increases in the North-South direction.

3.3.2 One-hour Net Load Gradients

The unit commitment process is organized in hourly time periods in many power markets. The frequency and temporal distributions of hourly ramp rates are thus an important measure for short-term flexibility requirements of the power system. The impact of those ramps on system operation depends on whether they were forecasted or not. If they are predictable, even slower power plants can be started up early enough to be available exactly when the ramp occurs. However, accurateness of prediction is lower the day ahead and increases when temporally closer to the event [97]. Thus, the power system should be designed in a way to meet those 1-hour gradients by power plants that are already on-line or have a fast start-up (hydro, gas turbine). Alternative options like storage and DSM can also contribute here.

Even though countries in Europe have different resource potentials (Fig. 3.1) and wind and PV ramp properties (Fig. 3.3), the wind/PV mix has similar effects on the variability of net load. Fig. 3.3 shows this for the example countries Ireland, Germany

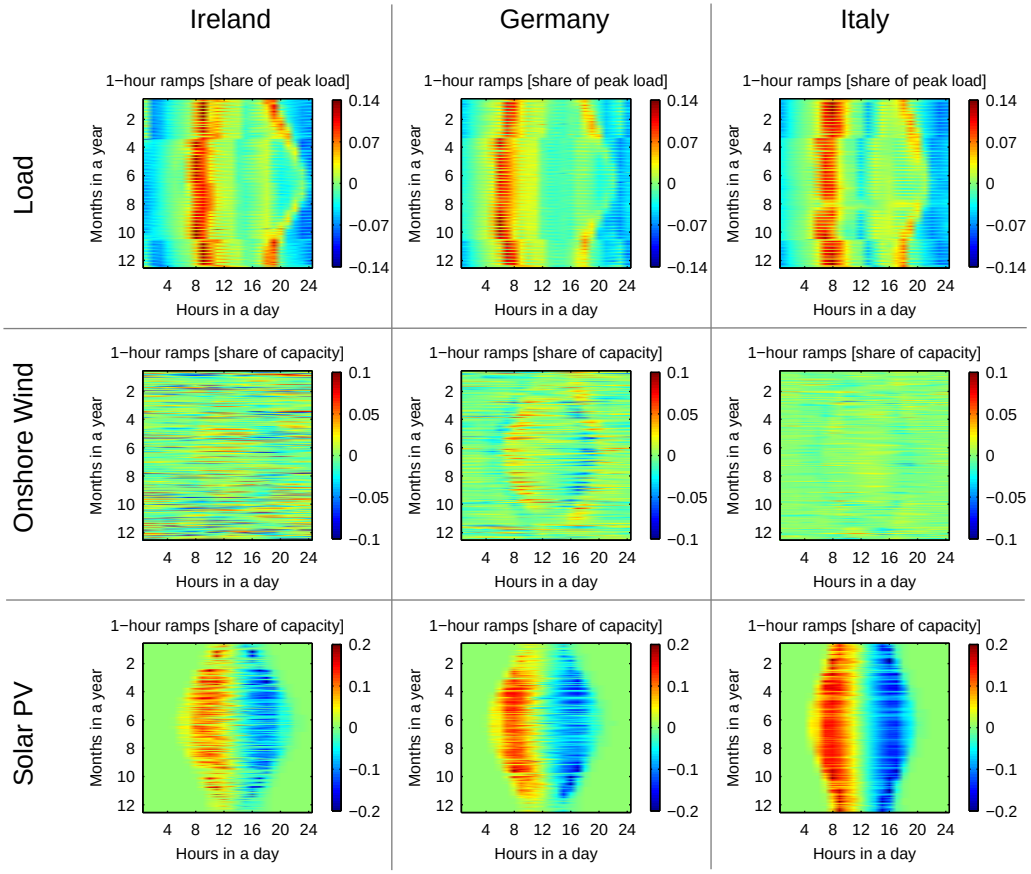

Figure 3.3: Temporal distribution of 1-hour ramps of load, wind and PV power in Ireland, Germany and Italy for the meteorological year 2011

and Italy, which differ considerably in terms of area as well as wind and PV FLH.

Fig. 3.4 shows the temporal distribution of the hourly net load ramps for those countries in the scenarios with renewable penetration $\alpha = 0.5$ and shares of PV in the VRE mix of $\beta \in \{0, 0.2, 0.4\}$. The plot shows that PV has a far stronger influence on the increase of hourly ramp rates than is the case for wind power. At the 100% wind mix, the hourly net load ramps are distributed randomly but are still mostly dominated by the load ramps. With an increase of PV to 20% ($\beta = 0.2$), the morning rise in load is compensated by PV power generation, which reduces ramps. However, this reduction in the frequency of large net load ramps in the morning is counteracted by an upward ramp pattern in the late afternoon when PV power production slows down and load increases at the same time. With 40% PV ($\beta = 0.4$), the ramps of PV power dominate the net load variability. The frequency of high net load ramps increases dramatically, with downward ramps in the morning and upward ramps in the evening. Ramps of magnitude higher than the morning load rise are maintained over 3–4 consecutive hours in each direction for a significant part of the year in all analyzed European countries.

As shown in Fig. 3.5 on the example of Germany, the frequency distributions of hourly net load gradients at $\alpha = 0.5$ are close for the mixes with high share of wind at $\beta = \{0, 0.2\}$ and this relationship holds for all analyzed countries. Compared to the

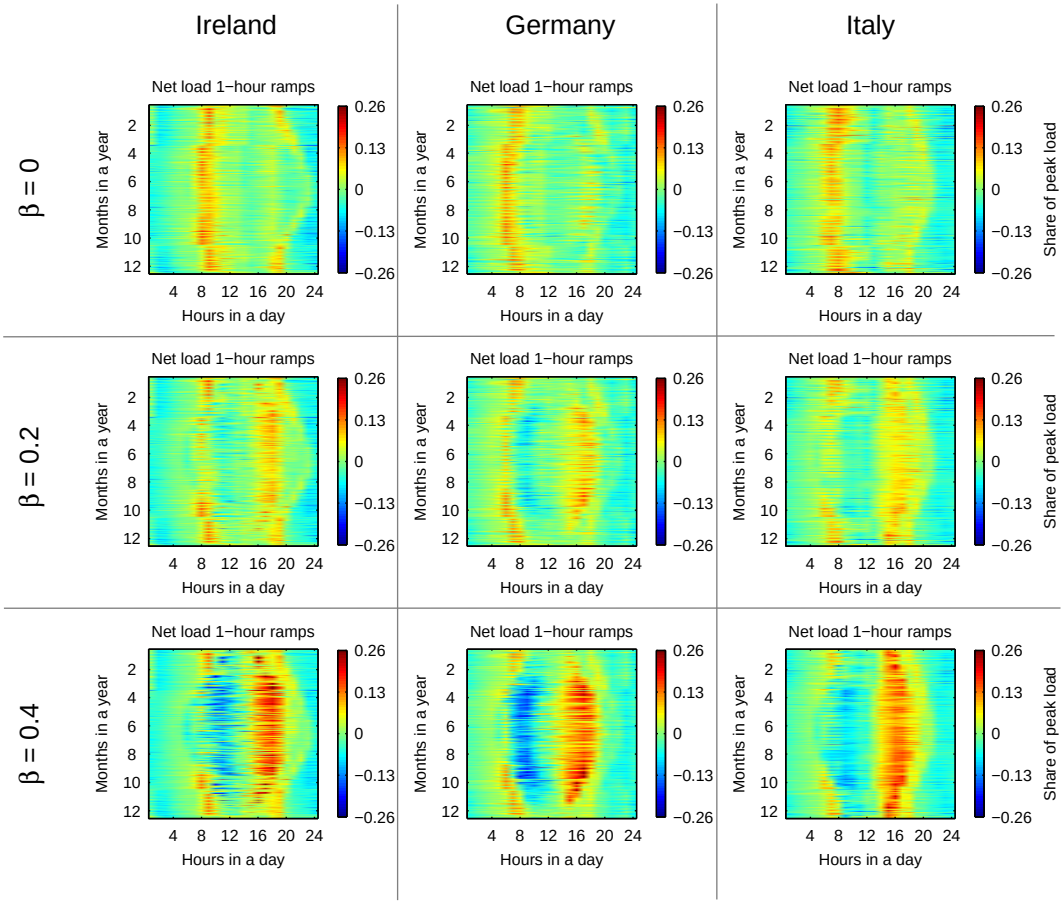

Figure 3.4: Temporal distribution of 1-hour net load ramps for different shares of PV in the wind/PV mix β at 50% penetration of variable renewables

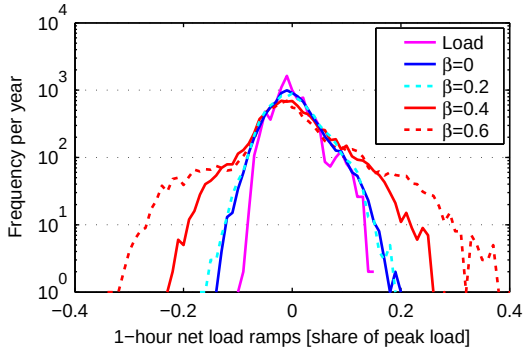

Figure 3.5: Frequency distribution of 1-hour net load ramps for different shares of PV in the wind/PV mix β at 50% variable generation penetration in Germany, 2011

load gradient, the frequency of ramps close to zero is reduced nearly by half. Up to a threshold share of 20% PV in the VRE mix (in some countries up to 30%) which is equivalent to 10–15% of annual consumption, the frequency distribution of net load ramps remains of similar shape as for a 100% wind mix. Adding more PV capacity to the system above this threshold results in a large increase in the frequency of high ramps. Depending on country area and full load hours, extreme net load ramps can occur also with high shares of wind in the system, which is analyzed in Section 3.4.

3.3.3 Multihour Net Load Gradients

The UC and ED process in power system operation requires considering more than just one hour. Many of the conventional power plants included in this process have flexibilities that require a planning period of up to 24 hours. The start-up times for coal power plants range up to 12 hours and for nuclear power plants even longer [183]. Even CCGT power plants, which are often considered as a flexible option, require up to 4 hours for a cold start [65]. Therefore, the ramping capabilities of the power plant fleet in a system over multiple hours are crucial for system integration of variable renewables. Net load ramp requirements over different time horizons determine the optimal portfolio of conventional power plants and other flexible resources. Portfolios can differ tremendously; few fast power plants can in certain circumstances provide the same flexibility as many slow plants [65].

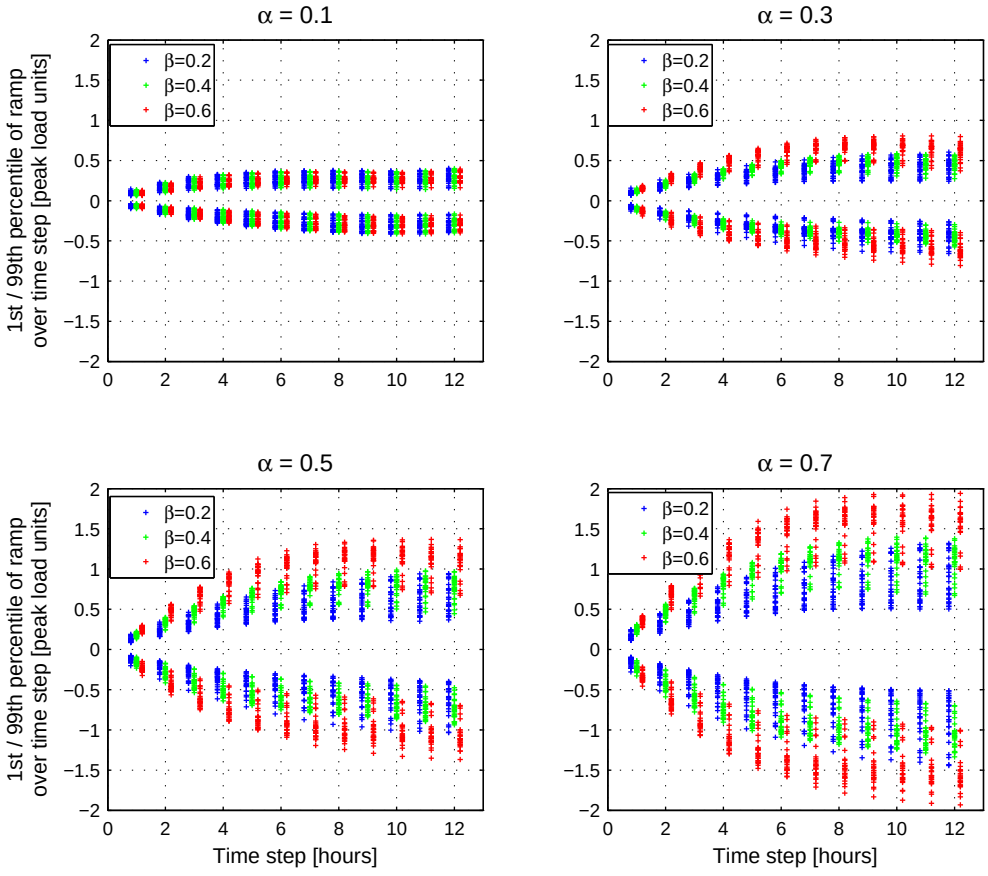

Figure 3.6: Ramp envelopes for 27 European countries for different variable generation penetrations α and shares of PV in the wind/PV mix β, 2011. Each plotted symbol represents one country.

A method to display and analyze the ramp requirements over multiple hours are ramp envelopes as introduced e.g. in [121]. Fig. 3.6 depicts ramp envelopes for the 27 European countries at levels of renewable penetration $\alpha \in \{0.1, 0.3, 0.5, 0.7\}$ and shares of PV power in the VRE mix $\beta \in \{0.2, 0.4, 0.6\}$. Depicted are the 1st and the 99th percentiles of gradients, which are crucial for future power system design: extreme

values will most probably not be predictable even shortly before occurrence and will thus be balanced by spinning reserves. This, however, is not the scope this research, but it seems reasonable that higher variability in net load will also lead to higher uncertainty and thus higher requirements for spinning reserves.

Several interesting observations which have implications for power system planning can be described from Fig. 3.6:

- At low penetrations of $\alpha = 0.1$, the gradient envelopes of all countries and all β are close; differences are rare. The major gradients might still come from variation in load. 1-hour gradients are in the region of 10% of peak load. Even at a time horizon of 6 hours, the ramps are all below 30% of peak load.
- Beginning with $\alpha = 0.3$, the ramps become significantly larger and mixes differentiate. Except for countries with very low wind FLHs, the ramp envelope is shifted outwards with increasing β.
- An important trend that becomes evident with higher shares of VRE ($\alpha = 0.5$ and $\alpha = 0.7$) is a clustering according to the three values of β. The differences arising from varying shares of PV power in the mix β tend to be larger than the differences between countries. At $\alpha = 0.5$, for each β-value, the differences in the 1-hour gradients between countries show a standard deviation of only 2–3% of peak load, whereas the difference in the mean value of all countries, for example between $\beta = 0.4$ and $\beta = 0.6$, is 18% to 26%.

Table 3.1 and Table 3.2 present the 1st and the 99th percentiles of the 1-hour and 6-hour net load gradients averaged across the 27 European countries for six different scenarios. The range and the standard deviations show the dispersion of values that the net load extremes can reach in different countries.

Table 3.1: 1-hour net load ramp rates – mean of all countries and their statistical dispersion

α	β	1-hour ramps [share of peak load]	
		99th percentile **mean** (min/max/stdev)	1st percentile **mean** (min/max/stdev)
0.3	0.2	**0.10** (0.07/0.16/0.02)	**-0.08** (-0.13/-0.05/0.02)
	0.4	**0.12** (0.09/0.15/0.02)	**-0.10** (-0.14/-0.07/0.02)
	0.6	**0.15** (0.12/0.19/0.02)	**-0.13** (-0.19/-0.08/0.02)
0.5	0.2	**0.13** (0.09/0.19/0.03)	**-0.11** (-0.20/-0.08/0.03)
	0.4	**0.18** (0.13/0.22/0.02)	**-0.16** (-0.23/-0.10/0.03)
	0.6	**0.26** (0.20/0.30/0.03)	**-0.23** (-0.32/-0.15/0.04)

Table 3.2: 6-hour net load ramp rates – mean of all countries and their statistical dispersion

α	β	6-hour ramps [share of peak load]	
		99th percentile **mean** (min/max/stdev)	1st percentile **mean** (min/max/stdev)
0.3	0.2	**0.34** (0.23/0.48/0.07)	**-0.34** (-0.52/-0.20/0.07)
	0.4	**0.44** (0.33/0.50/0.05)	**-0.36** (-0.44/-0.26/0.04)
	0.6	**0.62** (0.45/0.72/0.07)	**-0.50** (-0.62/-0.30/0.08)
0.5	0.2	**0.50** (0.34/0.73/0.12)	**-0.47** (-0.80/-0.30/0.13)
	0.4	**0.72** (0.51/0.84/0.09)	**-0.60** (-0.75/-0.37/0.11)
	0.6	**1.04** (0.71/1.23/0.14)	**-0.91** (-1.09/-0.55/0.15)

In a next step, two points on the envelope curves, the 1st and the 99th percentiles of the 6-hour ramps, are considered and depicted on the net load gradient duration curves in Fig. 3.7. On average, every second day a positive or a negative ramp occurs outside the 1st–99th percentile range whereas 2.4 ramping events per day occur on average outside the 5th–95th percentile range. Again, the differences between countries for one mix are smaller than the divergence caused by different mixes.

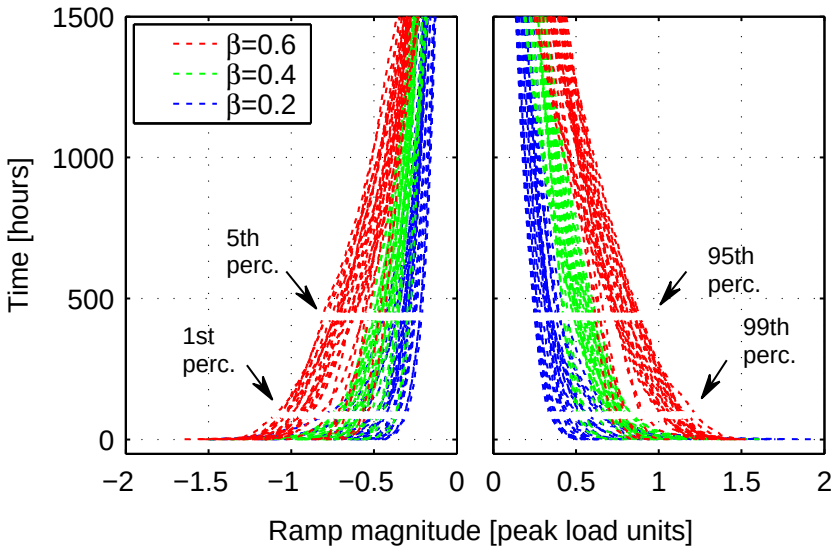

Figure 3.7: Top and bottom 1500 hours of the 6-hour net load ramp duration curves for 27 European countries at 50% share of variable renewables and different shares of PV in the wind/PV mix β

In a last analysis focusing on the influence of the wind/PV mix, Fig. 3.8 shows the 99th percentiles for the 1-hour and 6-hour net load gradients, again for Ireland, Germany and Italy. The first impression is that the images for the countries look similar supporting the finding that the mix is more important than the country analyzed. The maximum value is set to one for both time horizons. A net load ramp rate of one means that the whole conventional power plant park (including storage plants) has to ramp up in 1 or 6 hours. The figure illustrates that 1-hour ramps are moderate (less than 25% of

peak load) as long as α is below 0.3. From there on, the ramp rates start to increase dramatically, especially with β higher than 0.3. The behavior of Ireland and Germany is very similar whereas Italy shows lower gradients. For 6-hour ramps, a net load ramp of one is achieved with much lower α. Beginning with $\alpha = 0.3$ and high β above 0.5, the peak load has to be achieved within 6 hours. For PV shares β below 0.2, a much higher share of renewables can be integrated with lower 6-hour ramps.

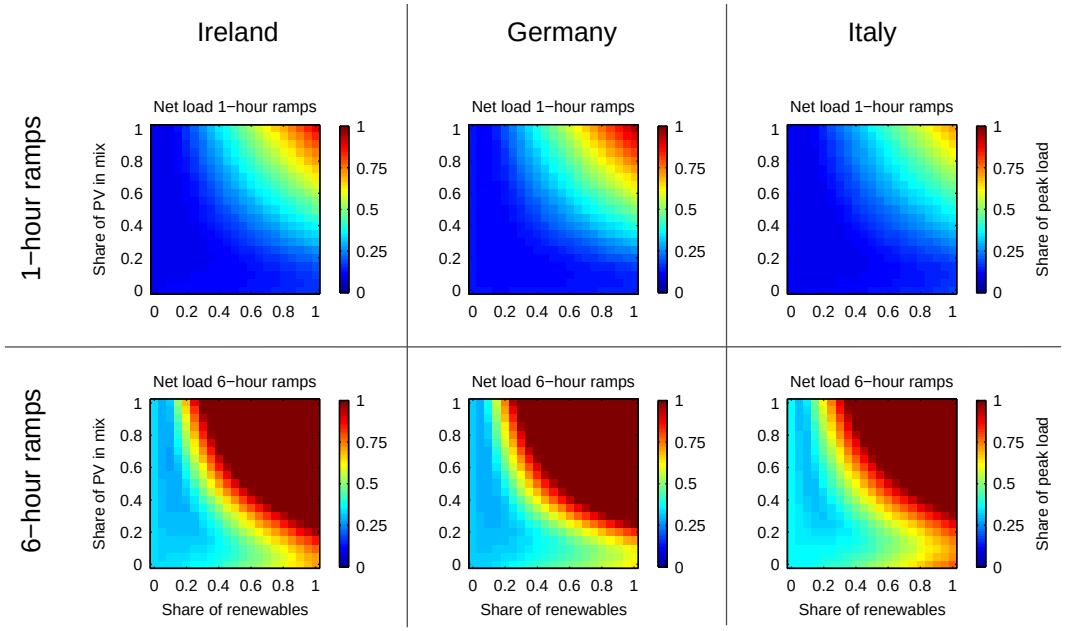

Figure 3.8: 99th percentiles of 1-hour and 6-hour net load ramps as a function of the variable Generation Penetration Level α and the Share of PV in the Wind/PV Mix β

The graphs in this section show the meteorological year 2011, however, the development of the envelope curve is the same for the years 2001 to 2011. Even if the ramp rates were surprisingly similar in the analyzed countries, differences remain. An attempt to explain them is conducted in the next section.

3.4 Why are Countries Different? – an Attempt to Explain Diversity

The standard deviation of all countries for the 1st and 99th percentiles of one-hour ramps proved to be low with 2–3% of peak load (Table 3.1). Still, there are several countries where ramps have greater deviations from the European mean (up to three times the standard deviation). This sections aims to identify region-specific factors with strong influence on the flexibility requirements arising from variable generation. The factors analyzed are system size and the regional wind and PV ramp characteristics as well as full load hours determined by geographic location.

The focus of the analysis lies on hourly net load gradients and look particularly at the highest and the 1st/99th percentiles of net load ramp occurrences because ramp behavior differs among countries the most in the extremes. Furthermore, hourly values

are of particular interest for system operation and scenarios with higher hourly ramps were also shown to feature higher ramps over multiple hour time horizons (see Fig. 3.6).

Fig. 3.9 plots three interpercentile ranges of the net load ramp distribution for each country against the chosen region-specific factors: the minimum–maximum range, the 1st–99th and the 5th–95th percentile ranges. Scenarios are shown with shares of PV in the mix $\beta \in \{0.2, 0.4, 0.6\}$ at combined VRE penetration $\alpha = 0.5$. To account for the interannual variability of wind and solar power, net load time series are simulated using wind and PV data for each of the meteorological years 2001–2011. The percentiles of the net load ramp time series are then calculated for each year and finally averaged over all years. Those percentiles are plotted in Fig. 3.9 against the average wind and PV full load hours over the same period.

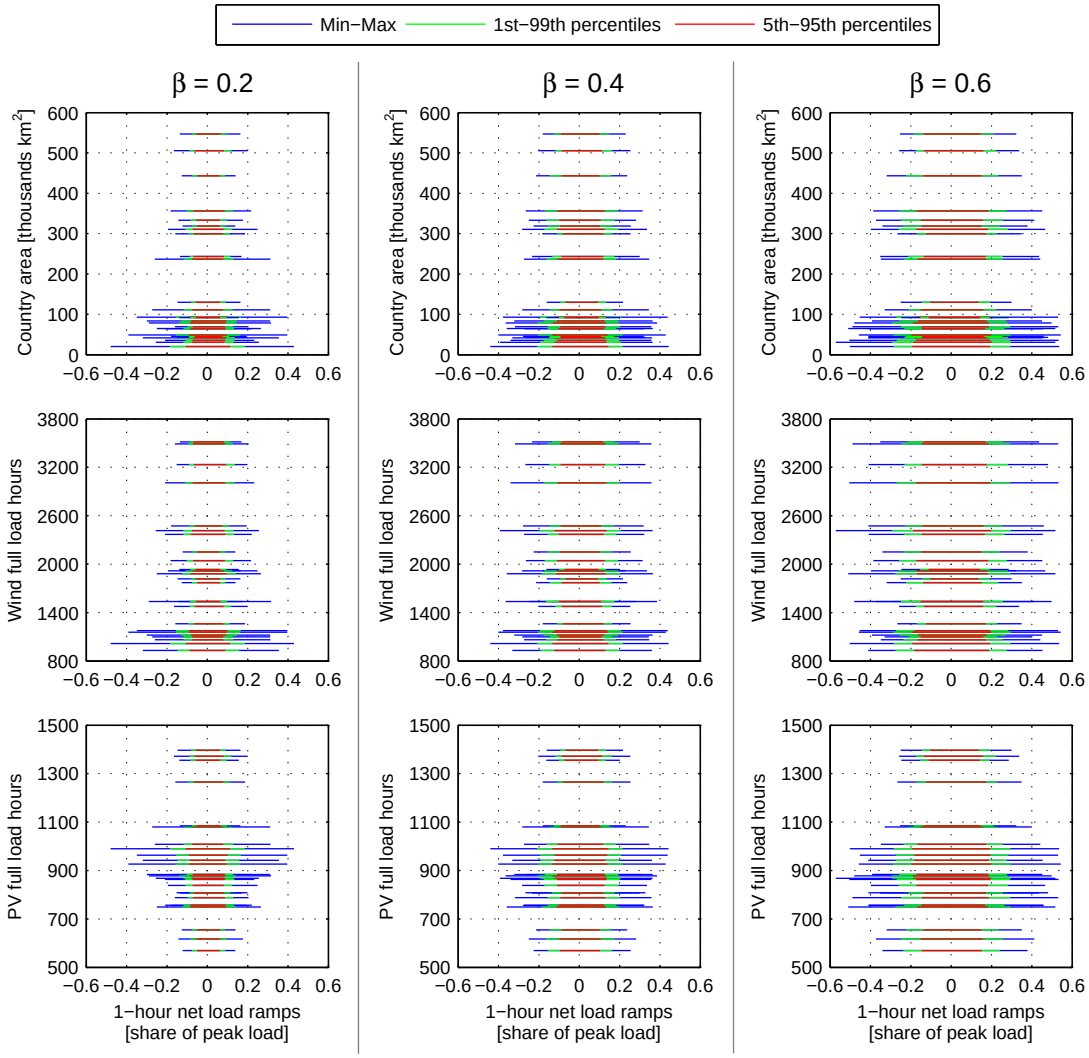

Figure 3.9: Three interpercentile ranges of 1-hour net load ramps for different shares of PV in the Wind/PV Mix β at 50% penetration of variable renewables

3.4.1 System Size

The first row of Fig. 3.9 shows the relationship between country area and the magnitude of extreme hourly net load ramps. The smoothing effect of geographical dispersion on wind power fluctuations is well-known [48, 100] and can be clearly observed in the wind power ramp rates in the model data used. Although the ramp behavior of small regions is highly heterogeneous, large countries experience 1.5 to 2 times less extreme net load ramps than smaller ones in the mix with 80% share of wind ($\beta = 0.2$). Examining the effect of country area on the PV ramp time series shows that the magnitude of extreme ramps is only slightly reduced through larger system size and has almost no influence on the range between the 5th and 95th percentiles. That is why the smoothing effect of a larger region becomes less pronounced with a higher share of PV in the energy mix. This analysis provides another important argument for increasing system size when wind power is deployed: it does not only reduce backup capacity requirements but also flexibility requirements.

3.4.2 Wind and PV Full Load Hours

The second influential factor to explain differences between countries is the resource availability in terms of FLHs from wind and PV. The second row in Fig. 3.9 shows the influence from wind FLH, the third row from PV. Regarding the influence of wind power, higher net load ramp extremes for lower FLH are observed, which can be explained by the fact that the same share of wind energy in electricity consumption requires more installed capacity in a region with low FLH. The required capacity rises especially steeply in countries with wind FLH below 1500 per year. The effect of capacity dominates over the ramp structure of wind power production, whose impact is in the opposite direction: wind power ramps reach higher extremes in countries with high wind FLH than in those with low FLH. No systematic variation is observed between net load ramps and wind FLH with higher shares of PV in the system as PV ramps are not related to wind resource availability.

Regarding the influence of PV FLHs, the third row of Fig. 3.9 shows that especially countries with medium FLH face high hourly net load ramp rates. This relationship holds both for systems with high wind and high PV shares in the mix and can be attributed to two effects in the same direction. First, it is partly not PV but wind power that causes the ramps: for all three interpercentile ranges the largest wind power ramps occur in countries with medium PV FLH between 900 and 1100 hours per year. This could be attributed to the stronger diurnal cycle of wind in Central Europe as shown in Fig. 3.3. In some countries such as Hungary and Slovakia, this effect is amplified by low wind FLH, which increase the requirements for installed wind capacity. Second, the PV ramp extremes are highest for countries with average PV FLH. In countries with higher PV FLH in the south of Europe, the impact of the lower PV capacities required dominates over the consistent increase in ramp extremes in the North-South direction. In Northern countries with low FLH the opposite is true – the effect of lower ramps inherent in the PV power structure outweighs the need for higher capacity.

3.5 Benefits from Cooperation

As shown in Fig. 3.9, larger geographical system size correlates with lower net load ramp extremes. This Section quantifies more precisely the reduction in flexibility requirements that can be achieved by interconnecting smaller regions into a large power system.

In order to illustrate potential effects, net load gradients in Saxony, Germany and Europe as a whole are compared (see Section 3.2.2 for the derivation of the net load for Europe). Saxony was chosen as it has wind and PV characteristics which are most similar to those of entire Germany. Fig. 3.9 showed that the gradient dependence on the region size is higher with larger shares of wind. It is mainly wind power extremes that can be reduced through leveling over regions. Thus, a mix with $\beta = 0.2$ is chosen for further analysis. Fig. 3.10 plots the hourly ramp duration curves at the three spatial scales. The effects from cooperation are tremendous, especially at the tails of the curves. At 50% wind and solar penetration, the maximum gradient is reduced from about 30% of peak load at the regional scale to 12% for interconnected Europe in the optimal case without transport restrictions. To what extent this ramp reduction potential will be exploited in the European system depends on the reduction of grid restrictions between countries and the integration of their electricity markets.

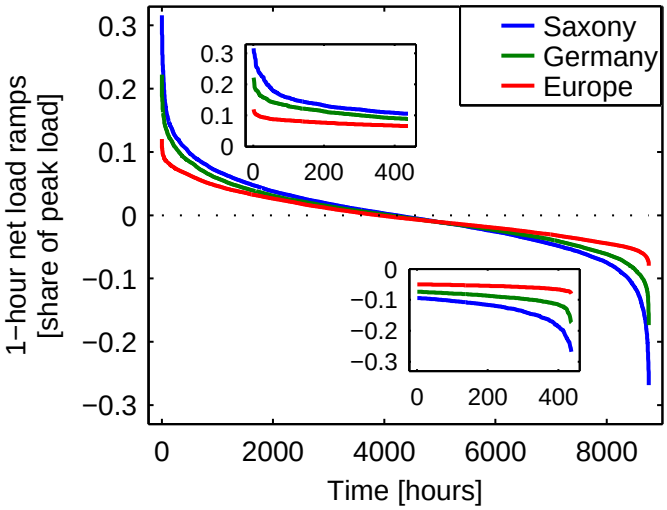

Figure 3.10: 1-hour net load ramp duration curves at the regional, country, and European scale at 50% share of renewables and 20% PV in the wind/PV mix for the meteorological year 2009

Having seen the benefits of cooperation in the 1-hour time horizon, multihour ramps are analyzed next. Fig. 3.11 compares the ramp envelopes for Saxony, Germany and Europe again in the scenario with $\alpha = 0.5$ and $\beta = 0.2$. The 1st/99th percentile envelopes contain 98% of all gradients in each time horizon. Scenarios are simulated with each of the meteorological years 2001 to 2010, the percentile values are calculated for each of those scenarios and then averaged (shown by the solid lines). The range over this period is represented by the gray-shaded area. This plot shows clearly that gradients over all time steps are much lower if power systems are operated cooperatively. Furthermore,

the variation between years (grey-shaded area) becomes smaller with larger systems. This allows for less uncertainty in the system planning period. The effect is similar for the maximum ramps of each duration.

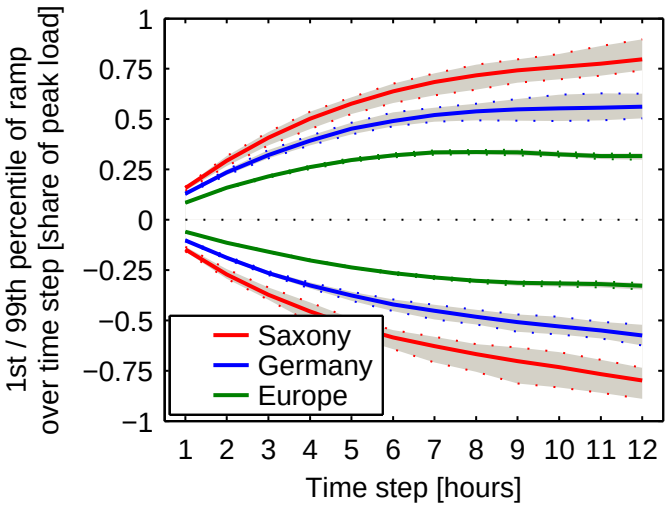

Figure 3.11: 1st/99th percentile ramp envelope at the regional, country, and European scale at 50% share of renewables and 20% PV in the Wind/PV mix; average values for the period 2001–2010 and their range

Requirements for the conventional power plants will decrease dramatically. These reductions in ramp rates will most probably lead to less start-ups and wearing of the remaining thermal power plants, which can reduce costs and emissions [118].

Fig. 3.12 shows the reduction of extreme hourly net load ramp rates (the minimum/-maximum and the 1st/99th percentiles) for the individual countries compared to the interconnected European system at 50% VRE penetration. The values are again averaged over scenarios for the years 2001–2010. As discussed before, small countries have the highest ramp rates and will consequently benefit the most from a powerfully interconnected European power system. The maximum hourly change of net load in the European system is 11% of the peak load whereas small countries face hourly ramp extremes of 30–50% of peak load, e.g. in Switzerland and Slovenia. Even large countries like Germany can reduce the maximum ramp from 20% to 11%. Only very few countries like the Nordic countries would not benefit substantially; the ramp rates in Norway and Sweden are only slightly higher than in a European system.

The analysis provides additional arguments in support of large-scale transcontinental power systems with strong transmission grids, besides the benefits of reducing backup energy needs [14]. In Czisch [48] or Huber et al. [106], a power system spanning Europe and North Africa is shown to be cost-effective, mainly because of wind power smoothing. Several studies propose even a global super-grid to efficiently integrate renewable power sources [2, 38]. Other authors focused on the very short term advantages of dispersing PV power generation [145]. The results in this thesis show advantages of cooperation in the timescale of 1–12 hours between the very long-term horizon, concerned with capacity adequacy, and the short-term scales.

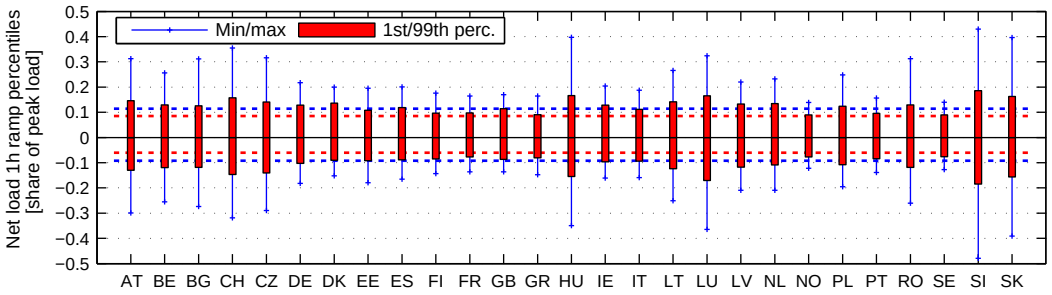

Figure 3.12: Boxplot with 1-hour net load ramp extremes for individual countries (solid lines/bars) and Europe (horizontal dashed lines) at 50% share of renewables and 20% PV in the Wind/PV mix

3.6 Conclusion and Outlook

This chapter presented an analysis of time series of load, wind, PV and the resulting net load in scenarios for Europe that allow to quantify flexibility requirements in future power systems with high shares of variable generation. The analysis focused on deterministic flexibility needs at the temporal scale of 1–12 hours. This time frame is important for the UC and ED process in power system operation. Since the regional scope of the analysis is Europe, results might depend on its particular climate and weather situation.

Increasing wind and solar power generation above a 30% share in annual electricity consumption will dramatically increase flexibility requirements. Especially, large PV contributions of more than 20–30% in the wind/PV mix will foster this trend. In scenarios about future net load, the penetration level of wind and PV as well as their mix affect most European countries in a similar way. Still, differences between countries exist which can to some extent be explained by country size as well as by the annual wind and PV full load hours. In scenarios with high wind penetration, larger systems tend to face lower ramps. For example, at 50% variable generation, the most extreme hourly net load ramp drops from 30% of peak load at the regional level to 22% for a large country and 11% for an interconnected Europe. Balancing larger, well-interconnected power systems can thus reduce ramp requirements substantially. This allows for advantages to be realized from cooperation among countries in Europe.

In summary, the research suggests that the future flexibility requirements in power systems in Europe will depend on three major parameters: the share of variable renewables, their mix and the balancing area size. Accommodating high shares of wind and solar power will require that manufacturers develop more flexible components for power systems. System operators will have to fit their system to the upcoming renewable installations. Incentives for highly flexible power plants, storage as well as demand-side response will be beneficial for the system. The results also provide further arguments for aiming at transnational solutions as the most efficient way for large-scale integration of renewable power sources.

Part II

Modeling

Chapter 4

Unit Commitment and Load Flow Modeling

Setting up a modeling framework is crucial for the evaluation of concepts for future power systems. In this chapter, the applied methodology is described and new developments that improve state-of-the-art modeling are highlighted. Before starting with the actual modeling framework, some preliminaries on the basic market environment considered and the main ideas of the mixed-integer (linear) programming (MIP) approach are given. A major part of this Chapter presents joint work with Matthias Silbernagl and René Brandenberg (i.e. Sections 4.3.4, 4.4, 4.5 [185], and Section 4.6 [111]).

4.1 Modeling Operation with Perfect Market Assumption

In this thesis, a perfect market is assumed, which means that all power plants in Germany/Europe or the considered model region are operated with the goal of cost-minimization. Possible sub-optimal solutions arising from monopolies and information asymmetry (e.g. [137, 214]) are neglected in this framework. Still, the unit commitment models that are developed in the course of this thesis can be applied for a utility that has to plan its power plant operations as well. This explicitly includes strategic behavior and decision-making under uncertainty as long as power plant modeling and optimization is required. When being applied by an utility, the improved accuracy of the model approach might even be more important; model features can be exploited more effectively when data availability on power plant technology is better and when less power plants have to be considered.

In this thesis, the focus lies on evaluating flexibility components within large power systems, i.e. the German and the European power system. All results achieved might be an outcome of a stylized ideal market where a central planner optimizes plant behavior. In Europe, that is not the case as there are several market zones, and a harmonized European market is planned and worked on but not yet achieved [11, 156]. In contrast, several ISOs (Independent System Operators) in the US and in other world

regions have a central planning of operations including power plant scheduling and grid management [98]. The modeling approach in this thesis can be interpreted as the complete European Power system being operated by one ISO with all rights on infrastructure operation from unit commitment to reserve scheduling. Results will reveal what is possible from a technical point of view after all regulatory and political obstacles are overcome.

4.2 Mixed-Integer Programming as Basic Approach

The operational planning of (hydro-)thermal power systems is well known as the unit commitment and economic dispatch problem (see e.g. Baldick [6]). Finding cost-optimal solutions to this problem has been an active field of research since almost the beginning of electrification [114], and a huge variety of optimization approaches have been applied (see e.g. Sheble et al [184] or Padhy [161] for a literature overview). In the last decade, mixed-integer programming (MIP) (or more specific mixed-integer linear programming), which was applied to the UC problem in the 1960s for the first time [78], has replaced Lagrangian relaxation to become the major technique applied in industry. For example, the largest wholesale electricity market PJM changed over to MIP in 2005 [160].

The basic formulation of an MIP can be expressed with an integer variable $\boldsymbol{x}$ and a real variable $\boldsymbol{y}$ by:

$$\begin{aligned} \min_{x,y} \boldsymbol{c}^T\boldsymbol{x} + \boldsymbol{b}^T\boldsymbol{y}, \qquad \text{s.t.} \quad & \boldsymbol{x} \in \mathbb{Z}, \qquad \boldsymbol{y} \in \mathbb{R} \\ & \boldsymbol{A}\begin{bmatrix}\boldsymbol{x}\\ \boldsymbol{y}\end{bmatrix} \leq \boldsymbol{B} \\ & \boldsymbol{x} \geq 0 \\ & \boldsymbol{y} \geq 0 \end{aligned} \tag{4.1}$$

Mixed-Integer linear programming (MILP) can be seen as a special case of the more general MIP. In the latter, also non-linear terms would be allowed while MILP is constraint to linear equations. For the models described in this thesis, mostly MILP is employed and, more specifically, the models are formulated as binary problem. Power plants can be either on-line or switched off which is represented by $\boldsymbol{x} \in \{0, 1\}$ instead of $\boldsymbol{x} \in \mathbb{Z}$. In the following, all integer approaches are referred to as the most general MIP and specification are given when necessary. A special case being used for some illustrations and explanations later on is pure IP (integer programming). These problems only consist of integer variables without any linear variables, i.e. only the first part of equation (4.1) is considered.

The main advantage of MIP over other approaches for solving integer problems is its ability to provide guarantees on the optimality gap / degree of optimality that accompanies the achieved solutions. A prevalent employed approach for solving MIPs is branch and cut, constituting a combination of branch and bound and cutting plane

methods, whose basic ideas are described below in Section 4.2.1. The main drawbacks of the approach are the restricted modeling flexibility and the high computational efforts required. Both issues have been mitigated by new UC formulations, faster solvers, and greater computational power; still, further progress is vital. The approach described in this thesis contributes by further improving the formulation of an important part of the UC model: the start-up costs.

An MIP formulation of the unit commitment problem that is currently widely used in academic research was published in 2006 by Carrión and Arroyo [37]. Based on this formulation, progress in several areas of development have been made in past years, including amongst others: an application to the self scheduling problem with a more accurate start-up process [186], attempts to tighten the quadratic production costs function [76, 205, 212], a more efficient formulation for start-up and shut-down ramping [149], and a formulation with three instead of one binary variable per unit which showed to be more efficient in many cases [150]. Recently, new research is focusing again on a more accurate and efficient formulation of start-up costs, e.g, see Tuffaha and Gravdahl [199], showing the relevance of the topic.

4.2.1 Quality of MIP Formulation and Solution Algorithms

The number of algorithmic steps to find the optimal solution of an MIP problem can, in the worst case, be exponential with the number of binary variables n, leading to 2^n possible combinations. In unit commitment, there is basically one binary variable per modeled period $t \in \mathcal{T}$ and power plant $n \in \mathcal{N}$ leading to a problem size of $\mathcal{O}(2^{|\mathcal{N}||\mathcal{T}|})$. To give an idea of the problem size considered within this thesis: more than 1000 individual plants are included in the European dataset and 36 hours are to be computed in the day ahead planning. Computational efficiency is hence an important premise when solving UC models with large-scale datasets. An important criteria for the effectiveness of an MIP model formulation is the so-called "integrality gap". This gap is the relative difference between the optimal MIP solution Z_{MIP} and the solution of the relaxed linear program (LP) given as Z_{LP}, leading to

$$\text{INTgap} = \frac{Z_{\text{MIP}} - Z_{\text{LP}}}{Z_{\text{MIP}}}. \tag{4.2}$$

The relaxed MIP can be interpreted as a problem where $x \in \mathbb{Z}$ is replaced by $x \in \mathbb{R}$ in equation (4.1); all other constraints of the problem are kept at status quo.

Fig. 4.1 provides a simplified illustration of the integrality gap and compares two different formulations. The grid points are the possible values of the two integer variables x_1 and x_2. The region described by the linear inequalities is marked in orange and feasible solutions are marked in blue while all other values of the variables which lie outside the orange region are marked in gray. In the left figure, the difference between the integer optimal solution Z_{MIP} and the solution of the relaxed problem Z_{LP} is higher than in the example in the right one. The model formulation illustrated by the right figure has a smaller integrality gap and solving might eventually be easier (see description of algorithms below).

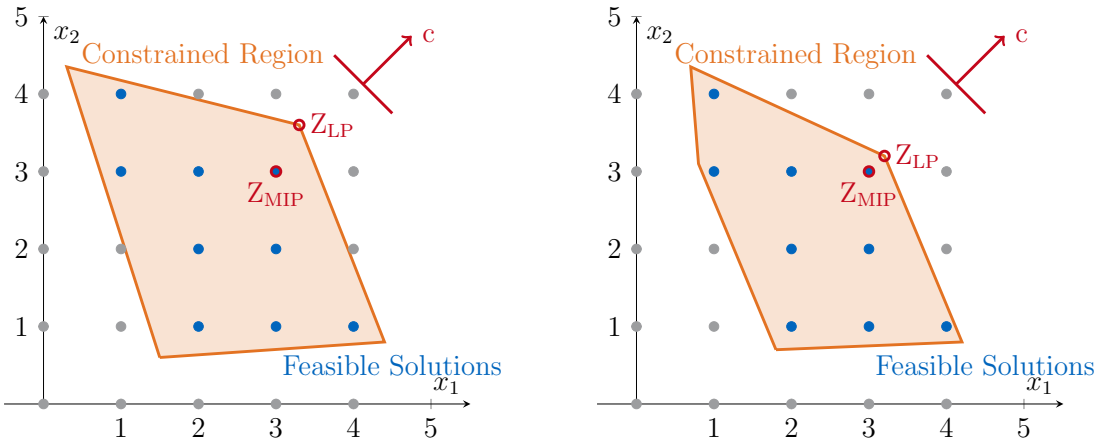

Figure 4.1: Illustration of the integrality gap. The formulation of constraints on the right figure has a lower integrality gap then the formulation depicted on the left.

Solution Algorithms Two algorithms are predominant at present: the cutting plane algorithm and the branch and bound algorithm. Those two approaches are combined in the so-called branch and cut algorithm that is used for solving the MIPs within this thesis. A very short and illustrative explanation is presented below which is based on the illustration in Fig. 4.2 for the cutting plane and Fig. 4.3 for the branch and bound algorithm. Both show the solution finding process for the MIP model which is displayed in Fig. 4.1 on the left. The major idea of both approaches is to reduce the integrality gap of the initial problem. The remaining gap during this process is called the (relative) MIP gap which is in the case of CPLEX defined by [77]:

$$\text{MIPgap} = \frac{|\text{bestbound} - \text{bestinteger}|}{1e^{-10} + \text{bestinteger}}, \tag{4.3}$$

with "bestbound" being the best current solution of the linear relaxation and "bestinteger" the best solution that has been found so far.

Cutting Plane Algorithm Starting with the cutting plane algorithm, the idea of the algorithmic procedure lies in adding additional constraints to the original problem (so-called "cuts"). These additional constraints will then reduce the feasible region of the problem and bring the LP solution closer to the MIP solution. The MIP solutions have to be found by heuristics and whenever the MIP gap is below a given limit (MIP-tolerance), the solution is considered optimal. An illustration of the procedure of adding cuts is given by the sequence in Fig. 4.2.

There are different strategies for finding cuts including both user specific cuts which require problem specific knowledge and general purpose cuts. Gomory [83] was the first to introduce a cutting plane algorithm for solving general integer problems; a short summary of the idea is given in the following.

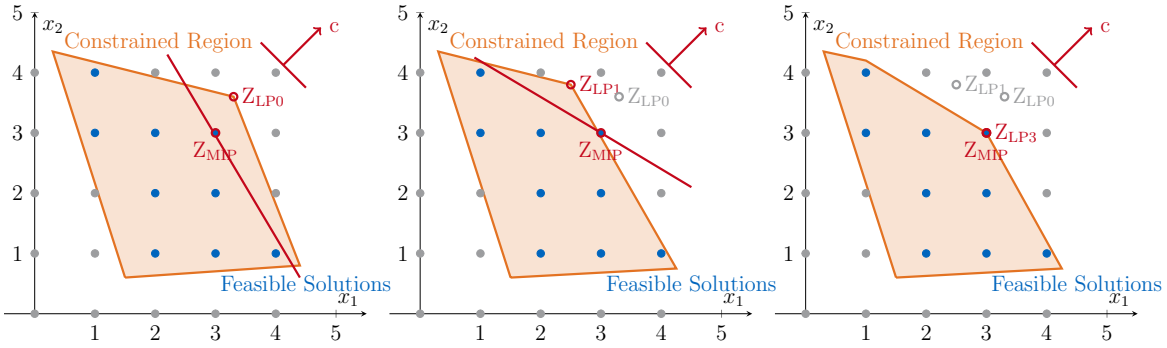

Figure 4.2: Illustration of cutting plane method. Own illustration inspired by a talk of Morales-España [148].

The starting point for the algorithm is the final simplex tableau of the relaxed problem which could in general form be described as [44]:

$$x_i + \sum_{j \in \mathcal{N}} \bar{a}_{i,j} s_j = \bar{b}_i, \tag{4.4}$$

with x_i being a basic variable, s_j the nonbasic variables, and $a_{i,j}$ the fractional coefficients (for details on simplex see e.g. Bazaraa et al. [12]). In order to depict the basic idea of how Gomory cuts are constructed, a simple numerical example is taken here [24] with $i = 1, \bar{a}_1 = \frac{9}{4}, \bar{a}_2 = 14$, and $\bar{b}_1 = \frac{9}{4}$:

$$x_1 + \frac{9}{4} s_1 - \frac{1}{4} s_2 = \frac{9}{4}. \tag{4.5}$$

The steps for constructing a Gomory cut are the same for the general formulation, however, this simple numerical example is more illustrative. In a first step, fractional and integer values are separated, leading to

$$x_1 + \left(2 + \frac{1}{4}\right) s_1 - \left(1 - \frac{3}{4}\right) s_2 = 2 + \frac{1}{4}. \tag{4.6}$$

Bringing all fractional values to the right hand side gives

$$x_1 + 2s_1 - 1s_2 - 2 = -\frac{1}{4} s_1 - \frac{3}{4} s_2 + \frac{1}{4}. \tag{4.7}$$

As all variables are integer and as $s_1, s_2 \geq 0$, it follows that:

$$-\frac{1}{4} s_1 - \frac{3}{4} s_2 + \frac{1}{4} \leq \frac{1}{4}. \tag{4.8}$$

As the the left hand side of equation (4.7) is integer, the additional constraint (the Gomory cut) can be defined to

$$-\frac{1}{4} s_1 - \frac{3}{4} s_2 + \frac{1}{4} \leq 0. \tag{4.9}$$

Branch and Bound Algorithm The branch and bound method is more complicated to be described. The method is based on dividing the original problem in several steps as depicted by the illustrative sequence in Fig. 4.3. The first LP solution of the original problem lies in between 3 and 4 for both x_1 and x_2. In a first step, the problem is divided according to variable x_2 and LP solutions are computed (LP "bounding"): in one subproblem, x_2 is set to be lower or equal than 3 ($x_2 \leq 3$) which leads to the solution Z_{LP1}. In the other subproblem, x_2 has to be larger or equal than 4 ($x_2 \geq 4$) and the solution obtained is Z_{LP2}. The solutions are then compared and Z_{LP1} is found to be the better one. In a next step, the subproblem with the better solution is further divided ("branched"), this time according the x_1 variable. Setting $x_1 \leq 3$ and setting $x_1 \geq 4$ leads to the solutions Z_{LP1*} and Z_{LP3}, where Z_{LP1*} is proved to be an optimal solution of the MIP problem. An illustrative example of the same style with given numbers can be found in Conforti et al. [44].

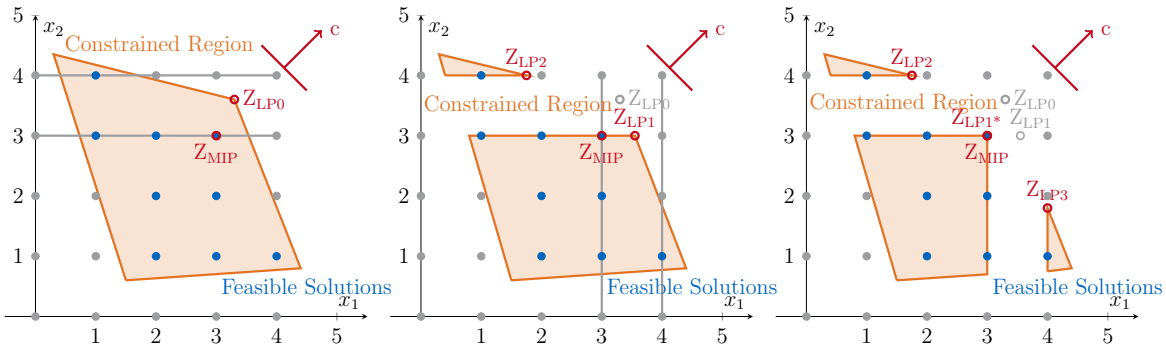

Figure 4.3: Illustration of branch and bound method. Own illustration inspired by a talk of Morales-España [148].

It has to be noted that those descriptions and illustrations are very simplified and only provided to give a basic idea about solution procedures and a reason why some formulations of the same MIP might be easier to solve than others. In the case of unit commitment modeling as described in this thesis, the variables are binary, which is a special case of an integer variable. They can only have the value 0 or 1. Branching thus means setting the values to either 0 or 1. The UC problems for realistic test cases have a tremendous amounts of variables which leads to high dimensional polytopes that cannot be illustrated.

4.2.2 Literature Review on Modeling Approaches

A widely used unit commitment model was presented by Carrión and Arroyo [37], describing a formulation of the start-up costs based on Nowak and Römisch [158]. Since then, numerous advancements have been published. The list here is restricted to mentioning only those with a relevant focus. The start-up types introduced by Muckstadt and Wilson [153] are enhanced by Simoglou et al. [186] to model the start-up process, including synchronization times, soak times, and power trajectories. Even when disregarding the start-up process, these start-up types lead to tighter formulations of the start-up costs (see Morales-España et al. [150]).

Tighter UC formulations have been of interest in general. Lee et al. [135] consider minimal up- and down-time constraints and prove that the feasible operational schedules can be described by $\mathcal{O}(2^T|\mathcal{I}|)$ inequalities. By using start-up and shut-down status variables, Rajan and Takriti [175] characterize the same feasible set with $\mathcal{O}(|\mathcal{I}|T)$ inequalities—an example of how representations of polytopes may be simplified by introducing additional variables.

The quadratic production costs have commonly been modeled by piecewise linear approximations. Frangioni et al. [76] present tight valid inequalities for such costs, enabling an iterative approximation scheme. A similar approximation scheme with different valid inequalities is given in [205]. Finally, Ostrowski et al. [159] improves solution times by using valid inequalities for the ramping process.

4.3 State-of-the-Art UC Models

This section describes the basics of the two prevalent MIP models in recent publications: the approach of Carrión and Arroyo [37] with one binary variable per unit and period ("1-Bin") as well as the approach with three binaries ("3-Bin") according to Ostrowski et al. [159], which were proved to model start-up costs more efficiently by Morales-España et al. [150].

4.3.1 Base Model

The goal of the UC problem is to fulfill the electricity demand D^t in each period t by power generation p_i^t from power plants i at minimal cost. The costs comprise two parts: production costs cp_i^t and start-up costs cu_i^t. Using the production costs cp_i^t and the start-up costs cu_i^t, the UC problem may be modeled as

$$\min \sum_{i\in\mathcal{I},t\in\mathcal{T}} cp_i^t + cu_i^t, \quad \text{s.t.} \tag{4.10}$$

$$\sum_{i\in\mathcal{I}} p_i^t = D^t \qquad \forall\, t \in \mathcal{T}. \tag{4.11}$$

The start-up costs are discussed separately in Section 4.3.3. The production costs are non-convex [93, 165] and approximated by a piecewise linear function of Carrión and Arroyo [37]. In this thesis, simple linear production costs, as described by Morales-España [150], are used. The costs depend linearly on the binary operational state v_i^t and the production p_i^t with the parameter A_i for the fixed part and B_i for the linearly increasing part:

$$cp_i^t = A_i v_i^t + B_i p_i^t \qquad \forall\, i \in \mathcal{I}, t \in \mathcal{T}. \tag{4.12}$$

The fixed part of the productions costs A_i is also referred to as no-load cost and leads to lower efficiency in part-load operation (see next Section for details).

Generally used constraints of thermal power plants regard the minimal production $P_i^{\min}$, the maximal production $P_i^{\max}$, maximal up and down ramping speeds RU_i and RD_i as

well as maximal ramping at start-up SU_i and shut-down SD_i. The production limits are formulated with the power plant state v_i^t as

$$P_i^{\min} v_i^t \leq p_i^t \leq P_i^{\max} v_i^t \qquad \forall\, i \in I, t \in \mathcal{T}. \tag{4.13}$$

Ramping constraints can then be formulated according to Carrión and Arroyo [37] by:

$$p_i^t \leq p_i^{t-1} + RU_i v_i^{t-1} + SU_i(v_i^t - v_i^{t-1}) + P_i^{\max}(1 - v_i^t) \;\; \forall\, i \in \mathcal{I}, t \in [2\,..\,T], \tag{4.14}$$

$$p_i^t \geq p_i^{t-1} - RD_i v_i^t - SD_i(v_i^{t-1} - v_i^t) - P_i^{\max}(1 - v_i^{t-1}) \;\; \forall\, i \in \mathcal{I}, t \in [2\,..\,T], \tag{4.15}$$

$$p_i^t \leq P_i^{\max} v_i^{t+1} + SD_i(v_i^t - v_i^{t+1}) \quad \forall\, i \in \mathcal{I}, t \in [1\,..\,T{-}1]. \tag{4.16}$$

The last term of equation 4.14 guarantees that p_i^t remains positive when power plants are shut down ($v_i^t - v_i^{t-1} = -1$). The last term of equation 4.15 prevents influences on the start-up process from the equation constraining shut-down speed.

Options to tighten the ramping constraints are described by Ostrowski et al. [159], where the interested reader is referred to. Those tightened constraints are only used in the numerical example to support the efficiency of the temperature model but not in the large-scale numerical simulations of Section 7.

In many unit commitment formulations, minimum up and downtimes are modeled. The following constraints as developed by Rajan et al. [175] are used for the extended model in the numerical test cases of this Section:

$$\sum_{k=t-UT_i+1}^{t} y_i^k \leq v_i^t \qquad \forall\, i \in \mathcal{I}, t \in [UT_i\,..\,T], \tag{4.17}$$

$$\sum_{k=t-DT_i+1}^{t} z_i^k \leq 1 - v_i^t \qquad \forall\, i \in \mathcal{I}, t \in [DT_i\,..\,T], \tag{4.18}$$

with y_i^t being the start-up indicator, z_i^t the shut-down indicator, UT_i the minimum uptime and DT_i the minimum downtime.

In the large-scale numerical simulation of Chapter 7, however, minimum up and downtimes are not considered. From a technical point of view, minimum downtimes are only very short and mostly below one hour, representing the time that is required to aerate the turbines. A technical report prepared by The Union of the Electricity Industry (Eureletric) [68] reports the minimum downtime of all conventional power plants to be non-existent supporting the approach of neglecting them. Minimum uptimes can also hardly be explained by technical constraints since power plants must be able to shut down in emergency cases anytime. Kirschen and Strbac [122] argue for minimum uptimes with a limitation of damage that is caused by frequent start-ups. However, this is mainly an economic argument and gives reason to neglect the constraint whenever start-up costs are modeled appropriately.

4.3.2 Modeling Part Load Efficiencies

The linear production costs as described above in equation (4.12) automatically model an important property of thermal power plants: lower efficiencies in part load. While

being a linear equation, the offset by the so called "no-load costs" represented with A_i is proportionally lower with a higher power output and, in turn, fuel efficiency increases. In Fig. 4.4 on the left, the costs or fuel inputs are illustrated as a function of electricity output. When calculating the efficiency η as the ratio of output p to fuel input, the result is a concave function as illustrated in Fig 4.4 on the right.

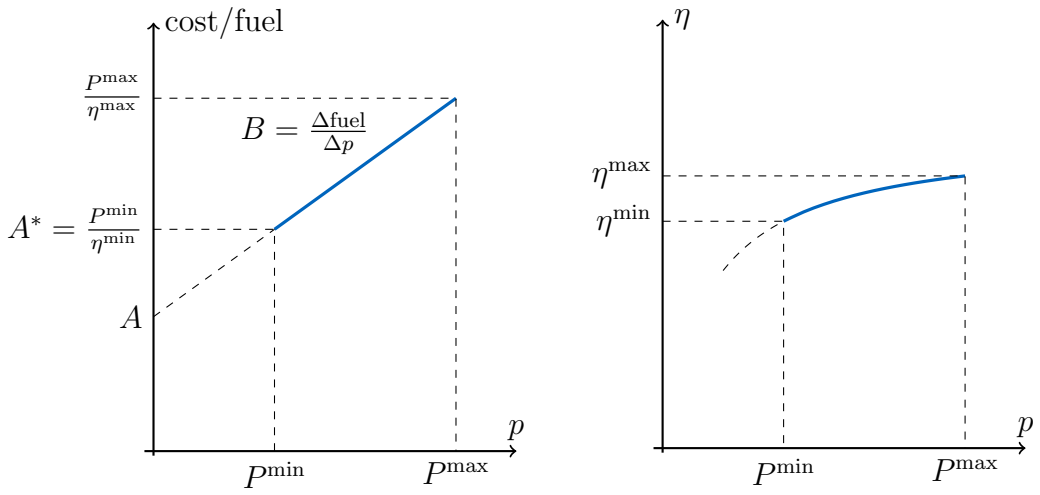

Figure 4.4: Visualization of the cost function and reduced efficiency in part load. The power plant considered here has a minimum production of 40%, a minimal efficiency of 50% and a maximal efficiency of 60%.

The two parameters A_i and B_i for each power plan i can be computed from the efficiency at minimal load $\eta^{\min}$, the efficiency at maximal load $\eta^{\max}$, and the minimal power output $P^{\min}$ by

$$\text{cost/fuel} = \frac{P^{\min}}{\eta^{\min}} + (p - P^{\min}) \cdot \frac{\left(\frac{P^{\max}}{\eta^{\max}} - \frac{P^{\min}}{\eta^{\min}}\right)}{(P^{\max} - P^{\min})}. \tag{4.19}$$

This equation can be reformulated to equation (4.12) by defining A and B as

$$A^* = \frac{P^{\min}}{\eta^{\min}}, \quad B = \frac{\left(\frac{P^{\max}}{\eta^{\max}} - \frac{P^{\min}}{\eta^{\min}}\right)}{(P^{\max} - P^{\min})}, \rightarrow \quad A = A^* - P^{\min} B. \tag{4.20}$$

4.3.3 Start-up Costs

A special focus and the main area of improvements presented in this thesis is the modeling of start-up costs. The start-up costs K_i^l depend on the amount of time l that a unit has been off-line before a start-up, and on the heat-loss coefficient λ_i. For thermal power plants, they are typically modeled according to Wood et al. [211] and Spliethoff [188] as

$$K_i^l = V_i(1 - \mathrm{e}^{-\lambda_i l}) + F_i \quad \forall\, i \in \mathcal{I}, l \in \mathbb{N}, \tag{4.21}$$

where F_i are the fixed start-up costs and V_i are the maximum variable start-up costs, such that the costs for a complete cold start are $V_i + F_i$. The fixed costs include labor

costs as well as time-independent wear-and-tear costs. As the modeled time range is discretized into periods, only integer off-line times $l \in \mathbb{N}$ may occur. An illustration of the start-up costs is given in Fig. 4.5 below.

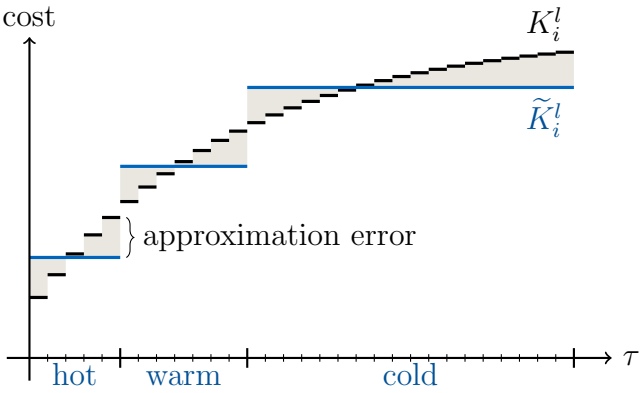

Figure 4.5: Time-dependent start-up costs K_i^l and a three-step approximation $\widetilde{K}_i^l$.

Formulation with one binary variable ("1-Bin") The cost function is modeled by an increasing step function, i.e. a piecewise constant, increasing function (see Fig. 4.5). According to Carrión and Arroyo [37] or Nowak and Römisch [158], this can be formulated with the power plant state v_i^t at time t and preceding time steps l as well as the offtime dependent start-up costs K_i^l as

$$cu_i^t \geq K_i^l \Big(v_i^t - \sum_{n=1}^{l} v_i^{t-n} \Big) \quad \forall\, i \in \mathcal{I}, t \in \mathcal{T}, l \in [1\,..\,t{-}1] \text{ with } K_i^l > K_i^{l-1}. \tag{4.22}$$

Formulation with three binary variables ("3-Bin") Simoglou et al. [186] and Morales-España et al. [150] show that by using the start-up status y_i^t, the shut-down status z_i^t, and the previous downtime PD_i as described by Garver [78],

$$y_i^1 - z_i^1 = \begin{cases} v_i^1 & \text{if } PD_i > 0, \\ v_i^1 - 1 & \text{else,} \end{cases} \quad \forall\, i \in \mathcal{I}, \tag{4.23}$$

$$y_i^t - z_i^t = v_i^t - v_i^{t-1} \quad \forall\, i \in \mathcal{I}, t \in [2\,..\,T], \tag{4.24}$$

the start-up costs may be modeled computationally more efficient than by using solely v_i^t as in 1-Bin. To this end, for each unit i, the off-times $[1\,..\,T{-}1]$ are grouped by their start-up costs into a minimal number E_i of intervals $L_i^1 \dot\cup \ldots \dot\cup L_i^{E_i} = [1\,..\,T{-}1]$ with

$$K_i^l = K_i^{l'} \qquad \forall\, i \in \mathcal{I}, e \in [1\,..\,E_i], l, l' \in L_i^e.$$

If unit i starts up in period t after l off-line periods with $l \in L_i^e$, then the start-up is of type e, expressed by $g_i^t(e) = 1$. According to Simoglou et al. [186] this is modeled by

$$y_i^t = \sum_{e \in [1\,..\,E_i]} g_i^t(e) \qquad \forall\, i \in \mathcal{I}, t \in \mathcal{T}, \tag{4.25}$$

$$g_i^t(e) \leq \sum_{l \in L_i^e} z_i^{t-l} \qquad \forall\, i \in \mathcal{I}, e \in [1\,..\,E_i{-}1], t \in \mathcal{T} \text{ with } t > \max L_i^e. \tag{4.26}$$

While $g_i^t(e)$ may be used to model the start-up process and its power production [186], the comparison in this thesis considers only the start-up costs by substituting the variables cu_i^t in the objective function (4.10) by

$$cu_i^t := \sum_{e \in [1\,..\,E_i]} K_i^{\min L_i^e} g_i^t(e) \qquad \forall\, i \in \mathcal{I}, t \in \mathcal{T}. \tag{4.27}$$

The minimum operator in equation (4.27) is required to select one element of the interval L_i^e. Each other arbitrary element could be selected here as well.

4.3.4 Improving the 1-Bin and 3-Bin Formulations

The subsection presents joint work with Matthias Silbernagl and René Brandenberg [185]. We present a modification of the constraints in (4.22) that tightens 1-Bin, and a method to control the approximation error of the time-dependent start-up costs in both 1-Bin and 3-Bin.

Tightening the 1-Bin formulation The inequalities (4.22) can be tightened by lessening the coefficients of the variables v_i^{t-n},

$$cu_i^t \geq K_i^l v_i^t - \sum_{n=1}^{l} (K_i^l - K_i^{n-1}) v_i^{t-n} \quad \forall\, i \in \mathcal{I}, t \in \mathcal{T}, l \in [1\,..\,t{-}1] \text{ with } K_i^l > K_i^{l-1}. \tag{4.28}$$

Each of these inequalities is trivially fulfilled if unit i is off-line in period t, since then its right-hand side is non-positive. If unit i is on-line in period t, consider all $n \in [1\,..\,l]$ with $v_i^{t-n} = 1$. If no such n exists, then both the start-up costs cu_i^t and the right-hand side of the inequality equal K_i^l. Otherwise, choose a minimal n with this property. Then, the start-up costs cu_i^t equal K_i^{n-1} and the right-hand side is at most K_i^{n-1}. As these inequalities dominate those in (4.22), i.e. as they provide a stronger bound on cu_i^t, they still properly model the start-up costs. The impact of the tightening on the integrality gap is depicted in Fig. 4.8 in Section 4.6.5.

Approximating the time-dependent start-up costs To keep computational efforts reasonable, the time-dependent start-up costs are often approximated either by a constant value (see e.g. [78, 153]) or by up to three steps: hot-, cold-, and possibly warm-start (see e.g. [195]). In the light of cool-down times of up to 120 hours for large thermal units [188], these approaches result in considerable approximation errors (see Fig. 4.5 above). This is addressed in [158, 186] and subsequently in [37, 150, 159], where an arbitrary number of steps are allowed.

When solving MIPs, the goal typically is to reach a certain maximal relative optimality gap. Hence, the approximation $\widetilde{K}_i^l$ of K_i^l needs to guarantee a maximal relative error K_{tol},

$$\left| \widetilde{K}_i^l - K_i^l \right| \leq K_{\text{tol}} \cdot K_i^l \qquad \forall\, i \in \mathcal{I}, l \in [1\,..\,T{-}1]. \tag{4.29}$$

Algorithm 1 below determines, given a certain approximation tolerance K_{tol}, how to choose $\widetilde{K}_i^l$ with a minimal number of steps. The algorithm was introduced by Brandenberg and Silbernagl [26].

Algorithm 1: Approximate Start-up Costs

$a \leftarrow 1$
while $a < T$ **do**
  $b \leftarrow a$
  while $b \leq T \ \wedge \ \frac{K_i^{b+1} - K_i^a}{K_i^{b+1} + K_i^a} \leq K_{tol}$ **do**
    $b \leftarrow b + 1$
  for $l \in [a \,..\, b]$ **do**
    $\widetilde{K}_i^\tau \leftarrow \frac{2K_i^a K_i^b}{K_i^b + K_i^a}$
  $a \leftarrow b + 1$

4.4 The Temperature Model

This section presents joint work with Matthias Silbernagl and René Brandenberg [185]. We introduce the temperature as a new model variable. The first subsection shows how the time dependent start-up costs depend on physical power plant temperatures and their cooling behavior, then, the subsequent subsection presents the temperature model as used throughout the scenario calculations in Chapter 7.

4.4.1 Start-up Costs of Thermal Units

The step-wise start-up cost model considered in the previous section is applicable for all increasing start-up cost functions. However, as mentioned in the last section, the start-up cost function of a thermal unit is commonly (e.g. [211]) defined much more restrictively as

$$K_i^l = \underbrace{V_i \left(1 - \mathrm{e}^{-\lambda_i l}\right)}_{\text{variable cost}} + \underbrace{F_i}_{\text{fixed cost}} \qquad \forall\, i \in \mathcal{I}, l \in \mathbb{N}, \tag{4.30}$$

where l denotes the off-line time. The fixed costs are derived from the start-up status y_i^t as in constraints (4.23) and (4.24). The variable costs originate from the reheating process at start-up, where fuel needs to be burned and where the unit experiences thermal stress.

Here, the term $(1 - \mathrm{e}^{-\lambda_i l})$ is proportional to the heat loss of the power plant incurred while off-line, and models the exponential decay of the temperature,

$$\overline{\text{temp}}_i(l) = \mathrm{e}^{-\lambda_i l} \qquad \forall\, i \in \mathcal{I}, l \in \mathbb{R}_{\geq 0}, \tag{4.31}$$

assuming the operational temperature is normalized to 1 and the environmental temperature is normalized to 0. As shown in Fig. 4.6, equation (4.31) is discretized by a step-wise constant function with steps according to

$$\widehat{\text{temp}}_i^t := \begin{cases} 1 & \text{if } v_i^t = 1, \\ \overline{\text{temp}}_i(l_i^t) = \mathrm{e}^{-\lambda_i l_i^t} & \text{else,} \end{cases}, \qquad \forall\, i \in \mathcal{I}, t \in \mathcal{T}, \tag{4.32}$$

where l_i^t denotes the number of periods that unit i is off-line prior to period t.

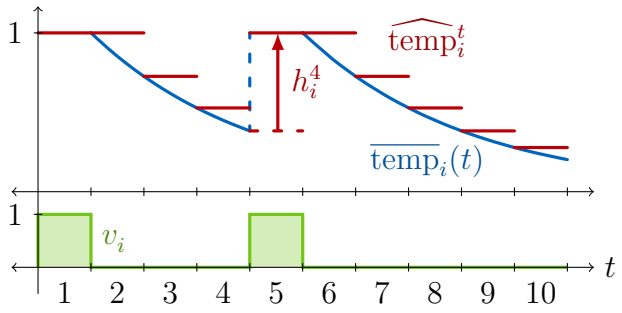

Figure 4.6: Discretization of a unit's temperature function. Following the operational schedule, the unit exhibits the temperature function $\overline{\text{temp}}_i$ which is discretized to $\widehat{\text{temp}}_i$, with resulting heating h_i according to (4.38).

The above nonlinear definition of $\widehat{\text{temp}}_i^t$ may be restated recursively as

$$\widehat{\text{temp}}_i^1 = \begin{cases} 1 & \text{if } v_i^1 = 1, \\ \mathrm{e}^{-\lambda_i PD_i} & \text{else,} \end{cases} \qquad \forall\, i \in \mathcal{I} \tag{4.33}$$

$$\widehat{\text{temp}}_i^t = \begin{cases} 1 & \text{if } v_i^{t-1} = 1 \text{ or } v_i^t = 1, \\ \mathrm{e}^{-\lambda_i} \widehat{\text{temp}}_i^{t-1} & \text{else,} \end{cases} \qquad \forall\, i \in \mathcal{I}, t \in [2\,..\,T], \tag{4.34}$$

with PD being the previous downtime.

4.4.2 Temperature as a New Variable in the Modeling Framework

In this section, the temperature loss derived in the last section is modeled by explicitly capturing the temperature of a unit as the new state variable temp_i^t and the amount of heating as the new variable h_i^t. Combined with the start-up status y_i^t (cf. 4.4.1), they are used to model the start-up cost function as defined in equation (4.21).

The new variables, temperature temp_i^t and applied heating h_i^t, are continuous and non-negative,

$$\text{temp}_i^t \in \mathbb{R}_{\geq 0} \qquad \forall\, i \in \mathcal{I}, t \in \mathcal{T}, \tag{4.35}$$

$$h_i^t \in \mathbb{R}_{\geq 0} \qquad \forall\, i \in \mathcal{I}, t \in [0\,..\,T{-}1]. \tag{4.36}$$

The operational temperature is expressed as

$$v_i^t \leq \text{temp}_i^t \leq 1 \qquad \forall\, i \in \mathcal{I}, t \in \mathcal{T}, \tag{4.37}$$

enforcing a temperature of exactly 1 during operation. The recursion in equations (4.33) and (4.34) is modeled as

$$\text{temp}_i^1 = \mathrm{e}^{-\lambda_i PD_i} + h_i^0 \qquad \forall\, i \in \mathcal{I}, \tag{4.38}$$

$$\text{temp}_i^t = \mathrm{e}^{-\lambda_i}\text{temp}_i^{t-1} + (1 - \mathrm{e}^{-\lambda_i})v_i^{t-1} + h_i^{t-1} \qquad \forall\, i \in \mathcal{I}, t \in [2\,..\,T], \tag{4.39}$$

which causes the temperature

- to decay exponentially while the unit is off-line ($v_i^t = 0$),
- to stay constant at 1 while the unit is on-line ($v_i^t = 1$), and
- to rise by h_i^t if the unit is heating.

Finally, the start-up costs are modeled as

$$cu_i^t = V_i h_i^{t-1} + F_i y_i^t \qquad \forall\, i \in \mathcal{I}, t \in \mathcal{T}, \tag{4.40}$$

with V_i being the variable part of start-up costs and F_i the fix part as described in equation (4.21).

Next, the exactness of the model is explained. It is easy to check that $y_i^t = 1$ exactly if there is a start-up in period t, and $y_i^t = 0$ otherwise. Thus, the constant part of the start-up costs is modeled correctly. The temperature losses increase proportionally with $\text{temp}_i^t - v_i^t$. Thus, in a cost-minimal solution, heating is applied such that the temperature is minimal while fulfilling $\text{temp}_i^t \geq v_i^t$. This entails two consequences:

1. Heating is applied only in the period prior to each start-up. Earlier heating could be postponed until this period, thus saving heating costs.
2. The amount of heating is exactly such that the temperature reaches 1. Excessive heating could either be postponed until the period prior to the next start-up, or be avoided if there is no such start-up.

Therefore, in a cost-minimal solution, the temperature variables temp_i^t match the discretized temperatures $\widehat{\text{temp}}_i^t$ as given in equation (4.32), and the start-up costs cu_i^t equal 0 if unit i does not start-up in period t.

Given a cost-minimal solution, assume that unit i starts up in period t after l off-line periods. By period $t-1$, the unit has cooled down for $l-1$ periods, and in period t, the temperature after start-up has to be 1 again,

$$\text{temp}_i^{t-1} \overset{(4.32)}{=} \mathrm{e}^{-\lambda_i(l-1)} \quad \text{and} \quad \text{temp}_i^t \overset{(4.37)}{=} 1.$$

Thus, the needed heating, considering the further cooling during period $t-1$, matches the expected temperature loss,

$$h_i^{t-1} \overset{(4.39)}{=} \text{temp}_i^t - \mathrm{e}^{-\lambda_i}\text{temp}_i^{t-1} + (1 - \mathrm{e}^{-\lambda_i})\overbrace{v_i^{t-1}}^{=0} = 1 - \mathrm{e}^{-\lambda_i l}.$$

This means, the variable part of the start-up costs is modeled correctly too, leading to $cu_i^t = K_i^l$.

While this model uses new additional variables, it reduces the number of constraints significantly in comparison to 1-Bin, 1-Bin* (the tightened version of 1-Bin), and 3-Bin, even with a start-up cost approximation tolerance of $K_{\text{tol}} = 5\%$ (see Section 4.5.3). Fig. 4.8 suggests that the integrality gap of this model is on average smaller, while the solution times of the linear relaxation remain comparable to 1-Bin and 3-Bin (see Fig. 4.7). Both factors are crucial for the improved number of solved instances shown in Fig. 4.9.

4.5 Numerical Examples Demonstrating Advantages of Temperature Model

This section presents joint work with Matthias Silbernagl and René Brandenberg [185]. We present results from numerical examples which show the benefits of the new modeling approach. After introducing the modeling setup and reporting problem sizes and solution times of the linear relaxation, its reduced integrality gap is highlighted. This advantage leads to an overall faster optimization procedure and enables larger models to be solved. The experiments are performed using the CPLEX solver.

4.5.1 Scenarios and Data Description

Two scenarios are investigated, one based on the German power system with 223 units, and one based on the IEEE 118 bus system with 54 units and 118 nodes in a transmission network. The German system slightly differs to the dataset described in Chapter 6, as an updated version is used for the flexibility evaluation studies. The complete datasets including power plants, residual loads, and the transmission grid is available in form of ancillary files at `http://arxiv.org/abs/1408.2644`.

German power system The raising requirements for fossil-fuel power plants, which stem from a more volatile residual load, include more start-ups and hence result in a higher ratio of start-up to operational costs [118]. A higher percentage of start-up costs will lead to higher solution times and increase the advantages of the temperature model approach. To consider the impact of a more volatile residual load in the numerical experiments, a forecast scenario for the year 2025 is employed.

Power plant data of the German power system of 2014 are published by the German Federal Network Agency [33], comprising 228 individually controlled power plants. The data is augmented by assumptions regarding minimal production, efficiency, and start-up costs, which are partly based on [56, 66, 128]. As the year 2025 is modeled, all nuclear power plants are phased out in favor of four additional combined cycle gas turbines, reducing the number of plants to 223. Again, this assumption is different to the dataset development described in Chapter 6, where thermal power plants are kept at status quo for future scenarios as well.

The main benefits of this dataset compared to existing test datasets (e.g. as used by Carrión and Arroyo [37]) are

- an adequate number of power plants, representing the diversity of a real power system, and
- detailed thermal start-up cost functions given by coefficients F_i, V_i, and λ_i (see (4.30)).

In addition to power plant data, the model requires data of the residual load, i.e. of the difference between load and electricity production from must-run renewable power sources. The load data is taken from ENTSO-E [62] and scaled to a yearly electricity consumption of 520 TWh. Wind and solar electricity generation profiles are computed based on the NASA MERRA database [177] for the same base year. Afterwards, these profiles are scaled according to the respective installed capacity (50 GW wind, 50 GW solar). Biomass and hydro power plants are assumed to produce at full capacity (5.5 GW biomass, 4.5 GW hydro).

Each experiment is performed using 14 time ranges of length $T=72$ (Sections 4.5.3 and 4.5.5), length $T=240$ (Section 4.5.4) or varying length (Section 4.5.6), starting in the S-th hour of the year with $S \in \{624k + 433 : k \in [0\,..\,13]\}$. This set is chosen such that each time range starts at midnight, the time ranges are uniformly distributed over the year 2025, and two time ranges start on any day of the week, respectively.

IEEE 118 bus system This scenario is based on the IEEE 118 bus test system published in [146], and again augmented to include the relevant power plant data. Apart from being well-studied, its major benefit is its realistic transmission network.

The test system provides load values for 24 hours and 20 wind scenarios which are concatenated into a residual load of 480 periods. Since the low average wind production of 5.4% of the load leads to a lower ratio of start-up to operational costs than in the scenario of the German power system, the advantage of the new approach is expected to be less pronounced. Analogous to the German power system, 14 uniformly distributed starting points are given by $S \in \{24k+1 : k \in [0\,..\,13]\}$.

4.5.2 Compared Model Formulations

The approach is evaluated by comparing it to the state-of-the-art start-up cost formulations introduced in Section 4.3.3:

1. 1-Bin: Start-up costs modeled by inequality (4.22).
2. 1-Bin*: Same as 1-Bin, with the tightened start-up cost inequalities (4.28) instead of the original inequalities (4.22).
3. 3-Bin: Same as 1-Bin, except that start-up cost inequalities (4.22) are replaced by the inequalities (4.23)-(4.26), and the start-up costs are defined as in (4.27).

4. Temp: New approach with explicit modeling of the power plant temperature, as described in Section 4.4.2, including inequalities (4.35)-(4.39) and start-up costs defined in (4.40).

These formulations are embedded into the two models described in Section 4.3.1,

- the basic formulation composed of (4.10)–(4.13), (4.14)–(4.16), and
- the extended formulation composed which further includes the tighter ramping constraints according to Ostrowski et al. [159] as well as grid constraints with power transfer distribution factors (PTDF) as described in Section 4.9.

The basic UC problem uses the German power system, while the extended UC problem includes load flow constraints and thus requires the networked IEEE 118 bus system.

In 1-Bin, 1-Bin*, and 3-Bin, the start-up costs are approximated with tolerance $K_{\text{tol}} \in \{0\%, 5\%, 20\%\}$ (see Section 4.3.4). Using $K_{\text{tol}} = 0\%$, the modeled start-up costs are equal to Temp, resulting in equivalent problems and solutions, which is required when comparing integrality gaps. With $K_{\text{tol}} = 20\%$, the start-up cost functions are approximated very roughly with 2.3 steps on average. Finally, as in the presented scenarios, start-up costs amount to up to 10% of the total costs, $K_{\text{tol}} = 5\%$ is a sensible choice leading to a maximal error of $10\% \cdot 5\% = 0.5\%$ of the objective value.

4.5.3 Problem Sizes

Table 4.1 lists the number of variables and inequalities for the four start-up cost models and for different start-up cost approximation tolerances K_{tol} in the basic formulation. Their number of additional variables and inequalities remains constant in the extended formulation, except for the start-up and shut-down indicators which are already part of 3-Bin and Temp but have to be added in 1-Bin and 1-Bin*.

While Temp uses twice as many variables as 1-Bin and 1-Bin*, the model requires significantly fewer inequalities than the state-of-the-art formulations at $K_{\text{tol}} = 5\%$. Naturally, higher tolerances K_{tol} result in fewer inequalities: a number of inequalities approximately equal to Temp is reached by 1-Bin and 1-Bin* at $K_{\text{tol}} \approx 11.3\%$, and by 3-Bin at $K_{\text{tol}} \approx 19.2\%$.

4.5.4 Computational Effort for Solving the LP

A criterion for the quality of a formulation is the computational effort for solving its (initial) linear relaxation. To stay as close as possible to the practical application, all integrality-specific algorithms of the solvers were disabled, i.e. presolve, integrated cuts, and heuristics. The experiments were conducted with an interior point algorithm, which proved to be significantly faster than the dual simplex across all formulations. Applying the latter decreases the difference between 3-Bin and Temp slightly, while 1-Bin and 1-Bin* are considerably slower.

Table 4.1: Problem sizes and average number of steps in the approximation of the start-up cost function of all start-up cost formulations for $K_{\text{tol}} \in \{0\%, 5\%, 20\%\}$ for $T = 72$ periods and 223 units (basic formulation).

Model	K_{tol}	Avg. steps	Variables	Inequalities
None			32112	79683
1-Bin	0%	71.00	48168	649671
	5%	6.48	48168	166334
	20%	2.32	48168	111423
1-Bin*	0%	71.00	48168	649671
	5%	6.48	48168	166334
	20%	2.32	48168	111423
3-Bin	0%	71.00	634435	665950
	5%	6.48	151098	182613
	20%	2.32	96187	127702
Temp			96336	127851

Fig. 4.7 compares solution times of the linear relaxations taken over 14 time ranges of length $T = 120$ as described in Section 4.5.1 and using a start-up cost approximation tolerance of $K_{\text{tol}} = 5\%$. The results show that Temp significantly outperforms 3-Bin. While 1-Bin and 1-Bin* are on average faster than Temp in the German power system, this is reversed in the IEEE 118 bus system where Temp yields the fastest linear relaxation by a considerable margin.

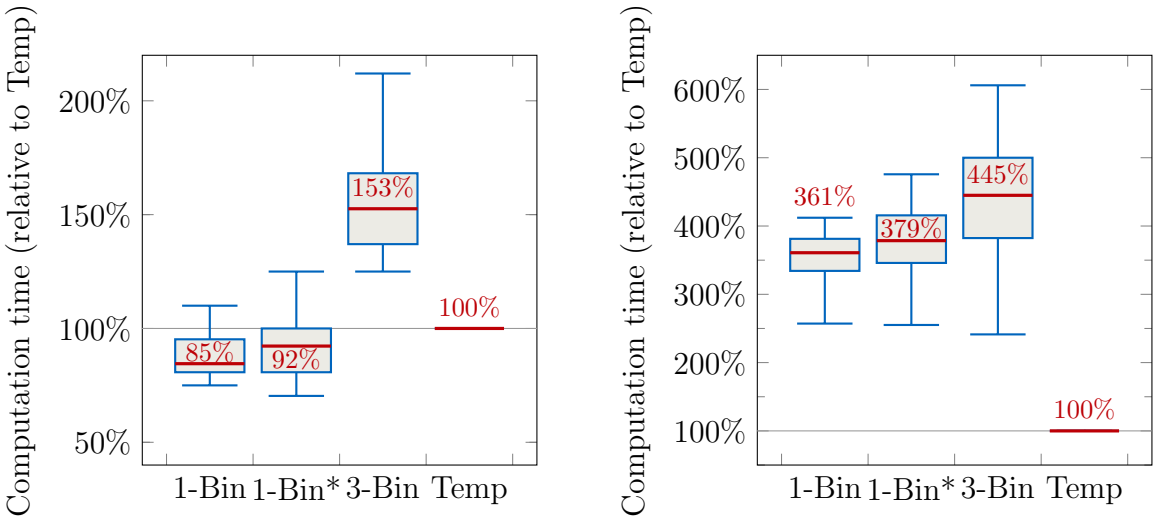

Figure 4.7: Solution times of the linear relaxation for 14 test cases with $T = 120$ periods and $K_{\text{tol}} = 5\%$ in the German power system (left chart) and the IEEE 118 bus system (right chart). Temp outperforms 3-Bin consistently.

4.5.5 Integrality Gap

Another important criterion of a problem formulation is its integrality gap, which measures the influence of the integrality constraints on the optimal solution. It is defined as $z_{\text{MIP}} - z_{\text{LP}}$, where z_{MIP} denotes the optimal value and z_{LP} the optimal fractional value, and normalized to $(z_{\text{MIP}} - z_{\text{LP}})/z_{\text{MIP}}$ for comparability across test cases.

Smaller integrality gaps mean better lower bounds, which lead to faster solution times. The best possible integrality gap is 0, which would mean that the optimal objective value of the formulation does not depend on the integrality constraints.

Fig. 4.8 shows the integrality gap of all four models relative to Temp for the same test cases as in Fig. 4.7, but with $K_{\text{tol}} = 0\%$ and $T = 72$. Note that the medians of the relative integrality gaps are similar in both formulations, but the German power system exhibits a much higher variance. This can be attributed to the highly volatile residual demand in the forecast of the year 2025. Moreover, the complexity of the extended formulation for the IEEE 118 bus system results in a higher absolute integrality gap, with a median of 1.4% compared to 0.7% in the basic formulation with the German system.

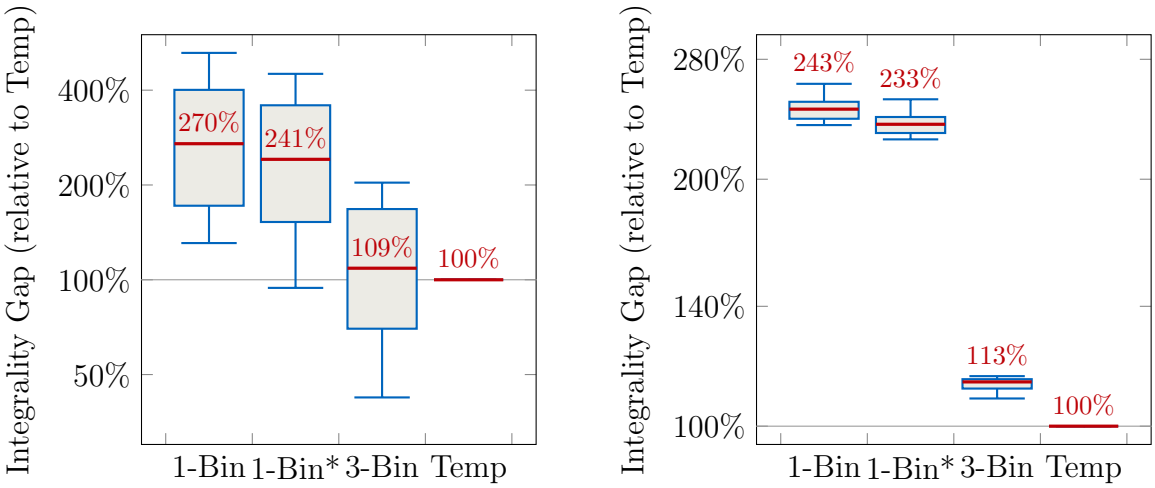

Figure 4.8: Integrality gaps relative to 3-Bin, for 14 test cases with $T = 72$ periods in the German power system (left chart) and the IEEE 118 bus system (right chart). In both, 3-Bin dominates 1-Bin and 1-Bin*, but is on average inferior to Temp. Results in the IEEE 118 bus system exhibit less variance.

Fig. 4.8 clearly illustrates the advantage of modeling the temperature as an explicit variable. Since the inequalities (4.28) of 1-Bin* dominate the inequalities (4.22) of 1-Bin, 1-Bin* must have a lower integrality gap (11% and 4% decrease). 3-Bin consistently provides a lower integrality gap than 1-Bin*, with an average reduction of 55% and 51%, corresponding in magnitude to the results in Morales-España et al. [150]. Temp further decreases the average integrality gap of 3-Bin by 9 and 13 percentage points and proves to be the tightest model analyzed.

4.5.6 Performance With Scaling to a Larger Number of Periods

An essential aspect in computational efficiency is the behavior with model scaling. Especially scaling to a greater number of modeled periods seems to be highly relevant for future operational planning for two reasons:

1. As the residual load will become more volatile it will be beneficial to increase the time resolution [50].
2. As renewable generation changes over several days and weeks, the storage management requires to consider longer time horizons than today where it is mainly driven by day and night variation of load.

The scaling behavior is analyzed with 14 sets of test cases. The test cases have start periods S as described in Section 4.5.1, a varying number of time steps considered T ranging from $T=24$ to $T=444$, and start-up costs approximated to tolerances $K_{\text{tol}} \in \{0\%, 5\%, 20\%\}$. Fig. 4.9 shows the number of instances which have been solved to an optimality gap of 1% within 30 minutes for the German power sytem (upper chart) and the IEEE 118 bus system (lower chart).

In both cases, 3-Bin dominates 1-Bin and 1-Bin*, confirming the results of [150]. However, even if allowing the highest start-up cost approximation tolerance $K_{\text{tol}} = 20\%$, Temp consistently solves more instances than all other models.

Unsurprisingly, the superiority of the temperature model is more emphasized in the basic formulation, since the higher complexity of the extended formulation and the lower share of start-up costs in the IEEE 118 system lessen the impact of the start-up cost model.

4.6 Modeling Start-up Times

This section presents joint work with Matthias Silbernagl [111]. The temperature model showed advantages compared to previous model formulations in terms of computational efficiency and accuracy of modeling start-up costs. Furthermore, the formulation with the temperature variable brings the model closer to the real physics of the power plants. One aspect for taking advantage of this formulation is the modeling of start-up times [128].

Modeling start-up times is an important feature for operational planning. In deterministic models, the start-up time is important for defining when to begin the start-up process. Thereby, the required amount of time (the start-up speed) is not an operational constraint since even plants that require multiple hours for a cold start can be on-line exactly when needed. As soon as uncertainty is considered – which is the case in real world applications – the possible start-up speed becomes an important parameter and fast-starting units become more valuable as they allow operators to react quickly to changes in forecast of demand.

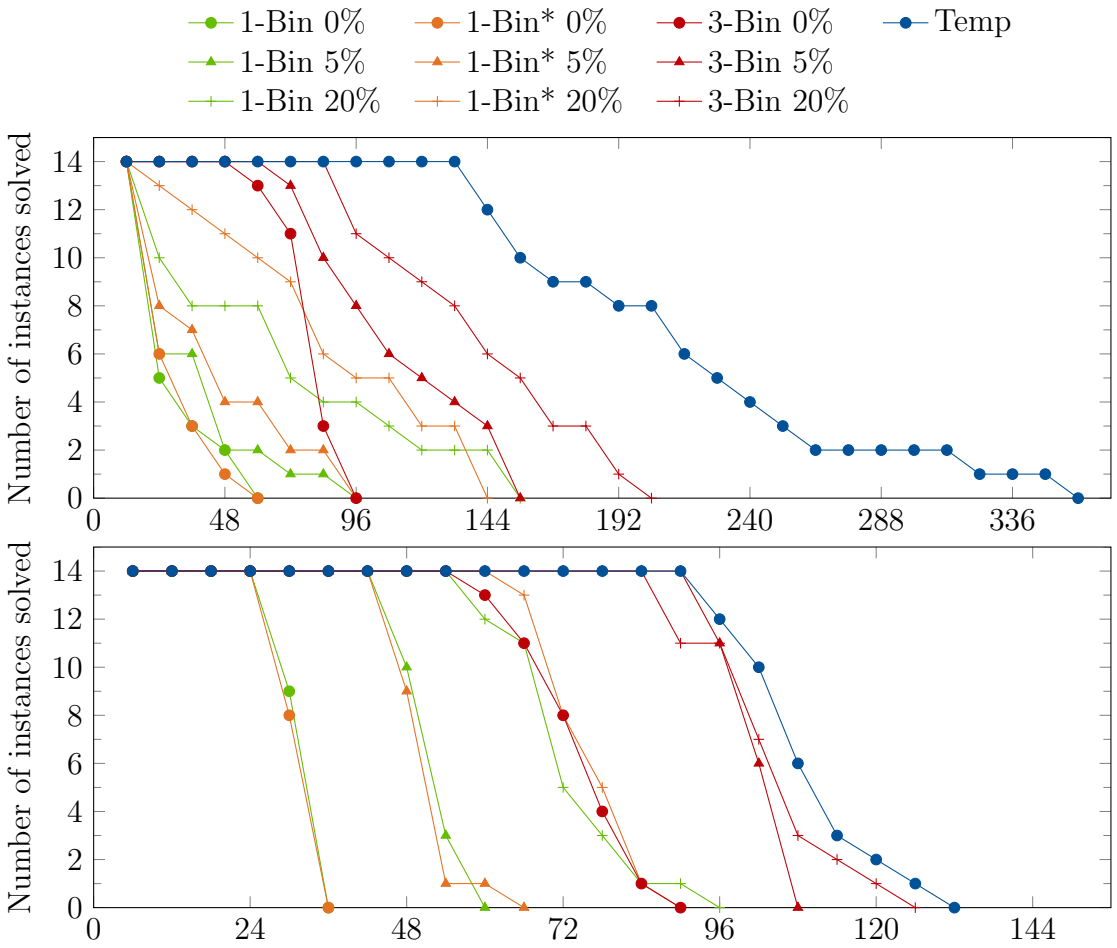

Figure 4.9: Scaling of computational effort with problem size for all formulations and different start-up cost approximation tolerances K_{tol}. The upper chart shows the number of instances solved to an optimality gap of 1% within 30 minutes of computation time for the German power system, the lower chart shows the same for the IEEE 118 bus system.

Start-up of power plants is mostly restricted by either thermal stress in the components, which can be expressed as a temperature increase, or by limited heating capabilities, which can be expressed by limiting the applied heating. This Section presents approaches to integrate start-up times in the temperature formulation for either

- units with limited heating speed (c.f. Fig. 4.10 on the left), or
- units with limited temperature increase (c.f. Fig. 4.10 on the right).

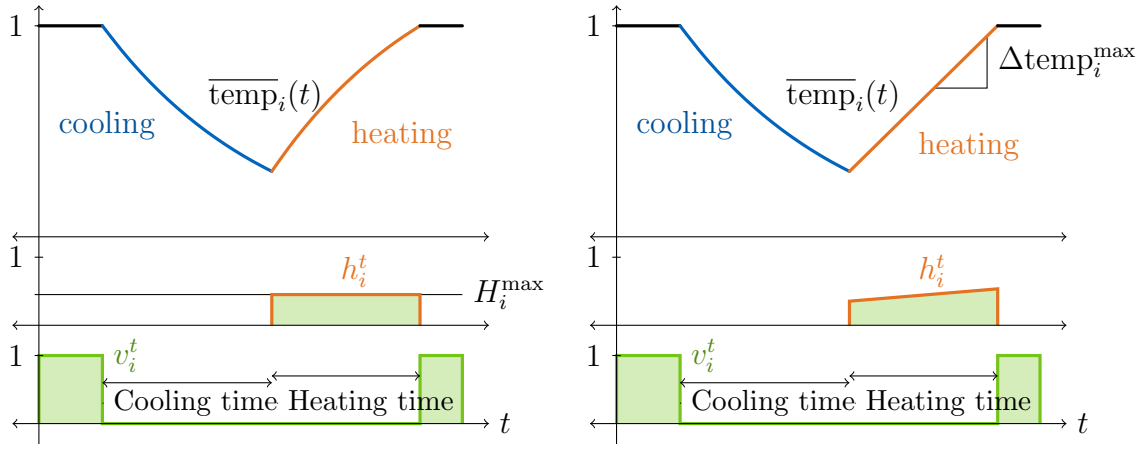

Figure 4.10: Cooling and heating during the off-line time of a unit with limited heating speed (left) and of a unit with limited temperature increase per period (right).

For both types of units, the resulting start-up time and costs are derived and compared in Section 4.6.4. The start-up time, which is defined as the number of periods during which the unit heats up, is denoted by $SUT_i(l)$. The sum of the variables h_i^t during start-up is denoted by $TH_i(l)$, such that $V_i \cdot TH_i(l)$ equals the variable start-up costs in 4.40.

First, the development of the temperature of a unit in a continuous model is derived. The off-line time can be split in two phases: the unit cools down and, subsequently, it is reheated before the start-up takes place (c.f. Fig. 4.10 on the left).

During the entire off-line time, the unit continuously loses heat at a rate of $\lambda_i \text{temp}_i^t$. As shown above, the modeled temperature of unit i equals $\mathrm{e}^{-\lambda_i l}$ after l offline periods. During heating, the temperature is increased by supplying heat at a rate of $\overline{h}_i(t)$. Assuming the heating phase starts at $t = 0$, the continuous temperature $\overline{\text{temp}}_i(t)$ may be modeled as

$$\begin{aligned} \overline{\text{temp}}_i(0) &= \mathrm{e}^{-\lambda_i l}, \\ \frac{\mathrm{d}\overline{\text{temp}}_i(t)}{\mathrm{d}t} &= -\lambda_i \overline{\text{temp}}_i(t) + \overline{h}_i(t). \end{aligned} \tag{4.41}$$

While heating, the unit continues to lose further heat. Therefore, units heat as fast as possible in a cost-minimal solution. So far, unbounded heating, which models the typical start-up costs (4.30), was assumed. As noted, the following two sections consider the effect of limiting the heating speed and the temperature increase.

4.6.1 Limited Heating Speed

The start-up time of a unit may stem from its limited ability to heat (c.f. Fig. 4.10 on the left). Assuming a heating speed of at most $H_i^{\max}$, the continuous model for cost-minimal heating in 4.41 can be simplified by substituting $\overline{h}_i(t)$ with $H_i^{\max}$. Considering the initial temperature of $\overline{\text{temp}}_i(0) = \mathrm{e}^{-\lambda_i l}$, the solution of the differential equation (4.41)

can be computed to

$$\overline{\text{temp}}_i(t) = \mathrm{e}^{-\lambda_i(l+t)} + \frac{H_i^{\max}}{\lambda_i}(1 - \mathrm{e}^{-\lambda_i t}). \tag{4.42}$$

This function fulfills the recursion

$$\overline{\text{temp}}_i(t+1) = \mathrm{e}^{-\lambda_i}\overline{\text{temp}}_i(t) + \frac{1 - \mathrm{e}^{-\lambda_i}}{\lambda_i} H_i^{\max}. \tag{4.43}$$

Since the temperature development in equation (4.39) is modeled as

$$\text{temp}_i^t = \mathrm{e}^{-\lambda_i}\text{temp}_i^{t-1} + (1 - \mathrm{e}^{-\lambda_i})v_i^{t-1} + h_i^{t-1},$$

the limit on the heating speed may, in the UC model, be expressed as

$$h_i^t \leq \frac{1 - \mathrm{e}^{-\lambda_i}}{\lambda_i} H_i^{\max} \qquad \forall\, i \in \mathcal{I}, t \in [0\,..\,T{-}1]. \tag{4.44}$$

In the continuous model, the start-up heating finishes at time t^* with $\overline{\text{temp}}_i(t^*) = 1$. Equation (4.42) is the basis for

$$t^* = \frac{1}{\lambda_i} \ln\left(1 + \frac{1 - \mathrm{e}^{-\lambda_i l}}{H_i^{\max}/\lambda_i - 1}\right),$$

which results in $\lceil t^* \rceil$ periods of heating in the unit commitment formulation, and hence in a start-up time of

$$SUT_i(l) = \left\lceil \frac{1}{\lambda_i} \ln\left(1 + \frac{1 - \mathrm{e}^{-\lambda_i l}}{H_i^{\max}/\lambda_i - 1}\right) \right\rceil. \tag{4.45}$$

If t^* is integral, and therefore $SUT_i(l) = t^*$, the unit heats at maximal speed in the unit commitment problem, and the total heating equates to

$$TH_i(l) = \frac{1 - \mathrm{e}^{-\lambda_i}}{\lambda_i} H_i^{\max} SUT_i(l). \tag{4.46}$$

If t^* is not integral, and therefore $SUT_i(l) > t^*$, the unit needs to heat at sub-maximal speed in the first heat-up period to reach a final temperature of exactly 1. As this is equivalent to keeping the unit warm for the initial part of that period, it results in a slightly higher total heating than $TH_i(l)$. However, the difference is generally small (c.f. Fig. 4.11).

4.6.2 Maximum Temperature Increase

Alternatively, a unit may have a maximally allowed temperature change $\Delta\text{temp}_i^{\max}$ (c.f. Fig. 4.10 on the right),

$$\begin{aligned} \overline{\text{temp}}_i(0) &= \mathrm{e}^{-\lambda_i l}, \\ \frac{\mathrm{d}\overline{\text{temp}}_i(t)}{\mathrm{d}t} &= \Delta\text{temp}_i^{\max}, \end{aligned} \tag{4.47}$$

which is solved by

$$\overline{\text{temp}}_i(t) = \mathrm{e}^{-\lambda_i l} + t\Delta\text{temp}_i^{\max}. \tag{4.48}$$

This function fulfills the recursion

$$\overline{\text{temp}}_i(t+1) = \overline{\text{temp}}_i(t) + \Delta\text{temp}_i^{\max}, \tag{4.49}$$

and may be modeled as

$$\text{temp}_i^t \leq \text{temp}_i^{t-1} + \Delta\text{temp}_i^{\max} \qquad \forall\, i \in \mathcal{I}, t \in [2\,..\,T] \tag{4.50}$$

in the unit commitment formulation.

As the temperature after l off-line periods equals $\mathrm{e}^{-\lambda_i l}$, the required start-up time can be derived as

$$SUT_i(l) = \left\lceil \frac{1 - \mathrm{e}^{-\lambda_i l}}{\Delta\text{temp}_i^{\max}} \right\rceil. \tag{4.51}$$

Assuming now that $\Delta\text{temp}_i^{\max}$ divides $1 - \mathrm{e}^{-\lambda_i l}$ evenly, i.e. that the unit heats at maximal speed for the entire start-up time, the required heating in each period equals

$$h_i^t = \text{temp}_i^{t+1} - \mathrm{e}^{-\lambda_i}\text{temp}_i^t = (1 - \mathrm{e}^{-\lambda_i})\text{temp}_i^t + \Delta\text{temp}_i^{\max}.$$

Noting that the temperature in the j-th period of heating equals $\mathrm{e}^{-\lambda_i l} + (j-1)\Delta\text{temp}_i^{\max}$, the sum of the heating variables can be derived as

$$TH_i(l) = (1 - \mathrm{e}^{-\lambda_i l})\left(1 + \frac{1 - \mathrm{e}^{-\lambda_i}}{2}\left(\frac{1 + \mathrm{e}^{-\lambda_i l}}{\Delta\text{temp}_i^{\max}} - 1\right)\right). \tag{4.52}$$

If $\Delta\text{temp}_i^{\max}$ does not divide $1 - \mathrm{e}^{-\lambda_i l}$ evenly, then the effective total heating slightly surpasses $TH_i(l)$; yet $TH_i(l)$ remains an excellent approximation (c.f. Fig. 4.11).

4.6.3 Objective Function

In (4.43) and (4.49) the continuous model of the heating process in (4.41) was discretized using the period length 1. Choosing a different period length $f \in \mathbb{R}_{>0}$ yields the same model, albeit with scaled parameters $\tilde{\lambda}_i = f\lambda_i$, $\tilde{H}_i^{\max} = fH_i^{\max}$ and $\Delta\tilde{\text{temp}}_i^{\max} = f\Delta\text{temp}_i^{\max}$.

Apart from scaling and rounding, the resulting start-up time $\tilde{SUT}_i(l/f)$ matches the original start-up time $SUT_i(l)$, i.e. $f\tilde{SUT}_i(l/f) \approx SUT_i(l)$. The same however does not hold for the total heating, which varies significantly depending on f.

This discrepancy arises from the modeling of the variable h_i^t, which represents the temperature increase in period t due to heating; In the context of start-up times however, one should instead consider the heating speed $\overline{h}_i(t)$ in (4.41).

A heat increase h_i^t is equivalent to heating at speed

$$\overline{h}_i(t) = \frac{\lambda_i}{1 - \mathrm{e}^{-\lambda_i}} h_i^t \qquad \forall\, i \in \mathcal{I}, t \in \mathcal{T}$$

during period t. Introducing this factor in (4.40) as

$$cu_i^t := V_i \frac{\lambda_i}{1 - \mathrm{e}^{-\lambda_i}} h_i^{t-1} + F_i y_i^t \qquad \forall\, i \in \mathcal{I}, t \in \mathcal{T}, \tag{4.53}$$

results in start-up costs which remain approximately equal for equivalent operational schedules, regardless of the period length f. Within this thesis, the period length is set to 1 hour in all cases.

4.6.4 Comparison of Approaches

Due to differing power plant technology, the choice of the appropriate limitation depends on the individual unit, and some units may even require both limitations. This section compares the start-up time $SUT_i(l)$ and the total heating $TH_i(l)$ for an off-line time l in both approaches.

Fig. 4.11 on the left depicts the start-up time $SUT_i(l)$ for an exemplary unit with parameters $\lambda_i = 0.05$ and $H_i^{\max} = \Delta\mathrm{temp}_i^{\max} = 3\lambda_i$, showing that limiting the heating speed leads to higher start-up times. As defined, $SUT_i(l)$ equals the start-up time in the continuous model, rounded up to the next integer.

Using the same example, Fig. 4.11 on the right demonstrates that the approximations $TH_i(i)$ of the total heating given in (4.46) and (4.52) closely match the actual values. Furthermore, the figure shows that the required heating is highest when limiting the heating speed, and both limitations result in higher variable costs than when applying the model with unbounded heating.

4.6.5 Numerical Examples

This section describes the computational performance of the proposed approaches as well as the effect of the restrictions on the system costs. Both models are compared to the model without start-up time, i.e. with unbounded heating.

A scenario representing the German power system as described in Section 4.5.1 is used. Depending on the examined approach, the maximum heating speed $H_i^{\max}$ and the maximum temperature increase $\Delta\mathrm{temp}_i^{\max}$ of each unit i are set to $H_i^{\max} = \Delta\mathrm{temp}_i^{\max} = M\lambda_i$, where the factor M is varied to highlight the impact of the strictness of the limits $H_i^{\max}$ and $\Delta\mathrm{temp}_i^{\max}$.

Computational efficiency The introduction of either (4.44) or (4.50) leads to additional constraints, whose effect on the computational time is investigated in the following. Fig. 4.12 on the left shows the change of computational time for time ranges with $T = 72$ and $T = 144$ periods, and depending on the factor M. The figure indicates that the change in computational time is not significant for small models, but may

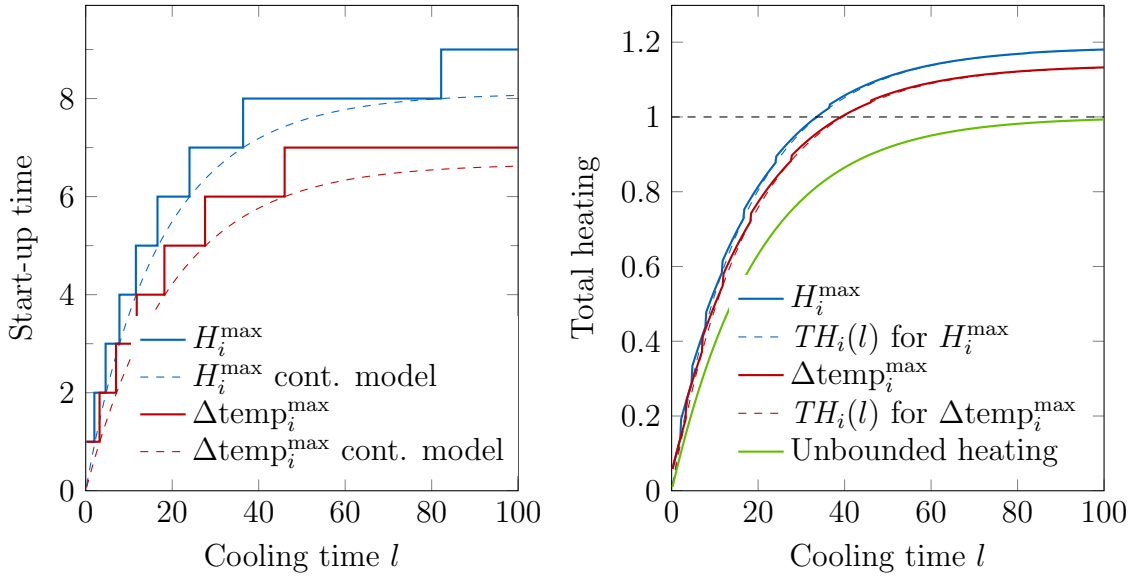

Figure 4.11: Start-up time (left) and total heating (right) when limiting heating/temperature increase for a unit with parameters $\lambda_i = 0.05$ and $H_i^{\max} = \Delta\text{temp}_i^{\max} = 3\lambda_i$. The total heating is compared to the respective approximations $TH_i(i)$ and the model with unbounded heating.

increase significantly for larger models and strict limits (small M). The model with limited heating is more efficient and only increases computational times moderately up to 200% compared to the model with unbounded heating. In contrast, the model with limited temperature increase may increase computational times by up to 600% at $M = 40$.

Effects on system costs As highlighted in Fig. 4.11, the required heating for a start-up increases when modeling the start-up time. Fig. 4.12 on the right analyzes the resulting increase in system costs, depending on $H_i^{\max}$ and $\Delta\text{temp}_i^{\max}$. The increase amounts to less than 0.5% even for very strict limitations.

This observation applies only to a deterministic model; in a stochastic model the start-up time may force a unit to stay at operational temperature during off-line time, possibly increasing the system costs considerably.

4.7 Start-up Type Depending Wear-and-Tear Costs

Part of the start-up costs are caused by wear-and-tear of the power plants. This includes shorter time intervals for maintenance as well as reduced lifetime. The reason for these costs is the thermal stress of power plant components [128]. Whenever plants start up, the temperature must be increased to the operating temperature from where it cools down again after shut-down. The same is true for increasing and reducing output during operations, but temperature differences are much lower than in the start-up and shut-down processes [128]. Berth et al. [16] estimate the wear-and-tear costs of a

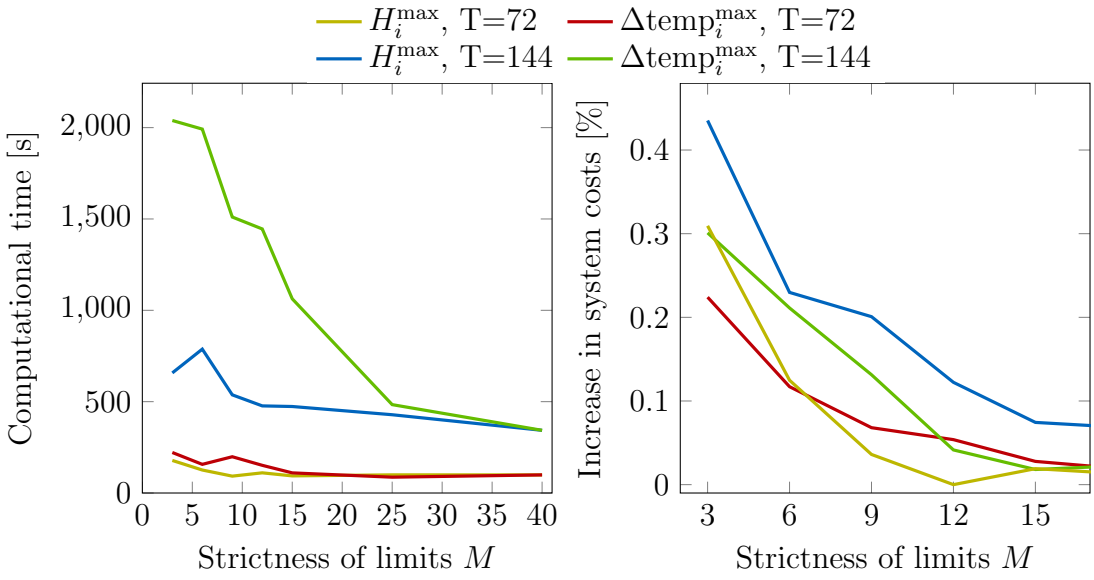

Figure 4.12: Increase in system costs and computational time with limited heating/temperature increase for test cases of two sizes and parameters $H_i^{\max} = M\lambda_i$ or $\Delta\text{temp}_i^{\max} = M\lambda_i$. The additional system costs amount to less than 0.5%.

start-up (so-called "indirect start-up costs") to 40% of overall cycling costs. The share of load following cycling is estimated to be only at around 5%. The authors also found that the share of cycling costs in total operating costs will increase dramatically from 1.7% without any renewables to 14% with a 50% penetration of wind and solar. Denny and O'Malley [51] simulated the additional cycling costs by introducing a carbon price. They predict that the share of additional fuel costs represents 2-50% of cycling costs – leaving at least 50% of costs coming from wear-and-tear, again pointing to the high importance of this cost factor in future power system operation.

The wear-and-tear costs depend on the speed of the temperature increase and the resulting thermal tensions. The temperature base modeling approach as presented in the previous sections allows to account for this fact by introducing start-up speed dependent costs. A piecewise linear function is employed which approximates quadratically increasing costs by faster heating due to the higher thermal stress. Fig. 4.13 illustrates this increasing characteristic of the start-up costs. The (additional) costs for wear-and-tear can be included in the model with the following equation:

$$cw_i^t \geq \zeta_i^c + \phi_i^c \cdot h_i^t \qquad \forall t \in \mathcal{T}, i \in \mathcal{I}, c \in \mathcal{C}, \tag{4.54}$$

with ζ_i^c being the fix part and ϕ_i^c the variable part of each line $c \in \mathcal{C}$.

In order to add those costs to the model, cw_i^t can be added to the total costs in equation (4.10). Start-up costs cu_i^t are then split into one part representing additional fuel requirements and one part for the wear-and-tear costs. The parameters of the start-up costs V_i and F_i have to be adjusted and only represent additional fuel costs then.

Including heating-speed dependent wear-and-tear costs in UC can change operations: while fast start-ups were the best option for keeping additional fuel consumption at lowest level, when including the start-up type depending wear-and-tear costs, slower

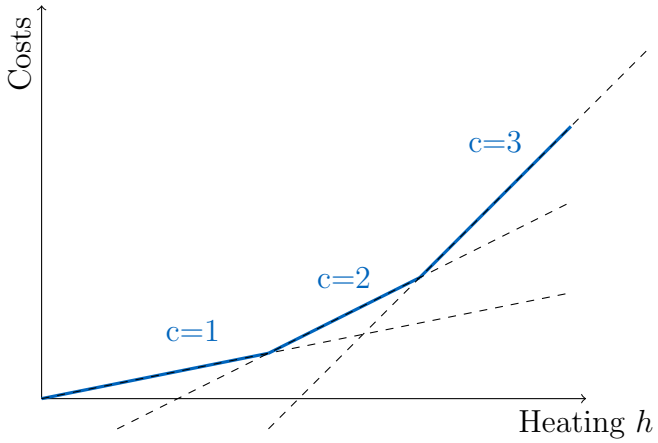

Figure 4.13: Exemplary illustration of wear-and-tear costs with number of lines $|\mathcal{C}| = 3$
.

start-ups can be the better option. In stochastic optimization, the effects of including variable wear-and-tear costs can be even more interesting: Postponing the start-up process leads to higher costs when power plants need to be started unexpectedly.

4.8 The Hot State - Reserves from Off-line Plants

While the percentage of electricity provided by thermal power plants tends to decrease, the requirements for flexibility in form of reserves are increasing. Ideas to bring power plants into an idle state where non-spinning reserves can be provided while no (or only very little) electricity is produced are being discussed at present [151]. An important variable in this technical discussion is the temperature of the plants; only plants that are kept in a very hot state can start quickly enough to contribute to reserves, i.e. tertiary reserves. Morales-España et al. [151] consider off-line units for tertiary reserves in their model by adding binary variables for units providing those reserves. The same can be done in the temperature model of this thesis. In this case, an additional state – the binary "hot" state w_i^t – is introduced. Considering such an extra state causes rising computational complexity. However, in future power systems and with further improved power plants, such a "hot" state could become more important. In our model, the constraint for a unit to change into "hot" state is the same as for the on-line state. The temperature has to equal one or the power plant has to be able to reach the temperature of one within x-minutes. The available time of x-minutes depends on the reserves types, e.g. 15 minutes for tertiary reserves in Germany. This constraint may be formulated as

$$\mathrm{w}_i^t \leq \mathrm{temp}_i^t + \Delta\mathrm{temp}_i^{\max} \cdot \frac{x}{60}, \tag{4.55}$$

with $\Delta\mathrm{temp}_i^{\max}$ being the maximally allowed temperature change within one hour.

A further constraint is required to guarantee that a power plant can either be in the "hot" state or in the on-line mode and given by

$$\mathrm{w}_i^t + v_i^t \leq 1. \tag{4.56}$$

A further discussion and additional constraint for considering non-spinning reserves is discussed in Section 5.3.2

4.9 Modeling of Power Flow and Flexible Transmission

In order to evaluate the effects of enhanced flexibility in realistic test systems like the European continental system or the German system, a suitable representation of the transmission grid must be found. This section gives an overview of different possible approaches and describes the applied methodology for load flow computations including the consideration of flexible transmission elements like phase shift transformers.

4.9.1 Overview of Load Flow Modeling Approaches

There are several possible approaches and levels of details that can be applied for transmission modeling:

Full AC modeling The basic formulation for the power flow on line $m \in \mathcal{L}$ between two nodes $a, b \in \mathcal{N}$ can be described by equations (4.57), (4.58) (for a detailed description and derivation see e.g. Andersson [5] or Kundur [129]):

$$f^L_{a,b} = V_a V_b \left(G_{ab} \cdot \cos(\delta_a - \delta_b) + B_{ab} \cdot \sin(\delta_a - \delta_b)\right), \tag{4.57}$$

$$q^L_{,ab} = V_a V_b \left(G_{ab} \cdot \sin(\delta_a - \delta_b) + B_{ab} \cdot \cos(\delta_a - \delta_b)\right). \tag{4.58}$$

In those equations, V is the voltage at each node, G is the conductance, and B is the susceptance of the lines. The difference in the phase angle is noted as $\delta_a - \delta_b$, the active flow as $f^L_{a,b}$, and the reactive flow is noted as $q^L_{a,b}$. These equations are nonlinear and must be simplified in order to be used in large-scale UC modeling.

DC modeling with angles A very common approach for simplified load flow modeling is the so-called DC modeling framework. Only active power is considered and voltage differences are neglected ($V_a \approx V_b$). As a further simplification, the reactive flow is assumed to be compensated and thus not considered anymore. Furthermore, the angle differences $\delta_a - \delta_b$ are assumed to be very small, which leads to:

$$\sin(\delta_a - \delta_b) \to (\delta_a - \delta_b), \qquad \text{for small angle differences.} \tag{4.59}$$

Assuming equal voltage at all nodes in the system by $V_a = V_b = V_0$, the (active) DC load flow can be formulated by

$$f^L_{a,b} = V_0^2 \cdot B_{ab} \cdot (\delta_a - \delta_b). \tag{4.60}$$

For a networked system, all flows can be described in matrix notation with the diagonal matrix (index d) of the susceptances $\boldsymbol{B}_d$, the incidence matrix $\boldsymbol{A}$, and the angles at all nodes $\boldsymbol{\delta}$ as

$$\boldsymbol{f}^L = V_0^2 \cdot \boldsymbol{B}_d \cdot \boldsymbol{A} \cdot \boldsymbol{\delta}. \tag{4.61}$$

When implementing this formulation, the angle at each node is a variable in the optimization process. The usefulness of the DC model for techno-economic power system simulations was, for instance, shown by Van Hertem et al. [94].

DC modeling with PTDF The variable δ_N can be replaced by a set of equalities in a formulation using so called power transfer distribution factors (PTDF). This formulation is often applied in UC models whenever grid constraints are considered. The concept is widely used and the description given here is mostly built on Van den Bergh et al. [18]. The basic idea is to formulate the balance of each node, the nodal flow f_a^N, by

$$f_a^N = V_0^2 \sum_{b \in \mathcal{N}, b \neq a} B_{ab}(\delta_a - \delta_b) \qquad \forall a \in \mathcal{N}, \tag{4.62}$$

and in matrix notation by

$$\boldsymbol{f}^N = V_0^2 \cdot \boldsymbol{A}^T \cdot \boldsymbol{B}_d \cdot \boldsymbol{A} \cdot \boldsymbol{\delta}. \tag{4.63}$$

By combining (4.61) and (4.63), the angles can be replaced leading to a formulation where the flow on each line $\boldsymbol{f}^L$ depends on the feed in on each node $\boldsymbol{f}^N$

$$\boldsymbol{f}^L = ((V_0^2 \cdot \boldsymbol{B}_d \cdot \boldsymbol{A})(V_0^2 \boldsymbol{A}^T \cdot \boldsymbol{B}_d \cdot \boldsymbol{A})^{-1}) \cdot \boldsymbol{f}^N. \tag{4.64}$$

The voltage level V_0^2 is a scalar that can be cancelled out. This simplifies the line flow to

$$\boldsymbol{f}^L = ((\boldsymbol{B}_d \cdot \boldsymbol{A})(\boldsymbol{A}^T \cdot \boldsymbol{B}_d \cdot \boldsymbol{A})^{-1}) \cdot \boldsymbol{f}^N. \tag{4.65}$$

The impact of nodal feed-in (nodal flow) on the line flow is represented by the matrix of power transfer distribution factors **PTDF** which can be defined as

$$\mathbf{PTDF}^{|\mathcal{L}|\mathrm{x}|\mathcal{N}|} = (\boldsymbol{B}_d \cdot \boldsymbol{A})(\boldsymbol{A}^T \cdot \boldsymbol{B}_D \cdot \boldsymbol{A})^{-1} \tag{4.66}$$

with dimension number of lines $|\mathcal{L}|$ times number of nodes $|\mathcal{N}|$. The power flow formulation with **PTDF** is then stated as

$$\boldsymbol{f}^L = \mathbf{PTDF} \cdot \boldsymbol{f}^N. \tag{4.67}$$

The **PTDF** contains values that reflect the effect of a feed-in at each single node on the entire resulting line flows. For each network, a slack node has to be defined (multiple slack nodes are required to model Europe with its DC lines, see the paragraph on modeling DC lines in Section 4.9.2 for further details). The slack node is required as the system of equations would otherwise be linearly dependent, which results in a determinant of $(\boldsymbol{A}^T \cdot \boldsymbol{B}_D \cdot \boldsymbol{A})$ being zero and a singularity of its inverse. Slack nodes are incorporated by deleting rows and columns in $\boldsymbol{B}_d \cdot \boldsymbol{A}$ and $\boldsymbol{A}^T \cdot \boldsymbol{B}_D \cdot \boldsymbol{A}$ as follows:

- $\boldsymbol{B}_d \cdot \boldsymbol{A}$: This is a matrix of size $|\mathcal{L}|\mathrm{x}|\mathcal{N}|$, the column of each slack node has to be replaced by zeros.

- $\boldsymbol{A}^T \cdot \boldsymbol{B}_D \cdot \boldsymbol{A}$: This is a matrix of size $|\mathcal{N}|$x$|\mathcal{N}|$, the column and the line corresponding to each slack node has to be replaced by zeros.

The equation can be written in index notation by

$$f^t_{m,AC} = \sum_{n \in \mathcal{N}} \text{PTDF}^m_n \left[\sum_{i \in \mathcal{I}_n} p^t_i + \sum_{s \in \mathcal{S}_n} \text{ps}^t_s - D^t_n \right] \qquad \forall t \in \mathcal{T}, m \in \mathcal{L}, \tag{4.68}$$

with $\left(\sum_{i \in \mathcal{I}_n} p^t_i + \sum_{s \in \mathcal{S}_n} \text{ps}^t_s - D^t_n\right)$ being the nodal net injection / nodal flow at node n and $f^t_{m,AC}$ being the line flow over AC lines.

When applying the DC modeling framework with the **PTDF**, two constraints need to be considered in addition to the power flows according to equation (4.68). The sum of all net injections $f^{t,N}_a$ must equal zero in all periods by

$$\sum_{a \in \mathcal{N}} f^{t,N}_a = 0, \qquad \forall t \in \mathcal{T}, \tag{4.69}$$

and the power flow over each line must stay within its limits:

$$-f^{L,\max}_m \leq f^t_{m,AC} \leq f^{L,\max}_m \qquad \forall t \in \mathcal{T}, m \in \mathcal{L}. \tag{4.70}$$

Transport modeling In the transport modeling framework, electricity can be transported like any physical good without consideration of phase angles. This is the simplest approach and is suitable for transmission extension optimization, which requires high computational efforts. Since it is not applied in the models described in this thesis, the reader is referred to other studies, e.g. Schaber et al. [181] apply the approach to study cost-optimal grid extensions in Europe.

Modeling losses There are several approaches for modeling losses in power sytems. Often, quadratic losses are assumed and modeled by a piecewise linear approach, e.g. [53, 139]. The idea that loss minimization is a physical principle which is also leading to the basic DC flow equations is described by Ahlhaus and Stursberg [4]. Therein, piecewise linear approximated losses are used to better approximate power flows in a capacity extension model. For all models analyzed in this thesis, losses are neglected since the focus of the analysis lies in the flexibility adequacy of the system.

4.9.2 Flexible Elements in the Transmission Grid

Adding flexibility to the power system is not restricted to enhancing generation or storage but can also be incorporated in the grid itself. Flexibility in the grid does not yield advantages in the time domain but in the spatial domain by allowing a control of the interregional power flows. Two major ideas are described: the introduction of high voltage DC lines (HVDC) and the introduction of phase shift transformers (PSTs).

High voltage DC lines HVDC lines connect two nodes by an AC-DC and a DC-AC converter that are fully controllable. Electricity can be transported from one node to another according to a predefined schedule.

The basic idea of modeling HVDC lines in the DC modeling approach is to subtract the power that is fed to the AC-DC converter from the total nodal injection P_N by

$$\boldsymbol{f}_{AC}^{N} = \boldsymbol{f}^{N} - \boldsymbol{f}_{DC}^{N}. \tag{4.71}$$

The nodal injections to the DC line and the line flow are related with the transposed incidence matrix of all DC lines $\boldsymbol{A}_{DC}^{T}$ according to

$$\boldsymbol{f}_{DC}^{N} = \boldsymbol{A}_{DC}^{T} \cdot \boldsymbol{f}_{DC}^{L}. \tag{4.72}$$

Combining those two equations shows the effect of DC flows on nodal AC flows by

$$\boldsymbol{f}_{AC}^{N} = \boldsymbol{f}^{N} - \boldsymbol{A}_{DC}^{T} \cdot \boldsymbol{f}_{DC}^{L}. \tag{4.73}$$

The basic equation of the PTDF formulation in Section 4.9.1 was

$$\boldsymbol{f}_{AC}^{L} = \mathbf{PTDF} \cdot \boldsymbol{f}_{AC}^{N}. \tag{4.74}$$

Replacing $\boldsymbol{f}_{AC}^{N}$ by the formula of equation (4.73) leads to

$$\boldsymbol{f}_{AC}^{L} = \mathbf{PTDF} \cdot \boldsymbol{f}^{N} - \mathbf{PTDF} \cdot \boldsymbol{A}_{\boldsymbol{DC}}^{T} \cdot \boldsymbol{f}_{DC}^{L}, \tag{4.75}$$

and to the definition of the so-called direct current distribution factor (DCDF) matrix (an equivalent to PTDF matrix in functionality but applied for the DC lines) by

$$\mathbf{DCDF} = -\mathbf{PTDF} \cdot \boldsymbol{A}_{DC}^{T}. \tag{4.76}$$

For a matrix-vector notation of an example grid, the reader is referred to Van den Bergh et al. [18].

Phase shift transformers (PSTs) Another possibility for increasing the system flexibility is the introduction of PSTs which allow for a partial routing of electricity in the grid. PSTs can change the angle between two nodes by the phase shift angle which is modeled by the variable psa_m. More details on the underlying technology can be found e.g. in Verboomen et al. [204]. The equations describing the load flow including the phase shift of psa_m can be formulated as [18]:

$$f_{a,b}^{L} = V_0^2 B_{ab}(\delta_a - \delta_b + \text{psa}_{ab}) \tag{4.77}$$

and in matrix notation as

$$\boldsymbol{f}^{L} = V_0^2 \cdot \boldsymbol{B}_d \cdot \boldsymbol{A} \cdot \boldsymbol{\delta} + V_0^2 \cdot \boldsymbol{B}_d \cdot \boldsymbol{psa}. \tag{4.78}$$

Following [18], the equations can be written for nodal balances as

$$f_a^N = V_0^2 \sum_{b \in \mathcal{N}, b \neq a} B_{ab}(\delta_a - \delta_b + \text{psa}_{ab}), \tag{4.79}$$

and in respective matrix notation as

$$\boldsymbol{f}^N = V_0^2 \cdot (\boldsymbol{A}^T \cdot \boldsymbol{B_d} \cdot \boldsymbol{A}) \cdot \boldsymbol{\delta} + V_0^2 \cdot (\boldsymbol{B_d} \cdot \boldsymbol{A})^T \cdot \boldsymbol{psa}. \tag{4.80}$$

By combining (4.78) and (4.80) (analog to the reformulation as described in equation (4.64)), the line flow can be described by

$$\begin{aligned} \boldsymbol{f}^L = &\left((V_0^2 \cdot \boldsymbol{B}_d \cdot \boldsymbol{A})(V_0^2 \cdot \boldsymbol{A}^T \cdot \boldsymbol{B}_D \cdot \boldsymbol{A})^{-1})\right) \cdot \boldsymbol{f}^N \\ &+ \left(V_0^2 \cdot \boldsymbol{B}_d - (V_0^2 \cdot \boldsymbol{B}_d \cdot \boldsymbol{A})(V_0^2 \cdot \boldsymbol{A}^T \cdot \boldsymbol{B}_D \cdot \boldsymbol{A})^{-1}) \cdot (V_0^2 \cdot \boldsymbol{B}_d \cdot \boldsymbol{A})^T\right) \cdot \boldsymbol{psa}. \end{aligned} \tag{4.81}$$

Inserting the definition of the **PTDF** according to (4.66) and shortening the voltage level where possible leads to

$$\boldsymbol{f}^L = \mathbf{PTDF} \cdot \boldsymbol{f}^N + V_0^2 \cdot \left(\boldsymbol{B}_d - \mathbf{PTDF} \cdot (\boldsymbol{B}_d \cdot \boldsymbol{A})^T\right) \cdot \boldsymbol{psa}. \tag{4.82}$$

Finally, a matrix of phase shift distribution factors (PSDF), which indicates the changes of flows that are induced by a phase shift on one line to all other lines in the network, can be defined by

$$\mathbf{PSDF}^{|\mathcal{L}|\mathrm{x}|\mathcal{L}|} = \boldsymbol{B}_d - \mathbf{PTDF} \cdot (\boldsymbol{B}_d \cdot \boldsymbol{A})^T. \tag{4.83}$$

It is important to note that the PSDF matrix as defined must be multiplied by V_0^2 to transform the resulting power flows into Watts. Additionally, the values must be divided by 57.3 when *psa* is given in degrees instead of radians (see equation (4.84)-(4.85)).

Van Hertem et al. [94] investigated the usefulness of analyzing the impact of PSTs within the simplified DC modeling framework. The authors compared the load flows of a test system with PSTs in the full AC case to the simplified DC version and found a small increase of the error through introduction of PSTs. Their conclusion was that the error is small enough that the simplified DC flow is suitable for testing PSTs as done in this thesis.

Complete power flow equations Combining all definitions and elements of the power flow equations that allow to include DC lines as well as PSTs and setting the voltage to $V_0 = 380$ kV leads to

$$\boldsymbol{f}^L_{AC} = \mathbf{PTDF} \cdot \boldsymbol{f}^N + \frac{380000^2}{57.3} \mathbf{PSDF} \cdot \boldsymbol{psa} + \mathbf{DCDF} \cdot \boldsymbol{f}^L_{DC}. \tag{4.84}$$

The equation can be written in index notation and by transforming the power unit from [W] to [MW] by

$$\begin{aligned} f^t_{m,AC} = &\sum_{n \in \mathcal{N}} \mathrm{PTDF}^m_n \left[\sum_{i \in \mathcal{I}_n,} p^t_i + \sum_{s \in \mathcal{I}_n} \mathrm{ps}^t_s - D^t_n\right] + \frac{380^2}{57.3} \sum_{m' \in \mathcal{L}_{AC}} \mathrm{PSDF}^m_{m'} \cdot \mathrm{psa}_{m'} + \\ &\sum_{m' \in \mathcal{L}_{DC}} \mathrm{DCDF}^m_{m'} \cdot f^t_{m',DC}, \qquad \forall m \in \mathcal{L}_{AC}, t \in \mathcal{T}, \end{aligned} \tag{4.85}$$

where the set of lines $\mathcal{L}$ is split into AC lines and DC lines, $\mathcal{L}_{AC} \cup \mathcal{L}_{DC} = \mathcal{L}$.

The principle of all matrices, i.e. **PTDF**, **DCDF**, **PSDF** is similar. Their elements are factors that indicate the effect of a change of a nodal feed-in (**PTDF**), a change in DC flow in DC lines (**DCDF**), or a change in phase angle of all lines with phase shifters (**PSDF**) on the considered line m. Concerning the change in phase angles, the elements of the PSDF matrix must be multiplied by a scalar, in the case of this thesis given by $380^2/57.3$. For general purposes, the entire system of equations can also be computed in per-unit values. In this case, the PSDF must be multiplied by the power base [18].

Synchronous vs. asynchronous systems The calculation of the power distribution factors as described above assumes a power grid where all nodes are located within one synchronous zone. However, the European system comprises five subzones (see Fig.4.14) that are not synchronous but only connected via DC links. In order to consider this fact, a slack node must be incorporated for each zone and included in the computation of the **PTDF**. In mathematical terms, this is achieved by deleting columns of slack nodes in $\boldsymbol{B}_D \cdot \boldsymbol{A}$ and columns and lines of respective slack nodes in $\boldsymbol{A}^T \cdot \boldsymbol{B}_D \cdot \boldsymbol{A}$ (see Section 4.9.1) and inserting zeroes in the resulting PTDF matrix. Power flows in one synchronous zone do not affect flows in another zone despite the controllable electricity transmission via DC links. Hence, the import of electricity by DC links into one region can be considered in the same way as generation in the importing region.

The constraint for the sum of all net injections being zero (equation (4.69)) must hold separately for each synchronous zone. In addition to the five synchronous areas in Europe that are shown in the map of Fig.4.14), two additional zones are incorporated for Corsica and Sardinia as they are connected to the continent by DC lines.

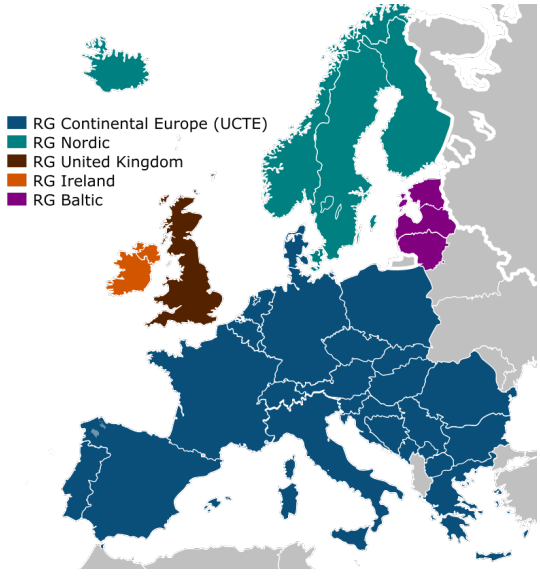

Figure 4.14: The synchronous grids of Europe: map of the European network of transmission system operators for electricity. Image: Wikimedia Commons [208]

4.9.3 Zonal Approach

In the model used for the numerical studies presented in Chapter 7, zones are defined for Europe. In order to reduce complexity and due to data availability, Europe is

divided into 268 zones according to the NUTS classification (see Section 6.1) and only interzonal transmission is considered. Estimating an adequate PTDF matrix for this reduced grid is a complicated task and methods for grid reductions are discussed for example by Van den Bergh et al. [18] or Hasche [88].

Computation of zonal PTDFs A common approach is to compute the zonal PTDF with a model comprising the entire grid topology. One zone is defined as the reference zone and effects of transmission from each other zone to this reference zone are computed with the complete, original grid. By using the transitivity of the PTDF matrix, the results of flows from each region to the slack node/zone are enough for constructing a zonal PTDF (see e.g. Duthaler [55]). As alternative, Van den Bergh [18] suggests an approach where a zonal PTDF is computed directly from the nodal PTDF by several matrix operations.

The approach applied in this thesis (see Chapter 6 on dataset development) is to count all lines that cross regions and to define an equivalent circuit. The simplicity and the reduced requirement on grid data are major reasons for this choice. Future research must evaluate and compare this simple approach to the more complex methods described above. In general, the usefulness of reducing a system into regions and employing zonal PTDFs is still discussed in the scientific community.

Discussion of applicability of zonal models The application of zonal DC modeling / zonal PTDF leads to some problems and inaccuracies. Hogan [99] argues that zonal models should not be employed for real-time operations as not all congestions are considered correctly and market power might be exercised. Furthermore, prices are not correct and the simplifications in trading are not observed as promised. Baldick et al. [7] analyzed the effects of zonal PTDFs for Texas and showed that erroneous results will lead to wrong incentives and thus to an inefficient market allocation. Duthaler [54, 55] discussed the application of zonal PTDFs for a European system. The author showed that the aforementioned arguments are also true for the European system.

All of these studies analyzed the applicability of zonal PTDFs for realtime operations. In this thesis however, off-line simulations that will give insights into further planning and future investments are analyzed. Additionally, Duthaler [55] reduced the European grid to zones for each country which is less accurate than the partition according to NUTS. The smaller the zones, the fewer intrazonal congestion is expected, and in turn the higher the correctness of the zonal PTDFs [7].

Due to computational limits, a reduction of the European grid is necessary when including the grid constraints into a UC model (see also Van den Bergh et al. [18]). Still, the DC model will still show more realistic results than a simple transport model. The improvements of zonal DC models over transport models are discussed by Hasche [88] and a superiority of applying a zonal DC model over simple transport models is shown. Especially in situations with high wind penetration, when transportation is important, the zonal DC model resembles the real system behavior more accurately.

Another strong argument to use the DC modeling framework in this thesis is that the

dataset that is developed (see Chapter 6) is regarded as a stylized real power system. Its realistic behavior and general system properties are more essential than the exact representation of the European system - which is not fully possible in reduced models anyway. Hence, the focus in the interpretation of results in this thesis is giving general understandings on a networked power system with high shares of fluctuating generation but not necessarily concrete policy recommendations for individual line upgrades.

In real world systems, operators must consider contingencies in their operational planning. A commonly used method is computing so-called outage transfer distribution factors (OTDF), which can be interpreted as PTDFs for a post contingency state [40,192]. Computation of such OTDFs for the reduced power system and considering thermal contingency constraints seems to be a promising option for future research. So far, the security constraints (N-1) are approximated by reducing the maximal line capacities to 70% of the computed transmission limit.

4.10 Modeling of Storage

Another crucial and concurrent source of flexibility in power systems is storage. Storage has several aspects that need to be considered: a maximum power (can be negative and positive), a maximum storage content, and a ramping speed for power output. Model equations can be formulated as follows:

- The supply-demand equation (4.11) changes by adding the storage power to

$$\sum_{i \in \mathcal{I}} p_i^t + \sum_{s \in \mathcal{S}} \mathrm{ps}_s^t = D^t \qquad \forall\, t \in \mathcal{T}. \tag{4.86}$$

- The power output of the turbine ($\mathrm{ps}_s^t > 0$) and the pump ($\mathrm{ps}_s^t < 0$) has to be within boundaries of a maximum pump capacity ($-PS_s^{\max}$) and maximal turbine capacity ($PS_s^{\max}$), which are assumed to be identically at

$$-PS_s^{\max} \leq \mathrm{ps}_s^t \leq PS_s^{\max} \qquad \forall\, t \in \mathcal{T}, s \in \mathcal{S}. \tag{4.87}$$

- The storage content develops over time according to

$$\mathrm{es}_s^t = \mathrm{es}_s^{t-1} - \mathrm{ps}_s^t \qquad \forall\, t \in \mathcal{T}, s \in \mathcal{S}. \tag{4.88}$$

- The content must always be within its boundaries which is guaranteed by

$$0 \leq \mathrm{es}_s^t \leq ES_s^{\max} \qquad \forall\, t \in \mathcal{T}, s \in \mathcal{S}. \tag{4.89}$$

In the case that storage plays a part in providing reserve power, additional constraints must be considered. They are explained in Section 5.3.

4.11 Modeling of Demand Side Management

In this last section on modeling, the inclusion of demand side management (DSM) is described. DSM is often perceived to be a promising possibility to counterbalance fluctuations [194]. Depending on the country, there are different promising options like cooling, heating, industrial appliances, household appliances and many more. A frequently discussed option is the usage of electric vehicles (EVs). Charging EVs offers great flexibility in demand as cars are parked for most of the time (e.g. Kempton and Tomic [120] state that cars are only used in 4% of the time for transportation). Incorporating flexible demand in UC modeling is being researched at present and different approaches have been developed. Madzharov et al. [142] describe an approach where 7 groups of EVs are considered according to their driving and charging patterns. Charging control is incorporated in the UC decision making and allows to shift charging to times with lowest electricity generation costs. The approach developed within the research of this PhD thesis [112] is comparable to the one described by Madzharov et al. [142] but with a larger number of groups considered. Its basic idea is that EVs want to recharge their battery as much as possible during each parking period. To fulfill this task, an aggregator (e.g. a parking lot) can decide when the charging takes place within this possible time slot depending on market prices. In the model, a perfect market outcome is considered by directly including the charging decisions into the UC model.

Fur this purpose, a flexible load from EVs, the charging load cl^t, is added to the demand D^t and the sum has to be provided by the power plants according to

$$\sum_{i \in \mathcal{I}} p_i^t = D^t + \mathrm{cl}^t \qquad \forall\, t \in \mathcal{T}. \tag{4.90}$$

The flexible charging load can be shifted within boundaries that result from the parking behavior of EVs. Fig. 4.15 exemplarily illustrates the parking times of several EVs over the modeling horizon of 36 hours. After each parking process, EVs should be fully charged. When considering all EVs within a larger power system, e.g. a whole country, a large number of cars with different parking processes each must be considered. In order to reduce complexity, all parking processes with the same start and end time are summarized. For an illustration of this approach, the bars representing identical behavior are highlighted with identical colors that deviate from the standard light blue tone in Fig. 4.15. In addition, the maximal considered parking duration is limited to 24 hours. During this time, EVs must be charged even though their parking time might be longer.

With this reduction of complexity, $|\mathcal{T}|$ possible arrival times remain, which can be combined with 24 different options for the parking duration. A table of values $CT(t_a, t_p)$ for each pair of t_a and t_p is the major input to the flexible charging model. In order to guarantee that EVs are charged according to this table, the sum of charging loads $\mathrm{cl}^t_{\mathrm{aux}}(t_a, t_p)$ over all modeled time steps t_m from the arrival time t_a to the end of parking

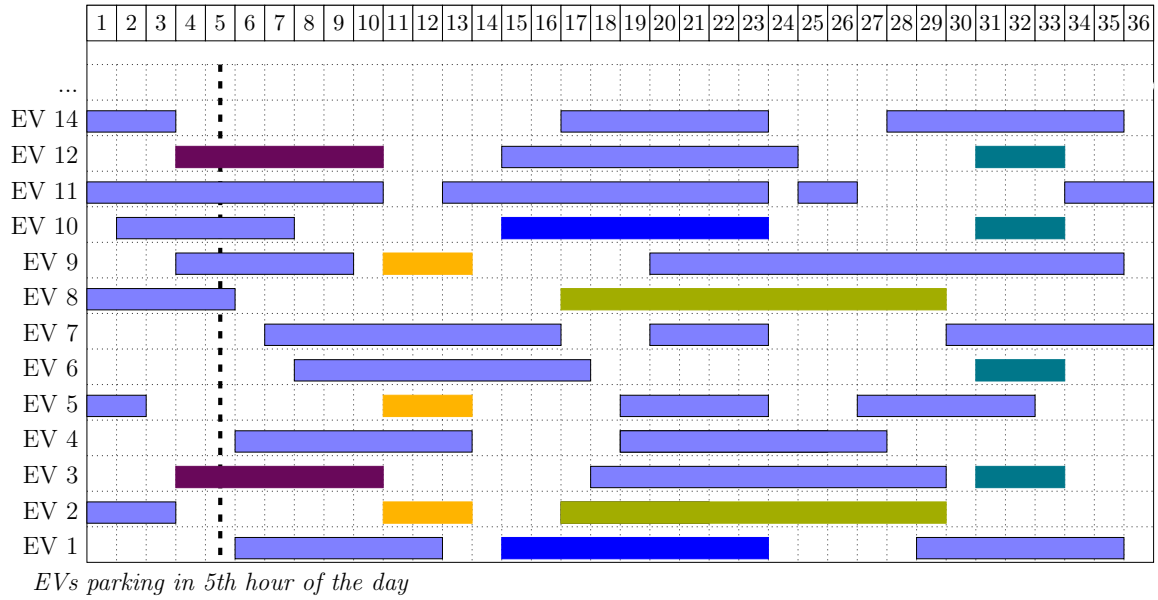

Figure 4.15: EV parking durations. The different EVs are illustrated on the y-axis and their parking behavior on the x-asis. The colored bars indicate that the EV is parking during the respective time frame.

at $t_a + t_p - 1$ has to equal the respective value from the charging table:

$$CT(t_a, t_p) = \sum_{t=t_a}^{t_a+t_p-1} \mathrm{cl}^t_{\mathrm{aux}}(t_a, t_p), \quad \forall t_a \in \mathcal{T}_a, t_p \in \mathcal{T}_p, \tag{4.91}$$

with $\mathcal{T}_a = \mathcal{T}$ and $\mathcal{T}_p = 1, 2, ..24$.

In order to compute the charging load as a function of modeling periods t only, the sum over all arrival times t_a and parking durations t_p is computed by

$$\mathrm{cl}^t = \sum_{t_a \in \mathcal{T}_a} \sum_{t_p \in \mathcal{T}_p} \mathrm{cl}^t_{\mathrm{aux}}(t_a, t_p) \qquad \forall t \in \mathcal{T}. \tag{4.92}$$

As an approximation for the maximal charging capability of the connected EVs, this load over all EVs must be below a maximal charging load $CL^{t,\max}$, which is computed by the number of EVs parking, their maximal charging power, and some factor for security margin, leading to

$$\mathrm{cl}^t \leq CL^{t,\max} \qquad \forall t \in \mathcal{T}. \tag{4.93}$$

The approach is computationally extensive and data on behavior of agents is required. It is therefore not included in the large-scale models of the European and German power system in Chapter 7. Test calculations applying the methodology were conducted for a model of Singapore [112]. Three different charging strategies were tested: full charging at arrival until fully charged ("Dumb Charging"), charging with equal power over the entire parking period ("Mean Charging") and charging according to UC cost optimization ("Smart Charging"). The basic results and effects from applying "Smart Charging" are illustrated by Fig. 4.16 and summarized to:

- Peak load is reduced compared to “Mean” and “Dumb” charging.
- Load develops into a step function that reflect the optimal operating points of thermal power plants.
- Flexibility allows for more efficient power plant operation and leads to a reduction of costs and CO_2 emissions.

The electricity demand for “Mean” and for “Dumb” are very similar which is in contrast to other research (e.g. Kefayati [119]). Reasons for this lie in the constraints that require EVs to be fully charged after each parking event and the possibly smaller mileage of cars in Singapore compared to Texas or other states/countries. Other parameters and different constraints for charging like charging only at home might alter the results significantly and should analyzed in future research.

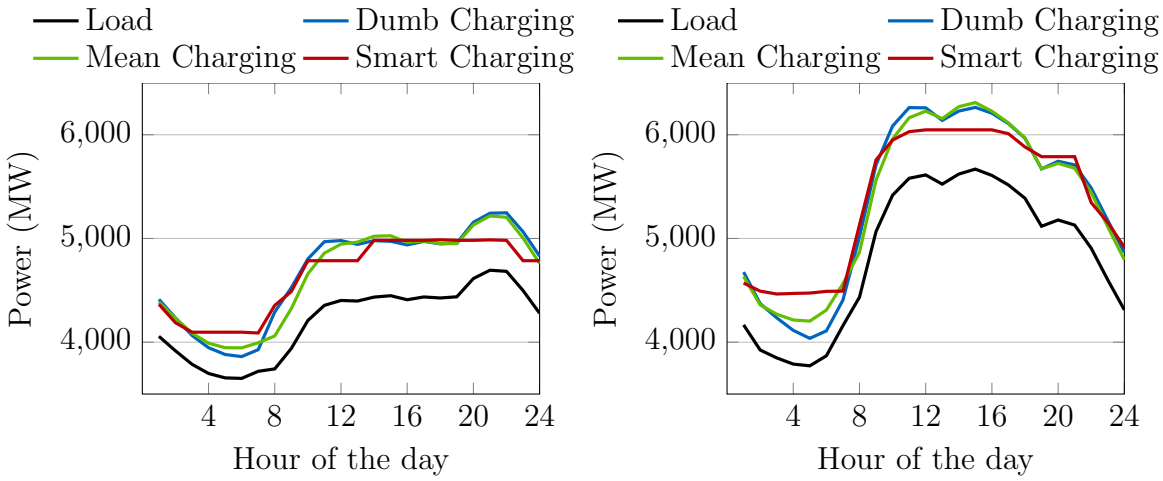

Figure 4.16: Comparison of electricity demand with different EV charging strategies in Singapore. On the left: a typical Sunday, on the right: a typical weekday.

Chapter 5

Uncertainty in Power System Operation

Power systems had to handle uncertain events since the very beginning of electrification. Power plant or line tripping incidents occurred and operators had to balance those unexpected events [114]. Even though load predictions were never accurate, accuracy increased over time reaching a forecast error of 1-2% in most modern power systems today [34]. Forecast accuracy decreased slightly from a standard deviation of 1.7% of peak load to more than 2% of peak load after liberalization in Germany. However, new techniques that promise to reestablish formerly known forecast quality are developed [29]. While the quality of forecasts has increased over time, more uncertain production has been integrated at the same time, bringing uncertainty management (again) high on the agenda of power system operators [138].

Based on the modeling framework as described in Chapter 4, this chapter provides some approaches of how to deal with the challenge of uncertainty. Uncertainty in operational planning means future generation can only be predicted with a certain error, e.g. in the form of multiple possible scenarios or a bandwidth of generation. Fig. 5.1 schematically illustrates a forecasting approach with multiple scenarios. The red line in the figure represents the actual wind power production (ex post) while the

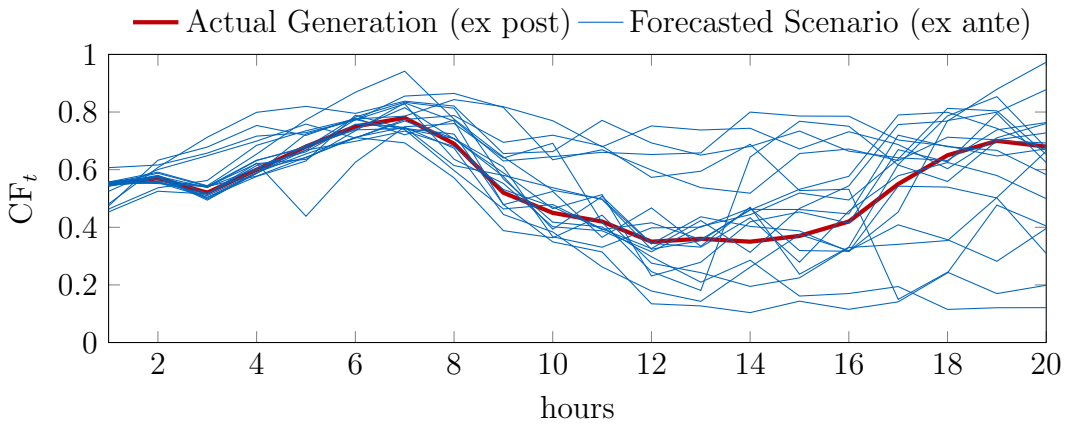

Figure 5.1: Exemplary illustration of uncertain VRE generation and possible forecasts

blue lines denote possible scenarios (ex ante). Research must not only provide point forecasts (one single scenario), but it should also specify ranges and the likelihood of those forecasts [166]. Depending on the quality and characteristic of the forecasts, the computational capacities, and the operational schemes, different strategies for incorporating uncertain information into daily planning can be considered.

In this chapter, several concepts are introduced that allow analyzing the additional challenges arising from the uncertainty in the system. The most prominent of them are applied within the numerical studies of Chapter 7. Considering the modeling concepts introduced, this chapter also points out the advantages of the temperature model developed in Chapter 4 that can be realized once uncertainty is considered in future research and planning.

5.1 General Classification of Approaches to Manage Uncertainty

Handling uncertainty requires decisions in the present with respect to a future that is unknown or only known imprecisely. In power systems, many actors are faced with decision making under uncertainty. In systems with a powerful ISO, the operator has to decide which power plants to put on-line a day ahead while load and generation from renewables are uncertain. In decentralized markets, power-producing companies must determine their offers and bids without knowing the behavior of competitors and the resulting price. The decision making process requires policies that define the actions in the current state. According to Powell and Meisel [169–171], four basic policy paradigms can be defined and some of them find applications in power system operation:

- Policy function approximations (PFA): Each possible state in the present is mapped to an action based on look-up tables or on certain parametrized functions. Prominent examples are neural networks that are employed e.g. in control of heating systems in buildings and other small-scale applications.

- Cost function approximation (CFA): The cost function or constraints are adjusted in a way that the system is prepared for uncertain events. The introduction of reserves in power systems is an example for these policies and is described below.

- Value function approximation (VFA): The value of different possible states after the decision is considered in the optimization. In the example of storage operation (given in [171]), the value assigned to having a specific state of charge in a point of time t is defined a priori and considered in the optimization process.

- Lookahead policies: Decisions are based upon expectations about the future development of several parameters/variables. The basic lookahead model assumes a deterministic forecast and optimizes the system accordingly. In a receding manner, actions are taken and forecasts are updated. Forecasts can also be of stochastic nature, which is usually called stochastic optimization in power systems.

For the topic of power system operation, the most common approaches belong to a combination of lookahead policies with cost function approximations. A description of these approaches is given in the next sections. Afterwards, the advantages of including the temperature model to uncertainty modeling are explained.

5.2 Receding Horizon - a Necessary Lookahead Policy

Operational planning in power systems often takes into account future expectations in a receding manner. Constraints like start-up times and storage operation require planning for at least several hours in advance to be able to make rational planning choices. Fig. 5.2 exemplarily depicts decision making with a receding horizon. Thirty-six hours of production are planned in advance but only the first 24 hours are used in the final schedule, while the next 12 hours are recalculated with new information in the next planning step. The reasons for such a modeling and planning process are diverse.

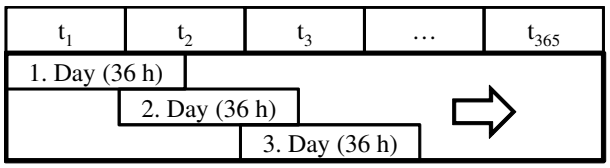

Figure 5.2: Receding horizon in power system planning

In real-world operations, limited and changing information about future events are the major issues requiring lookahead policies, e.g. there is no sense in planning power plant operations for an entire upcoming year on an hourly basis. Price information is not available and operating constraints concern several subsequent hours or days but not entire years, except for dam storage hydro generation or maintenance planning. The latter requires planning of entire years but with lower temporal resolution. When power systems are modeled for system evaluation (as conducted within this thesis), a computational limitation requires dividing a year into smaller optimization problems even though all relevant information for the entire year is available. However, a positive effect of using such receding horizons in system studies is that real world operation is resembled. The receding horizon can also be a first approach to model uncertainty by introducing (partly) changing forecasts (compare Section 5.4).

5.3 Deterministic Approach - Scheduling of Reserves

5.3.1 Basics and Classification

The most basic mechanism to prepare the system for uncertain events is the utilization of ancillary services such as the Automatic Generation Control (AGC) and the speed control (see Section 2.5). Often, ancillary services are divided into primary, secondary,

and tertiary control, which must be scheduled in addition to energy. The first two are spinning reserves which means that only power plants that are on-line are allowed to provide them. Tertiary reserve can also be provided by fast-starting units like single cycle gas turbines or units that are kept in a warm status. To give an example of the magnitude of reserves required, Table 5.1 depicts the requirements for the reserve types in Germany.

Table 5.1: Reserves types and their activation time in Germany according to Ziems et al. [213]

	Primary	**Secondary**	**Tertiary**
Reserve required	650 MW	2230 MW	1800/2500 MW (positive/negative)
Activation time	30 sec	5 min	15 min
Delivery period	5 min	30 min	45 min

In terms of the classification given in Section 5.1, the reserve scheduling approach for preparing for uncertain events can be interpreted as a cost function approximation [170, 171]. Additional constraints have to be added to the system that will result in higher system costs while guaranteeing system security. This section describes the required constraints as they are also employed in the numerical experiments of Chapter 7.

Ancillary services have to be provided even in power systems without any VRE generation since load is uncertain and outages can occur at anytime. As soon as variable renewable generation is introduced to the system, the adjustment of those reserves is discussed. One option that is often discussed and applied for scenario calculations, e.g. by Ziems et al. [108, 213], is to increase reserve requirement in times with VRE feed-in. Several studies suggest that reserve requirements will increase with more VRE [59] while the question of calculating the optimal amount remains unanswered. Paradoxically, reserve requirements in many European countries have not been increasing but decreasing with more VRE generation so far [96]. While increased variability might lead to higher requirements on the one hand, some drivers, like improved forecasts, improved scheduling due to 15-minute trading, and transnational and TSO cooperation, amongst others, might reduce requirements on the other hand [96].

For the simulations in this thesis, the AGC approach is considered in its most basic form: primary and secondary reserves must be provided at current levels which are given in Table 5.1. This considers the tradeoff between efforts for reduction and the increase through higher percentages of VRE integration. Tertiary reserves are not considered as they might mostly be provided by off-line plants. The provision of reserves from off-line power plants with their “hot” state is also described below. However, computational limits have led to the decision of neglecting this feature in the large-scale simulations of Chapter 7.

5.3.2 Mathematical Formulation

The requirements $R^t_{o,r}$ for each of the reserve types $r \in \mathcal{R}$ in each control area $o \in \mathcal{O}$ have to be provided by power plants $\mathrm{rv}_i^{t,r}$ or storage $\mathrm{rvs}_s^{t,r}$ in the control area according to equation (5.1). Within the simulations of this thesis, the different reserve types $r \in \mathcal{R}$ include positive and negative primary and secondary reserves. Further reserves can be added without limiting the generality of the equations.

$$\sum_{i \in \mathcal{I}_o} \mathrm{rv}_i^{t,r} + \sum_{s \in \mathcal{S}_o} \mathrm{rvs}_s^{t,r} \geq R^t_{o,r} \qquad \forall t \in \mathcal{T}, o \in \mathcal{O}, r \in \mathcal{R} \tag{5.1}$$

Power plant constraints Power plants are limited in supplying reserves by both capacity and ramp rates. During the full period of offering reserves, the upward/downward ability to ramp and the required capacity needs to be guaranteed.

The scheduled power p_i^t minus the sum of all negative reserves $\mathrm{rv}_i^{t,r}, r \in \mathcal{R}^-$ has to remain above a minimum power output. In the other direction, the sum of scheduled power p_i^t plus the sum of all positive reserves $\mathrm{rv}_i^{t,r}, r \in \mathcal{R}^+$ has to remain below the rated capacity. Furthermore, power plants cannot provide upward reserves in t when they will be shut down in $t+1$, which leads to the following capacity constraints:

$$p_i^t - \sum_{r \in \mathcal{R}^-} \mathrm{rv}_i^{t,r} \geq p_i^{\min} \cdot v_i^t \qquad \forall t \in \mathcal{T}, i \in \mathcal{I}, \tag{5.2}$$

$$p_i^t + \sum_{r \in \mathcal{R}^+} \mathrm{rv}_i^{t,r} \leq P_i^{\max} \cdot v_i^t - (P_i^{\max} - SD_i) z_i^{t+1} \qquad \forall t \in \mathcal{T}, i \in \mathcal{I}. \tag{5.3}$$

The next set of constraints ensures that power plants are capable of providing the required ramps. As stressed by Morales-España et al. [151], the required ramp rates must be available on top of the ramping that is executed for the planned schedules. Fig. 5.3 illustrates the additivity of different ramping tasks.

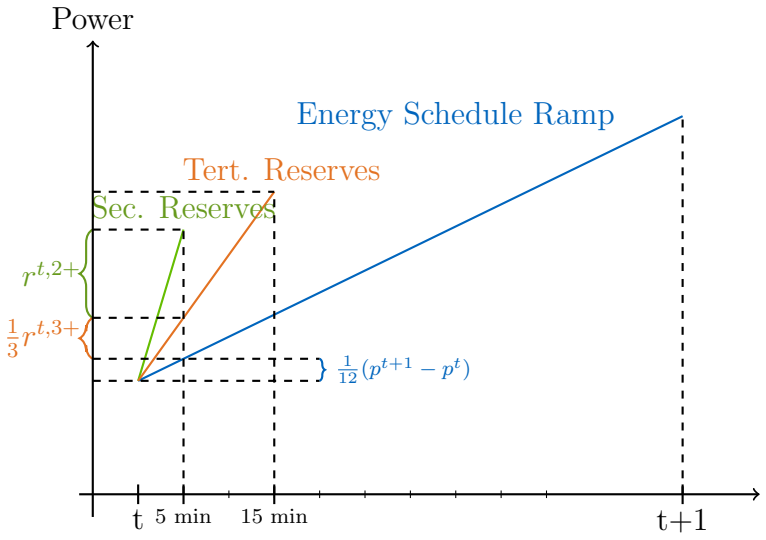

Figure 5.3: Ramping requirements for a power plant with scheduled power increase and provision of positive secondary and tertiary reserves.

The blue line shows the scheduled ramping for meeting the energy schedule in a linear matter. On top, the orange and the green lines represent the ramps for the provision of tertiary reserves and secondary reserves that have to be added. Morales-España et al. [151] assume a power-based UC model and define all constraints for reserves within that paradigm. The power-based approach reflects technical capabilities of the plants more accurately. Energy-based scheduling, however, is still the common practice in most electricity markets and is therefore employed for this thesis. In energy-based scheduling, power plants often ramp even faster than in power-based scheduling in order to fulfill their block bid as accurately as possible. At the same time, they may be able to change the ramping behavior in situations where reserves are activated which makes the definition of constraints a difficult task.

The exact ramping process for the energy ramps depends on the market rules: markets might allow a smooth ramping, schedule 15-min blocks, or force power plants to follow the average hourly power output as closely as possible. In discrete steps, an exact following of the schedule is not possible and a common rule in many markets is to fulfill only the energy requirement. Fig. 5.4 depicts possible generation pathways of a fast unit (blue line) and a slow unit (red line) that both satisfy energy schedules (orange bars) but deviate from the power schedules (hourly average of energy schedules). This figure illustrates the difficulty of finding the exact constraints for the maximally allowed ramping. In the scenarios considered in this thesis, power plants are assumed to ramp up the average power output of the energy schedules from p_i^t to p_i^{t+1} within one hour, which is an optimistic assumption. During this whole ramp-up process, the power plant has to be capable to provide the scheduled reserves.

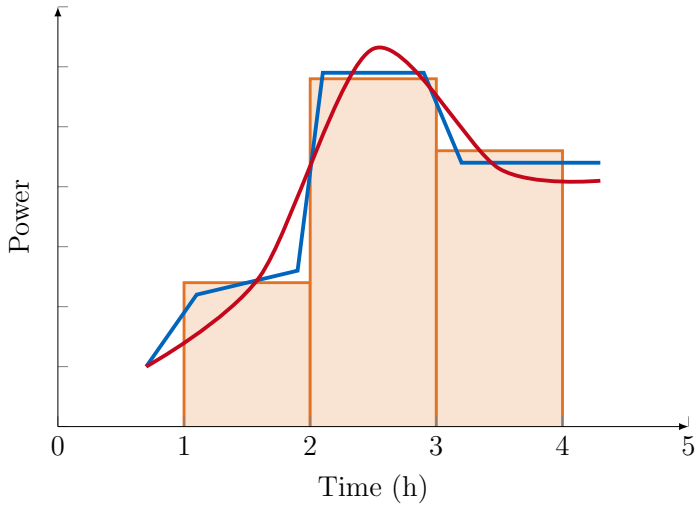

Figure 5.4: Energy schedules and possible behavior of power plants (illustrative only). The blue line shows a power plant that is capable of resembling the block bid reasonably well while the red line symbolizes a power plant with slow ramping that only provides energy over an hour but deviates from the block bid in terms of power. Author's graph based on [61].

According to Fig. 5.3, the complete secondary reserves, one third of the tertiary as well as one twelfth of the scheduled power increase have to be provided after 5 minutes. Thus, the ramp-up capability for those five minutes is restricted by (5.4) and (5.5):

$$\frac{1}{12}(p_{t+1}^i - p_t^i) + \mathrm{rv}_i^{t,\mathrm{sec}^+} + \frac{1}{3}\mathrm{rv}_i^{t,\mathrm{ter}^+} \leq RU_i \cdot 5 \qquad \forall t \in \mathcal{T}, i \in \mathcal{I}, \tag{5.4}$$

$$\frac{1}{12}(-p_{t+1}^i + p_t^i) + \mathrm{rv}_i^{t,\mathrm{sec}^-} + \frac{1}{3}\mathrm{rv}_i^{t,\mathrm{ter}^-} \leq RD_i \cdot 5 \qquad \forall t \in \mathcal{T}, i \in \mathcal{I}, \tag{5.5}$$

with RU_i/RD_i being the maximal possible up/down ramps per minute of a power plant.

For the simulations in this thesis, the constraints are assumed to dominate the ramp requirements after 15 minute ramping. This simplification is valid as long as the maximal ramping speed is the same for the first 15 minutes as for the first five minutes. Due to the conservative parameter assumption used in the scenarios of Chapter 7, it is assumed that power plants can ramp with RU_i/RD_i for the entire hour. If more detailed parameters for power plant ramping are available, different values for 5 min, 15 min, and hourly ramping could be included.

Here, only primary reserves are considered separately, as ramp capabilities for primary reserves RU_i^{prim} and RD_i^{prim} might be higher since plants have to ramp up/down for 30 seconds only. Further, primary reserves are only employed in the extremely short term and are not required anymore after five minutes. The constraint for primary reserves are modeled by

$$\mathrm{rv}_i^{t,\mathrm{prim}^+} \leq RU_i^{\mathrm{prim}} \cdot 0.5 \qquad \forall t \in \mathcal{T}, i \in \mathcal{I}, \tag{5.6}$$

$$\mathrm{rv}_i^{t,\mathrm{prim}^-} \leq RD_i^{\mathrm{prim}} \cdot 0.5 \qquad \forall t \in \mathcal{T}, i \in \mathcal{I}. \tag{5.7}$$

Due to data unavailability, the ramp rates for primary reserves are set to the same value as the overall ramp rates ($RU_i^{\mathrm{prim}} = RU_i$) in the numerical studies. This can be interpreted as a conservative assumption concerning power plant capabilities.

Effects of increased flexibility Depending on the reserve provision of power plants, the remaining range for energy provision is reduced. Fig. 5.5 shows the available capacity for reserve and energy provision and compares different flexibility options for enhancing power plants. The "Base" option depicts the standard version of the power plants with the green area being the operational range when providing primary and secondary reserves. In the "Flex1" setup, the ramp-up/down parameters RU_i/RD_i are increased which allows to provide more reserves. In "Flex2", the minimum power output is reduced which increases the operational range. Finally, in "Flex3", both the ramp rates and the minimum power output are improved. The effects of those flexibility enhancements are evaluated in Chapter 7.

Keeping units warm An advantage of the temperature model introduced in this thesis is that information of the power plant temperature can be used. Whenever a unit is warm enough and in the so-called "hot" state, positive tertiary reserves can be provided (see also Section 4.8).

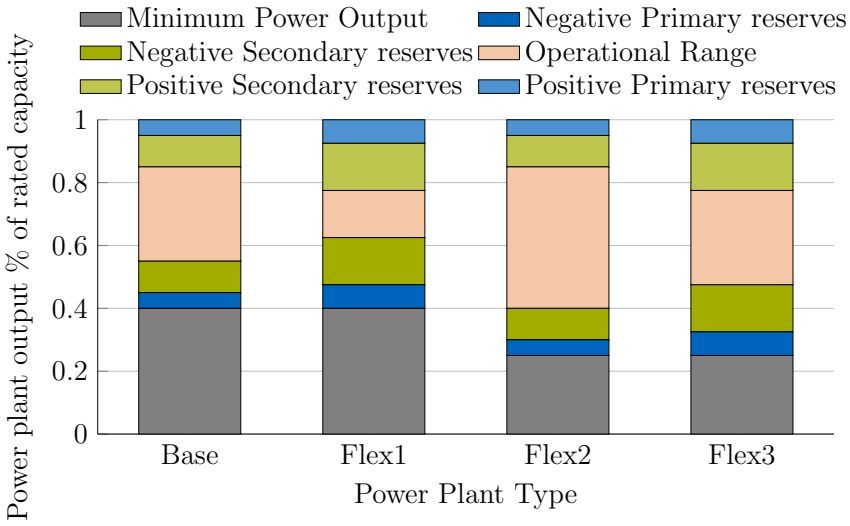

Figure 5.5: Operational range of a power plant with different options for flexibility enhancements. Own illustration based on Ziems et al. [213].

Power plants must be in the "hot" state (w_i^t=1) in order to be able to provide tertiary reserves. The reserves provided by "hot" but off-line power plants are indexed with "stby" for stand-by reserve $rv_i^{t,stby}$, leading to

$$rv_i^{t,stby} \leq w_i^t \cdot P_i^{max} \qquad \forall t \in \mathcal{T}, i \in \mathcal{I}. \tag{5.8}$$

Power plants can only be in the "hot" state whenever starting within the activation time of the reserve of x-minutes is possible. Depending on the maximal temperature increase $\Delta temp_i^{max}$ in 1/hour, this requirement can be formulated by

$$w_i^t \leq temp_i^t + \Delta temp_i^{max} \cdot x/60 \qquad \forall t \in \mathcal{T}, i \in \mathcal{I}, \qquad \text{with x=15 in this case.} \tag{5.9}$$

The maximal available reserves are limited by the power output that can be achieved within the 15-minute activation time of tertiary reserves. A possible assumption is that power plants are at minimum power output P_i^{min} as soon as a temperature of 1 is achieved. Afterwards, reserves above this minimum output can be provided by ramping up with the maximal ramping speed RU_i in the remaining time. The constraint can be formulated by

$$rv_i^{t,stby} \leq P_i^{min} + RU_i \cdot \left[15 - \frac{1 - temp_t^i}{\Delta temp_i^{max}} \cdot 60\right] + (1 - w_i^t) \cdot RU_i \cdot \frac{1}{\Delta temp_i^{max}} \cdot 60 \quad \forall t \in \mathcal{T}, i \in \mathcal{I}. \tag{5.10}$$

The maximal temperature increase $\Delta temp_i^{max}$ can also have values above one which does not change anything with respect to the hourly start-up process (see Section 4.6.2). Yet, it allows ramping to higher values for reserve provision. The last part of equation (5.10) has to be added to prevent the term being negative for long remaining start-up times, i.e. for a lower current temperature $temp_t^i$ and/or low heat-up speed $\Delta temp_i^{max}$.

As power plants operate above their minimum output whenever started, the reserves offered by off-line units must be above this value:

$$\mathrm{rv}_i^{t,stby} \geq \mathrm{w}_i^t \cdot P_i^{\min} \qquad \forall t \in \mathcal{T}, i \in \mathcal{I}. \tag{5.11}$$

Finally, equation (4.56) from Section 4.8 is required to guarantee that only off-line plants can provide standby reserves (power plants can be either online or in hot state).

Concerning the real-world application of the approach, the exact requirements of the power plants must be considered. Several power plants might not be allowed burning fuel at these low levels and dumbing of heat would be required. Other power plants might require technical reconfiguration before this status can be employed.

Storage constraints Reserve provision is not restricted to power plants but storage can be employed as well. Storage is modeled linearly without any minimum power output requirement. Thus, capacity constraints for reserve provision can be defined by equations (5.12) and (5.13). The power output p_s^t of storage can be negative when pumping or positive when the turbine is activated. The maximal power capacity of the turbine and the pump is assumed to be symmetric leading to the following constraints:

$$-p_s^t + \sum_{r \in \mathcal{R}^-} \mathrm{rvs}_s^{t,r} \leq PS_s^{\max} \qquad \forall t \in \mathcal{T}, s \in \mathcal{S}, \tag{5.12}$$

$$p_s^t + \sum_{r \in \mathcal{R}^+} \mathrm{rvs}_s^{t,r} \leq PS_s^{\max} \qquad \forall t \in \mathcal{T}, s \in \mathcal{S}. \tag{5.13}$$

Additionally, the energy content es_s^t must be positive even after provision of scheduled energy and reserves:

$$\mathrm{es}_s^t + \mathrm{ps}_s^t - \sum_{r \in \mathcal{R}^-} \mathrm{rvs}_s^{t,r} \geq 0 \qquad \forall t \in \mathcal{T}, s \in \mathcal{S}, \tag{5.14}$$

and below the maximal reservoir capacity $ES_s^{\max}$:

$$\mathrm{es}_s^t + \mathrm{ps}_s^t + \sum_{r \in \mathcal{R}^+} \mathrm{rvs}_s^{t,r} \leq ES_s^{\max} \qquad \forall t \in \mathcal{T}, s \in \mathcal{S}. \tag{5.15}$$

Storage plants have to respect ramping constraints in the same way that power plants do when providing reserves. The change of power output within 5 minutes is restricted to

$$\frac{1}{12}\left(\mathrm{ps}_s^{t+1} - \mathrm{ps}_s^t\right) + \mathrm{rvs}_s^{t,\mathrm{sec}+} + \frac{1}{3} \cdot \mathrm{rvs}_s^{t,\mathrm{ter}+} \leq RU_s \cdot 5 \qquad \forall t \in \mathcal{T}, s \in \mathcal{S}, \tag{5.16}$$

$$\frac{1}{12}\left(-\mathrm{ps}_s^{t+1} + \mathrm{ps}_s^t\right) + \mathrm{rvs}_s^{t,\mathrm{sec}-} + \frac{1}{3} \cdot \mathrm{rvs}_s^{t,\mathrm{ter}-} \leq RU_s \cdot 5 \qquad \forall t \in \mathcal{T}, s \in \mathcal{S}. \tag{5.17}$$

5.4 Stochastic Approach Based on Scenarios

An intuitive approach to include uncertainty is scenario-based stochastic programming. The basic idea of stochastic programming is to consider multiple scenarios for the realization of variable generation and resulting net load or other stochastic events like power plant outages [144]. An illustrative example of possible scenarios for one actual development of generation from wind power is given in Fig. 5.1.

5.4.1 Method

Single-stage problems The most essential notion of a stochastic problem is to find the minimum of the expected value over all possible realizations of the uncertain variable, e.g. the load or production from renewable sources. For the base form of the UC problem, this can be formulated with scenarios $\omega \in \Omega$ for the uncertain demand $D^{t,\omega}$ and the probability of occurrence π_ω by [52]

$$\min \sum_{\omega \in \Omega} \pi_\omega \cdot \sum_{i \in \mathcal{I}, t \in \mathcal{T}} A_i v_i^{t,\omega} + B_i p_i^{t,\omega} + c u_i^{t,\omega}, \tag{5.18}$$

$$\text{s.t.} \sum_{i \in \mathcal{I}} p_i^{t,\omega} = D^{t,\omega} \qquad \forall\, t \in \mathcal{T}, \omega \in \Omega, \tag{5.19}$$

where different scenarios of demand $D^{t,\omega}$ have to be fulfilled. Technical constraints on the power generation $p_i^{t,\omega}$ can be included by defining the equations of Chapter 4 over all scenarios $\omega \in \Omega$, respectively. Takriti et al. [196] describe such a single-stage model and develop an efficient parallel solution algorithm.

With this single-stage approach, no reactive actions take place and planning is only conducted once. In real-world operation, planning is updated and reactive actions are usually executed [52]. Therefore, single-stage models promise to be mostly relevant for system studies or infrastructure planning, but not for real operations scheduling. For the latter, so-called two-stage problems are the most common approach.

Two-stage problems In such problems, decisions on a variable must be made in the "here and now" with an uncertain future which is considered by scenarios $\omega \in \Omega$. Depending on the realization of the uncertain variable, corrective actions must be carried out [21]. This will have different costs depending on the first-stage decisions. These second-stage costs are included in the optimization problem.

For the case of the UC problem, two possible formulations for a two-stage problem formulation are explained here. The most prominent one considers a day-ahead planning that includes the UC decisions for the next day as the first-stage decision (the "here and now"). In the second stage, the intra-day scheduling with determination of exact production levels is fixed. The overall goal is to minimize the sum of commitment costs (start-up-costs and no-load costs) and the expected second stage costs (production costs) depending on a set of scenarios Ω for the uncertain realizations of VRE production. For

the base form of the UC model, this two-stage model may be described by [36]

$$\min \sum_{i\in\mathcal{I},t\in\mathcal{T}} A_i v_i^t + cu_i^t + \sum_{\omega\in\Omega} \pi_\omega \sum_{i\in\mathcal{I},t\in\mathcal{T}} B_i p_i^{t,\omega}, \tag{5.20}$$

$$\text{s.t.} \sum_{i\in\mathcal{I}} p_i^{t,\omega} = D^{t,\omega} \qquad \forall\, t\in\mathcal{T}, \omega\in\Omega. \tag{5.21}$$

The approach could be modified by assuming quick starting units that can also be started during the intraday planning. Such a model was presented by Carøe and Schultz [36] and integer variables are then required in both stages.

Another approach to distinguish the two stages is the temporal dimension. Meibom et al. [144] employ a stochastic UC model where fixed UC (and dispatch) decisions are made for the three succeeding hours of the "here and now". Afterwards, the second stage problem (or multiple additional stages) takes the first three hours for granted and optimizes the system with respect to the different scenarios given. In order to give a mathematical description, the set of considered periods $\mathcal{T}$ is split up into periods with fixed demand $\mathcal{T}^{\text{det}}$ and periods with uncertain demand $\mathcal{T}^{\text{sto}}$. Therewith, the problem may be formulated as

$$\min \sum_{i\in\mathcal{I},t\in\mathcal{T}^{\text{det}}} A_i v_i^t + B_i p_i^t + cu_i^t + \sum_{\omega\in\Omega} \pi_\omega \sum_{i\in\mathcal{I},t\in\mathcal{T}^{\text{sto}}} A_i v_i^{t,\omega} + B_i p_i^{t,\omega} + cu_i^{t,\omega}, \tag{5.22}$$

$$\text{s.t.} \sum_{i\in\mathcal{I}} p_i^t = D^t \quad \forall\, t\in\mathcal{T}^{\text{det}}, \quad \text{and} \quad \sum_{i\in\mathcal{I}} p_i^{t,\omega} = D^{t,\omega} \quad \forall\, t\in\mathcal{T}^{\text{sto}}, \forall\omega\in\Omega. \tag{5.23}$$

The system operator can change the commitment/scheduling plan (first stage) whenever new information on the forecasted generation is available. An increasing frequency of forecast updates thereby significantly improves decision making [144, 200].

An example of an implemented stochastic optimization model can be found, for instance, in Meibom et al. [144]. The paper studies Ireland's power system with significant amounts of wind production. The production schedules (including the UC decisions) are updated in a rolling manner, i.e. every three hours, whenever improved information on future wind production becomes available. The study found that the additional costs rising from uncertain wind and demand realizations are, compared to overall operational costs, very small. The study also found that power systems with higher shares of flexible power plants, i.e. gas turbines, are less influenced by system uncertainties than systems with high percentages of base load plants, i.e. coal fired plants. Abrell and Kunz [3] compare a stochastic model to a deterministic model in order to evaluate impacts from VRE integration and find a shift towards operation of more flexible power plants as soon as stochastic planning is considered. Those two studies are examples that show the relevance of uncertainty consideration when evaluating the value of power plant portfolios and the value of enhancing their flexibility.

While the approach is intuitive and several studies show the benefits over deterministic approaches [162], there are two major drawbacks of the idea:

- Generating scenarios requires detailed information about forecast errors and their development over time. Furthermore, the probability of occurrence has to be

defined for each scenario, which is hardly possible. The latter question is tackled for instance by Pinson [166, 167] or by Lee et al. [134].

- The optimization problem grows exponentially with the number of independent variables that are represented in a single scenario tree. To illustrate this problem, consider generation from PV and wind at three different locations that are not depending on each other. When considering three scenarios for each technology and location, combining all scenarios would lead to $3^{(3 \cdot 2)} = 729$ scenarios. As there are 268 regions with three VRE technologies for the European model applied in Chapter 7, this would require $3^{(3 \cdot 268)}$ scenarios when only considering three scenarios for each technology in each region. This clearly shows the computational challenge ahead. Scenario reduction techniques are required to make these models solvable, e.g. by finding patterns in wind and PV generation. An approach for scenario reduction for VRE modeling can be found in Barth et al. [10].

5.4.2 Special Case: Single Scenario with Changing Forecasts

A simple case of a stochastic model is to use only one scenario for each variable. The computational burden for this case is not increased in comparison to the deterministic forecast. In the deterministic case with perfect forecasts, the required time for a start-up is (almost) not relevant since even a slow plant requiring ten hours for a cold start can be on-line exactly when needed. Considering changing forecasts, imperfect prognosis might require units to start-up faster or stop a start-up process that was started already. Abrell and Kunz [3] compare a changing forecast for wind generation to a stochastic model with multiple scenarios and a purely deterministic approach. The authors find that, in terms of overall costs, the changing forecasts resemble the stochastic model closer than the deterministic model. Furthermore, shifts in the fuel mix point in the same direction of changing forecasts and stochastic modeling: Less lignite and more coal are used as the latter is modeled with higher flexibility. In terms of start-up costs, changing forecasts lead to the highest costs while the stochastic model shows the lowest, as power plants are kept at low output levels to be prepared for different scenarios in the latter. All in all, this paper illustrates that simple changing forecasts are worth to be analyzed.

The approach of changing forecasts can be understood as a two-stage stochastic approach according to equations (5.22) and (5.23). Therein, the stochastic part contains only one scenario $|\Omega| = 1$. After updating the system, a new (changed) scenario is computed for the stochastic periods. Fig 5.6 illustrates the approach: the green part is the fix part of the rolling horizon, while the blue part is recomputed in the next step. In the first run (picture on top), the deterministic forecast considers the hours 1-7 (the fixed part + one additional hour to avoid infeasibilities), while the hours 8-36 have a forecast for renewable production that deviates from the deterministic generation. After one run, the rolling horizon is shifted by six hours and the former fixed part is not considered anymore (gray part in the second figure). Hours 7-13 are now the deterministic section and the blue line represents a new, changed forecast. Another step in the rolling horizon

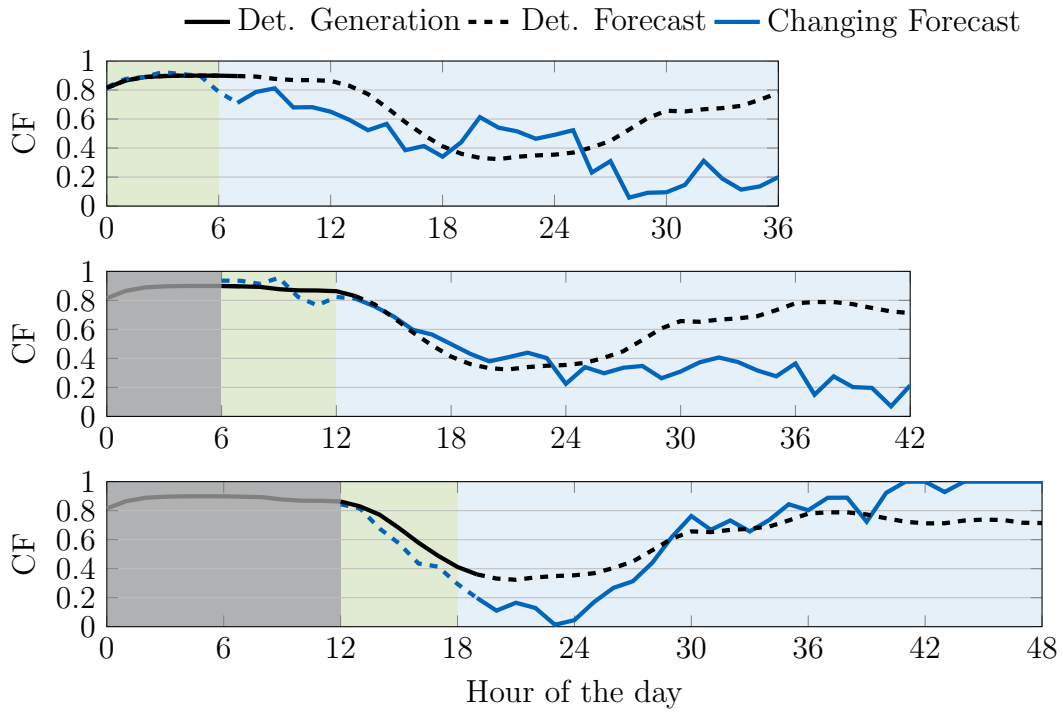

Figure 5.6: Development of forecasts with updated information every 6 hours

is depicted in the figure on the bottom with a deterministic part from hour 13 to 19. Occurring deviations in the deterministic hours are assumed to be balanced by speed control and AGC.

As the effects of uncertainty are only analyzed qualitatively in this thesis, a very simple approach for generating this changing forecast for each renewable generation technology is employed. The major assumptions of the forecasts are: a decreasing accuracy with longer time horizons k, a forecast that deviates from deterministic generation with a normally distributed random number, and a higher probability for deviations in the same direction as in preceding periods by taking into account the deviation of previous period Δ^{t-1}. The calculation of the forecasted generation $\widehat{p^t}$ is described in mathematical terms by:

$$\widehat{p^t} = \mathrm{N}(\mu, \sigma) \qquad \text{with} \quad \mu = p^t + \Delta^{t-1} \quad \text{and} \quad \sigma(k) = \sigma^0\sqrt{k} \tag{5.24}$$

and with the definition of Δ^{t-1} by:

$$\Delta^{t-1} = \widehat{p^{t-1}} - p^{t-1}. \tag{5.25}$$

The capacity factor has to remain within [0,1] so that all values above or below are set to either 1 or 0, respectively. The standard deviation is increasing by the forecast horizon k with: $\sigma(k) = \sigma^0\sqrt{k}$. Here, a value of $\sigma^0 = 0.02$ is assumed. As the same parameters are assumed for all types of VREs in all locations, this is only a rough estimation and more research is required for a sound analysis beyond the qualitative statements achieved in this thesis. The standard deviation with this assumption ranges from 2% for the upcoming hour to 12% for planning 36 hours ahead which is in the

same magnitude as the RMSE of actual predictions (see literature in Section 3.1 and Lenzi et al. [136]).

This approach was developed as a simple intuitive solution but might be categorized as ARMA (Autoregressive-Moving Average) model, where $\Delta(t-1)$ can be seen as both the moving average and as autoregressive term. However, the development of stochastic scenarios is not the focus of this thesis and detailed discussions on that issue go beyond the purpose of the chosen method. Further reading on generating adequate forecasts can be found in Barth et al. [10], Pinson et al. [167], or von Roon [179], amongst others.

5.5 Alternative: Robust Optimization Approach

The main disadvantages of the scenario-based approach are the scalability of the problem and the unknown distribution of forecasts. Those two major problems can be overcome with a robust optimization approach. The essential idea of this approach is optimizing over a continuous spectrum of expectations. The approach was applied to power systems and the UC problem by Bertsimas et al. [20]. Again, a two-stage situation is considered: an ISO optimizes the UC decisions in a first stage and then determines the exact schedules in a second stage. Thereby, the first-stage decision is made under the assumption of a worst-case second-stage outcome. In mathematical terms (compact matrix formulation, without formulation of constraints), this is formulated as min-max problem to

$$\min_{x} \boldsymbol{c}^T \boldsymbol{x} + \max_{\boldsymbol{d}\in\mathcal{D}} \boldsymbol{b}^T \boldsymbol{y}(\boldsymbol{d}) \quad \text{with} \quad \boldsymbol{x} \in \{0,1\}, \tag{5.26}$$

with uncertainty variable $\boldsymbol{d}$, the first-stage commitment decisions $\boldsymbol{x}$, and second-stage dispatch $\boldsymbol{y}$. The parameters $\boldsymbol{c}^T$ and $\boldsymbol{b}^T$ determine the operational costs for each schedule. Reformulating the second stage to a max-min problem leads to

$$\min_{x} \boldsymbol{c}^T \boldsymbol{x} + \max_{\boldsymbol{d}\in\mathcal{D}} \min_{\boldsymbol{y}\in\Omega(\boldsymbol{x},\boldsymbol{d})} \boldsymbol{b}^T \boldsymbol{y}, \quad \text{with} \quad \boldsymbol{x} \in \{0,1\} \tag{5.27}$$

with $\Omega(\boldsymbol{x},\boldsymbol{d})$ being the solution space resulting from the first stage decisions and the realization of $\boldsymbol{d}$.

The approach showed promising results as scalability to multiple uncertain variables is easier and distributions are not required. Still, there are problems with the solution algorithm that require solving a bilinear problem and might not converge to feasible solutions. The general solution idea is to build the dual of the second-stage scheduling problem in order to obtain a single maximization problem. This, in turn, requires solving a bilinear problem. All in all, the approach must be considered when thinking of incorporating uncertainty in UC. However, solving the bilinear problem might require new developments of algorithmic procedures that enable solving the problem with some guarantees of optimality and feasibility.

5.6 Alternative: Stochastic Approach Employing Ramp and Capacity Reserves

Another very promising approach was suggested by Morales-España et al. [147]. The approach considers two major restrictions to secure operation against uncertain renewable realizations: the system is required to have enough ramp reserves allowing to react to fast increasing or decreasing VRE production. Additionally, the system is required to have enough capacity reserves in order to be able to provide the lack of power in case of unexpectedly low production from VRE. The approach allows considering grid constraints which is an advantage compared to traditional reserve scheduling as described in Section 5.3. The model can be categorized as a mix of a deterministic reserve-based system and a stochastic approach as the objective function includes three scenarios: a nominal VRE generation (the most probable) as well as the minimal and maximal production expected. In the following, the major features of the approach are explained to provide the reader with the general idea. When implementing the model however, the reader is referred to the original publication for all details and equations. In the original article, the authors consider wind generation uncertainty only, while in this thesis all generation from VRE is considered.

Reserve requirements A major assumption of the approach is that VRE generation can be curtailed at no costs and at any time. A forecasted range of VRE generation for the upcoming hours/days is the basis for commitment decisions in the present. Both a forecast for maximal expected generation and for minimal expected generation (according to some reliability criterion) are required. Given this information, the system operator can define a scheduled range of VRE generation. Here, the minimum and the maximum of the scheduled range can be equal or below the respective values of the forecasted range as curtailment is allowed. The scheduled range defines all possible values of renewable generation that can be integrated.

Fig. 5.7 on the left illustrates the forecasted range with $VRE_n^{t,\min}$ being the minimal forecasted generation and $VRE_n^{t,\max}$ the maximal forecasted generation. The scheduled range of renewable generation (blue area in Fig. 5.7) is bounded by the scheduled minimum generation $vre_n^{t,\min}$ and the scheduled maximal generation $vre_n^{t,\max}$. The nominal values (which can be interpreted as the most probable ones) for the dispatched renewable generation vre_n^t have to be below the forecasted nominal values VRE_n^t as well. In mathematical terms, this leads to

$$0 \leq vre_n^{t,\min} \leq VRE_n^{t,\min}, \quad 0 \leq vre_n^t \leq VRE_n^t, \quad 0 \leq vre_n^{t,\max} \leq VRE_n^{t,\max} \quad \forall n \in \mathcal{N}, t \in \mathcal{T}. \tag{5.28}$$

The scheduled nominal renewable generation must be within the limits of scheduled minimal and maximal generation:

$$vre_n^{t,\min} \leq vre_n^t \leq vre_n^{t,\max} \quad \forall n \in \mathcal{N}, t \in \mathcal{T}. \tag{5.29}$$

An illustration of the maximal possible up and down ramps is given with Fig. 5.7 on the right and the maximal scheduled ramps can be defined to $(vre_n^{t,\max} - vre_n^{t-1,\min})$

and $(vre_n^{t-1,\max} - vre^{t,\min})$, respectively. The definitions of the maximal up and down ramps as well as the illustration of those ramps highlight the purpose of scheduling below forecasted values: the required maximal ramps can be reduced.

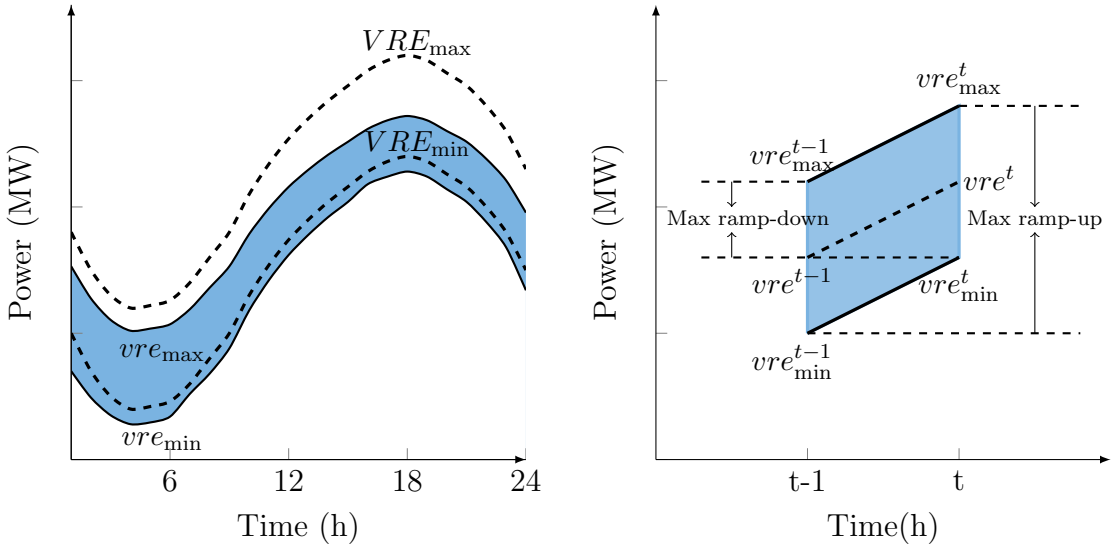

Figure 5.7: Determination of the maximal required ramps according to scheduled VRE generation. The figure on the left shows the forecasted range (dotted lines, range from $VRE_t^{\min}$ to $VRE_t^{\max}$) and the scheduled range (in blue, range from $vre_t^{\min}$ to $vre_t^{\max}$).

Given this scheduled range in between $vre_n^{t,\min}$ and $vre_n^{t,\max}$, the greatest up and down ramps on top of the nominal ramp $(= vre_n^t - vre_n^{t-1})$ are named $vre_n^{t,R+}$ and $vre_n^{t,R-}$ and can be computed by

$$vre_n^{t,R+} = (vre_n^{t,\max} - vre_n^t) + (vre^{t-1} - vre_n^{t-1,\min}) \quad \forall n \in \mathcal{N}, t \in \mathcal{T}, \tag{5.30}$$

$$vre_n^{t,R-} = (vre_n^{t-1,\max} - vre_n^{t-1}) + (vre_n^t - vre^{t,\min}) \quad \forall n \in \mathcal{N}, t \in \mathcal{T}. \tag{5.31}$$

After defining the required ramp reserves at each node, the system constraints can be formulated. These include the provision of demand D_n^t at each node n and period t by thermal producers p_i^t and by nominal production of renewable generation vre_n^t at all nodes:

$$\sum_{i \in \mathcal{I}} p_i^t = \sum_{n \in \mathcal{N}} D_n^t - \sum_{n \in \mathcal{N}} vre_n^t, \qquad \forall t \in \mathcal{T}. \tag{5.32}$$

Additionally, capacity reserves $\mathrm{rv}_i^{t,C+}$ and $\mathrm{rv}_i^{t,C-}$ have to be provided:

$$\sum_{i \in \mathcal{I}} \mathrm{rv}_i^{t,C+} \geq \sum_{n \in \mathcal{N}} (vre_n^t - vre_n^{t,\min}) \quad \forall t \in \mathcal{T}, \tag{5.33}$$

$$\sum_{i \in \mathcal{I}} \mathrm{rv}_i^{t,C-} \geq \sum_{n \in \mathcal{N}} (vre_n^{t,\max} - vre_n^t) \quad \forall t \in \mathcal{T}. \tag{5.34}$$

The capacity reserves guarantee the integration of every possible VRE generation outcome within the scheduled range. This can include decreasing power output of

thermal generation in the case of high VRE generation at $vre_n^{t,\max}$ or increasing thermal power output in order to counterbalance low generation at $vre_n^{t,\min}$.

Furthermore, ramp reserves ($\mathrm{rv}_i^{t,R+}$, $\mathrm{rv}_i^{t,R-}$) have to be provided according to the requirements $vre_b^{t,R+}$ and $vre_b^{t,R-}$ which were defined by equations (5.30)-(5.31) above. Ramp reserves guarantee that the system is flexible enough to react to all unforeseen changes in renewable generation. The ramp reserve requirements are defined by

$$\sum_i \mathrm{rv}_i^{t,R+} \geq \sum_{n\in\mathcal{N}} \inf\left(\widehat{VRE}_n^{t,R+}, vre_n^{t,R+}\right) \quad \forall t \in \mathcal{T}, \tag{5.35}$$

$$\sum_i \mathrm{rv}_i^{t,R-} \geq \sum_{n\in\mathcal{N}} \inf\left(\widehat{VRE}_n^{t,R-}, vre_n^{t,R-}\right) \quad \forall t \in \mathcal{T}, \tag{5.36}$$

with $\widehat{VRE}_n^{t,R+}$ and $\widehat{VRE}_n^{t,R-}$ being the maximal deviations from the nominal forecasted ramp, which is a parameter that has to be defined by the system operator a priori.

The infimum functions guarantee that ramp requirements are neither higher than the maximal deviation from the scheduled range nor higher than the maximal deviations from the forecasted range. When implementing the approach including an MIP formulation of the infimum function, the reader is referred to the original article [147].

Unit constraints When providing these reserves, each unit has to respect individual constraints, which include the general minimum power output, the commitment logic, and the ramp constraints as described in equations (4.13)-(4.18). Additional constraints include the capacity reserve restrictions which are similar to those of (5.2) and (5.3) by replacing the reserves with $\mathrm{rv}_i^{t,C+}$ and $\mathrm{rv}_i^{t,C-}$.

Finally, all reserves have to be positive and several constraints have to hold that interrelate the power and ramp capacity reserves which are described in detail in [147].

Network constraints and reserve deployment An encouraging aspect of the approach is the inclusion of network constraints for the nominal case as well as for the cases where maximal and minimal reserves have to be deployed ($\mathrm{rdp}_i^{t,\max}$ and $\mathrm{rdp}_i^{t,\min}$, respectively). The minimal and maximal reserve deployments of each unit are limited by the scheduled ramp reserves $\mathrm{rv}_i^{t,R+}$ and $\mathrm{rv}_i^{t,R-}$. The deployed reserves must respect the maximal ramp reserves by

$$-\mathrm{rv}_i^{t,R-} \leq \mathrm{rdp}_i^{t,\max} - \mathrm{rdp}_i^{t-1,\max} \leq \mathrm{rv}_i^{t,R+} \quad \forall t \in \mathcal{T}, \forall i \in \mathcal{I}, \tag{5.37}$$

$$-\mathrm{rv}_i^{t,R-} \leq \mathrm{rdp}_i^{t,\min} - \mathrm{rdp}_i^{t-1,\min} \leq \mathrm{rv}_i^{t,R+} \quad \forall t \in \mathcal{T}, \forall i \in \mathcal{I}. \tag{5.38}$$

In order to guarantee the balances of demand and supply and the network constraints in all cases, reserve deployments for minimal and maximal VRE generation are defined by the maximal deviation of VRE generation from the nominal case:

$$\sum_i \mathrm{rdp}_i^{t,\max} = \sum_n (vre_n^t - vre_n^{t,\max}) \quad \forall t \in \mathcal{T}, \tag{5.39}$$

$$\sum_i \mathrm{rdp}_i^{t,\min} = \sum_n (vre_n^t - vre_n^{t,\min}) \quad \forall t \in \mathcal{T}. \tag{5.40}$$

For both the maximal and the minimal VRE generation and the respective reserve deployments, network constraints have to be fulfilled. The constraints are the same as in equation (4.85), but VRE generation and reserve deployments are added. Constraint (5.41) guarantees line constraints for maximal generation and constraint (5.42) the same for minimal generation:

$$-f_m^{L,\max} \leq \sum_{n\in\mathcal{N}} \mathbf{PTDF}_n^m \left(\sum_{i\in\mathcal{I}_n} \left(p_i^t + \mathrm{rdp}_i^{t,\max}\right) + vre_n^{t,\max} - D_n^t \right) \leq f_m^{L,\max} \quad \forall t \in \mathcal{T}, \forall m \in \mathcal{L}, \tag{5.41}$$

$$-f_m^{L,\max} \leq \sum_{n\in\mathcal{N}} \mathbf{PTDF}_n^m \left(\sum_{i\in\mathcal{I}_n} \left(p_i^t + \mathrm{rdp}_i^{t,\min}\right) + vre_n^{t,\min} - D_n^t \right) \leq f_m^{L,\max} \quad \forall t \in \mathcal{T}, \forall m \in \mathcal{L}. \tag{5.42}$$

Including the grid constraints for the both extremes guarantees that reserves are not only available within the system but can also be provided to the nodes where required.

Objective function The objective function considers the nominal case as well as the extreme cases for VRE generation, thus leading to a two-stage stochastic model with the objective function

$$\min \sum_{i\in\mathcal{I},t\in\mathcal{T}} A_i v_i^t + cu_i^t + B_i \left[\gamma_1 \left(p_i^t\right) + \gamma_2 \left(p_i^t + \mathrm{rdp}_i^{t,\max}\right) + \gamma_3 \left(p_i^t + \mathrm{rdp}_i^{t,\min}\right)\right], \tag{5.43}$$

with $\gamma_1 + \gamma_2 + \gamma_3 = 1$ being the weights for the three scenarios. The model framework as proposed by [147] does not schedule energy but ramps. However, the approach is in principal adjustable to energy scheduling as well.

This method is worth being considered for future system studies as major obstacles of scenario-based stochastic modeling and robust modeling can be overcome: the model can be formulated as MIP and knowledge about scenarios and probability distributions is not required. The inclusion of the network constraints for the upper and lower bounds of VRE generation can be seen as a further advantage.

5.7 Conclusions From Uncertainty Considerations

5.7.1 Advantages of the Temperature-Based UC

For all of the approaches described, advantages or ideas of how to gain synergies by a combination with the temperature model can be found. The key advantages are: the introduction of a "hot" state for reserve provision, the ability to model start-up speed, and the ability to stop the starting procedure whenever updates on forecasts requires.

- Deterministic reserves provision: The "hot" state can be introduced to consider the reserve provision from off-line units as described above with equations (5.8)-(5.10).

- Changing forecast (single scenario): Whenever forecasts are updated, the start-up and commitment decisions for the next hours might be reconsidered reflecting the costs for interrupted start-up processes without any extra variables. Additionally, different costs for different start-up speeds as introduced in Section 4.7 could be considered in such a context.
- Stochastic (multiple scenarios): In addition to the rescheduling of start-up processes, keeping units at a certain higher temperature might be a strategy for being prepared for different scenarios. Again, no additional variables are required.
- Robust approach: This approach resembles the stochastic approach concerning the synergies with the temperature model. Keeping units warm promises to be a strategy to prevent high cost solutions.
- Ramp-based approach: Changing forecasts will also reflect changes in start-up plans. Additionally, the hot state can be introduced for units serving as capacity or ramp reserves.

5.7.2 Applications for Flexibility Evaluation

This chapter has discussed different approaches to deal with uncertainty in generation from VREs and showed that valuable research could be done in this field. The temperature model allows considering additional aspects for different kinds of uncertainty modeling approaches. Research should consider those aspects and develop improved methods for uncertainty management in power system operations.

Currently, the reserve adjustment approach is the most employed. However, the dimensioning of the additional reserves for VRE integration is unclear and might lead to suboptimal results by scheduling too much or too few reserves. Furthermore, grid restrictions and the spatial dimension of uncertainty are not included or only considered partly by regional reserve requirements. Vrakopoulou [206] discusses how to improve reserve provision: algorithms that find reserve requirements depending on AC power simulations are provided and could improve temporal and spatial allocation of reserves. Bucher et al. [30] introduce a metric that defines regional flexibility requirements for procuring reserves accordingly. Such ideas might allow reserve adjustment to be the method of choice also in future operation.

Looking at alternatives, the employment of other stochastic modeling approaches might take advantage of further benefits of the temperature model. Limited start-up times and disrupted start-ups can be integrated more simply. The robust approach also seems encouraging. Yet, it requires solving a bilinear problem. The model with ramp reserve requirements seems to be promising. However, storage is not included per se and many additional constraints are required. The stochastic approach with scenarios proves to be viable for real-world test cases but requires knowledge on scenarios and has a high computational burden. The simplified approach with only one scenario was discussed by Abrell and Kunz [3] and proved to resemble several of the system effects that also occur with the multiple scenario approach, i.e. system costs and fuel shifts.

While there are alternative approaches which might allow VRE integration at lower costs, reserves and reserve adjustments have been used in real-world applications until now. As being the standard method at present, it will also be applied for the large-scale system simulations in the evaluation chapter of this thesis (Chapter 7). Additionally, the method of changing forecasts is considered in several scenarios in order to estimate additional effects resulting from uncertainty. These scenarios give an outlook on the size and quality of additional effects that can be further studied from thereon.

Part III

Evaluation

Chapter 6

Development of a Test Dataset Representing Europe's Power System

In order to evaluate the different flexibility options, a model that reflects major characteristics of a real-world power system is required. A system that is currently in the transition to integrate large shares of VREs is the European power system. The European Union its member countries have committed themselves to targets for a significant reduction of their CO_2 emissions in the next decades. One important measure to achieve this goal is the introduction of renewable energy sources in the power systems. The European power system is therefore an ideal test case for the modeling framework and allows to gain insights to the value of different flexibility options which might help policy makers and system planners. This chapter presents an overview of the dataset developed. The dataset represents major aspects of the real European power system but remains an abstract test case for the course of this thesis. It lays the foundation for further development and calibration of a power system model employed for policy analysis and infrastructure planning at Technical University of Munich (TUM).

A country with especially high targets in renewable generation is Germany. Here, the discussion on increasing flexibility in generation has been prevailing (see e.g. publications on the topic by Brauner et al. [27] or Ziems et al. [213]). The country is connected to many neighbors and electricity is exchanged continuously. Still, in some analyses, Germany is considered as an island that must balance renewable generation independently. Discussions in some Eastern European countries to block electricity imports from Germany in order to prevent load flows [47, 174, 187] might make this assumption a relevant policy scenario. For these "Germany-only" scenarios, relevant data is extracted from the European dataset and all connections to neighboring countries are cut off.

The contributions of developing the described dataset based on publicly available data can be summarized to the following:

- A test system is established that allows applying the theoretical modeling framework of Chapter 4 in a realistic environment.

- A model platform to analyze flexibility options at the German and European level is set up. As the model data is deduced from a real-world power system, results can be highly valuable for future system planning. This is especially true for the general rules and system suggestions that are derived from the results.
- The models can be seen as the basis for future research and policy consulting (A first consulting project for the Bavarian Ministry of Economic Affairs and Media, Energy and Technology has already been conducted using the model and dataset of this thesis [86])

6.1 Basic Model Structure

Europe is divided into subregions based on the statistical entities of the Nomenclature of Territorial Units for Statistics (NUTS) classification with the granularity at NUTS 2 level [71]. After adjustments, 268 model regions are finally considered. Adjustments include the exclusion of Malta and several Greek islands that are not connected to the continental grid. Also, several cities were incorporated in their surrounding regions and very small regions were merged in order to keep complexity at a manageable level. The modeled regions as used for the scenario calculations are depicted in Fig. 6.1. The colors of the regions indicate their annual electricity consumption. Depending on the research question and computational capability, the entire European system or different parts of it were considered.

6.2 Electricity Consumption

The model requires time series data of electricity demand for each region. Historic data with hourly load for all European countries for the year 2011 is used (available from ENTSO-E [62]). The year 2011 is chosen due to the availability of renewable generation characteristics. Using synchronized load and generation data is important when studying VRE integration as characteristics might have temporal interdependencies, e.g. higher load on hot and sunny days with high PV generation. Concerning annual consumption, the hourly load characteristic is scaled to the most recent data available for each country, i.e. data from ENTSO-E [60] for the year 2014.

The annual consumption in each country, Demand_k, is distributed to the respective model regions $n \in \mathcal{N}_k$ with consideration of regional gross domestic product (GDP) and regional population. This data is available from the European Commission [72, 73]. Wherever regions are merged, GDP and population of the respective regions are summed up. The equation to calculate the annual demand in a region n of a country k is given by

$$\text{Demand}_n = (0.3\frac{pop_n}{pop_k} + 0.7\frac{GDP_n}{GDP_k}) \cdot \text{Demand}_k \qquad \forall n \in \mathcal{N}_k. \tag{6.1}$$

The distribution of load to the regions is illustrated in Fig. 6.1 with colors indicating the consumption relative to the respective area.

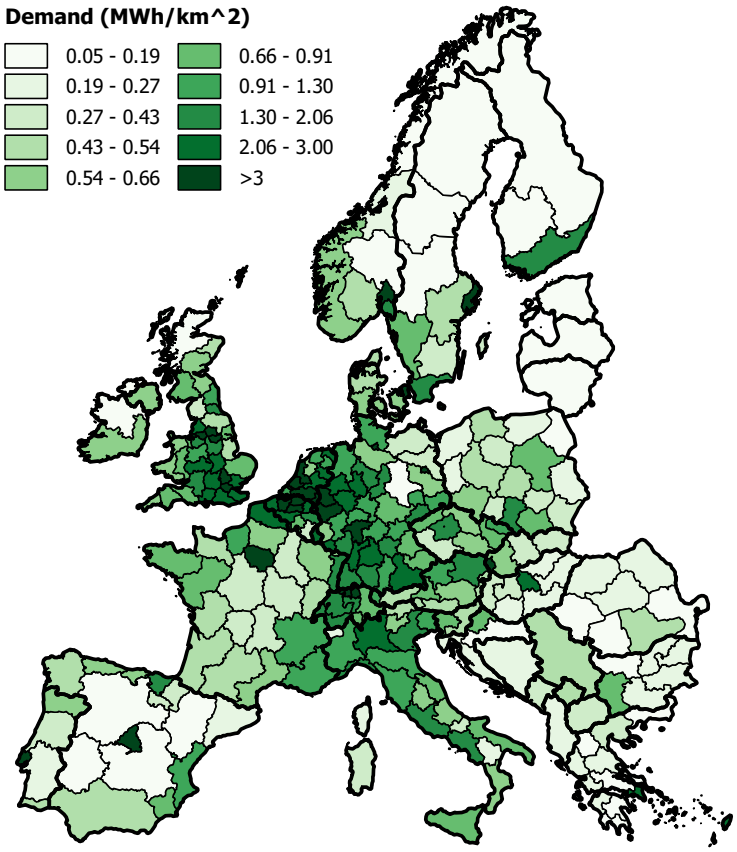

Figure 6.1: The 268 model regions and their electricity consumption relative to their area

6.3 Inter-Area Transmission

A reduced model of the European power grid where each node represents one model region is developed. A zonal DC power flow is used as described in Section 4.9.3. This requires estimating reactances and maximal allowed capacity for each connection between two regions, i.e. for the reduced grid. The basic idea for this estimation is to count lines that are crossing two neighboring regions. Together with the distance between the two model nodes, parameters for the reduced grid are computed. As discussed in Section 4.9.3, the grid model has to be seen as a stylized power system model based on the European network, which might result in power flows deviating from real-world power flows. Still, the model provides a test case for a large-scale power system with major characteristics and challenges as will be faced in Europe's system over the next years.

Electrical centers and line length For each region, the "electrical center" is defined as a geographical center of all substations available from Platts PowerVision [168] (commercial database). In some cases, the position of the electrical centers are moved closer to actual load manually, e.g. closer to large cities. The electrical centers are the endpoints of the connection lines and are depicted in Fig. 6.2.

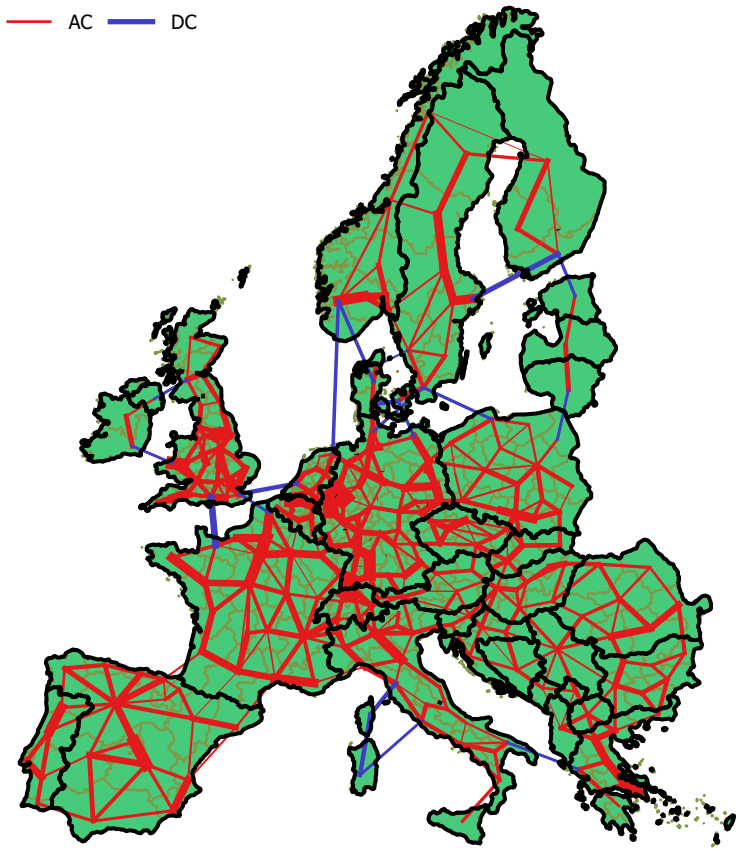

Figure 6.2: Illustration of the reduced transmission grid model consisting of AC and DC lines. The thickness of the lines gives a qualitative impression of the differences in capacity.

Line capacities and reactances (AC lines) Information about the number and voltages of lines from one region to another is obtained from Platts PowerVision [168] and combined with the map of transmission lines from ENTSO-E [64]. The DC load flow model requires calculating the matrix of susceptances $\boldsymbol{B}$ to subsequently compute the PTDF matrix according to equation (4.66). The susceptances can be derived from reactances X according to

$$B = -\frac{X}{R^2 + X^2}, \tag{6.2}$$

which can be reduced to

$$B = -\frac{1}{X} \tag{6.3}$$

for the lossless case ($R = 0$).

The reactances for individual lines are computed based on a specific reactance x_{voltage}, which depends on the voltage level (see Table 6.1) and the respective line length by

$$X = x_{\text{voltage}} \cdot \text{length}. \tag{6.4}$$

The base voltage system of the network is set to 380 kV and all reactances X have to be transformed to this base voltage level accordingly. Reactances in the base voltage system are then noted by X^*. The transformation is described by

$$X^* = X \left(\frac{380\ kV}{V_{\text{line}}} \right). \tag{6.5}$$

Maximal transferable power for each connection is computed by the surge impedance loading (SIL) values as given in Table 6.1. SIL values present the (natural) power loading at a set point, i.e. reactive power is neither produced nor absorbed.

Table 6.1: Reactances and SIL values for high voltage transmission based on Egerer et al. [56] and Kundur [129] and internal discussions

Voltage	x_{voltage} (Ω/km)	SIL(MW)
220 kV	0.4	230
380 kV	0.33	670

For computing the maximal allowed power flow, the SIL values have to be multiplied by a loadability factor LA(length) according to the St. Clair curve [42], representing different limitations depending on the lengths of the transmission line. For short lines of up to 80 km, thermal limits constrain the maximal flow. For longer lines in the range of 80 km to 320 km, the voltage drop becomes the limiting factor and for even longer lines, angle stability issues become dominant [129]. For the dataset developed, the St.Clair curve and resulting loadability factors LA(length) are approximated by six discrete steps according to Table 6.2.

Table 6.2: Loadability factor LA(length) according to St.Clair curve

Length	LA(length)	**Length**	LA(length)
$0 \leq$ length $< 100\ km$	2.5	$300 \leq$ length $< 400\ km$	1.1
$100 \leq$ length $< 200\ km$	2	$400 \leq$ length $< 500\ km$	0.9
$200 \leq$ length $< 300\ km$	1.3	$500 \leq$ length $< 600\ km$	0.72

When comparing reactances and line capacities to other reduced power system data, e.g. Hasche [88] or Egerer et al. [56], reactances are similar. In terms of maximal capacity, values differ significantly. The reason lies in the different methods for line limitations, e.g. the use of a thermal transmission limit instead of the SIL approach.

Different cases must be distinguished for computing reduced line parameters. First, reactances X for individual connections $m \in \mathcal{L}$ must be computed from voltage levels and line length according to equations (6.2)-(6.5). Then, aggregated values are computed according to the descriptions and formulas below. Lines with a voltage of 110 kV and below are not considered and parameters of DC lines are computed separately.

- One connecting line: In case of only one connecting line, the calculation of the equivalent reactance is simple and defined by voltage and length of the line:

$$f_m^{L,\max} = \text{SIL}(\text{voltage}_m) \cdot \text{LA}(\text{length}_m), \tag{6.6}$$
$$X_m = X^*. \tag{6.7}$$

- Multiple connecting lines with same voltage levels and same reactances $X_i' = X^*$: The maximal capacities of multiple lines add up. Concerning the reactances, the lines are regarded as a parallel circuit:

$$f_m^{L,\max} = n \cdot \text{SIL}(\text{voltage}) \cdot \text{LA}(\text{length}_m), \tag{6.8}$$
$$X_m = \frac{1}{\sum_{i=1}^{n} \frac{1}{X_i'}} = \frac{X^*}{n}. \tag{6.9}$$

- Multiple connecting lines with different voltage levels: The principal idea of a parallel circuit remains but reactances X_i' between lines differ resulting in:

$$f_m^{L,\max} = \sum_{i=1}^{n} \text{SIL}(\text{voltage}_i) \cdot \text{LA}(\text{length}_m), \tag{6.10}$$
$$X_m = \frac{1}{\sum_{i=1}^{n} \frac{1}{X_i'}}. \tag{6.11}$$

  In this case, the lower voltage lines might limit the overall transmission capacity [8], and thus, the capacity is overestimated. Applying reactive compensation might help in reducing the problem and make the approach a reasonable assumption.

HVDC Lines In contrast to AC lines, high-voltage direct current (HVDC) lines can be controlled by the operators and line flows are not determined by the reactances. Only a maximal capacity is required as data input and values are set individually for each line according to the scenario considered.

Simplified N-1 In order to represent security constraints, the maximal line capacity is reduced to 70% of the above computed $f_m^{L,\max}$. This is a simple approximation and does e.g. not consider the different quantities and capacities of individual lines which are aggregated in the reduced grid. More sophisticated approaches could consider outage transfer distribution factors (OTDFs) for the inter-zonal line corridors [40,192], however, this is not the focus of this thesis.

6.4 Renewable Generation

This section describes the installed capacities as well as the generation profiles of different renewable sources. All considered technologies are assumed to be non-controllable but are running with a predefined characteristic.

6.4.1 Installed Capacities

The basis for the scenarios on renewable capacities is the EU Energy Trends report 2013 [69]. The installed capacities for the year 2015, 2025, and 2035 are considered according to the reference scenario. The national capacities are distributed to the model regions in a procedure which is explained in the following.

Wind and solar The installed capacity for renewable technology per region is defined in a similar approach as the aggregation of grid points in the calculation of capacity factors (CF) by Janker [116]: Regions with higher FLHs will install greater capacities. An exponential approach is used to compute the share of of capacity ψ_n for a specific region n in country k by

$$\psi_n = \frac{\mathrm{FLH}_n^2}{\sum_{n \in \mathcal{N}_k} \mathrm{FLH}_n^2} \qquad \forall n \in \mathcal{N}_k. \tag{6.12}$$

The installed capacities of wind and solar for the three model years are depicted in Fig. A.1 in the Appendix.

Hydro Concerning hydro power, open data sources (mainly Enipedia of Delft University of Technology (TU Delft) [49] and Wikipedia [209]) are used to distribute the installed capacity to the regions.

Biomass and geothermal Hardly any data is available on the geographical distribution of biomass or geothermal sources. Therefore, plants are distributed proportionally to electricity consumption. Especially for geothermal generation, this might be an erroneous assumption as geothermal fields are very local occurrences. However, since the overall installed capacity is low, a small error of this estimation appears tolerable.

6.4.2 Generation Modeling

Wind and solar Wind and solar generation time series are defined on the basis of the PhD thesis of Janker [116], where a global dataset for hourly renewable generation was developed. The dataset provides time series of hourly CFs on different levels of aggregation according to the "GADM database of Global Administrative Areas" [154]. The basis for each aggregation is raw data in a grid with a resolution of 0.5° N/S and 0.66° W/E. For each aggregated region, five different time series are available per technology: the best grid point in the region, the worst grid point, the average of all grid points, a linear interpolation where weights are given to the individual grid points based on full load hours, and an exponential interpolation where good sites are considered with higher weights.

The aggregated regions from Janker [116] are mapped to the model regions in a next step. For most cases, the aggregation level "country-1" matches the model regions exactly. Whenever regions do not fit, smaller regions from the global database ("country-2") are merged and the respective time series are averaged, e.g. for the regions within Finland or the United Kingdom (UK). In the case of Germany, "country-2" matches the model

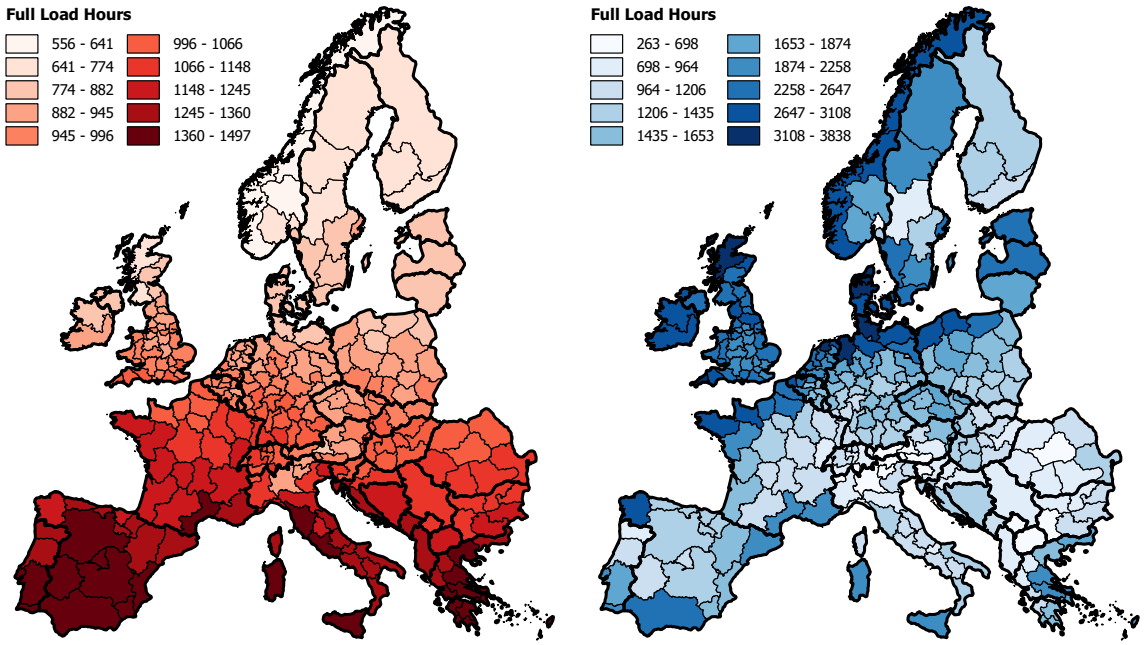

Figure 6.3: The FLH for PV (left) and wind (right) generation in the model regions

structure and is used directly. The different aggregations per region in the dataset of [116] are employed depending on the technology:

- PV: A linear interpolation of grid points is employed.
- Wind Onshore: For each of the model regions, the time series for the best grid point is used. Concerning the turbine height, 40 m or 80 m above ground are employed in order to compensate for the over-/underestimation of wind speeds for several regions. Mainly regions closer to the Alps and on the Iberian Peninsula are underestimated. Thus, the 80 m turbine model is employed there.
- Wind Offshore: The linear interpolation of grid points per region is employed. The turbine height is assumed to be at 60 m.

The resulting FLH for wind onshore and for PV are depicted in Fig. 6.3.

Hydro generation (except pumped storage) Another technology that relies on time series for hourly generation is hydropower. The hourly time series are based on monthly generation values that were published by ENTSO-E [63]. These monthly values are interpolated to hourly generation for each country and CFs for the model regions are identical to the ones of the respective country. An exact modeling of hydro generation is highly complex as parts of the power plants allow for control of water inflow (reservoir type hydro plants [67]). Especially in mountainous regions, many large storage facilites allow the inflowing water to be stored first and released later when needed. The reservoir sizes are variable and range from small ones for balancing daily fluctuations to very large ones for storing inflowing water over seasons [67]. The approach to consider this system flexibility is to install additional pumped hydro storage

with a simple rule: In mountainous regions, 30% of the hydro capacity is availably as a storage plant. An assumption that is reached by additionally installing pumped hydro capacity of such size. The storage volume of those "proxy" pumped hydro plants is 6 hours of maximal capacity. Their losses are 5% for charging and 5% for releasing water. In contrast to real pumped hydro storage, they are not allowed to participate in reserve markets. With these proxy pumped hydro plants, the reservoir type hydro plants is modeled and generation can be shifted within the 36 hours optimization time frame. Tests showed that, especially in Norway, this assumption allowed to reduce curtailment (negative slack) tremendously in the model for the year 2015; revealing the importance of this assumption.

As the seasonality of real-world storage is represented by the monthly generation, the addition of pumped hydro storage might be a valid approximation of the additional system flexibility. In further work with the model, the ideal capacity of proxy pumped storage should be evaluated by model calibrations.

Biomass Biomass is often seen as a further source of flexibility while currently most of biomass production is used as a constant source of supply. Within this thesis, biomass is also modeled as a constant source of supply with a utilization rate of 6000 FLHs per year.

Geothermal Geothermal and all other power sources mentioned in EU Energy Trends 2013 [69] are summarized and run with a constant power output and a utilization rate of 8000 FLHs per year.

6.5 Thermal generation

Capacities The database for all thermal generation is developed based on publicly available data sources. Major sources are the Wikipedia "List of Power Stations" [209] and the Enipedia database [49]. Other sources considered are listed in the database file upon publishing. All power plants for Germany are available from the Bundesnetzagentur [33] and data include capacity, fuel type, as well as the year of first initialization. Most of the sources provide fuel type, rated capacity, location, and the year of construction, which are the basic parameters to construct the required model input. All coal, lignite, and nuclear plants are assumed to be steam cycles. For gas-fueled power plants, a distinction is made based on capacity: plants with more than 100 MW are assumed to be combined cycle gas turbines, whereas below, single turbines are assumed. Oil-fueled plants are always assumed to be diesel generators.

The collected data is compared to the installed capacities for the year 2015 according to [69]. Most countries show a coverage rate of more than 90%. The missing capacity is then added with generic power plants in all cases. More capacity is installed in regions with higher electricity consumption. Individual decisions on power plant size and location are made manually, but all data will be made available on the TUM publication server "Mediatum" with the publication of this thesis. The maps of Fig A.2

in the Appendix show the installed capacities of coal, lignite, nuclear, gas, and oil power plants.

In contrast to renewable generation, no scenarios on the capacity change over the next decades are made. The thermal power plant fleet is kept at a status quo for 2025 and 2035. Decommissioning of plants would mainly influence capacity-relevant questions. It would have less impact on the flexibility-concerned questions addressed in this thesis. When applying the model to other concrete policy or investment decisions, data on decommissioning and new installations must be compiled.

Parameters For modeling power plant behavior in UC models, several parameters are required. The parameters for the base scenario are summarized in Table 6.3. Most of them are own assumptions based on experience from industry projects and literature (e.g. [27, 56, 128, 198, 213]). Parameters are assumed to be the same for power plants of the same fuel type and year of construction. Individual plant characteristics are neglected, which allows for future improvements to the database in this regard. As these power plant parameters determine their flexibility, they are varied in scenarios that analyze effects of increased power plant flexibility (see Table 7.1 in Section 7.2).

Two additional parameters are introduced with the temperature model: the heatloss factor λ and the maximal heating speed $H^{\max}$. The latter is often described in literature, even though seldomly used in UC models. The heatloss factor λ, however, is not directly available from current sources but can be derived from the minimal off-time after which a start-up is called "cold" start. Here, a cold start is defined whenever the temperature of the power plant is below 10% of temperature during operation. This will be the case after cooling times of around 50 h for coal, 60 h for lignite, 75 h for nuclear, 25 h for combined cycle gas turbines (CCGT), and 7 h for open cycle gas turbines (OCGT) and oil power plants. Given this assumption, λ can be calculated by

$$\lambda = \frac{\ln 0.1}{\text{cooling time}}. \tag{6.13}$$

Afterwards, the maximally allowed heating is estimated from the time required for an entire cold start; values are approximated from the start-up times given in [183]. Readers must keep in mind that all parameters are approximations and highly differing values exist throughout the literature (see e.g. Hasche [88] for a comparison).

Parameters that are discussed intensively and which show a high variation are the start-up costs. The costs for a power plant start-up result from additional fuel requirements for heating as well as from wear-and-tear. Especially the wear-and-tear costs are highly uncertain and companies do not publish the values they are assuming for internal planning. In countries with increasing shares of renewable energy sources, several power plants might be shut down in the next years. This dramatically reduces the current value of the plants and hence the costs of damage. In other cases, newly built plants might still be operated to minimize damage and extend lifetimes.

An extensive and often cited study on cycling and start-up costs was done by the National Renewable Energy Laboratory (NREL) [128] based on a utility questionnaire.

Table 6.3: Parameters of thermal power plants in the base case

	Gas CCGT	**Gas GT**	**Lignite**	**Coal**	**Nuclear**	**Oil**
$P^{\min}$ (%)	45	30	45	35	45	40
$\eta_{\max}^{2015}$ (%)	60	45	43	45	40	40
$\eta_{\max}^{1960}$ (%)	45	30	33	35	30	25
$\eta_{\min}$ (%$\eta_{\max}$)	82	65	90	92	95	65
λ (-)	0.1	0.3	0.04	0.06	0.03	0.3
$H^{\max}$ (-/hour)	0.2	1	0.12	0.15	0.1	1
RU (%/min)	5	10	2	3	4	5
RD (%/min)	5	10	2	3	4	5
SU (%/min)	50	90	50	50	45	70
SD (%/min)	50	90	50	50	45	70
V (€/MW)	60	20	130	110	100	20
F (€/MW)	40	40	110	90	150	40

Herein, the costs show a very high variation, e.g. the capital and maintenance costs of a small (< 300 MW) coal-fired sub-critical power plant range from around 50 $/MW to more than 400 $/MW. Table 6.4 depicts the cost values that were identified by [128], i.e. the median and the 25th/75th percentile of all power plants from the questionnaire. It must be noted that those values are assumed to be lower bounds for start-up costs. For this reason, values used within this thesis are oriented around the 75th percentile. In the case of coal, an average of small and large power plants is assumed when calculating the costs.

The sum of F and V is set to the 75th percentile value of a cold start as given in Table 6.3. For CCGT and coal, hot start costs are assumed to be at around 50% of a cold start. As hot starts can already include several hours of cooling, the variable costs are set to a slightly higher value than the fixed costs. For gas turbines, on the other hand, fixed costs have a higher share: costs for a hot start are more than 50% of costs for a cold start. Lignite and nuclear power plants are assumed to be slightly more expensive than coal power plants in terms of start-up costs [56, 213]. The exchange rates between $ and € are neglected as costs are lower bounds. In a study by Keatley et al. [118], the non-fuel cold start costs (only damage and maintenance) of a 400 MW are estimated at 73111 €, which corresponds approximately to 180 €/MW. In other studies, however, values for start-ups are much lower.

The efficiency of power plants depends on the operating point and the year of power plant construction. In the maximal power point, which is assumed to be the most efficient point of operation, the efficiency is computed according to the year of construction by

$$\eta_{\max}^{\text{year}} = \eta_{\max}^{1960} + \left(\eta_{\max}^{2015} - \eta_{\max}^{1960}\right) \cdot \frac{\text{year} - 1960}{2015 - 1960}. \tag{6.14}$$

In the scenario calculations, no minimum up- or downtimes are considered as they are assumed to be non-existent [88]. In a report of the Eurelectric [68], minimum downtimes are set to zero, which is a further indicator that this assumption is correct.

Table 6.4: Estimation of start-up costs according to Kumar et al. [128]

	CCGT	**GT**	**Large Coal (>300MW)**	**Small Coal (<300MW)**
Hot Start Median ($/MW)	35	19	59	94
Hot Start 25th ($/MW)	28	12	39	79
Hot Start 75th ($/MW)	56	61	68	131
Cold Start Median ($/MW)	79	32	105	147
Cold Start 25th ($/MW)	46	12	63	87
Cold Start 75th ($/MW)	101	61	124	286

6.6 Fuel Costs

Important parameters for UC modeling are the fuel costs which determine large shares of the operational costs. Fuel costs are a highly uncertain parameter as both the pure fuel costs as well as the costs for CO_2 emissions are fluctuating across time. For this thesis, fuel costs including costs for CO_2 emissions are set to 9.3 €/MW_{th} for coal, 41.4 €/MW_{th} for lignite, 22 €/MW_{th} for gas, 3.6 €/MW_{th} for uranium and 47 €/MW_{th} for oil. Values for fuel costs were set oriented on the values that were used in [213].

6.7 Storage

The model considers short term pumped hydro storage (optimization horizon is only 36 hours). The storage data is based on publicly available data from Eurelectric [67] which includes turbine power per country. The reservoirs are assumed to be able to store 6 hours of full turbine power. The distribution to the regions is conducted by individual research on storage and several open source data [49, 209]. The efficiency of the pumped hydro storage is 90% for pumping and for turbining which results in a cycle efficiency of 81%.

6.8 Evaluation of Data Quality

The dataset that is developed within the course of this thesis has to be seen as a first step towards a reliable and validated model of the European power system. While being an ideal test bed for the analysis conducted within this thesis, the model has to be calibrated with real-world behavior. Especially grid modeling and resulting load flows require additional investigations and calibrations as the zonal DC model with aggregated lines can lead to errors or inaccuracies (see 4.9.3). However, only a model that respects grid constraints which are based on physical flows instead of a simplified transport model (e.g. [180]) allows to investigate effects of congestion, loop flows, and grid flexibility enhancement.

Intensive testing and application of the model in further research projects will allow for a fine tuning of parameters. Within this process, several aspects should be emphasized:

- Hydropower: So far, generation from hydro power is modeled according to ENTSO-E monthly generation on a country basis. To improve the model, water flows should be regarded more regionally. As flexibility from dam storage is underestimated by pure run-of-river plants, additional proxy pumped storage plants were installed in several regions. An exact calibration of the optimal size of those proxy plants should be undertaken or, alternatively, a completely new approach for modeling dam storage plants could be introduced.

- Combined heat and power plants (CHP): CHPs might be restricted in their operational range. In this thesis, the operation of CHPs is oriented on electricity markets and neglects constraints from heat supply. This might overestimate system flexibility and improved approaches could shed light on this question.

- Wind generation onshore and offshore: The database of Janker [116] is a global database that includes all VRE generation. Underlying data are reanalysis data from NASA [177]; a calculation of CFs was conducted whereby several parameters like turbine height, turbine type, and many more have to be considered. Data is calibrated for Germany and shows larger deviations for other countries and regions across the globe. An individual calibration for all European countries could improve the dataset further.

- Power plant database: The goal was to develop a model that can be made available to the public. Details on power plants might still not be accurate for all regions but a steady process of improvement will increase accuracy in the next years of model employment.

- Capacity retirement: Capacity retirement is not considered so far while there will be several changes in Europe's thermal power plant structure like the nuclear phase out in Germany. Future research could develop a European retirement and investment plan to consider dynamic changes in the conventional power plant portfolios.

- Transmission network physics: The same is true for the transmission network which is also not a perfect dataset but an approximation that should be improved over time. The zonal reduction and the resulting PTDF should be calibrated, e.g. by setting up a model of the entire high voltage transmission system.

- Transmission network politics: Other constraints that are not represented in the model and dataset are legal issues concerning power exchange between countries. The limits of cross-country trading are not the physical constraints but the ex-ante defined maximal capacities. Those so-called net transfer capacities (NTC) are derived from physical limitations which are valid for all power flow situations independent of the actual situation in a specific point of time.

Chapter 7

Evaluation of Flexibility Sources

In this chapter, the effects of adding flexibility sources to a power system are evaluated. As mentioned in the dataset description (cf. Chapter 6), the employed scenarios should be understood as general test cases and results will give insights into the effectiveness of different flexibility measures in large-scale power systems in a general sense.

As the major focus of this thesis lies on the model development for representing thermal power plants in UC, there is also a focus on the effects from increased power plant flexibility in the numerical studies. Still, various other experiments on grid extensions and grid flexibilizations are conducted in the German as well as European context to illustrate the powerfulness of the developed model.

7.1 Models and Measures

This section gives an overview of the model specifications for different research questions to be addressed. First, the evaluation metrics are introduced. Afterwards, different model setups depending on the level of detail are described and then compared with respect to computational effectiveness. The last part describes the different technical measures and their combination with the model setups.

7.1.1 Evaluation Metrics - Efficiency, Costs, and Reliability

When evaluating the introduction of new elements into a system, measures have to be defined to value their effectiveness. In the case of power systems, the measures are derived from the concept of the energy policy triangle aiming at providing energy with respect to economical viability, environmental friendliness, and a high degree of security of supply.

Measures that are used in the following are defined as:

- Renewable integration: The major reason for power systems to become more flexible is the integration of VREs. Generation that cannot be integrated has to be curtailed, e.g. because of insufficient ramping or because of insufficient transport capacities. The amount of curtailed production serves as the most important indicator for effective measures.

- Costs: Operating costs that include fuel costs as well as start-up costs (including wear-and-tear costs). The differences in costs that can be achieved by certain measures have to be compared to the base scenario. Costs are highly related to the curtailed generation but include other aspects like start-up costs or a shift towards cheaper technology as well.
- Emissions: Overall CO_2 emissions can be compared between scenarios with newly introduced technologies and the base scenario. Again, the curtailed generation is a first proxy for this variable but changes in technology can have additional effects.

Measuring security of supply in all aspects is more complicated and requires a model with more technical details. One aspect of security of supply, however, is the ability to fulfill energy schedules and provide the demanded energy in every instance. The model in this thesis uses a so called "slack" variable whenever only an insufficient amount of energy can be provided and load is lost. The amount of "slack" required is interpreted as indicator for security of supply. Analyzing the results showed that "slack" is only required in the scenarios with changing forecasts; load can be provided throughout the year in all other scenarios and, therefore, the measure is not discussed for these scenarios.

7.1.2 Overview of Basic Models For Evaluation

Several options for the inclusion of different modeling aspects can be considered. The major equations that are modeled with some variations are:

- The basic unit commitment constraints are employed including equations (4.10)-(4.16) for cost definitions and basic technical constraints. The logic constraints according to (4.23) and (4.24) are employed for all power plants that are modeled with binary decisions.
- The temperature model is employed which includes equations (4.35)-(4.40).
- Limited heating is considered by adding constraint (4.44).
- DC load flow with the PTDF approach is modeled by equation (4.85) and equations (4.69)-(4.70) guarantee that line constraints are respected.
- Storage is modeled in all regions by introducing storage generation to the demand equation according to (4.86). Further constraints describe the operational range of storage by equations (4.87)- (4.89).
- Whenever reserves are considered (models named with "-ctr"), the equations from Section 5.3 are applied for the control areas. This includes reserve requirements for the different types according to (5.1), the technical constraints of power plants (5.2)-(5.7) and the additional constraints for storage plants providing reserves (5.12)-(5.17).

Different options for modeling details are described and tested. This includes the optional consideration of reserve constraints and the decision on whether all or only part of the power plants are modeled with binary decisions. The purpose is to understand the possibilities of current computing and the effects on results that arise from the constraints. Based on testing a variety of different levels of detail, appropriate variants are chosen for the large-scale simulations. The geographic region is either the entire European continent or Germany as a focus region. The reason for concentrating on Germany in part of the simulations stems from the high computational complexity of the European system. Furthermore, current data provides more details for the German system, especially the power plant database is more accurate than for the rest of Europe. Finally, Germany can be seen as a leader in terms of VRE integration. Thus, it yields a compelling test case for modeling this integration and its consequences.

The models that are distinguished and tested can be categorized and named as:

- $\mathrm{EU}^{\mathrm{MIP}}_{\mathrm{ctr}}$: All power plants are modeled with binary decisions and reserve requirements are assumed for all countries.
- $\mathrm{EU}^{\mathrm{MIP}}$: All power plants are modeled with binary decisions. Reserves are not considered.
- $\mathrm{EU}^{\mathrm{lin}}\mathrm{DE}^{\mathrm{MIP}}_{\mathrm{ctr}}$: Only the German power plants are modeled with binary decisions; all other European plants are modeled linearly. Reserves are considered for the German system only.
- $\mathrm{EU}^{\mathrm{lin}}\mathrm{DE}^{\mathrm{MIP}}$: Same as $\mathrm{EU}^{\mathrm{lin}}\mathrm{DE}^{\mathrm{MIP}}_{\mathrm{ctr}}$ but without considerations of reserves.
- $\mathrm{DE}^{\mathrm{MIP}}_{\mathrm{ctr}}$: Germany is modeled as an island and all grid connections to neighboring countries are cut. All power plants are modeled with binary decisions and reserves are considered.
- $\mathrm{DE}^{\mathrm{MIP}}$: Same as $\mathrm{DE}^{\mathrm{MIP}}_{\mathrm{ctr}}$ but without consideration of reserves.
- $\mathrm{EU}^{\mathrm{MIP}}_{\mathrm{ctr}}$-rel: All binary decisions are relaxed. The basis is the model $\mathrm{EU}^{\mathrm{MIP}}_{\mathrm{ctr}}$.
- $\mathrm{EU}^{\mathrm{MIP}}$-rel: All binary decisions are relaxed. The basis is the model $\mathrm{EU}^{\mathrm{MIP}}$.
- $\mathrm{DE}^{\mathrm{MIP}}_{\mathrm{ctr}}$-rel: All binary decisions are relaxed. The basis is the model $\mathrm{DE}^{\mathrm{MIP}}_{\mathrm{ctr}}$.
- $\mathrm{DE}^{\mathrm{MIP}}$-rel: All binary decisions are relaxed. The basis is the model $\mathrm{DE}^{\mathrm{MIP}}$.

For all models, uncertainty in form of changing forecasts can be introduced (with one scenario only, according to the method described in Section 5.4.2). For this thesis, this option is used to estimate additional benefits of flexible power plants with the Germany-only model $\mathrm{DE}^{\mathrm{MIP}}_{\mathrm{ctr}}$.

7.1.3 Effects of Modeling Different Levels of Detail

In this section, the basic scenario is computed and differences between model variations are depicted. Differences are analyzed with respect to the computational burden but also with respect to the results themselves. These findings shed light on the possibilities for modeling with current computational limits. The computer used has 128 GB of RAM and 64 cores with Intel(R) Xeon(R) processors of 2.70 GHz. The solver settings allow using up to 24 cores for the parts of the optimization process that can be parallelized. As computational power and effectiveness of solvers will continue to rise, more accurate modeling might be possible in the future. However, relative differences between model formulations might remain.

Comparison of runtimes and gap The computational burden of each level of detail that is modeled can be described by the runtime required to reach a certain MIP gap (see Section 4.2.1 for a definition) and the remaining gap after a maximal time. For the experiments, the target MIP gap is set to 0.0001 (0.01%) and the maximum runtime is 28800 seconds (8 hours). In those tests, the first 7 days of a year are modeled with a rolling horizon as described in Section 5.2 (36 hours are optimized at once whereof the first 24 hours are considered for the final results).

Fig. 7.1 on the left depicts the remaining MIP gap (average over 7 runs) after the maximal runtime. The right side shows the average runtime until the target MIP gap is reached. The remaining MIP gap indicates the ability of the models to be used for the evaluation of flexibility measures. When modeling all power plants in the entire European system with binary decisions (EU^{MIP}_{ctr} and EU^{MIP}), the average remaining MIP gap is above 0.6. Results with such high gaps cannot be interpreted reasonably and power plant dispatch is far from optimal. Modeling only the German power plants with binary decisions and all other power plants in Europe linearly, the solvability of the model depends on whether reserves are considered or not. For the models with reserve consideration ($EU^{lin}DE^{MIP}_{ctr}$), the remaining MIP gap is still high with 0.11 on average. Again, a sensible interpretation of results is difficult. Only when neglecting the reserve constraints ($EU^{lin}DE^{MIP}$), the model becomes solvable.

For the models considering Germany only, the remaining MIP gap is small for both models, with or without reserves. The relaxed models do not have any MIP gap by definition. Here, only the time that is required for solving must be regarded. Solving a relaxed model means solving a linear problem without any integer constraints. Such models can be solved much faster. For the Germany-only models, the solving time for the relaxed problem is only 60 seconds with reserves and 44 seconds without. Including binary constraints leads to an dramatic increase of computational times and adding reserve requirements further doubles the time required to achieve the defined MIP gap. For the European system, average runtimes are above 8 hours which means the limit was always reached before a solution was found. Runtimes of slightly above 8 hours are due to model building, which was not included in the runtime limitation.

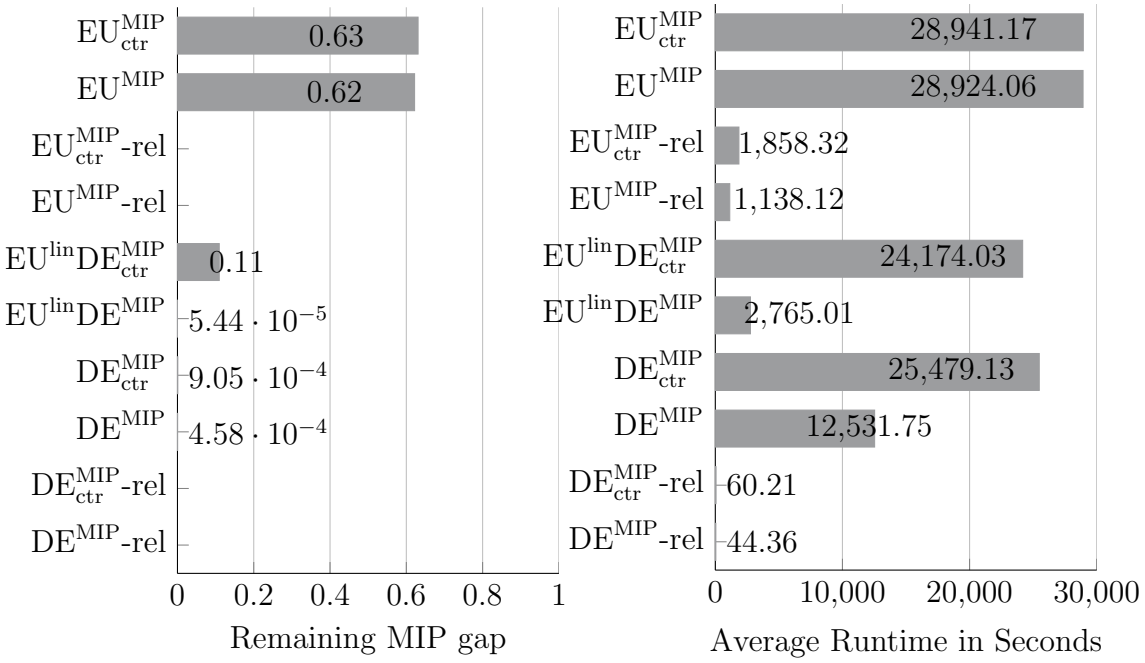

Figure 7.1: Remaining MIP gap (left) and runtimes (right) for different levels of modeling details

Comparison of costs and fuel mix Comparing the costs of the different approaches gives further insights into the model: what is the effect of mixed-integer constraints? What is the cost share of Germany within Europe? What is the burden of providing reserves? Fig. 7.2 illustrates the costs for the European system on the left and for the German system on the right, both for seven consecutive days. The models with very high MIP gaps show cost values that are far higher than for the models that were solved accurately. A real comparison is only possible for the German system, where all models were solved with a small remaining gap. The model with all binaries and reserves included leads to the highest costs of €131 m of which fuel costs account for €130 m. When neglecting reserves, the fuel costs are reduced from €130 m to €110 m, while start-up costs remain at the same level. Interestingly, costs are not reduced further when binary constraints are relaxed; for both, the model with and the model without reserves, costs remain the same. The tests only consider the first seven days and results might deviate as soon as entire years are considered.

As a last aspect to compare the different approaches, Fig. 7.3 shows the change in fuel mix as a percentage of overall thermal generation. In the European system, a shift from gas-, oil-, and coal-fired plants to the cheaper nuclear and lignite sources is observed. Both the constraint for a binary on/off state and the additional constraints for reserve provision lead to the same shift. Nuclear and lignite fired plants show lower costs but are less flexible at the same time. The shift is greater when neglecting the reserve requirement than when relaxing the binary constraint. The generation mix in $EU^{lin}DE^{MIP}_{ctr}$ has to be considered carefully as the MIP gap was too high. Still, tendencies might remain but be less pronounced when being solved with a smaller MIP gap.

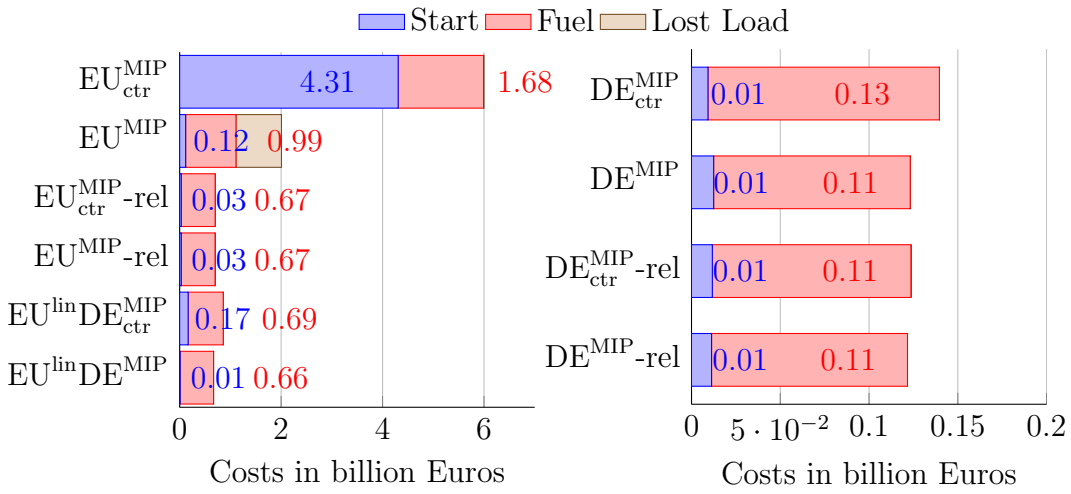

Figure 7.2: Comparison of operational costs for seven days depending on the level of modeling details. The figure on the left depicts models of the entire European system and the figure on the right shows models with Germany modeled as an island.

For the German system, this is exactly the case. A shift towards more lignite and less (hard) coal and gas is observed but at lower amplitude. Constraints like binary decisions or reserve requirements necessitate more expensive solutions with power plants of higher flexibility. An additional slight shift towards less nuclear generation can be observed, which is difficult to explain. However, as the latter effect is very small, it might originate from a special situation in the analyzed week.

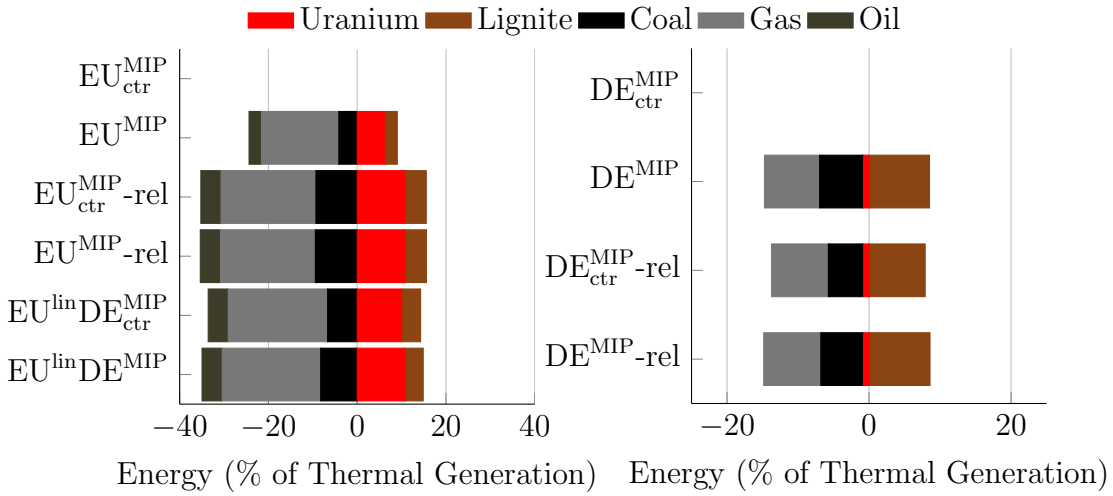

Figure 7.3: Comparison of the shift in generation mix with different levels of modeling details. The figure on the left shows values for Europe, the figure on the right the same values for Germany when modeled as an island. The figures illustrate the results of one model week.

Conclusions for modeling of details The experiments show the computational limitations of the model. Modeling all power plants with binary decisions is only possible with a remaining MIP gap of 0.63 after 8 hours of computation. Hence,

achieving reliable results in large-scale numerical studies is not possible. The model becomes solvable when modeling binary decision only for German power plants and when neglecting reserve constraints. Since the latter leads to an underestimation of the value of flexible generation, the approach does not appear to be appropriate for evaluating enhanced generation technologies. An idea to overcome computational problems is to improve the relaxed solution by adding valid inequalities as e.g. discussed by Hua and Baldick [104]. While the problem remains continuous, the resulting solution might be in closer correspondence to the original integer problem. This might allow modeling larger parts with relaxed equations while still being able to derive valid and interesting insights. Another option that might allow computing the entire system is to employ decomposition techniques, in which each zone is optimized on its own and the subsystems are then coordinated in a master problem. Such multi-region UC might also resemble the current power system of Europe with its separated market zones more realistically.

Following this analysis, two models seem to be the most relevant: models $\mathrm{DE}_{\mathrm{ctr}}^{\mathrm{MIP}}$ and $\mathrm{EU}^{\mathrm{lin}}\mathrm{DE}^{\mathrm{MIP}}$. Concerning the evaluation of effects from increased power plant flexibility, modeling of reserves and binary decisions is inevitable. Otherwise, ramping possibilities will not be as relevant in the model as they are in reality. Thus, the model $\mathrm{DE}_{\mathrm{ctr}}^{\mathrm{MIP}}$ is the method of choice when regarding effects of increased power plant flexibility. In order to be able to compare the effects of power plant flexibility to other measures, the same model is also applied for research on grid extension, grid flexibility, or storage extension in Germany. Investigation on a European scale can only be modeled with fewer details. Power plant flexibility enhancement is not investigated, but for all other questions, $\mathrm{EU}^{\mathrm{lin}}\mathrm{DE}^{\mathrm{MIP}}$ is employed.

In future research, a combined model might be a promising method. An initial approach in that direction was suggested by Trepper et al. [197]. In a first iteration, a relaxed problem with the entire European system is computed. Then, in a second step, results on power flows from and to Germany are set as parameters and the Germany-only model is re-optimized. In this case, results will present effects of increased flexibility for Germany within an interconnected European power system.

7.1.4 Modeling Flexibility Measures

Power plant flexibility A special scope of the thesis is modeling UC decisions and power plant operations. Different parameters of power plants are varied and their system impacts are analyzed. As discussed above, this issue is investigated for the German system only and input variation as well as results are presented in Section 7.2.

Storage Another very important measure discussed in the context of VRE integration is storage. In this thesis, the benefits of short-term storage (up to 36 hours) are evaluated for both the German and the European system. In several scenarios, the storage capacity of the system is doubled and their location is varied. Concerning the effects of seasonal storage, other types of models are required. A comprehensive overview over conducted studies can be found in the PhD thesis of Kühne [127].

Transmission extension Several studies showed the tremendous benefits of large-scale transmission extension for efficient renewable integration. Studies can be found with different regional scopes including Europe in [2], Asia in [109], or even a global scope [1, 2, 38]. In this thesis, analyses are restricted to a few extension experiments since the main focus of this section lies on demonstrating the ability of the developed model to find answers on grid extension questions. Results give clear indications on the importance of grid extension for the challenge of VRE integration within a German and within a European context.

DC lines Grid capability cannot solely be increased by extending the AC transmission system but also by adding DC lines or by switching existing AC lines to controllable DC lines. Several studies have already shown the positive effects of enhanced grid flexibilities by the introduction of DC lines (with and without capacity upgrades). Bucher et al. [31] evaluate the introduction of HVDC lines in a test grid and develop algorithms for optimal line placements. Results show that economic efficiency of the systems can be improved whenever DC lines are added to the system. Furthermore, a predefined flexibility metric significantly increases which indicates the positive effects for VRE integration. Chatzivasileiadis [39] defines an algorithm for placing DC lines with highest cost savings. The idea is connecting the nodes with highest marginal generation costs (highest nodal prices) with those showing lowest prices. Results indicate cost savings of up to 30% for placing new DC lines (very long lines, e,g, from Spain to Norway are considered). In the test cases of this thesis, only moderate DC extension on existing corridors are evaluated.

In contrast to extending and adding additional lines, switching of AC lines to DC lines does not increase transmission capacities. However, it allows for controlling the load flow and eventually prevents overloading of lines. Electricity flow that would overload a line can "bypass" through neighboring lines. Switching lines to DC might bring further advantages to the system since this hybrid transmission grid architecture enables more efficient optimal power flow as shown by Hotz and Utschick [103]. Further research could analyze whether the same lines allow for improved power flow computations and for techno-economic advantages.

Phase shift transformers (PSTs) PSTs could be another measure to prevent lines from overloading. Such elements allow to change the angle differences on a line and therefore shift load flow to neighboring lines. Currently, some Eastern European countries are using PSTs to prevent loop flows through their countries. For the evaluation within this thesis, PSTs are installed in order to eventually reduce congestion. The angle difference that is allowed for PSTs is limited to 30°, which is a typical value in industry [18], leading to

$$-30 \leq PSA_m^{\max} \leq 30 \quad \forall m \in \mathcal{L}. \tag{7.1}$$

7.2 Value of Enhancing Thermal Power Plants in Germany

The first measure for improved system performance is increased power plant flexibility. This section employs the developed models to analyze the effects of possible power plant enhancements. Several measures to increase the flexibility of power plants are evaluated by adjusting the following parameters:

- Reduced minimal power output $P^{\min}$ and increased part-load efficiency
- Increased heat-up speed $H^{\max}$ (only effective in stochastic settings)
- Increased ramp-up and ramp-down speed RU/RD
- Increased start-up and shutdown ramps SU/SD

Three scenarios ("Flex1": focus on ramps, "Flex2": focus on minimum power, "Flex3": focus on both) are defined where parameters are varied from the "Base" scenario as given in Table 6.3. Flexibility increases are not considered for nuclear plants (no new installations / replacements planned). The values for the flexibility measures are displayed in Table 7.1.

Table 7.1: Parameters of thermal power plants in scenarios. The different parameter sets concerning the plant flexibility are named "Base"|"Flex1"|"Flex2"|"Flex3".

	CCGT	**Gas GT**	**Lignite**	**Coal**	**Oil**
$P^{\min}$ (%)	45|45|30|30	30|30|15|15	45|45|30|30	40|40|20|20	40|40|30|30
$H^{\max}$ (%/hour)	20|40|20|40	100	12|24|12|24	15|30|15|30	100
RU (%/min)	5|10|5|10	10|20|10|20	2|4|2|4	3|6|3|6	5|10|5|10
RD (%/min)	5|10|5|10	10|20|10|20	2|4|2|4	3|6|3|6	5|10|5|10
SU (%/hour)	50|80|50|80	90|95|90|95	50|70|50|70	50|75|50|75	70|90|70|90
SD (%/hour)	50|80|50|80	90|95|90|95	50|70|50|70	50|75|50|75	70|90|70|90

The major results are derived with the option $\text{DEU}^{\text{MIP}}_{\text{ctr}}$ concerning modeling of details and key findings are presented in Sections 7.2.1 and 7.2.2. In order to estimate the influence of the chosen modeling framework and possible effects from uncertainty considerations, Section 7.2.3 compares system costs, number of start-ups, and emissions with two alternative approaches: an approach without reserve constraints and an approach with changing forecasts.

7.2.1 Comparison of Major Results

Costs The effect of increased flexibility on system costs is measured for the years 2015, 2025, and 2035. Results are depicted in Fig. 7.4 and illustrate that flexibility enhancements will become increasingly important with higher shares of VREs. While the maximal reduction of operational costs through increased power plant flexibility is only 1.8% in 2015, the value increases to 10.3% in the year 2035. Especially the reduction of minimum power output with "Flex2" becomes crucial with higher variability in residual

load. Cost reductions are almost as high as in the scenarios where both ramps and minimum downtimes are improved ("Flex3"). Increasing only ramp capability of the power plants ("Flex1") leads to higher start-up costs while fuel costs reductions are almost the same as in "Flex2". Here, generation is able to follow the variable load; power plants can be shut down even for shorter periods when necessary. With this "Flex1" scenario, cost reductions mainly result from reducing curtailment of excess generation.

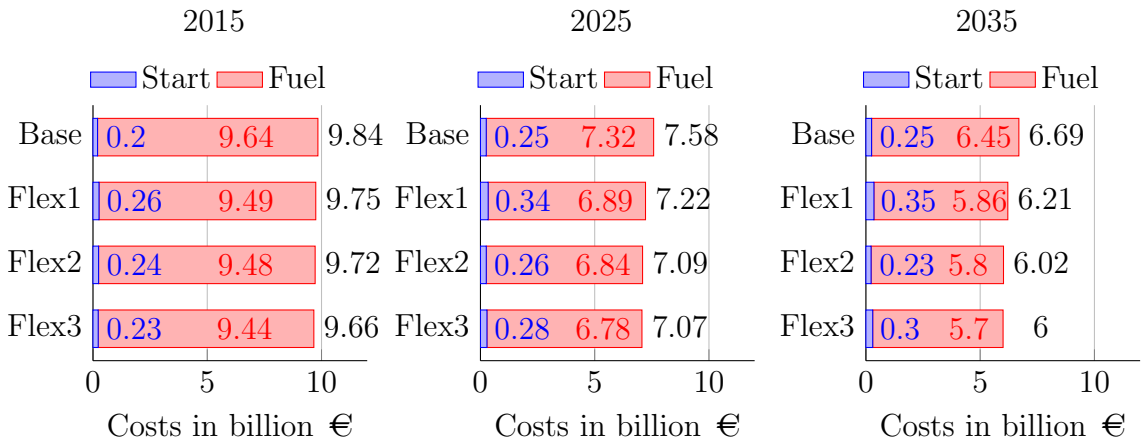

Figure 7.4: Operational costs for for different scenarios on power plant flexibility

(Renewable) Curtailment As depicted in Fig. 7.5, curtailment increases dramatically when larger capacities of VREs are installed. While curtailed energy is vanishingly small in the 2015 scenario, it increases to about 35 TWh in 2035 for the "Base" scenario. This number is as high as 6.4% of the annual production.

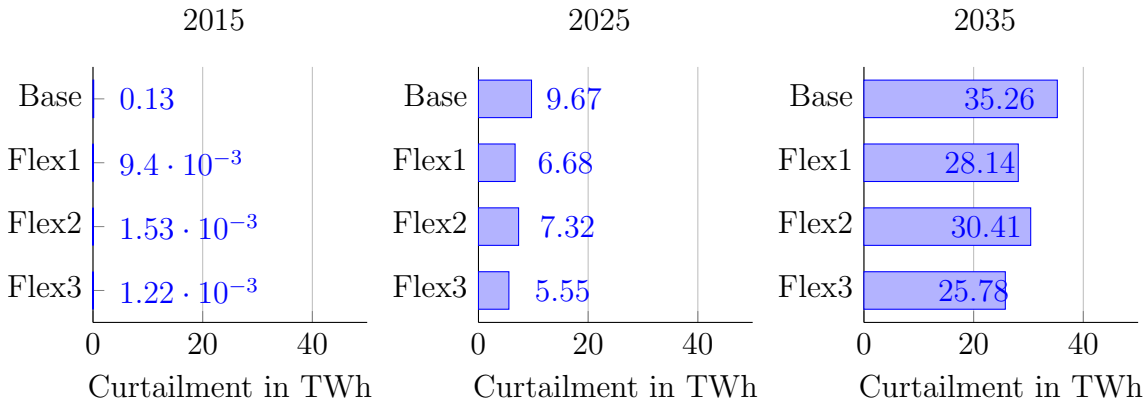

Figure 7.5: Power curtailment for different scenarios on power plant flexibility

The amount of curtailment can be reduced by 42.6% from 9.67 TWh to 5.55 TWh in 2025 and by 25.8% from 35.26 TWh to 25.78 TWh in 2035. Interestingly, the reduction is percentage-wise higher in the scenario for 2025. The reason is that only part of the curtailment is due to short-term flexibility requirements. In 2035 requirements for seasonal storage as well as grid constraints become more prominent.

In contrast to observations on system costs, increasing ramps seems to be slightly more effective concerning the reduction of curtailment. While curtailment with "Flex1" is reduced by 20% in 2035, only 13% are achieved with "Flex2". Increased ramps and start-up speeds allow for faster shutdown and restart whenever high VRE generation occurs. The higher start-up costs in "Flex1" can be interpreted as enabler for the reduction of curtailment. Combining the two measures with "Flex3", reduction of curtailment can be increased to 27%. Still, a curtailment of more than 25 TWh remains. Increasing flexibility of power plants proves to be an important measure for VRE integration. Nevertheless, it can only be part of the actions to be taken when aiming at the ambitious goals for renewable integration.

Emissions When analyzing power systems and VRE integration, an important measure that must always be considered is the amount of CO_2 emissions. Fig. 7.6 displays the changes arising from flexibilization of power plants. The figure shows several effects: emissions are reduced drastically by increased VRE generation. While emissions sum up to 256 Mio. tons in 2015, they can be reduced to 152 Mio. tons in 2035 (a reduction of 41%). In contrast, increasing the flexibility of fossil power plants only yields a very small effect and leads to slightly increased emissions in almost all instances.

Flexible generation allows integrating a higher share of VREs as illustrated by the reduced curtailment. More generally, it permits integrating a larger amount of generation from sources with low marginal costs. Besides VRE, lignite is a technology with very low marginal costs but with high emissions. A shift towards lignite away from gas and coal power plants leads to increased CO_2 emissions that overcompensate the reduction through prevention of curtailment.

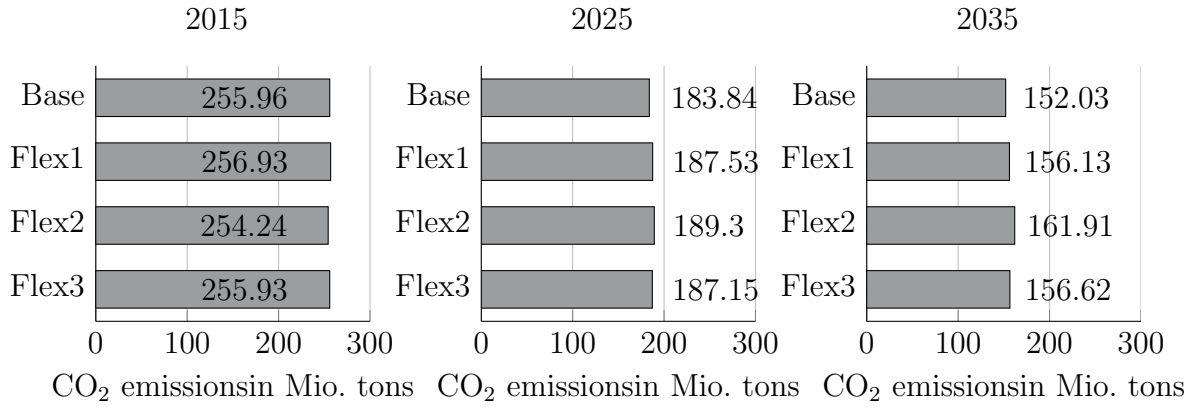

Figure 7.6: CO_2 emissions for different scenarios of power plant flexibility

Fuel mix The effect of a shift in the fuel mix is illustrated in Fig. 7.7. The upper charts show the overall fuel mix while the lower charts highlight the differences of the scenarios with increased flexibility compared to the "Base" scenario. The effects that were supposed to explain the increasing CO_2 emissions can be observed now: more lignite (and also slightly more uranium) is used while coal and gas generation is reduced. The figure also shows a reduction of overall utilization of thermal generation, reflecting the reduced curtailments. An additional 16 TWh of electricity production from lignite

is observed with "Flex3" in 2035. This causes higher emissions that overcompensate the savings of 20 TWh electricity generated by gas and 5 TWh generated by coal.

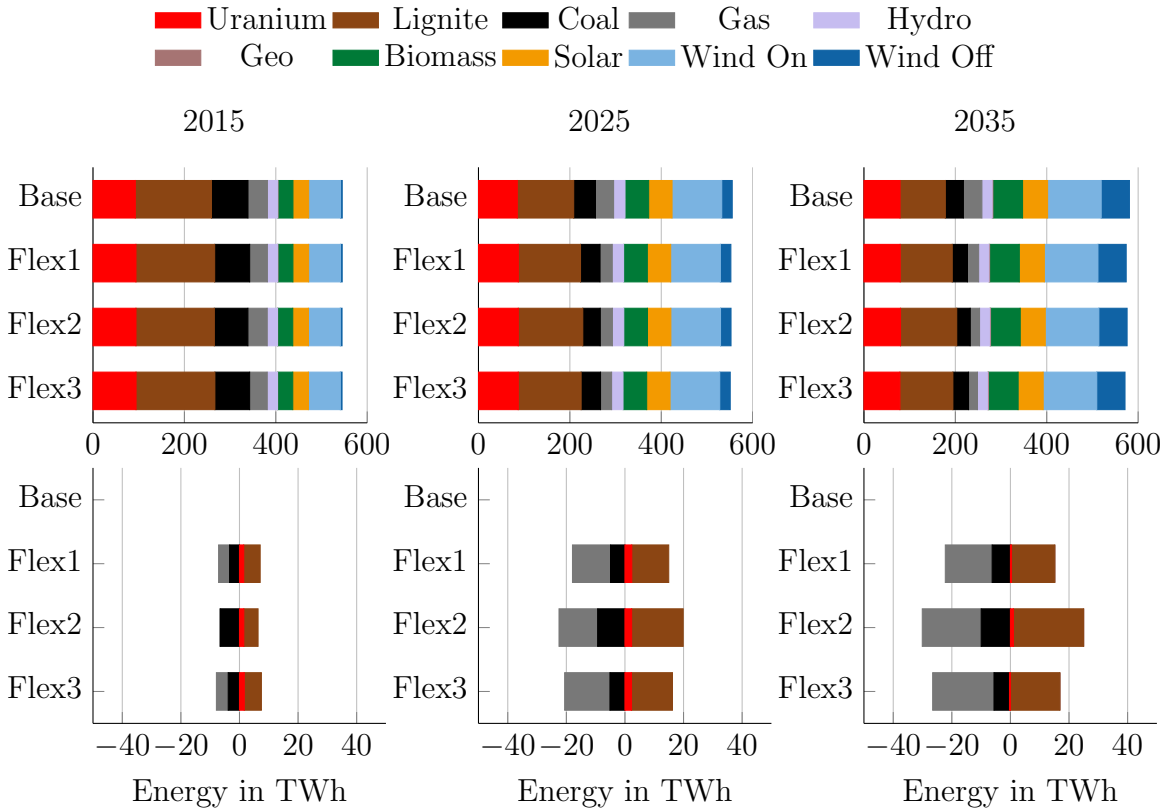

Figure 7.7: Generation mix for different scenarios on power plant flexibility. The upper charts illustrate the absolute values whereas the lower charts show the difference to the "Base" scenario.

7.2.2 Explanation and Further Analysis of Results

The previous section analyzed major effects of increasing flexibility of fossil power plants. Here, explanations of additional results are given.

Number of start-ups It is interesting to compare the absolute number of occurred start-ups (see Fig. 7.8). Remarkably, the number of start-ups slightly increases in 2025 but then decreases in 2035 for the "Base" scenario, for "Flex1", and for "Flex3". For "Base", the number of start-ups increases from 5438 in 2015 to 5501 in 2025 and then decreases to 4925 in 2035. In 2025, fossil fuels are required in most hours of the year to provide the variable load resulting in many start-ups and shut-downs of plants. In the scenario for 2035, several subsequent hours where fossil fuel generation is mainly required to provide reserves might occur. In those hours, generation is kept at minimum load and load following is mainly conducted by curtailing excess generation; start-ups and shutdowns are not possible/required.

Another interesting observation is that increasing flexibility tends to increase the number of start-ups. This finding is in contrast to former research, e.g. number of start-ups

decreased for an individual CCGT power plant in Huber et al. [108]. A reason for an increasing number of start-ups ("Flex1" and "Flex3") is an increased maximal speed of start-up and shut-down (SU and SD). Shutting down and starting up is possible in a shorter time frame and thus becomes more attractive. Additionally, increased ramps allow the provision of reserves with fewer power plants - allowing more power plants to be shut down during hours with very high generation from VREs.

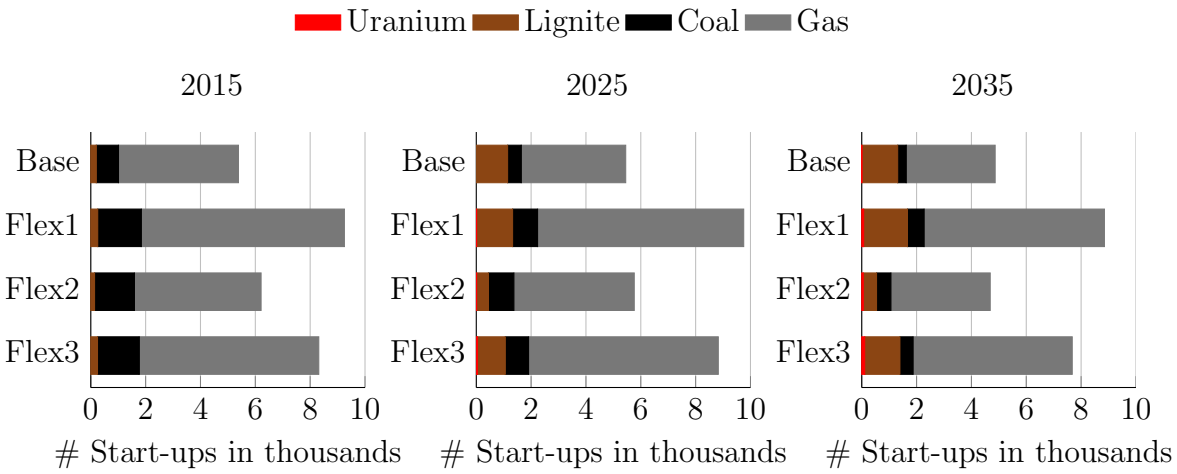

Figure 7.8: Number of start-ups in thousands according to generation technology

Reserve provision In all scenarios, reserve power must be provided as an important feature of current power systems to be prepared for unexpected events (see Section 5.3). The considered reserve types are primary and secondary reserves, both for positive and negative deviations. Here, the provision of secondary reserves is analyzed since more power is required and as storage is able to provide parts of it as well. Fig. 7.9 illustrates the contribution of different power plant types and storage to secondary reserve and provides several new insights. To start with, the upper charts depict the provision of positive secondary reserves and show that storage fulfills very large shares of this task in 2015 while fossil fuels become more important with higher shares of VREs. This can be explained by the fact that the "main task" of storage is storing energy in times with excess production and releasing the stored energy later on when demand is high. In other words, storage plants are required for their main purpose more often and more urgently in 2035 than in 2015. Another reason is that with increased VREs, more power plants are already operated in part load. Therefore, they can provide positive reserves in these times at no additional cost. The contrary effect is observed for negative reserves: power plants are increasingly operated close to their minimum power output, making the provision of negative reserves more difficult.

Comparing the different flexibility measures for thermal generation, some effects similar to those on the fuel mix results are observed. When improving reducing $P^{\min}$ ("Flex2"), more lignite is introduced to the system and then also provides more of the reserves. All power plant enhancement options allow providing reserves more easily which "frees" storage from providing negative reserves.

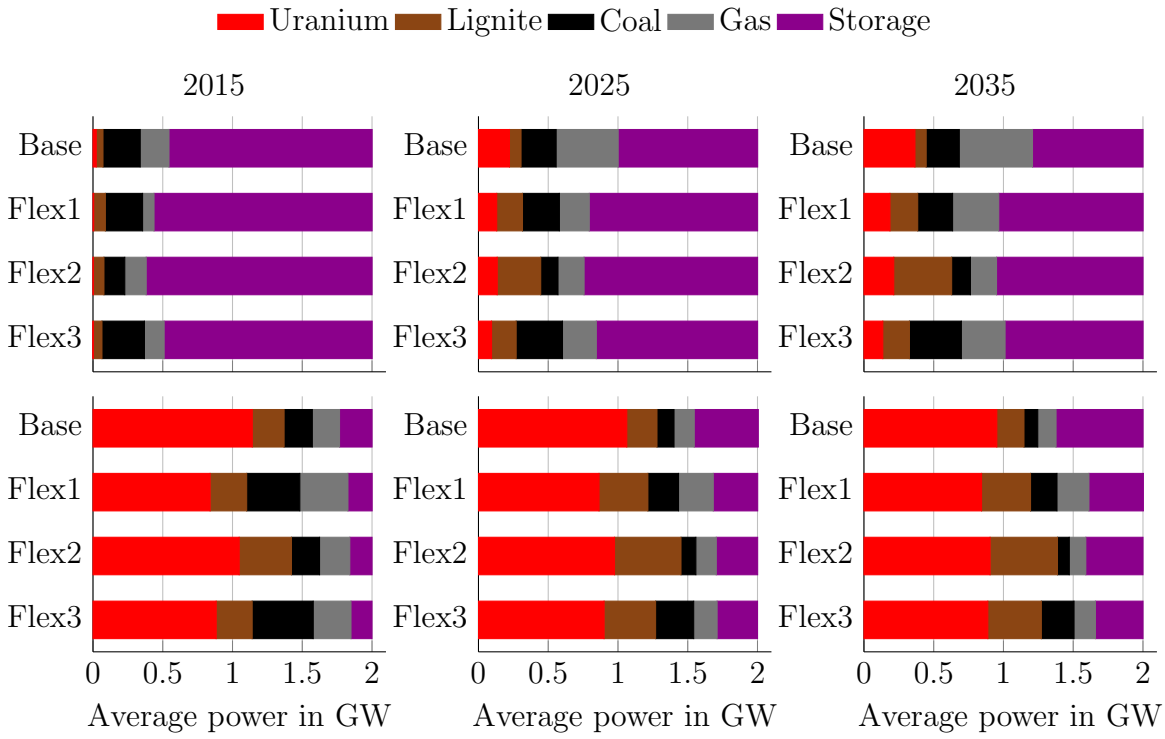

Figure 7.9: Provision of secondary control for different scenarios on power plant flexibility. The upper chart depicts the distribution of positive secondary reserve provision, the lower chart the same for negative secondary reserves.

Effects in hourly time resolution Fig. 7.10 shows the hourly generation profile for a summer week in the year 2035. The upper chart shows the "Base" scenario while the lower chart shows the generation with improved power plant flexibility ("Flex3"). In the first two days, large amounts of wind generation are fed into the system. In both scenarios ("Base" and "Flex3"), this leads to curtailment/excess generation (pink colored area). However, in the scenario with increased flexibility, curtailment is less. The conventional power plants that are still on-line during this long phase of high wind generation might mainly be used for reserve provision. Higher ramps allow providing the same amount of reserves with less capacity on-line.

Beginning with hour 40, wind calms down and additional generation from thermal plants is required. For "Base", a portfolio of sources including nuclear, lignite, coal, and gas provides this additional electricity. In the flexible scenario, the variety is lower: the increase is mostly provided by nuclear and lignite plants as their ability to increase their output (or to be started) is higher.

On the last day of the week beginning with hour 155, a very sunny day, generation from PV peaks at noon and then decreases in the afternoon. Thermal power plants are required to increase their output rapidly to fill the so-called "duck curve" (see Fig. 1.3 in the introduction). While gas and coal power plants run throughout the day and curtailment occurs in "Base", no gas and almost no coal power plant is running in "Flex3". Faster shutting down and restarting of plants allows for this more efficient behavior.

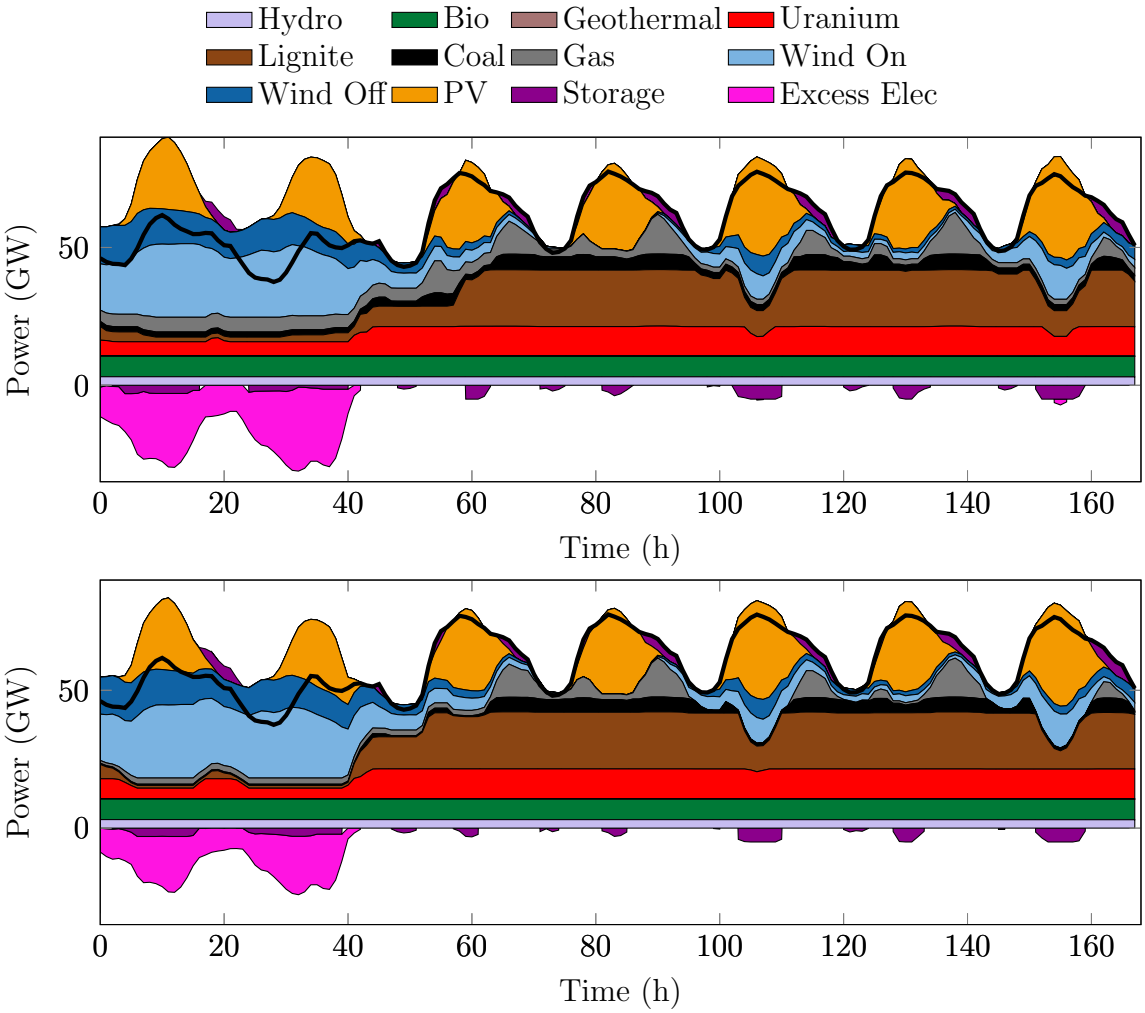

Figure 7.10: Generation profile for a typical summer week in 2035. The upper figures shows the "Base" scenario whereas the lower figure illustrates the scenario with improved flexibility ("Flex3").

7.2.3 Comparison with Alternative Scenarios

The results and analyses above show the contribution that increased flexibility of thermal power plants can have on the German power system as an island. The conducted runs include reserve requirements and grid constraints within the country. To better understand the measured improvements and verify whether these are upper or lower bounds, further tests are conducted:

- DE^{MIP}: An important comparison is a calculation that neglects the provision of reserves. This comparison allows quantifying how much of the benefits from improving thermal power plants result from the requirements to provide reserve power.
- DE^{MIP}-stoch: As discussed in Section 5.4, power systems might have to react to unexpected events by re-planning their schedules. The approach of Section 5.4 with a changing forecast is employed. This simplified stochastic approach gives

an idea of how results are influenced by uncertainty considerations leaving "real" stochastic considerations for future research.

All of those additional scenarios are considered for the year 2035 where effects from increased flexibility are highest.

Influences on costs A new component of costs must be introduced for analyzing the scenarios with changing forecasts: the cost of lost load. Whenever load cannot be fulfilled, e.g. due to "wrong" forecasts and inflexibilities in the system, a slack variable is employed in the model. This may be interpreted as consumers being cut off. The penalty for employing the slack variable is unknown and can only be speculated about. For the scenarios in this thesis, a value of 10.000 €/MWh is assumed.

Fig. 7.11 compares the costs for the alternative approaches: on the left, the results of the scenarios from previous sections are depicted and named as "standard"; in the middle, the scenarios without consideration of reserves are shown; on the right, the stochastic scenarios are depicted. For the scenario without any reserve considerations, very little effects of increased flexibility can be observed. Costs are reduced only slightly from €6.03 b to €5.91 b, which is a reduction of only 2% compared to the 10% reduction in the standard scenario. This reflects a main advantage of power plant flexibility: providing the system with reserves at low costs. When adding additional requirements for reacting to unexpected events by stochastic or changing forecasts (according to Section 5.4.2), effects from enhanced flexibility increase further. When including the value of lost load (which is only a guess), costs are reduced from €8.4 b to €6.07 b. But even when neglecting the cost of lost load, the system costs can be reduced from €6.88 b in "Base" to €6.06 b in "Flex3", which is a reduction of 12%. The results show the importance of increased ramp and start-up capabilities (including heat-up speed) which are available with "Flex1" and "Flex3" but neither in "Base" nor in "Flex2".

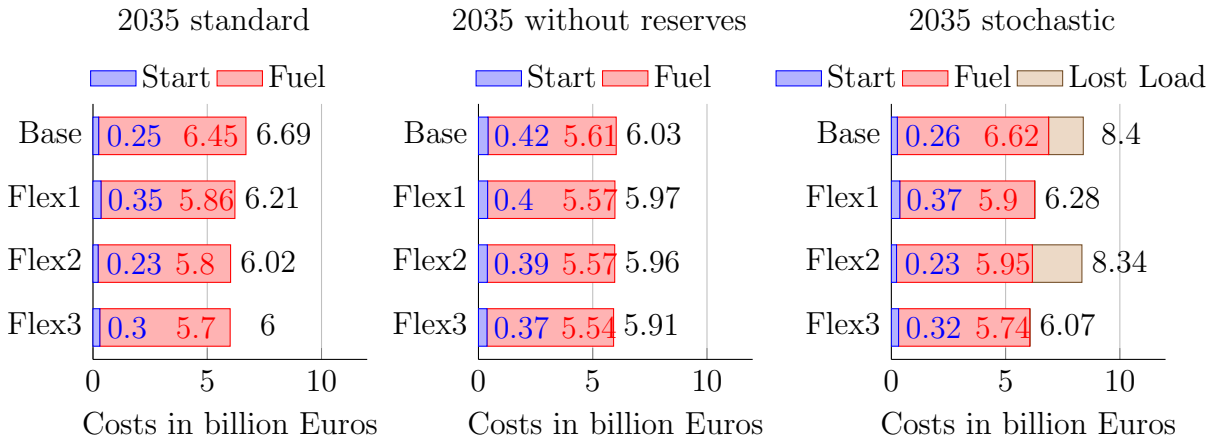

Figure 7.11: Operational costs in alternative scenarios. Different scenarios on power plant flexibility are evaluated in the standard model (left), a model without reserve consideration (middle), and a model with changing forecasts (right)

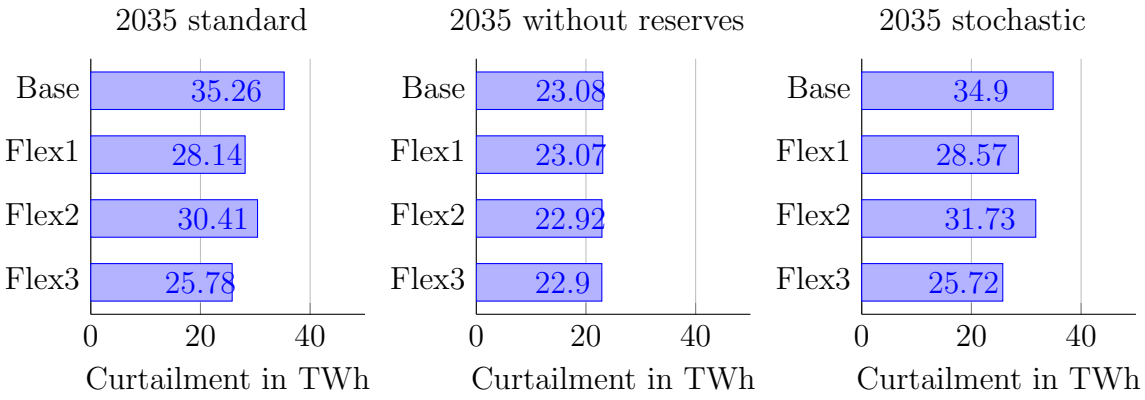

Figure 7.12: Curtailment in alternative scenarios

Influence on curtailment and lost load A comparison of those alternative modeling approaches in terms of curtailed energy is illustrated in Fig. 7.12. The figure shows that increasing flexibility does not have any significant effect when reserves are neglected. Curtailment is much lower for those scenarios, but the gap to the standard scenario converges with higher flexibility capabilities (for "Flex3", curtailment is 25.8 TWh in the standard scenario and 22.9 TWh for the scenario without reserves). With the introduction of uncertain forecasts, changes compared to the standard scenario are insignificantly small. The system seems to have enough downward flexibility. Power plants can be shut down very quickly while starting-up might take several hours.

Number of start-ups The number of start-ups is another noticeable aspect of the result and is depicted in Fig. 7.13. The effect of different flexibilization strategies is reduced when reserves are not considered. For the stochastic model, the number of start-ups increases dramatically reflecting the requirements for situations when less than planned production of renewable energy is fed in. Especially the start-ups of flexible plants, i.e. gas-fired plants as well as oil-fired plants are increased. While in the standard scenarios, oil-fired plants are not used at all, there is a significant number of start-ups from those plants when forecasts change. Especially in "Base" and "Flex2", oil-fired plants are required. For "Flex1" and "Flex3", most of required upward ramps can still be provided by gas-fired power plants and, as discussed above, no load is lost.

Discussion on the importance of flexible power plants Van den Bergh et al. [16, 17] show that the current portfolio of conventional power plants in Germany is capable of providing enough flexibility for the integration of up to 50% generation from wind and solar. While results in this thesis show occurring curtailment for the years 2025 and 2035, they still undermine the findings of Van den Bergh et al. for a unit commitment problem without considering reserve provision: curtailment cannot or can only slightly be reduced by increasing power plant flexibility. The curtailment might be a result of grid constraints or required mid-term/long-term flexibility. However, as soon as reserves must be provided, results change: Curtailment of renewable generation can be reduced significantly through increased flexibility of thermal power plants. Especially the increase of ramp capabilities with "Flex1"/"Flex3" proves to be helpful for the

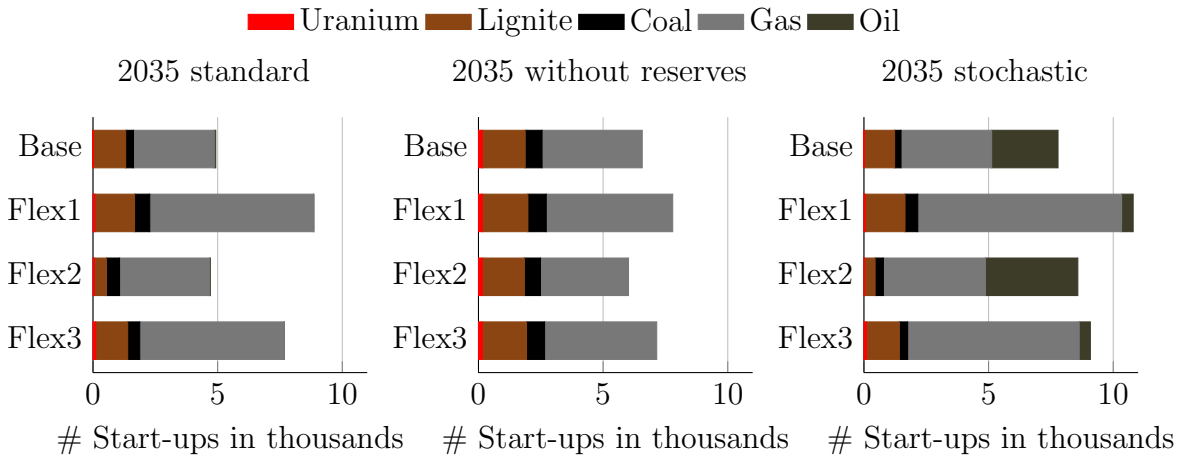

Figure 7.13: Number of start-ups in in alternative scenarios

system as soon as reserves and/or stochastic forecasts are considered. Since the real system requires reserves and as forecasts are always uncertain, results indicate that increased flexibility of power plants is indeed an important measure for improved renewable integration, but it is not sufficient for full VRE integration in 2035. The remaining curtailment does not require the short-term flexibility provided by power plants but might rather constitute excess generation in several hours that could be resolved by storage or grid constraints. Those two additional technological measures for improved integration of VRE are discussed in the next section.

The results of this section also point to the importance of uncertainty considerations. While the approach employed in this thesis is a first step, future research can be conducted to evaluate the benefits of improved power plants or entire power plant portfolios with increased flexibility capabilities. The temperature model is an ideal base for such modeling as constraints in start-up times are mostly a result of limited heating capabilities of plants.

7.3 Grid Enhancements and Storage Extension in Germany

As an alternative or as an additional measure for improved VRE integration, the installation of new transmission lines, the flexibilization of existing lines, and the extension of storage capacities are analyzed in this section.

7.3.1 Grid Extension in Germany

Simple AC extension ("All") The simplest approach for network extension is to increase all lines with a fixed factor. Here, all transmission lines are extended by allowing them to be operated at 100% of capacity instead of the 70% allowed when respecting the simplified N-1 criterion (See Section 6.3). In the base case case, the N-1 criterion has to be respected and the overall capacity (sum over the maximal allowed

flows over all lines) can be quantified to be at 248.7 GVA. Extending the lines in "All", i.e. neglecting the N-1 criterion, increases this number by 106.6 GVA to a total capacity of 355.4 GVA.

Selected AC lines ("Sel") In a more sophisticated approach, only selected connections are extended. The upper part of Fig. 7.14 illustrates the so-called shadow prices on grid capacities for the three model years with the "Base" scenario in terms of power plant flexibility. The shadow price can be interpreted as the benefit that could be achieved by lowering the capacity constraint by 1 MW: the higher the shadow price, the higher the expected benefit of the respective grid extension. In mathematical terms, the value is the marginal value of constraint (4.70) (positive for lower bound and negative for upper bound). The figure illustrates that only several lines show a high shadow price on capacities while many other lines are not congested. The applied extension strategy is to extend all connection which show a shadow price of above 1 €/MW in the 2035 scenario by two additional 380 kV lines. The overall extension after consideration of the N-1 criterion can be quantified to be at 12.9 GVA for this scenario. The individual connections that are extended are (see colored lines in Fig. 7.14 (c)):

- Kassel - Detmold
- Kassel - Braunschweig
- Lüneburg - Mecklenburg-Vorpommern
- Münster - Weser-Ems
- Oberfranken - Thüringen
- Münster - Detmold
- Hannover - Lüneburg

A further indication for the selection of lines to be extended are the line utilization rates which are displayed in Fig. 7.15, showing that the lines with highest shadow prices mostly also have the highest utilization rates. This gives further reason for their extension and validates the applied methodology of using the average shadow price as extension indicator.

DC Lines according to national plans ("DC") In this scenario, the currently planned DC lines are added. This includes five additional lines with each 2000 MW according to the German TSOs [80]. The overall capacity extension in this scenario can be quantified to be at 7 GW (after the N-1 criterion) but the lengths of extended lines are higher than in the other scenarios. Lines are added between the following regions:

- Schleswig-Holstein - Unterfranken
- Schleswig-Holstein - Stuttgart
- Weser-Ems - Düsseldorf
- Düsseldorf - Karlsruhe
- Dessau - Schwaben

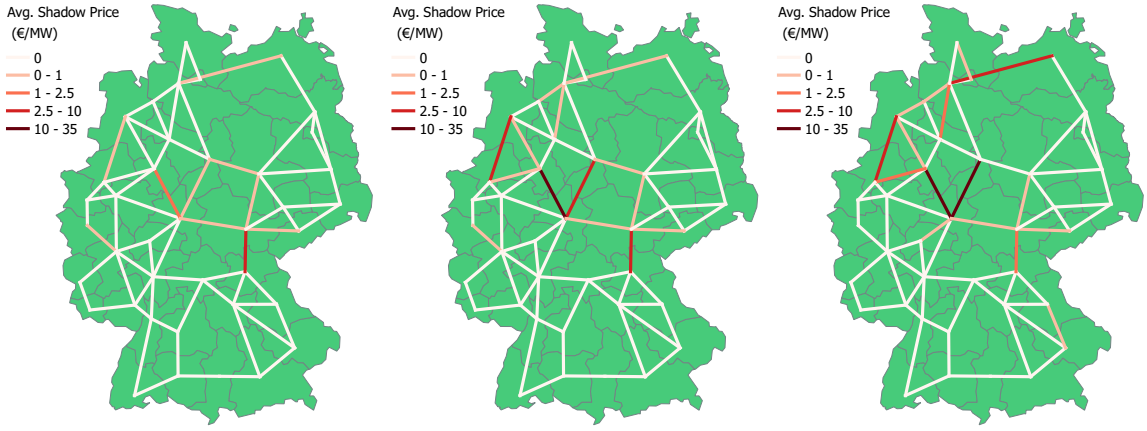

(a) 2015 (b) 2025 (c) 2035

Figure 7.14: Shadow prices on line capacities in Germany for the three modeled years

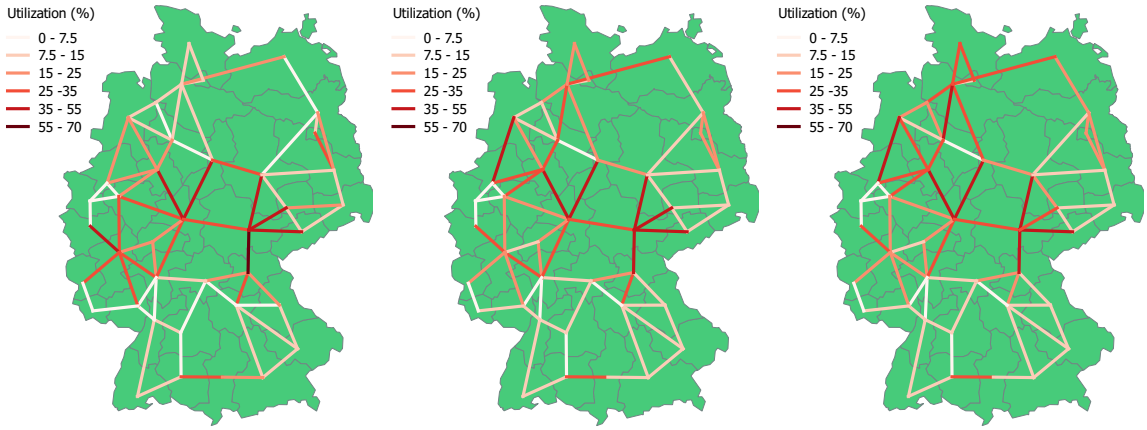

(a) 2015 (b) 2025 (c) 2035

Figure 7.15: Utilization of transmission capacities in Germany for the three modeled years

Effects of grid extension on costs in Germany Fig. 7.16 depicts the costs for the three different extension scenarios and allows drawing several conclusions. In 2015, grid extensions are not crucial as line limitations are still low and only very small effects can be achieved. These are the same for all extension scenarios and signify a cost reduction of only 0.2% from €9.84 b to €9.82 b. Cost reductions slightly increase in 2025 and are significant in 2035 with a reduction of €230 m from €6.69 b to €6.46 b (3.5%) in the DC scenario. Results show that the most cost-effective measure for grid extension is to install DC lines followed by increasing the capacity of selected AC lines ("Sel"). Extending all lines similarly ("All") is not as effective in terms of cost reductions. Congestions will still exist in the same lines and extending non-congested lines does not have positive effects (see below in paragraph on line utilization). Another observation is that the amount of start-up costs is not influenced significantly by grid extensions but will stay at a constant level.

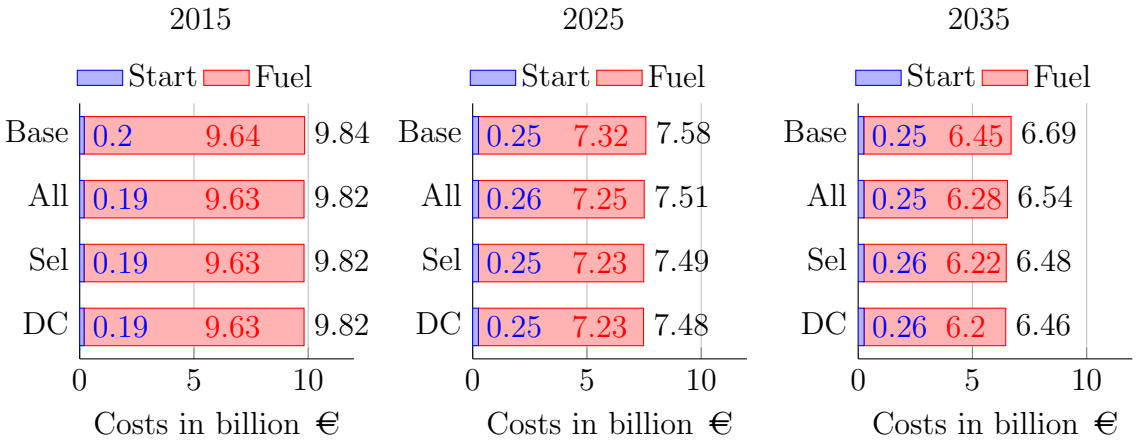

Figure 7.16: System costs for different grid extension scenarios in Germany

Effects of grid extension on curtailment in Germany The main reason for the cost reductions is the reduction of curtailment (see Fig. 7.17). Almost no curtailment occurs in 2015, while significant curtailment of 35.3 TWh emerges in 2035. Depending on the extension scenario, the value can be reduced to 26.2 TWh, which is a 25% reduction of the curtailment. The ranking of different extension strategies is the same as for the costs: setting up the DC lines is the most effective measure followed by the extension of selected congested lines. The achieved reduction in curtailment lies in the same order of magnitude as was achieved by power plant flexibilization.

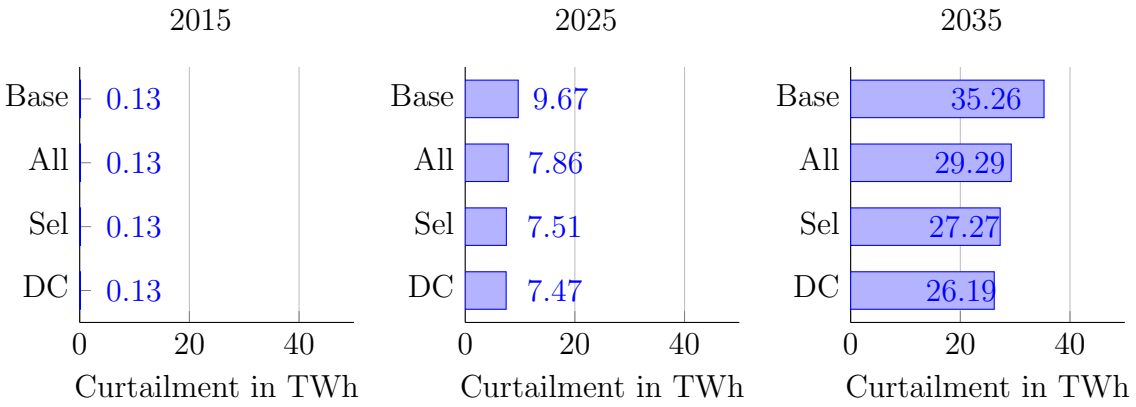

Figure 7.17: Power curtailment for different grid extension scenarios in Germany

Effects of grid extension on emissions in Germany Interesting effects are observed when analyzing CO_2 emissions as depicted in Fig 7.18. While grid extensions lead to slightly increased emissions in 2015 and to only very small reductions in 2025, greater reductions can be achieved in 2035. This reversing trend can be explained by the effect that transmission allows for a better integration of the cheapest sources throughout the year. In 2015, lignite/coal-fired plants are often the cheapest sources and grid extension allows using them with higher FLHs. In contrast, in 2035, heavy installations of VRE and an improved integration by better transport capabilities outweighs this

effect. CO_2 emissions can at most be reduced from 152 Mio. tons to 144 Mio. tons when installing the DC lines, which is a reduction of 5.3%.

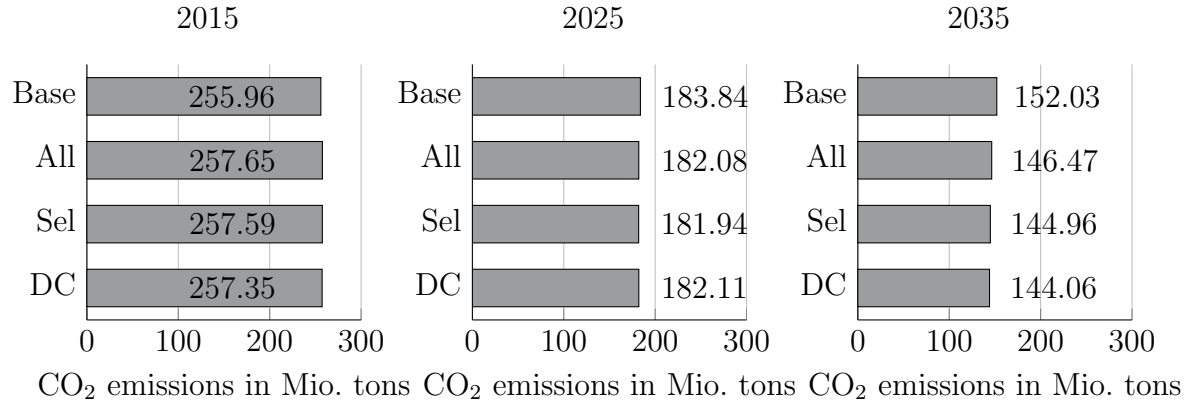

Figure 7.18: CO_2 emissions for different grid extension scenarios in Germany

Effects of grid extension on line utilization and shadow prices in Germany The illustration on line utilization and shadow prices can be found in the Appendix. It is explained in written form here. The effects on shadow prices (see Fig. B.4) are a proxy for the increased capabilities of the transmission grid after upgrades. When equally extending all lines ("All") in the year 2035, one line with average shadow price of more than 10 €/MW and two lines with an average shadow price of above 2.5 €/MW remain. In contrast, when selecting the extended lines or by adding the DC lines, congestion is reduced dramatically and only one line with a shadow price of more than 2.5 €/MW remains in "DC". The effect on line utilization (see Fig. B.3) is more difficult to see and explain. Extending specific constrained lines with "Sel" leads to a higher power flow in the western corridor on the north-south axis. Adding DC lines reduces the flow on the north-south corridors of the AC grid but allows for higher utilization of east-west lines in the south and the north of Germany. In other words, the DC lines transport electricity along the north-south corridor which can then be distributed towards east or west by the AC system.

Effects of grid extension on nodal prices in Germany An interesting aspect of the model results are the nodal prices. Nodal prices are the shadow prices on additional demand in a specific region, i.e. the marginal value of the equation that guarantees that demand is satisfied in each region. They reflect the additional costs that the consumption of one additional MWh would cause in the system.

Fig. B.2 in the Appendix compares the price development for the different grid extension scenarios. Especially in "Base" for 2035, price differences amongst the regions are significant. This might lead to political discussions on splitting the single price zone in Germany. While prices are as low as 18-21 €/MWh in the north, they are at 27-30 €/MWh in the south. Increasing all lines ("All") yields only a very small effect on this price divergence for the years 2025 and 2035, while "Sel" leads to complete uniform prices. The installation of DC lines ("DC") has a similar effect as "Sel" and leads to an almost complete compensation of price differences.

Discussion on grid extension in Germany The three scenarios on grid extension highly vary in the effort they would require to be implemented. Whereas "All" requires enormous new amounts of capacities, the scenarios "Sel" and "DC" require only about 10% of additional capacities compared to "All". The section shows the importance of a techno-economic evaluation for line extension planning as extending specific lines can lead to greater benefits than the mere extension of the entire network. The average shadow price seems to be a valid proxy for congestion and allows for a simple and applicable approach. Further research should evaluate whether iterative extensions according to those shadow prices will lead to optimal results. The model of this thesis can be a basis for such research and for respective policy evaluation.

Concerning the effects on renewable integration, grid extension proves to be very helpful and the achieved reduction of curtailment lies in the same order of magnitude as was achieved by a flexibilization of thermal power plants.

7.3.2 Grid Flexibilization in Germany

Another approach for enhancing the capabilities of the transmission grid without extending the installed capacities is to install flexible components: PSTs can be installed or former AC lines can be switched to controllable DC lines [43, 133]. It must be noted that those two measures can only be understood in an abstract model sense. They cannot be transferred directly to the real power systems as lines are aggregated in the model. In a real-world power system, switching lines would require switching all lines that connect the two respective regions and PSTs would have to be installed in several places; the real-world system is much more complex than the abstract model. Still, the results show the chances of these technologies and demonstrate the capabilities of the developed model for such evaluations.

Scenario setup Two different scenarios are investigated: one scenario where PSTs are installed and one scenario where AC lines are replaced by controllable DC lines. For both, the same lines that where extended with "Sel" are considered. The idea behind choosing the most congested lines is that flexibilization might allow to "shift" electricity transport to the neighboring and less congested lines.

Effects of grid flexibilization on line utilization and shadow prices in Germany In order to compare the effects, line utilization as well as line prices with and without the flexible elements are plotted in Fig. 7.19 (prices) and Fig. 7.20 (utilization). Installing PSTs and switching lines from AC to DC ("FlexDC") leads to a reduction of prices in several of the formerly congested lines. The effects of both measures are very similar and only slight differences are observed. Both measures allow for a (partial) control of power flows. The prices of the most expensive lines drop. At the same time, prices increase in other lines. This can be explained by looking at line utilization in Fig. 7.20. Both measures strongly increase grid utilization. Especially lines that are switched (lines with average shadow prices above 1 €/MW) and lines connected to them experience increased utilization.

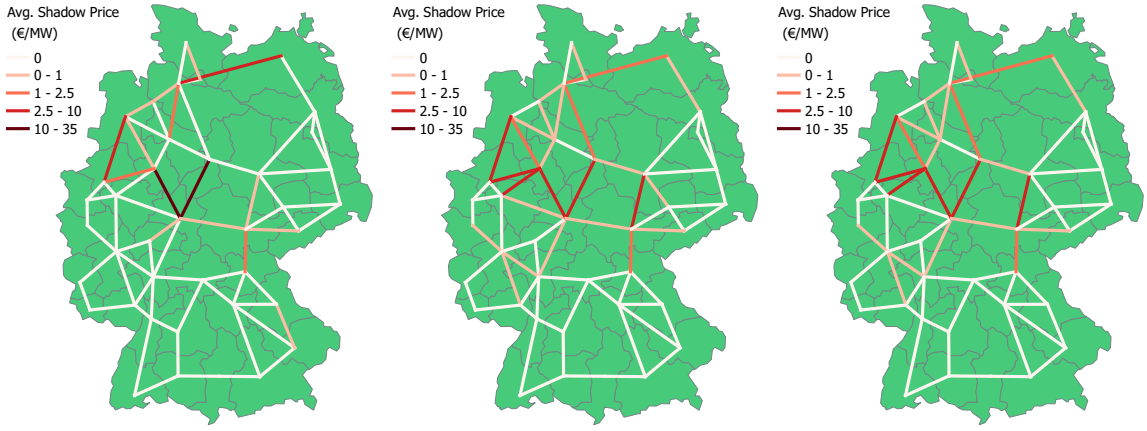

(a) 2035 Base (b) 2035 PST (c) 2035 FlexDC

Figure 7.19: Shadow prices on line capacities for grid flexibilization scenarios in Germany.

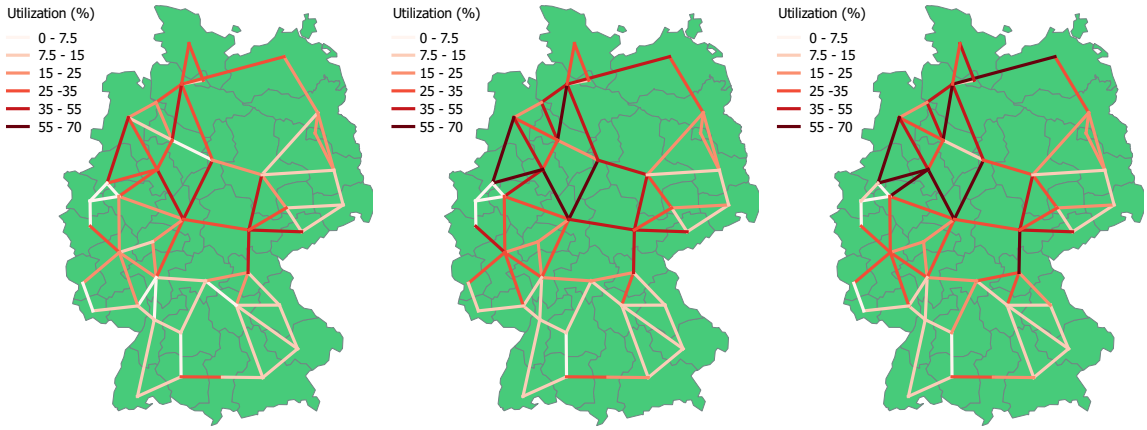

(a) 2035 Base (b) 2035 PST (c) 2035 FlexDC

Figure 7.20: Utilization of transmission capacities for grid flexibilization scenarios in Germany

Effects of grid flexibilization on costs and curtailment in Germany Fig. 7.21 depicts the operating costs for the grid flexilization scenarios. The higher the VRE integration, the higher the cost reductions. Cost reductions achieved by the two grid flexibility measures are at most at 1.5% in 2035. Still, in absolute terms, this signifies savings of up to € 100 million yearly, which might be enough for guaranteeing profitability of installing such components.

Fig. 7.22 illustrates the curtailment and possible reductions. With installing PSTs or with line switching, curtailment might at most be reduced by 3.55 TWh from 35.26 TWh down to 31.7 TWh (a reduction of 10%). These reductions are lower than the possible achievements by installing additional lines. Still, they contribute to an increased system efficiency at possibly low costs.

Effects of grid flexibilization on nodal prices in Germany When considering effects on regional price distributions, observations are similar to curtailment reduction. Fig. B.2 (in the Appendix) depicts nodal prices for the different grid flexibilization

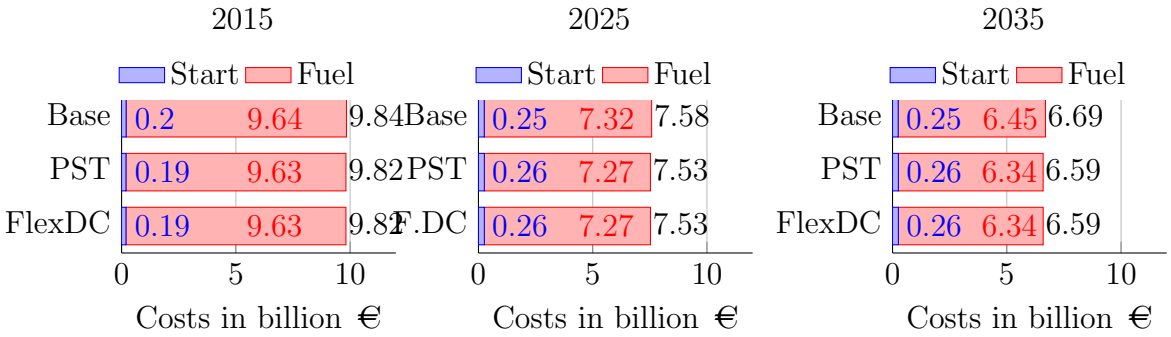

Figure 7.21: Operational costs for different grid flexibilization scenarios in Germany

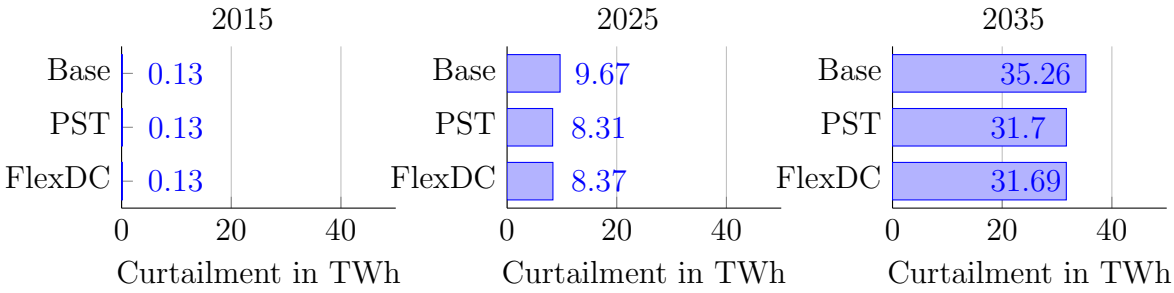

Figure 7.22: Curtailment for different grid flexibilization scenarios in Germany

scenarios. The leveling effect is visible with both approaches but less pronounced than with grid extensions that were discussed in the previous section.

Discussion on grid flexibilization in Germany Installing flexible grid components proves to be helpful for reducing congestion and improving VRE integration. In several analyzed aspects, effects are less pronounced than when extending lines. Still, grid flexibilization might be a promising alternative whenever line extensions are too expensive or not possible due to other constraints like environmental concerns or public resistance.

7.3.3 Storage Extension in Germany

Another measure that is discussed very often in the context of VRE integration is the installation of storage. In two scenarios, this measure is analyzed for the German power system. The scenarios imply the development and installation of new storage that is used for day-to-day balancing. Pumped hydro storage or batteries could be technologies that are modeled with this approach. Therefore, the evaluation will only value short- and medium-term advantages of storage installations. Other modeling approaches are required to evaluate seasonal storage extension strategies (see e.g. Kuhn [125] or Kühne [127]).

The current storage capacity is doubled under two different assumptions: in one scenario, storage capacities are doubled in the regions where storage plants are currently installed ("Sto1"). In a second variant, the same amount of additional storage is assumed but distributed across all regions equally ("Sto2"). The overall installed capacity of storage is 5037 MW with a reservoir capacity of 35 529 MWh in 39 regions. For the second

scenario, 129.15 MW (reservoir: 911 MWh) are installed in each region; the overall capacities remain the same.

Effects of storage extension on costs and curtailment in Germany Fig. 7.23 illustrates the effects of additional storage on operational costs. Reductions are quite small and smaller than achievements by plant flexibilization or by grid extensions. The achieved reductions are 1.0% in 2015 ("Sto1"), 1.4% in 2025 ("Sto2") and 3.0% in 2035 ("Sto2"). The installation of additional storage mostly reduces fuel costs while start-up costs are increased at the same time. Storage allows power plants to be shut down at times with high renewable generation by substituting reserve provision (see below).

Effects on curtailment are depicted in Fig. 7.24. In the year 2015, storage can lead to a complete reduction of curtailment. For the years 2025 and 2035, the effect of storage is also significant. Distributed storage leads to a complete prevention of curtailment in 2015, a 36.7% (3.6 TWh) reduction in 2025 and a 17.7% (6.2 TWh) reduction in 2035. While the reductions in 2015 and 2025 are in the same range as with the other scenarios, storage becomes less effective in 2035. This appears to be in contrast to other research, where storage becomes more important later, e.g. Kuhn [125] or Kühne [127]. However, the reason most likely lies in the fact that only short-term storage is analyzed here.

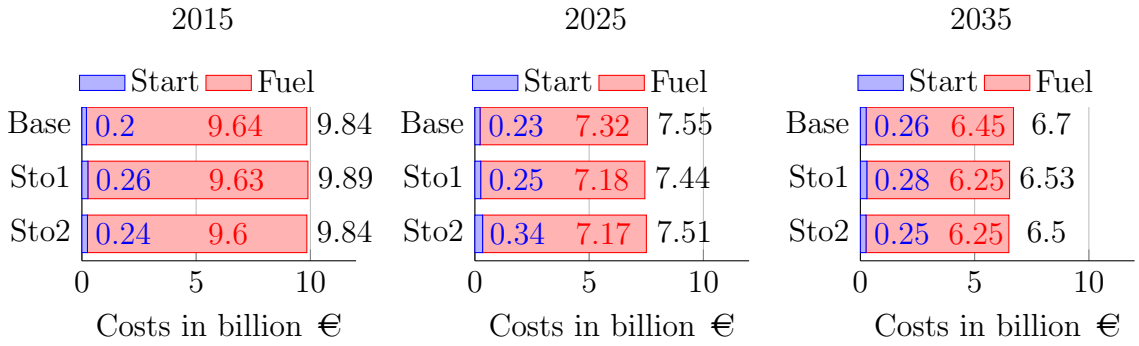

Figure 7.23: Operational costs for scenarios on storage extension in Germany

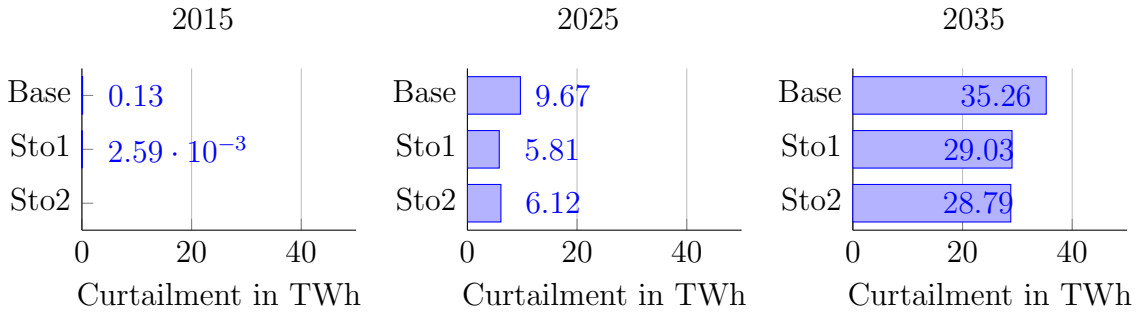

Figure 7.24: Curtailment for scenarios on storage extension in Germany

Effects of storage extension on reserve provision in Germany Regarding the effects of storage on VRE integration and reducing curtailment, two major aspects must be taken into account: storage can be used to store excess electricity and release it later, and storage can provide secondary control allowing thermal power plants to be shut down during times of high VRE generation. Fig. 7.25 depicts the effect: The share

of storage in reserve provision increases when storage capacity is extended. Especially the provision of positive reserves (which otherwise requires power plants to be on-line but producing below their maximum capacity) can be replaced by storage plants. In the year 2035, the share of storage for the provision of positive secondary reserves even doubles. The effect is higher when storage is doubled at the current locations ("Sto1"). Reserves can be provided independently from their location while distributed storage ("Sto2") can also be used to balance regional fluctuations.

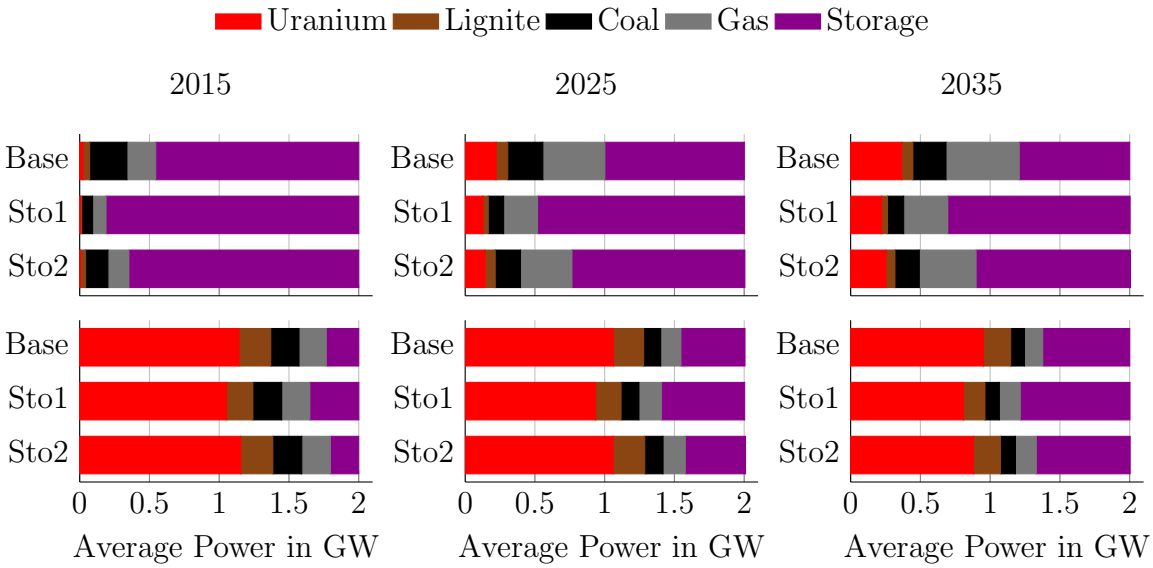

Figure 7.25: Provision of secondary reserves in storage extension scenarios in Germany. The upper charts shows the distribution of positive secondary reserve provision, the lower chart the same for negative secondary reserves.

Discussion on storage extension in Germany Storage seems to be another promising measure for reducing curtailment and improving VRE integration. While in 2015, the small amount of curtailment that exists can be fully integrated in the system with the help of storage, considerable amounts of curtailment remain with a doubled storage capacity in 2025 or 2035. Research could investigate whether all curtailment can be integrated by heavy installations of storage and how much seasonal storage should be installed in the system. Findings on the latter issue can be found with other modeling approaches e.g. in the work of Kuhn [125] or Kühne [127]. Doubling storage capacity reveals to be less effective than increasing power plant flexibility or installing the planned DC lines. Concerning the distribution of storage plants, a slightly greater effect can be achieved by distributing storage across the country since this might prevent line congestion. An optimized placement of storage promises to be an interesting topic for future research with the developed model. Generally, the model only allows evaluating the short-term effects of storage and other models are required for assessment of seasonal storage. Hence, the development of models which consider both, short-term and long-term effects is another interesting research topic. Iterative models that first optimize long-term storage operation and use the results in a UC model could be a first step.

7.4 Combining Measures and International Cooperation

The previous section demonstrated the effects of different measures on VRE integration. Results showed that each measure indeed does have positive effects. Yet, none of them allows for a complete prevention of curtailment. There seem to be different reasons that lead to curtailment in the system:

- Lack of flexible generation,
- Lack of transmission,
- Lack of short-term storage, and
- other reasons like requirements for long-term storage that are not considered.

This section tries to combine the measures and give an idea which of them might complement each other and, on the other hand, which of them address the same issues. Additionally, an outlook on possible reductions of curtailment through international cooperation is presented.

Combining measures in Germany Fig. 7.26 compares the different combinations of measures described in the previous section for the year 2035. It regards combinations with respect to curtailment, costs, and emissions and re-plots all collected results from above. Concerning curtailment, most of the individual measures allow a reduction of 5-10 TWh. Exceptions are the grid flexibility measures where reduction is less. When combining different measures, higher reductions of up to 20 TWh can be achieved. Especially the combination of DC extension and increased power plant flexibilities ("DCFlex3") seems to be very effective. A reduction from 35.26 TWh to 17.84 TWh (50%) can be achieved in this scenario. Adding storage to this combination ("Combined") only achieves one additional TWh in reduction of curtailment. The combination of increased power plant flexibility and storage ("StoFlex3") has the lowest effects of the combined measures. Both seem to be addressing short-term flexibility requirements such as fast ramping and provision of reserves. In contrast, the extension of the transmission grid helps integrating generation by transporting excess electricity from regions with high production to centers of consumption.

The analysis of costs and emissions shows additional effects. Regarding the costs, the combinations with increased power plant flexibility are the most effective including the combination with transmission extension ("DCFlex3") and the combination with storage ("StoFlex3"). In contrast to reduction of curtailment, "StoFlex3" is more effective than "DCSto" in this respect. The reasons are indicated when regarding emissions: "StoFlex3" shows the highest emissions by far. This is caused by increased production from lignite which has the highest specific emissions. The combinations including grid extensions are the most effective in terms of emission reduction. The combination "DCSto" is even better than "Combined" since flexibilization of power plants leads to increased emissions in all scenarios. However, further research should investigate power plant flexibility enhancement under different emission prices. When

prices are high enough, the shift towards lignite might not be relevant anymore and power plant flexibilities could also lead to reduced carbon emissions.

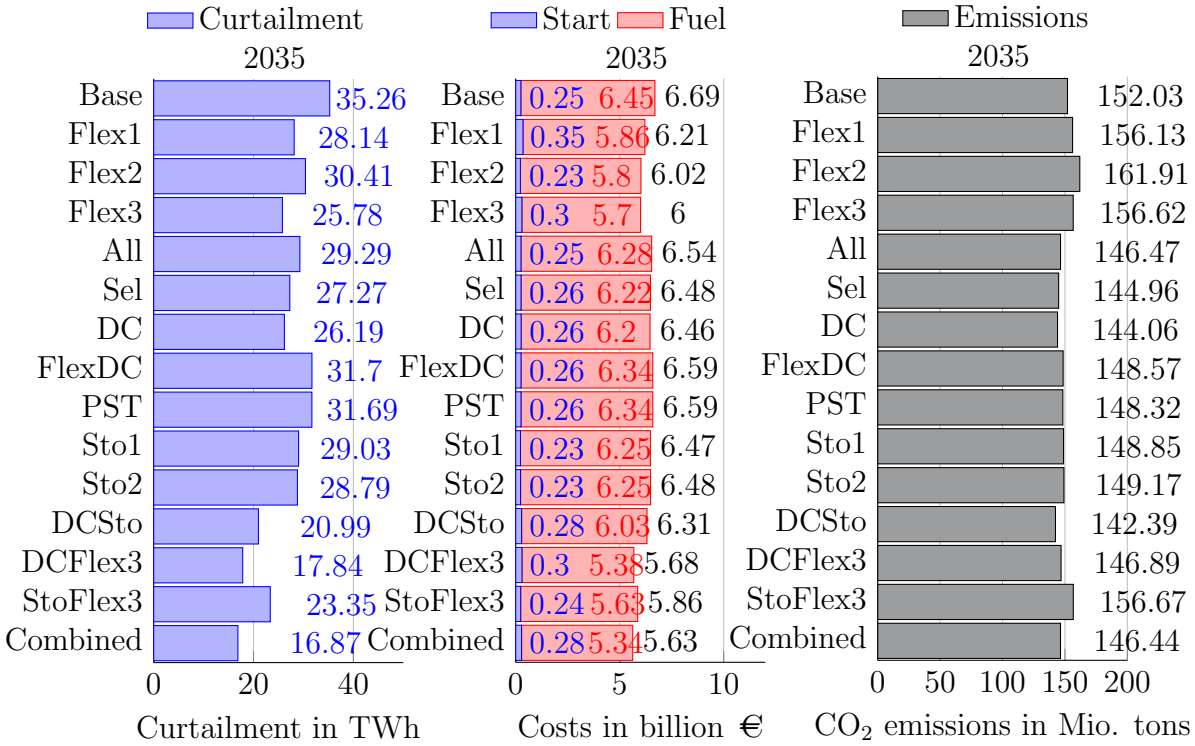

Figure 7.26: Effects of combining flexibility enhancement measures in Germany: curtailment on the left, operational costs in the middle, and emissions on the right.

International cooperation A recent study by Koch et al. [124] compares flexibility measures for the German power system. The study finds a curtailment of 30 TWh for the year 2030, which is very close to the results of this thesis and can be seen as a first validation of the model. The authors find that the connection of Germany into the European power system is the most important measure for large-scale VRE integration. The reduction achieved by the integration of Germany into the European system was found to be at 16 TWh. All other measures, like storage or DSM, showed values of around or below 1 TWh, highlighting the importance of international cooperation.

Computational limitations did not allow computing the detailed German system within the European context. As an alternative, the approach with binary decisions in Germany but without reserves ($EU^{lin}DE^{MIP}$) was computed. The curtailment in Germany with this approach summed up to 12.3 TWh, which is a reduction of 9.8 TWh compared to the 22.1 TWh that were found for the isolated German system without reserves (DE^{MIP}, compare Fig. 7.12). The reduction is in the same order of magnitude of the one found by Koch et al. [124]. However, the influence of international electricity exchange on the effectiveness of other VRE integration measures cannot be estimated with this approach. Most probably, the effects might be lower as a large share of curtailment is already prevented by cross-border electricity flows.

Discussion on VRE integration measures in Germany To summarize this section, results showed that no single measure or technology will solve the problem of VRE integration in Germany. Curtailment can be reduced by all different kind of measures but a combination is the most promising. International cooperation seems a very important aspect and when being combined with increased flexibility of plants, inner German grid extension, and additional storage installations, an almost complete integration of estimated renewable generation in 2035 seems to be possible.

7.5 Grid Enhancements and Storage Extension in Europe

After analyzing the VRE integration case for Germany, the entire European system is investigated in this section. Computational restrictions do not allow to model reserve requirements and binary decisions for the entire model (see Section 7.1.3); effects of power plant flexibility are thus not measured in this context. The other two measures for improved VRE integration - grid enhancements and storage - are analyzed, showing the possibilities of the model as set-up right now. Future research could reduce the model (possibly only modeling Germany and its direct neighbors) in order to be able to compute with more detail while still including international electricity trade.

7.5.1 Grid Extension and Flexibilization in Europe

The extension of the European grid is often discussed as one of the most important measures for improved VRE integration and for reaching a common European power market, see e.g. Schaber et al. [181] amongst many studies. Currently, cross country trading is only allowed within the limits which are set by the NTCs. These values are computed with high security margins for not disturbing transport capacities within each country [22]. Switching to a flow-based market coupling that considers real physical behavior for the respective trading periods would allow utilizing current resources more efficiently [124]. In this thesis, such flow-based market coupling is assumed implicitly as all lines can be used up to the physical limits. A simplified N-1 criterion is included that permits to use only 70% of the capacity. No political or market constraints (as e.g. the NTC values) are incorporated; the model assumes a situation with cost-optimal operation.

The congestion of the grid is visualized by the average shadow price on line constraints in Fig. 7.27. The development of the shadow prices over the years and with more VRE integration shows only a slight increase. Compared to the German case, congestion is less influenced by VRE integration but already results from the diverse generation portfolios in the status quo. Connections from France to its neighbors, e.g. Spain and Italy show high shadow prices. This is due to the fact that cheap nuclear power is generated in France while Italy and Spain have to use a high share of more expensive gas-powered plants. The different generation portfolios are also reflected in the nodal prices of the scenarios in Fig. 7.32.

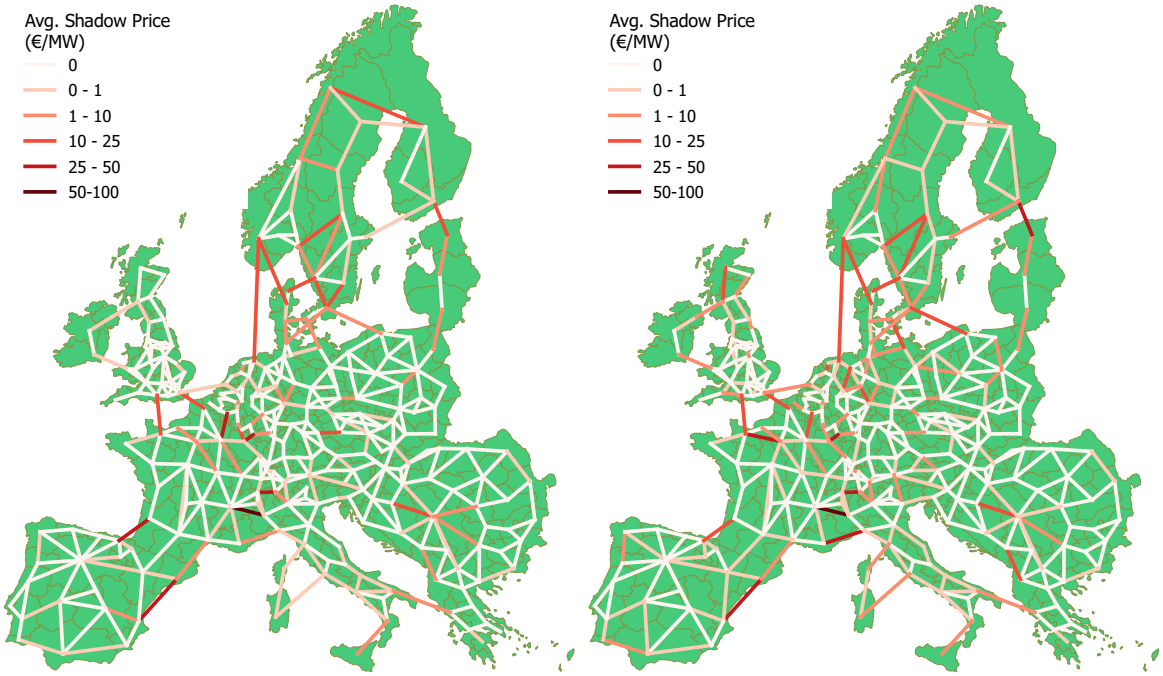

(a) 2015 (b) 2035

Figure 7.27: Shadow prices on line capacities in Europe for the years 2015 and 2035

All connections ("All") In the first transmission extension scenario, the N-1 criterion is neglected, which means an increase of transmission line capacities from 70% to 100%. In the European case, both AC and DC lines are extended and the overall capacity is 1670 GVA for AC lines and 14.4 GW for DC lines (instead of 1169 GVA and 10.1 GW when considering the simplified N-1 criterion).

Selected connections with aggressive extension ("Sel1") In the next scenario, grid extension is conducted based on scenario results for the year 2035. Similarly to the German case, all lines that showed shadow prices of above 1€/MW are extended. In Germany, 10 connections had a price above this value; for Europe, 77 lines are to be extended of which 18 connections are DC lines. The rule for the extension is that all AC lines are extended by two additional 380 kV lines while DC connections are extended by 2000 MW each. The overall extension (after consideration of N-1) is from 1169 GVA to 1271 GVA (+102 GVA) and from 10.1 GW to 32.3 GW (+22.2 GW).

Selected connections with conservative extension ("Sel2") The above scenario extends a high number of 77 lines and is thus an aggressive extension scenario. In a more conservative scenario, only the lines with a shadow price of above 10€/MW are extended which requires an extension from 1169 GVA to 1194 GVA (+25 GVA) and from 10.1 GW to 21.3 GW (+11.2 GW).

Selected connections but with DC ("DC") In this scenario, line extensions are the same as with "Sel2" but DC lines are employed for the extended connections; all connections with prices above 10€/MW are extended and modeled as DC lines.

Installing PSTs ("PST") and switching to DC ("FlexDC") The connections where PSTs are installed or which are switched from AC to DC are the same as the connections extended with "Sel2" or with "DC". This includes all lines that showed a shadow price on the line capacity of more than 10 €/MW. The PSTs allow the phase angle to be shifted by at most 30°, which is similar to the tests with the German system.

Effects of grid extension and flexibilization on costs in Europe The effects on costs are displayed in Fig. 7.28 for the three considered years. Results show that the most effective measure is to upgrade all lines with a shadow price of above 1 €/MW ("Sel1") which leads to a cost reduction of € 2.8 b (6.3%) in 2015, € 3.5 b (11.1%) in 2025 and € 3.9 b (15.2%) in 2035. Extending only the connections with a shadow price of above 10 €/MW ("Sel2") is still a better alternative than extending all lines from 70% to 100% ("All"). The scenario "DC", where all connections with a price of above 10 €/MW are extended and changed to DC is the second best alternative and leads to a reduction of € 2.4 b (10%) in 2035. Cost reductions are already significant in 2015, which is in line with findings for constrained lines due to countries' different generation portfolios (see Fig. 7.32)

Increasing the flexibility of the system by adding PSTs ("PST") or by switching lines from AC to DC ("FlexDC") seems to be less effective. For the year 2035, the reductions are € 0.9 b (3.6%) for "FlexDC" and only € 0.6 b (2.4%) for installing the phase shifters. This is much lower than the effect achieved by grid extensions. Capacity is constrained and no parallel lines are in place that could be used to unload congested lines.

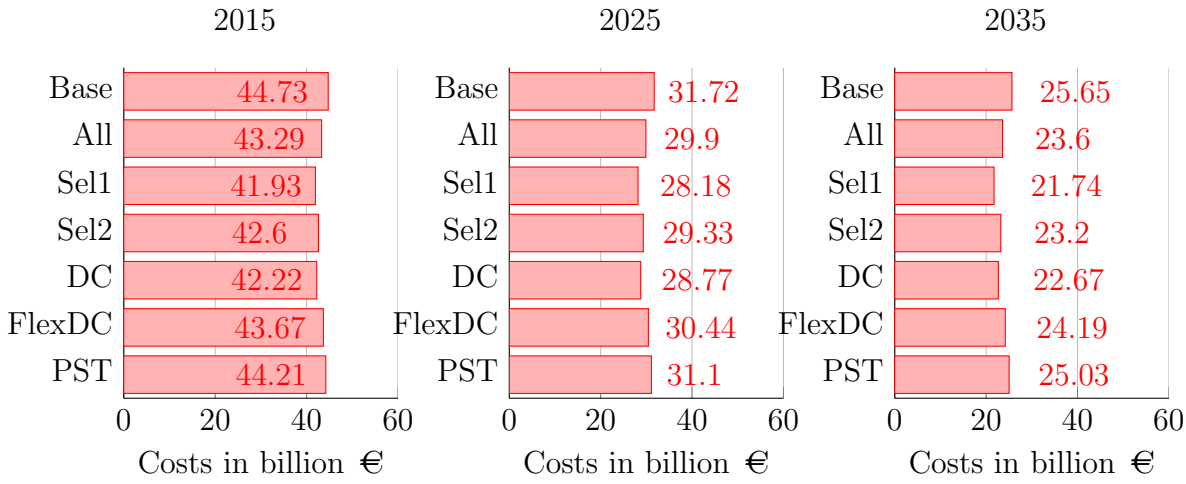

Figure 7.28: Operational costs for different grid extension and flexibilization scenarios in Europe

Effects of grid extension and flexibilization on curtailment in Europe The effects on curtailment are displayed in Fig. 7.29, where tremendous effects of grid extension can be observed. While curtailment is low in 2015, the amount raises to 17.8 TWh in 2025 and to even 72.0 TWh in 2035. The ranking of the different measures is the same as when regarding costs. The best scenario, "Sel2", leads to a reduction of curtailment from 17.81 TWh down to only 3.27 TWh in 2025, which is a reduction

of 14.5 TWh or 81.6%. In 2035, the effect is a reduction of 43.3 TWh (60.0%) from 72.02 TWh to remaining 28.76 TWh. When only extending the lines with a shadow price of above 10 €/MW, drastic reductions of curtailment can still be achieved with "DC", i.e. a reduction of 11.3 TWh (63%) in 2025 and of 33.7 TWh (47%) in 2035. Installing PSTs or switching lines also has some effects on reduction although the effects are less than for all extension scenarios. Further research could investigate the ideal placement of such components and possibly find better solutions than to place them directly at congested lines.

In comparison to the results for the German system, grid enhancements are more effective and more important when considering the entire European system. A larger part of the curtailment in Europe seems to be caused by transmission congestion. A very significant effect is already observed for 2025 while for Germany alone this is only the case for the scenarios of 2035.

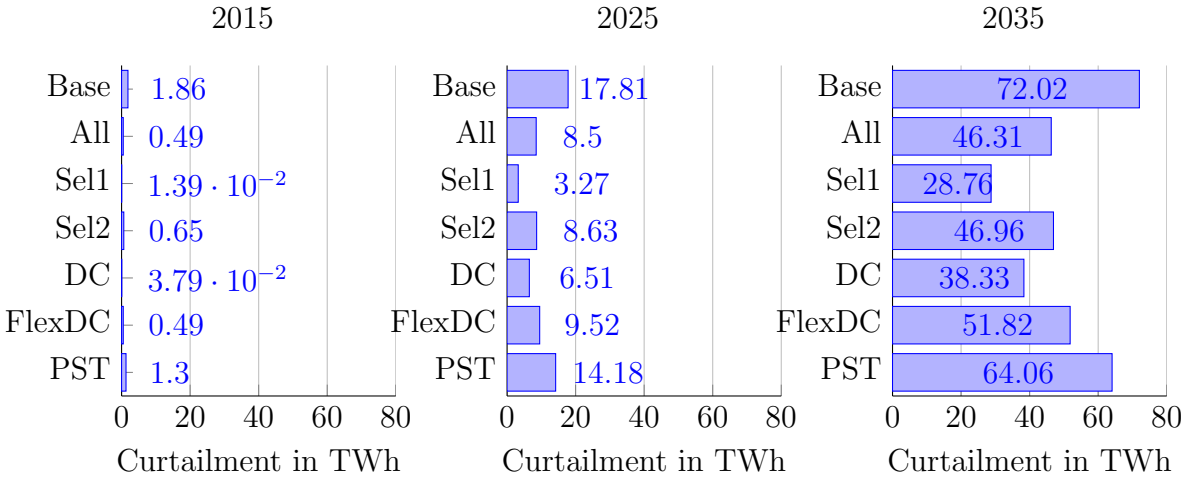

Figure 7.29: Curtailment for different grid extension and flexibilization scenarios in Europe

Effects of grid extension and flexibilization on emissions and fuel mix in Europe The effects on emissions are displayed in Fig. 7.30. Grid extensions and flexibilizations have positive effects on system emissions in all scenarios. This is again in contrast to the Germany-only case. While grid extensions helped to substitute expensive gas with cheap lignite in Germany, additional electricity from emission-free uranium can be integrated in the European system. Fig. 7.31 depicts the fuel mix for the scenarios on top and the differences to the "Base" scenario on the bottom. A clear shift towards higher shares of nuclear and away from gas, coal, and even lignite is observed. For the year 2035, the better integration of nuclear and the reduction of curtailment lead to very high abatements of emissions: the most effective scenario, "Sel1", leads to a reduction from 482.4 Mio tons to 371.5 Mio tons, i.e. a reduction of 110.9 Mio tons per annum (22.9% of overall emissions). When aiming at the ambitious goals for emission reductios in the European Union, these results suggest to put transmission extension and market integration high on the agenda. Even when only extending the connections

with shadow prices of above 10 €/MW ("Sel1"), reductions are at 15.3% (or 18.0% for extending and switching to DC at the same time with "DC").

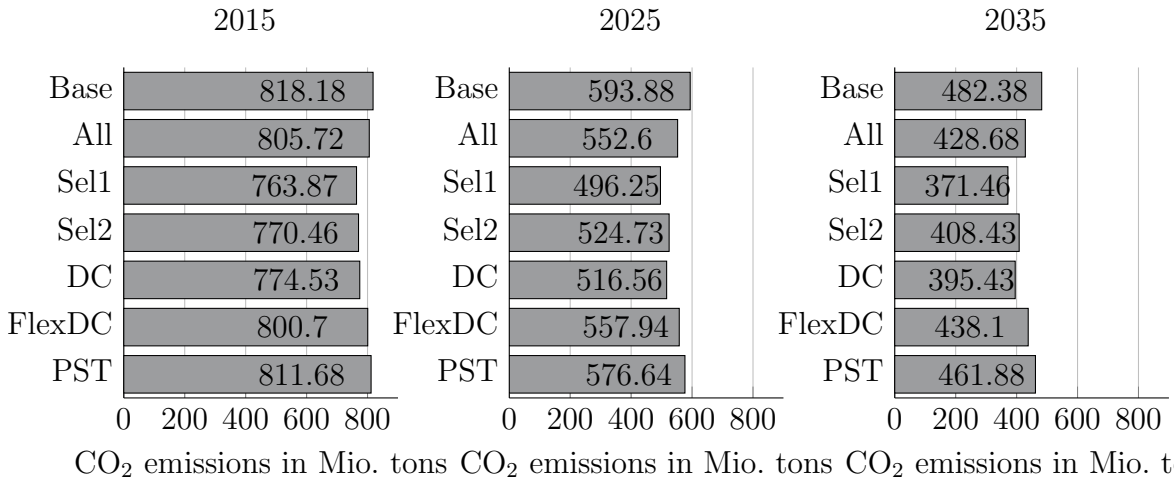

Figure 7.30: Emissions for different grid extension and flexibilization scenarios in Europe

Effects of grid extension and flexibilization on congestion in Europe The positive effects on improved VRE integration and reduced emissions are basically driven by a reduction of congestion, allowing for a more efficient dispatch of generation. An illustration of congested lines as well as the line utilization for the different scenarios can be found in the Appendix in Fig. C.2 (prices) and Fig. C.3 (utilization). The effects on shadow prices on line constraints that are caused by higher VRE integration are depicted in Fig. 7.27 above where shadow prices for 2015 and 2035 are compared. Effects of increased VRE integration on shadow prices are only small as many lines are already congested in 2015, caused by diverse generation portfolios. Especially the connections from and to France should be increased in order to export electricity from cheap nuclear sources. Other congested lines include the DC links to Scandinavia or from Great Britain to continental Europe.

When analyzing possible improvements with the different scenarios for grid enhancements (Fig. C.2), several conclusions can be drawn. The congested connection from France to northern Italy (average shadow price above 75 €/MW can be disburdened best with the inclusion of a flexible DC line, by either just replacing the existing AC line ("FlexDC") or by both extending and switching ("DC"). Other than that, the scenarios to increase the capacity of congested lines ("Sel1" and "Sel2") reduce the shadow prices of many of them. Since more lines are extended with "Sel1", more lines show decreased shadow prices. Several connections from continental Europe to Britain and Scandinavia are affected and congestion can be reduced. Most of the connections that are extended by two 380 kV lines still remain a constraint; highlighting the tremendous requirements for grid extensions in Europe.

Effects of grid extension and flexibilization on price diversity in Europe The nodal prices as depicted in Fig 7.32 can be interpreted as an indicator for the status of market integration. Large differences between regions are a results of grid

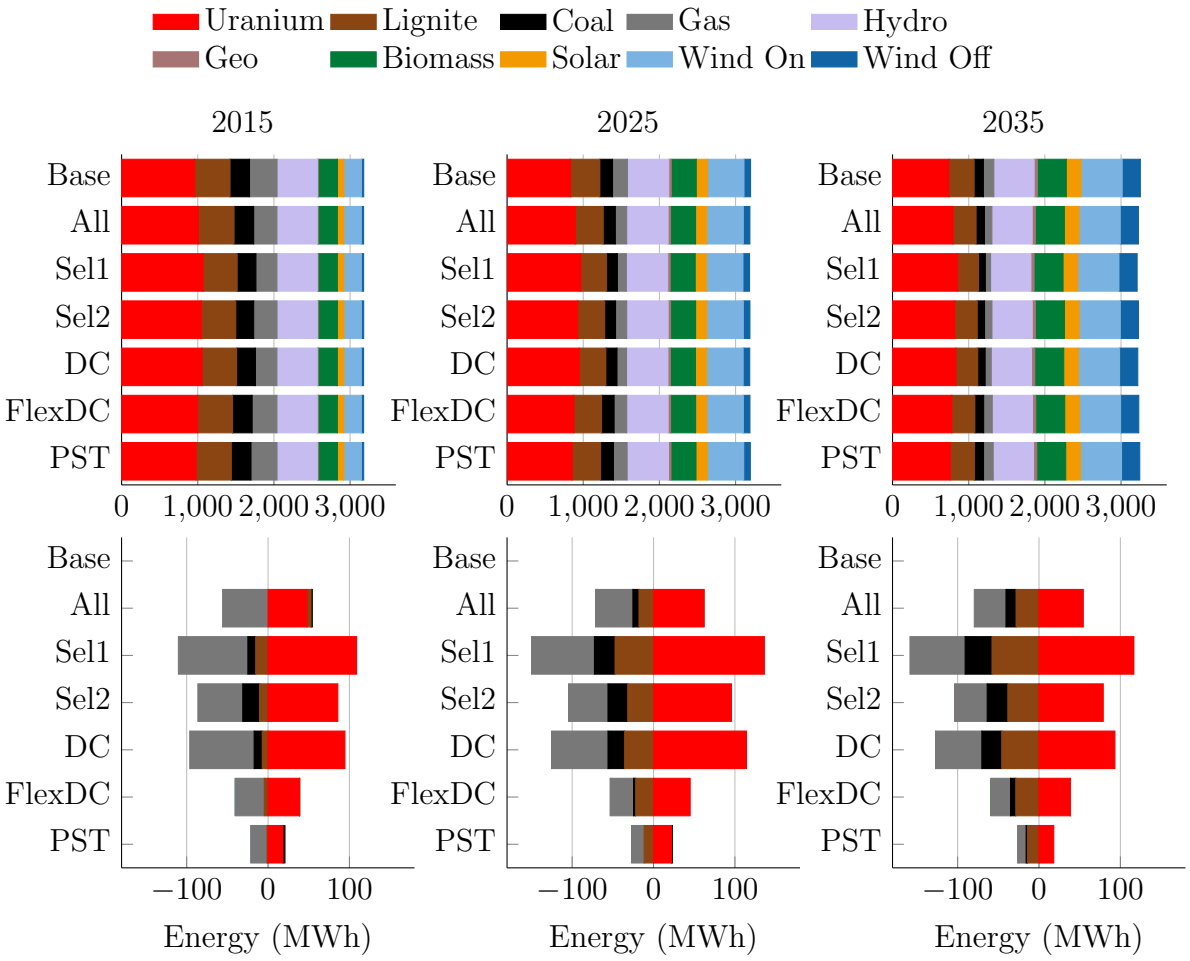

Figure 7.31: Fuel mix for different grid extension and flexibilization scenarios in Europe. The upper figures depict the absolute values while the lower figure depicts the change compared to the "Base" scenario.

constraints as discussed above. Trading between the regions is not possible despite existing comparative advantages. The figure shows that differences in zonal prices already exist in 2015 and might even flatten with the integration of VREs in 2035. The figure also shows that the regions constituting the political unit of a country face very similar prices. Inner-country regions are much better connected to each other than cross-country ones.

In 2015, France and Scandinavia show especially low prices (10-15 €/MWh) which can be explained by the high shares of nuclear generation in France and the high share of hydro power in Scandinavia. Also, Eastern and Southeastern European regions show lower prices of around 30-35 €/MWh compared to the 40-45 €/MWh in the UK, Western Germany, Austria, Italy, and Spain. The reason can again be found in the major sources for generation: while in Eastern Europe mostly coal or lignite are the price-setting marginal power plants, gas power plants are employed more often in the other countries. With the introduction of higher shares of VREs, the overall price level drops due to the so-called merit order effect (compare Fig. 2.2 in Section 2.3). Several of the former high-priced countries/regions converge with former cheaper areas.

This is true for the UK and the continental regions close to the coast (Netherlands, Northern Germany, Denmark) where large-scale wind farms will be installed. Still, already "cheap" countries like France will see a further drop in prices and some price differences will remain. The country with highest prices in 2035 seems to be Italy where average prices remain above 35 €/MWh as gas-fired plants are still required in many hours of the year.

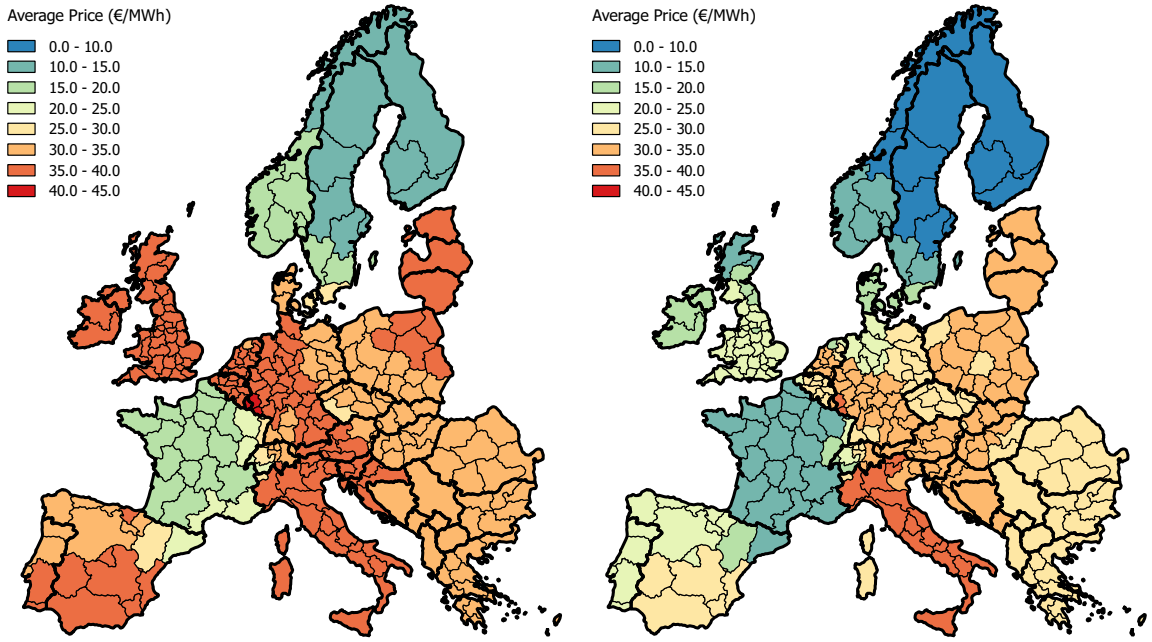

(a) 2015 (b) 2035

Figure 7.32: Regional prices for the "Base" scenarios in 2015 and 2035

The different scenarios for enhancing and extending the transmission capacities can be evaluated with regard to their possible effect on flattening the prices. Fig. C.1 in the Appendix displays the effects that are described here. Increasing system flexibility by switching connections to DC ("FlexDC") will only slightly change prices. However, some flattening can be achieved in some German regions, Austria, the Czech Republic, and Hungary. With the installation of additional lines, effects of flattening are higher. Especially the scenarios "Sel1" and "DC" have strong effects. All Italian regions become cheaper while prices in France increase at the same time. With all extension strategies, a large area including Germany, Austria, Eastern European and Southeastern European countries show all prices in the range of 20 €/MWh. These findings are in line with the findings of Schaber et al. [181], where similar smoothening effects in the same directions were found. Nevertheless, the absolute values differ as do the parameters of fuel prices and the level of VRE integration.

Discussion of grid extension and flexibilization in Europe The scenarios in this section emphasize the importance that grid extensions will play in a future European power system. This knowledge is not entirely new and many studies have found the effect that balancing of renewable generation is much easier in larger areas (e.g. Czisch [48] or

Huber et al. [106], amongst many others). Still, with the results of this thesis, a more detailed model is studied and, beyond demonstrating the model abilities, additional findings can be retrieved. Even though the zonal DC load flow model is a simplification and results might not be transferable exactly to the real-world European system, they clearly show the importance of selecting the lines for extension. The physics of the system does not allow to route electricity but congestion may occur in some connections while unused capacity remains in the parallel lines. Flexible components like PSTs can alleviate the problem and resolve grid constraints to some extent. System planners should consider this measure whenever grid extension is too expensive or not possible due to other circumstances.

7.5.2 Storage Extension in Europe

Scenarios on storage extension in Europe In a last section on results, the influence of adding storage to the system is discussed in the European context. 52,460 MW of pump/turbine power with 367,220 MWh of reservoir capacity are installed in the 268 regions for the "Base" scenario. In two scenarios, this capacity is doubled: either placed directly at current storage locations ("Sto1") or distributed across all model regions ("Sto2"). For the second variant, 195.75 MW/1370 MWh are installed additionally in each of the 268 regions.

Effects of storage extension in Europe Fig. 7.33 depicts the costs and Fig. 7.34 the curtailment for all scenarios. Compared with grid extensions, doubling storage capacities ("Sto1" and "Sto2") has only very little effect on costs and curtailment in the European context. In 2015, costs are reduced by €20 m (0.05%) and curtailment is reduced by 0.11 TWh (5.9% of curtailment in "Base"). The effects increase with greater installations of VRE. Cost reduction increases to €230 m (0.7%) in 2025 and to €330 m (1.3%) in 2035. Still, compared to possible cost reductions by grid extensions, those values are very low. The same is true for the reduction of curtailment which are at 3.3 TWh (4.5%) in 2025 and at 8.1 TWh (11.2%) in 2035. A larger effect of storage is achieved when the capacity is distributed across all regions; storage can then also be used for a more efficient power flow by feed-in at specific nodes whenever this improves the load flow in the system.

Discussion on storage extension in Europe The results show that storage has a lower importance on the European than on the German level. For a better integration of VREs in an European context, the extension of the transmission grid seems to be more important and should be a major focus of European energy politics. As already found by Kuhn [125] and Kühne [127], storage becomes most important at very high levels of renewable generation beyond 50% of electricity production. Especially long-term storage is predicted to be crucial in such cases. With the scenarios ranging only to the year 2035 for the entire European system, VRE penetration is still below such high penetrations and most of the renewable production can be integrated as long as transmission is possible.

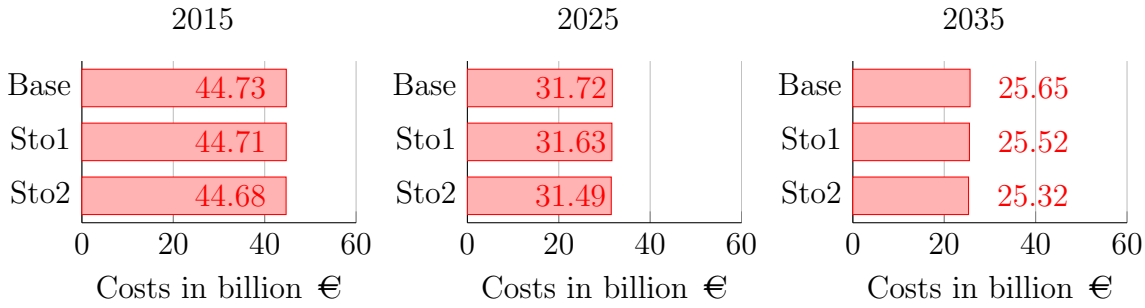

Figure 7.33: Operational costs for different storage extension scenarios in Europe

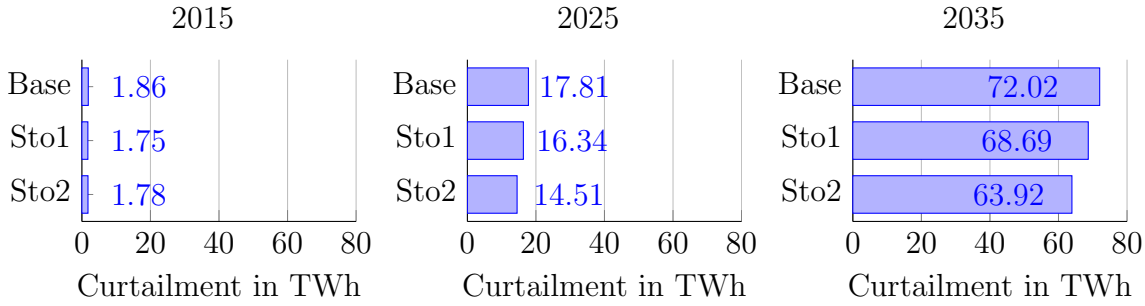

Figure 7.34: Curtailment for different storage extension scenarios in Europe

So far, the model is only able to capture requirements for short-term or day-and-night storage. Adding the ability to also investigate effects from seasonal storage yields more applications and new insights: storage might be more effective. Ideas could be an iterative model, where seasonal storage is optimized via a reduced model in a first step, followed by the detailed UC model with fixed long-term storage operation.

7.6 Résumé of Numerical Studies

The extensive numerical studies that were described in the last sections had two major purposes: Demonstrating the model capabilities and investigating the effects of different flexibility enhancement measures on performance of future power systems with large shares of renewable generation. Numerical studies were conducted for the isolated German system as well as for the entire European power system. The foci and methodology of both considered areas where slightly different. While reserve requirements and possible effects from unexpected events were included in the German system, only a simplified model without any reserve considerations was considered in the European context. Test runs demonstrated the computational limits: computations of the entire European system with binary decisions and reserves are not possible within a reasonable time limit. The most detailed model for the European system only allowed modeling German power plants with binary decisions but without reserve requirements. When regarding Germany as an island, all constraints including binary variables and reserve provision were modeled. Future research should try bringing those two cases together by developing a model that is able to consider both international electricity exchange and detailed modeling in focus areas. An iterative model could be a first approach. A very simple approach with changing forecasts highlighted the importance

of considering uncertainty when evaluating flexibility enhancement. Research in this direction seems to be very promising and the interplay of fast ramps/start-up speeds and uncertainty will be crucial in future operation. Research should employ the model's capability of including start-up speed depending wear-and-tear costs as an additional aspect of thermal power plant operation.

Concerning the results of the models and their implications for energy policy makers and system planners, they can be summarized with the following aspects:

- Results for the Germany-only case revealed the value of power plant enhancements for the system. Both lowering the minimum power output and increasing the ramping/heat-up speeds had significant effects on operational costs and the ability to integrate variable generation from renewable sources.
- Some simplified tests with changing forecasts gave a hint that the enhancements of ramping/heat-up speed might be even more important in a real-world power system where uncertain events happen.
- Comparing the results with and without reserve consideration shows the reason for the positive effect of power plant enhancements. Faster power plants are able to provide more reserves, and in turn, less power plants must be occupied by reserve provision. Furthermore, power plants can be shut down and restarted faster. This allows reacting more efficiently to hours with very high renewable generation. The lowering of minimum power output is also very helpful for efficient reserve provision. During times with high VRE generation, curtailment can be prevented by lowering the output while still being able to provide positive reserves.
- Grid extensions have significant effects in the German system and are of enormous importance in the European context. Extending grids in Europe allows reducing curtailment and emissions tremendously and should therefore be put high on the agenda of European and German energy policies.
- (Short-term) storage proved to be very helpful in the German system as reserve provision can be supported. Additionally, the share of renewable generation is higher in Germany than in the whole European system leading to a higher importance of storage here.

Chapter 8

Conclusions and Outlook

8.1 Summary and Conclusions

This thesis investigates power systems' ability to cope with variable and uncertain production from renewable energy sources like wind and solar. The thesis consists of three major parts with distinct research goals and approaches. In a first part, a statistical analysis of time series data on wind and solar generation is conducted. The results highlight the upcoming challenges arising with the integration of large amounts of renewable generation into existing systems: high ramps will occur that must be balanced by the residual system, i.e. thermal power plants and storage. In this thesis, ramps are investigated within time ranges from 1 to 12 hours and on different spatial scales. The results reveal the importance of the mix between wind and solar generation. While high shares of solar power will lead to very extreme ramps from one period to the next, ramps of wind power are less pronounced but range over longer periods. The analysis gives clear evidence that connecting larger areas by transmission lines will drastically reduce the requirements for balancing in the residual system. Furthermore, the analysis shows that, while differences between countries exist, several characteristics of the residual load are similar across countries, giving reason for transferability of system study results from one country to another.

The second and main part of the thesis is concerned with the mathematical modeling of power systems operation. Based on current state-of-the-art UC modeling, a new approach is introduced which includes the power plant temperature as an additional variable. The introduction of this new variable proved to be beneficial in several aspects. First of all, the formulation is computationally more efficient than previous approaches. Hence, other researchers as well as industry applications should consider this new approach in their work for this reason alone. The higher computational efficiency allows modeling start-up costs with more detail and modeling larger systems. Beyond the advantage in terms of computing, the inclusion of power plant temperature permits modeling additional features of real-world power plant operation. The required start-up time mostly depends on the allowed temperature gradients of critical materials in the power plants. When explicitly modeling temperature as a variable, an additional constraint can easily be included precisely representing this restriction on temperature

gradients. Additionally, the new approach allows modeling wear-and-tear costs arising from start-ups that depend on the heating speed: the higher the heating speed, the higher the temperature gradients and, therefore, the higher the costs. These additional modeling abilities promise to be especially interesting in a stochastic modeling environment. Several approaches for considering uncertainty are presented. The chosen method for most large-scale simulations consists of including reserve constraints. Furthermore, the ability of including changing forecasts is implemented and employed. Regarding transmission constraints, the developed model methodology and implementation includes a DC load flow model formulated with a PTDF matrix. The DC methodology is superior to a simple transport model as loop flows or congestion on individual lines can be represented and bottlenecks can be identified. The model with all its features allows testing different options that enable more efficient renewable integration, i.e. enhanced thermal power plants, storage, grid extensions, and grid flexibility measures like phase shift transformers or DC links.

After analyzing possible requirements on ramps in the system in a first step and defining and developing a model approach that allows evaluating different options for dealing with the fluctuating nature of renewables in a second step, the consequent third step of this thesis applies the methodology on a realistic test case. Therefore, data on the European power system is gathered and a simplified model based on 268 regions is developed. Most of the collected data stems from open sources, which allows the data set to be published and to provide additional value to the scientific community. Computational complexity permits modeling the entire European system with a simplified approach only while Germany alone is modeled with all model features including binary decisions for all thermal plants and reserve considerations. Results show that increasing the ability of thermal power plants to ramp up and down, to lower their output, and to heat up faster has significant effects on efficient integration of renewable energy sources. Especially when reserves are considered, which is the case in real-world operations, power plant enhancements are very beneficial. Storage also shows high effectiveness as soon as reserves are considered for the German system. In the overall European system, grid extensions are the most important actions policy makers should take when aiming at building a future power system with high shares of wind and solar power. Additionally, and in cases where extension is not possible, switching some lines to direct current or installing phase shift transformers might allow for a more efficient power flow and thereby reduce curtailment substantially.

Even though further validation of the proposed dataset and grid reduction is necessary, this part of the thesis demonstrates the power of the model theory and the dataset developed. In the process of writing this thesis, the model has already been applied in a project for the Bavarian Ministry of Economics. In that study, different energy policy options for the State of Bavaria were evaluated. This study already shows the relevance of the outcomes of this thesis beyond the pure scientific achievements: developing and establishing a ready-to-use model for policy research projects.

8.2 Further Research Questions Arising

Based on the progress achieved in UC modeling and the setup of a test case built on the European power system, this thesis yields many interesting research questions to be addressed in subsequent projects. Concerning the basic modeling framework, implementing a stochastic variant with a scenario approach in combination with the temperature formulation of this thesis promises to be an interesting modeling design. In a stochastic setting, different strategies for heating-up of power plants could be explored including keeping units warm and heating with different speeds.

Concerning the modeling of long-term storage and international electricity exchange while including all details of power plants at the same time, iterative modeling approaches might be an interesting option. First, the entire year (regarding seasonal storage) or the entire European system (concerning international electricity exchange) could be computed, while a more detailed model could follow in a second stage. An iterative approach could also be used for finding optimal grid extensions. After each iteration, the lines with highest marginal values on their capacity constraints would be extended until satisfactory system performance is achieved.

Another interesting model extension, that has already been initiated, entails coupling the model of this thesis with a more detailed full AC grid model. The coupling allows exploring whether it would also be possible to dispatch the outcomes of the simplified DC model computations when considering the detailed AC power flow including dynamic stability analysis. An interesting research question would be whether simplified constraints can be found in the UC model with DC power flow, which guarantees results that are also stable in a dynamic sense.

Concerning the dataset, a validation of the reduced transmission grid should be conducted as a next step. This will be done in the course of the model coupling to the full AC model. Additionally, a calibration of the model with historic real-world situations should be conducted including both, transmission and generation. So far, the model does not consider any outages, be it for regular maintenance or for unexpected events. As a consequence, the share of cheap sources like nuclear and lignite might be higher than in reality as plants are allowed to run all 8760 hours of the year. Future research could adjust the model to include such outages.

With the implementation of the suggested adjustments, the model will be helpful for different kinds of system studies: Research can evaluate different technological enhancements in regional as well as transnational power systems, which promises to be an increasingly important constituent of policy consulting. Beyond that, the model of this thesis can also be employed for regulatory questions concerning market zones and international electricity exchange - a field of growing national and international interest. Thus, the ideas for further research are manifold and creativity combined with a choice of relevant questions should allow for many high-level research studies to follow.

Finally, the model and all its further developments will be made available to the public in order to support the scientific community and to increase the transparency of research.

Appendix A

Additional Visualizations of the Dataset

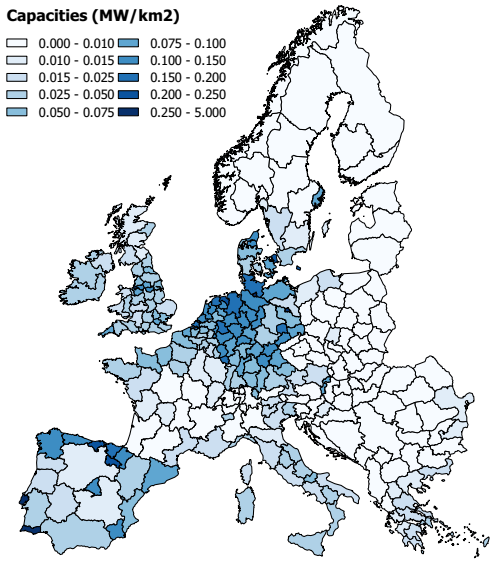

(a) Wind 2015

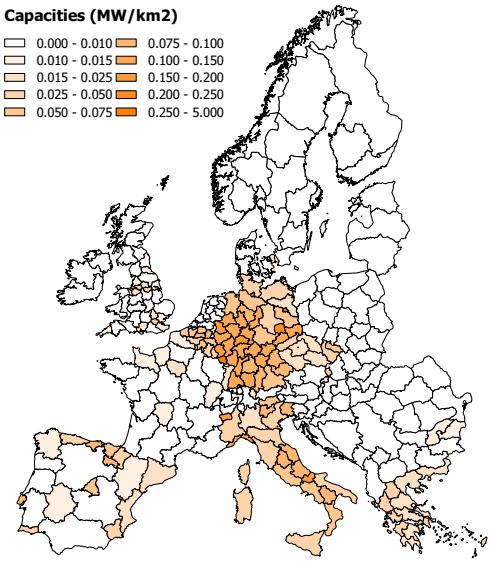

(b) PV 2015

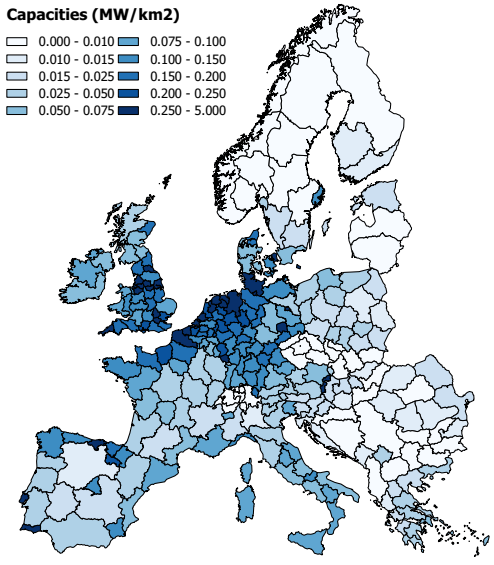

(c) Wind 2025

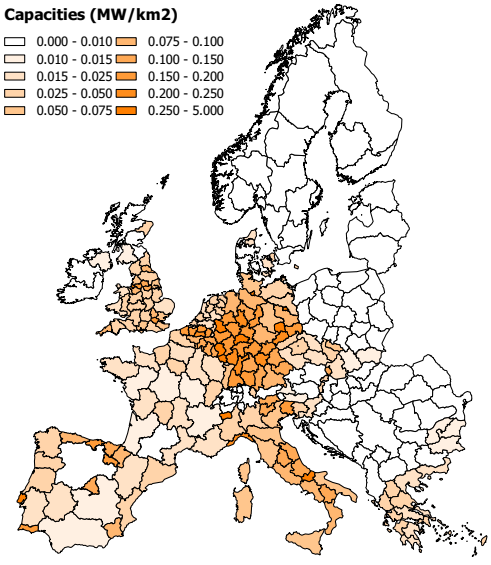

(d) PV 2025

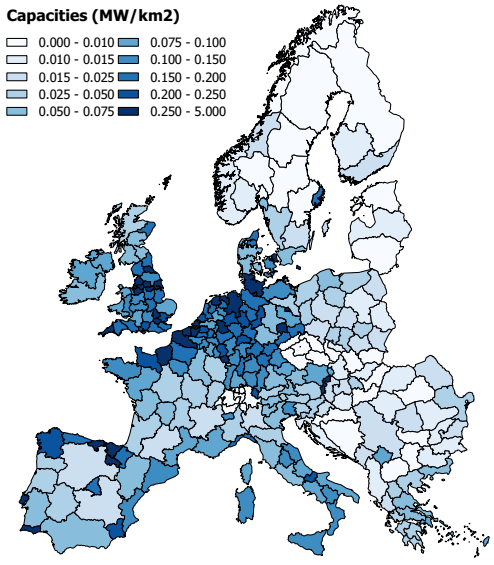

(e) Wind 2035

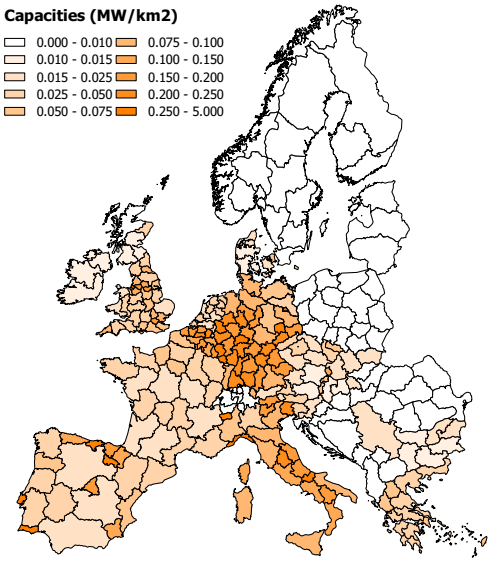

(f) PV 2035

Figure A.1: Capacities of VREs in the three model years

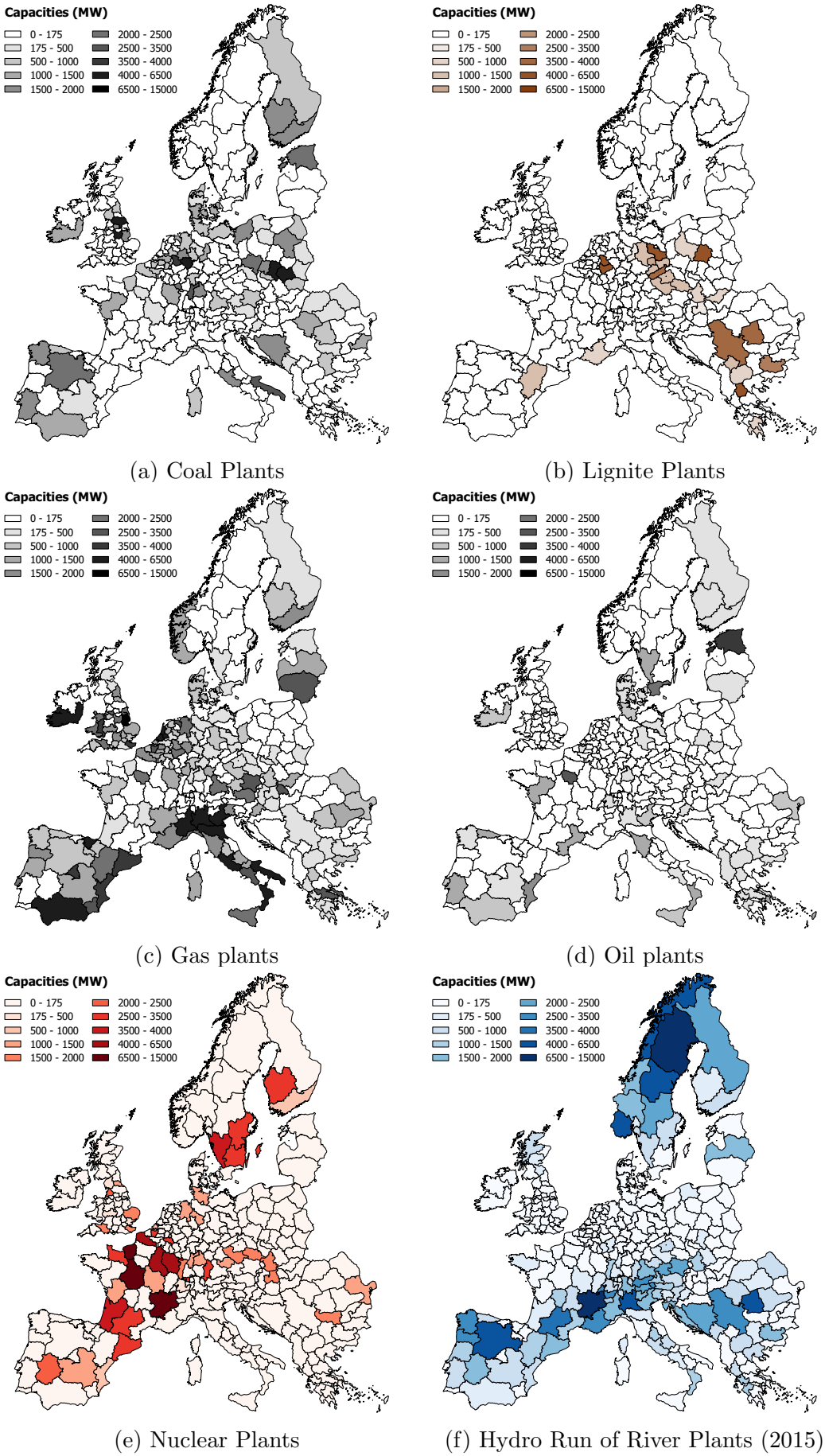

(a) Coal Plants

(b) Lignite Plants

(c) Gas plants

(d) Oil plants

(e) Nuclear Plants

(f) Hydro Run of River Plants (2015)

Figure A.2: Installed Capacities of hydro- and thermal generation (same for all model years)

Appendix B

Additional Results for the German System

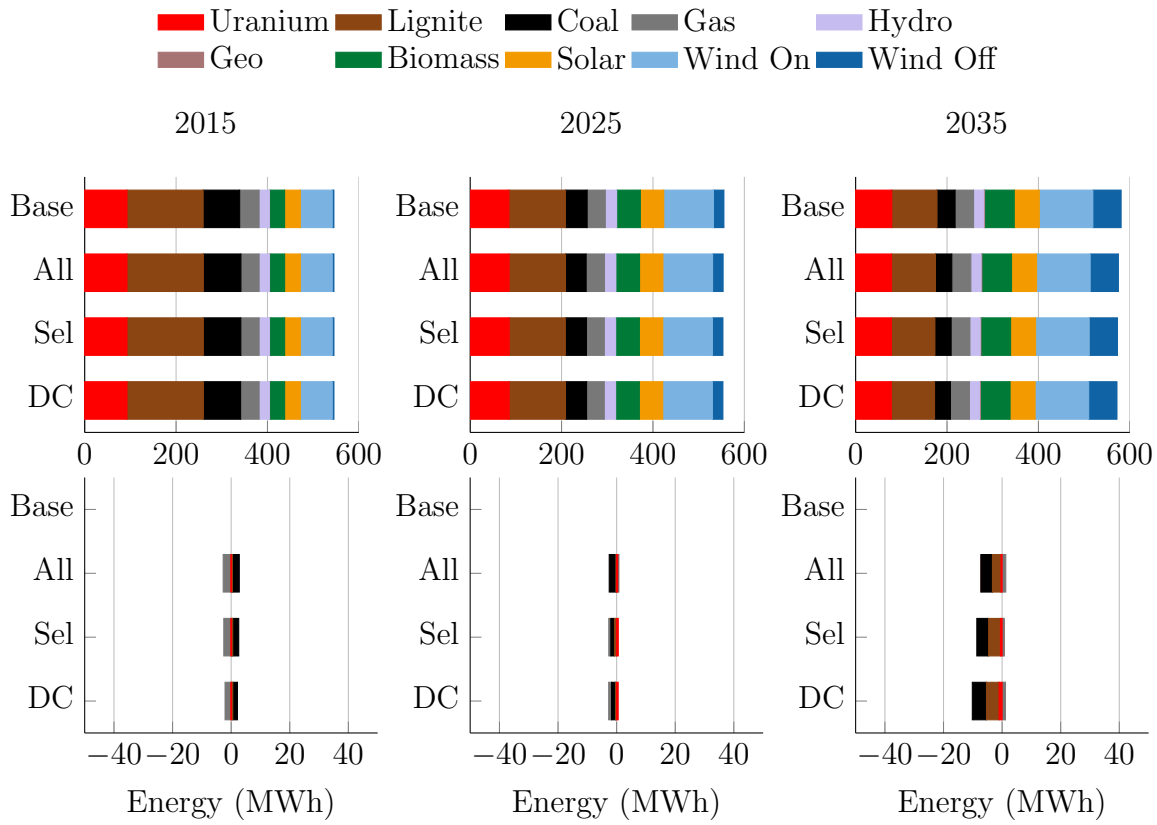

Figure B.1: Influence of grid extensions on generation mix in Germany

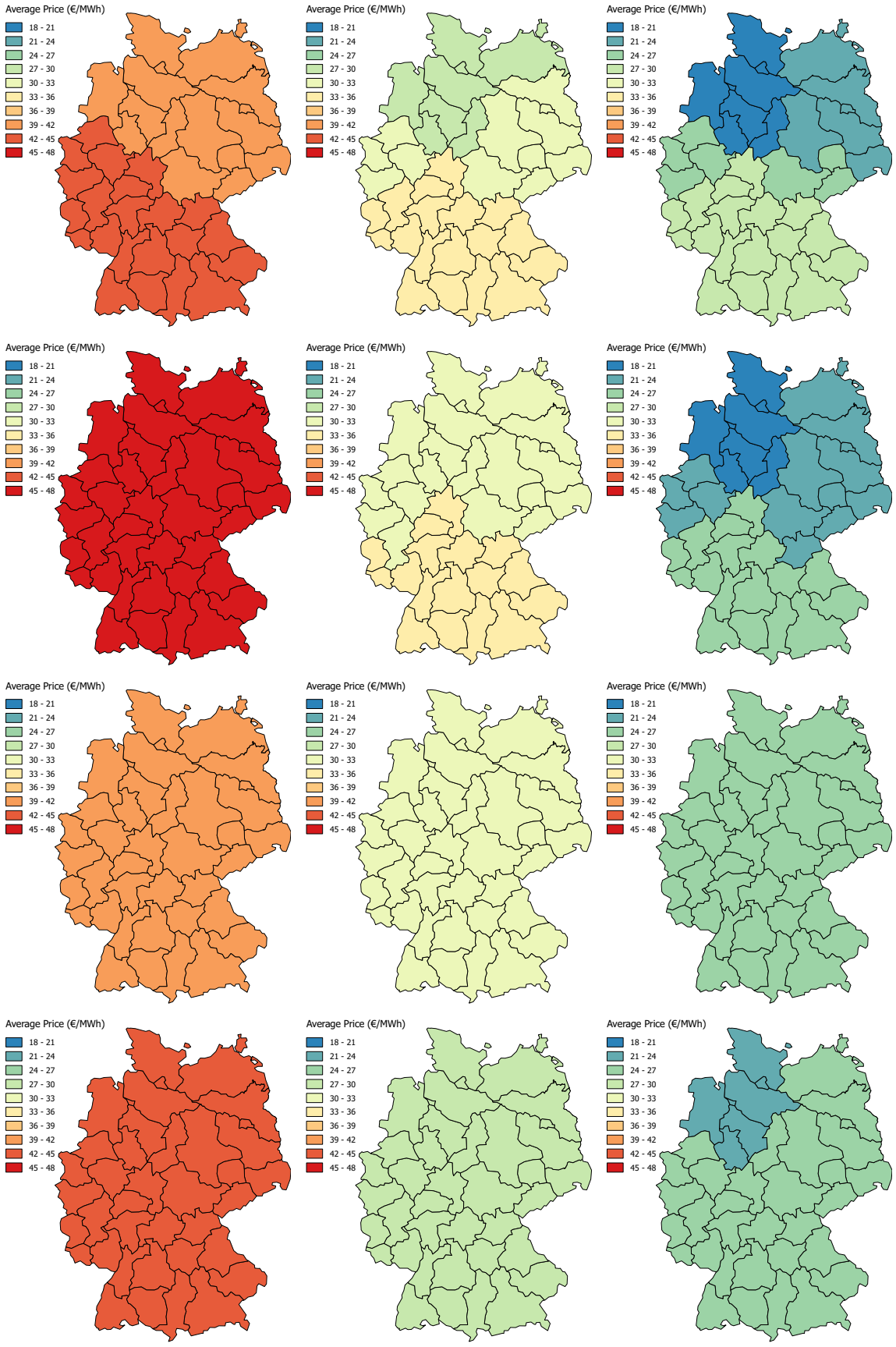

(a) 2015 (b) 2025 (c) 2035

Figure B.2: Nodal prices for different grid extension scenarios in Germany. The scenarios are ordered vertically from top to bottom: 1. Base scenario, 2. Extension of all AC lines (All), 3. Extension of selected AC lines (Sel), 4. Extension of DC lines

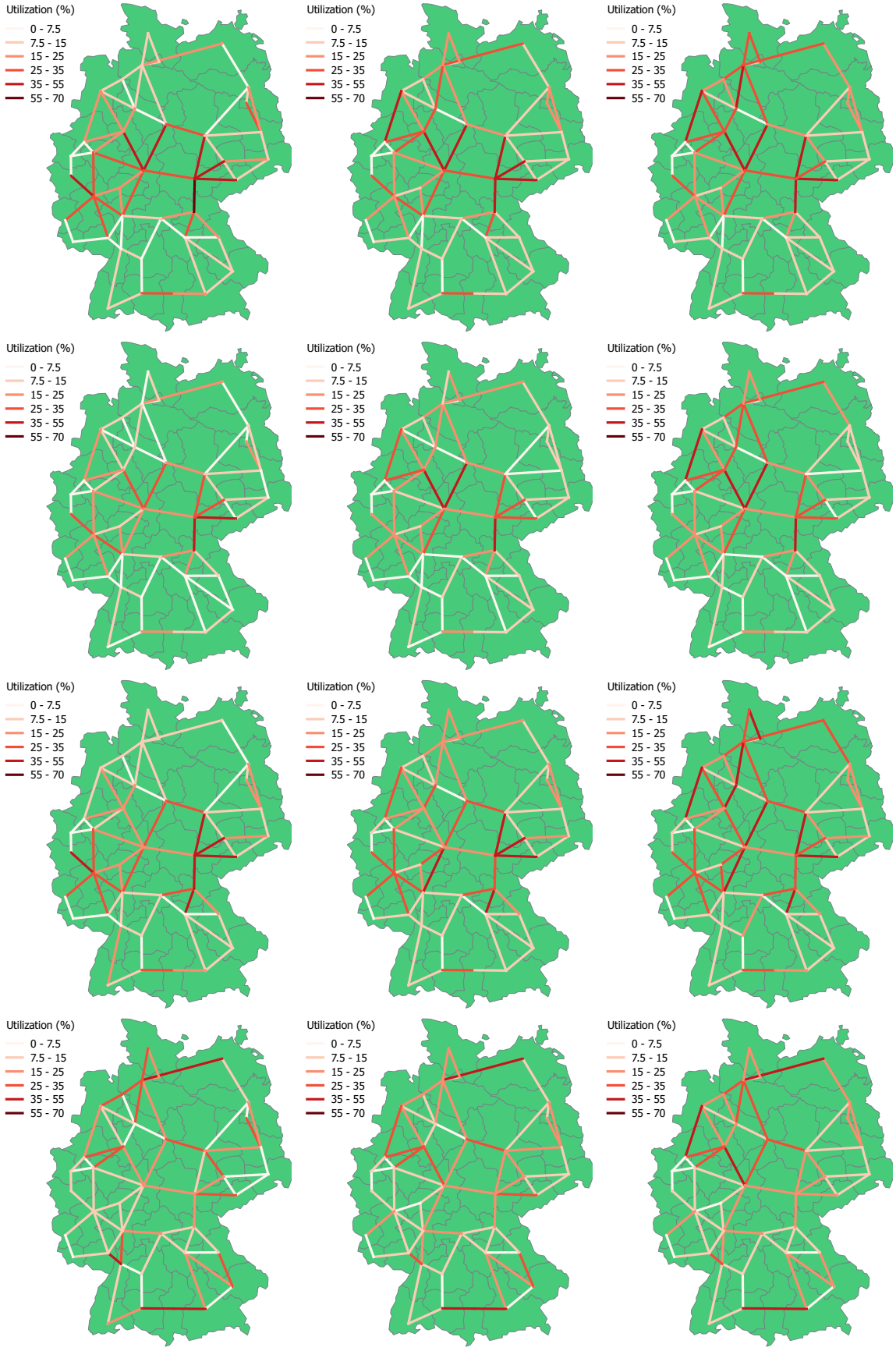

(a) 2015 (b) 2025 (c) 2035

Figure B.3: Grid utilizations for different grid extension scenarios in Germany. The scenarios are ordered vertically from top to bottom: 1. Base scenario, 2. Extension of all AC lines (All), 3. Extension of selected AC lines (Sel), 4. Extension of DC lines

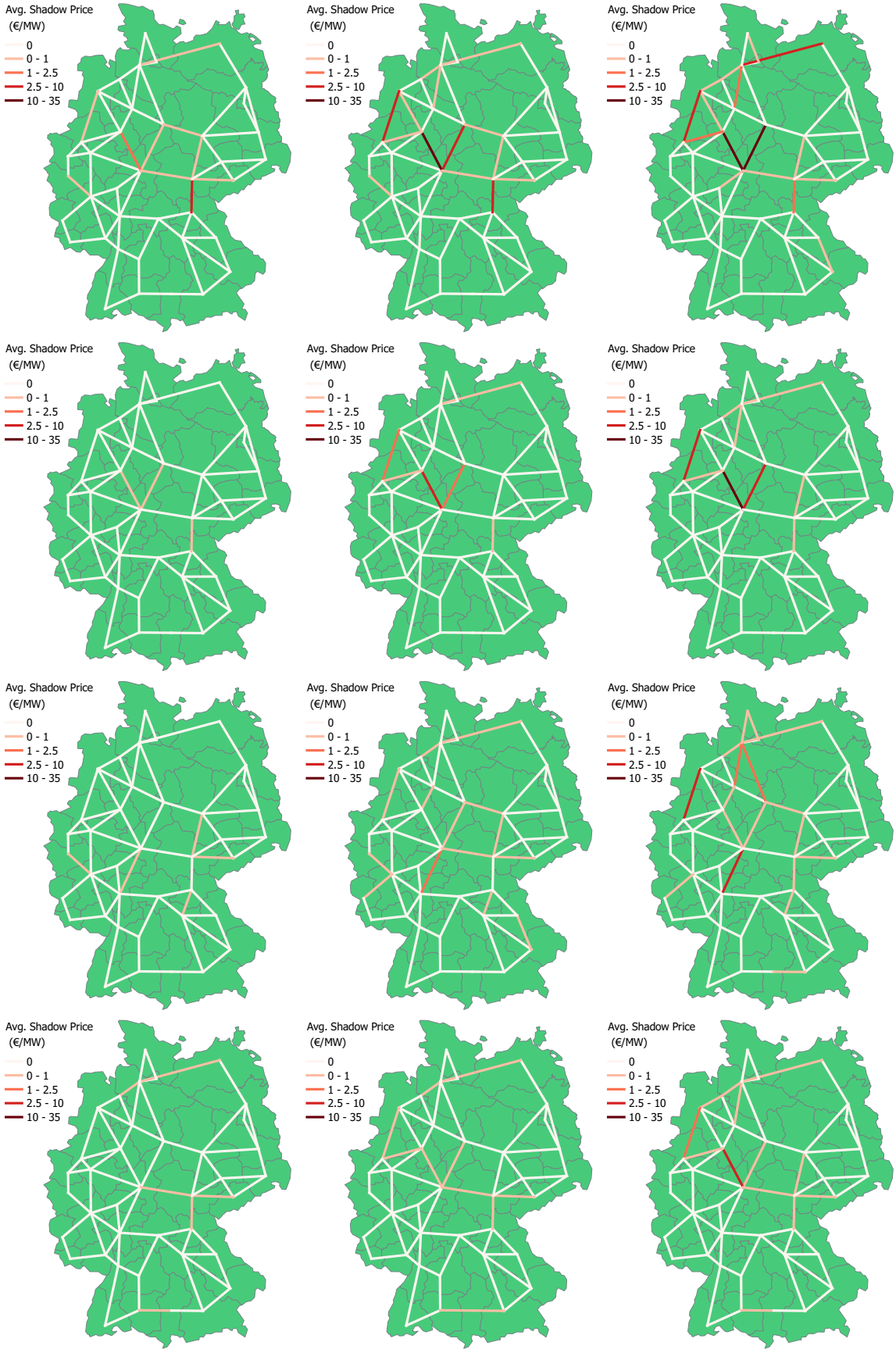

(a) 2015 (b) 2025 (c) 2035

Figure B.4: Shadow prices on line capacities for different grid extension scenarios in Germany. The scenarios are ordered vertically from top to bottom: 1. Base scenario, 2. Extension of all AC lines (All), 3. Extension of selected AC lines (Sel), 4. Extension of DC lines

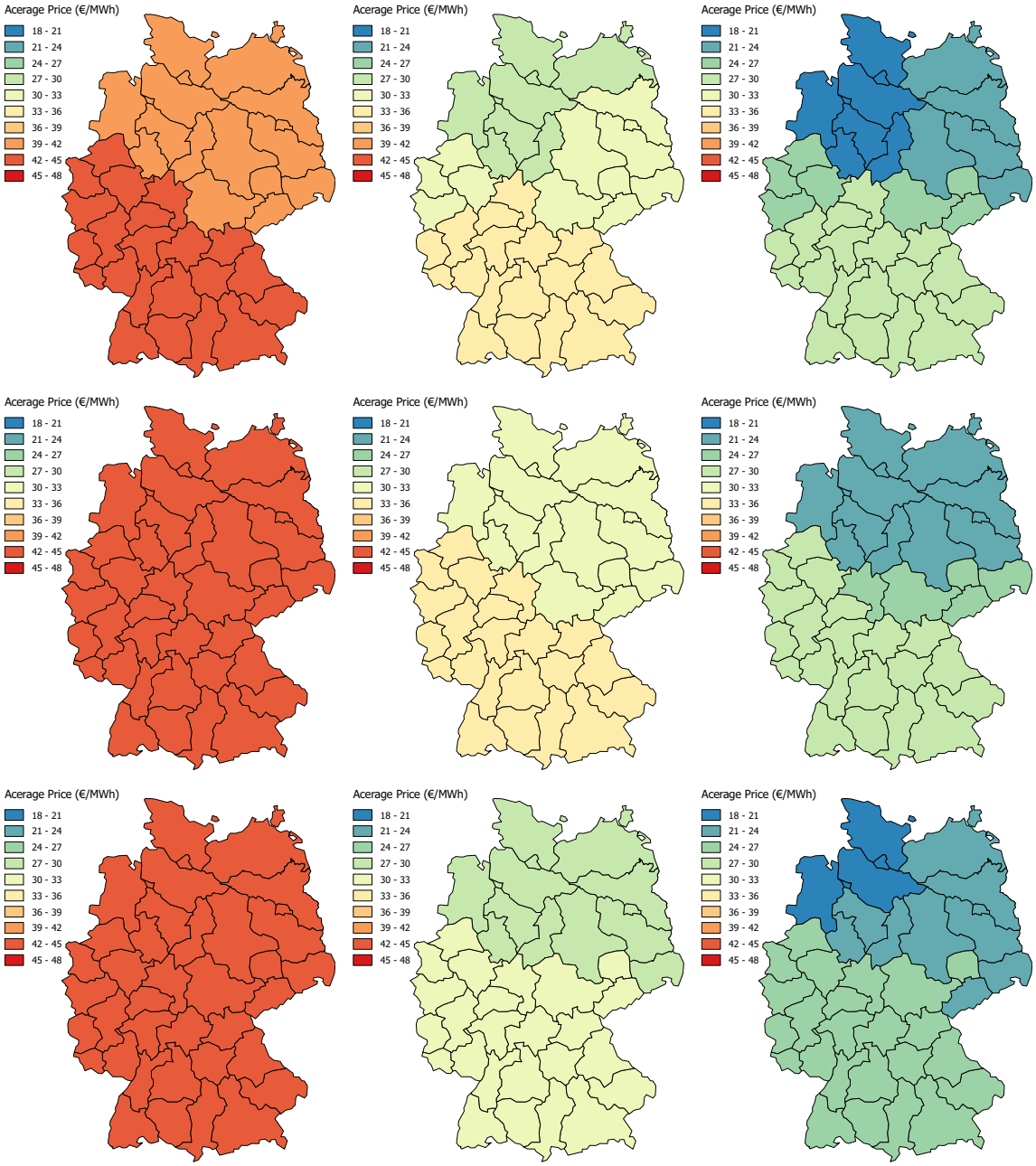

(a) 2015 (b) 2025 (c) 2035

Figure B.5: Nodal prices for different grid flexibility scenarios in Germany. The scenarios are ordered vertically from top to bottom: 1. Base scenario, 2. Switching of AC lines to DC, 3. Inclusion of PSTs

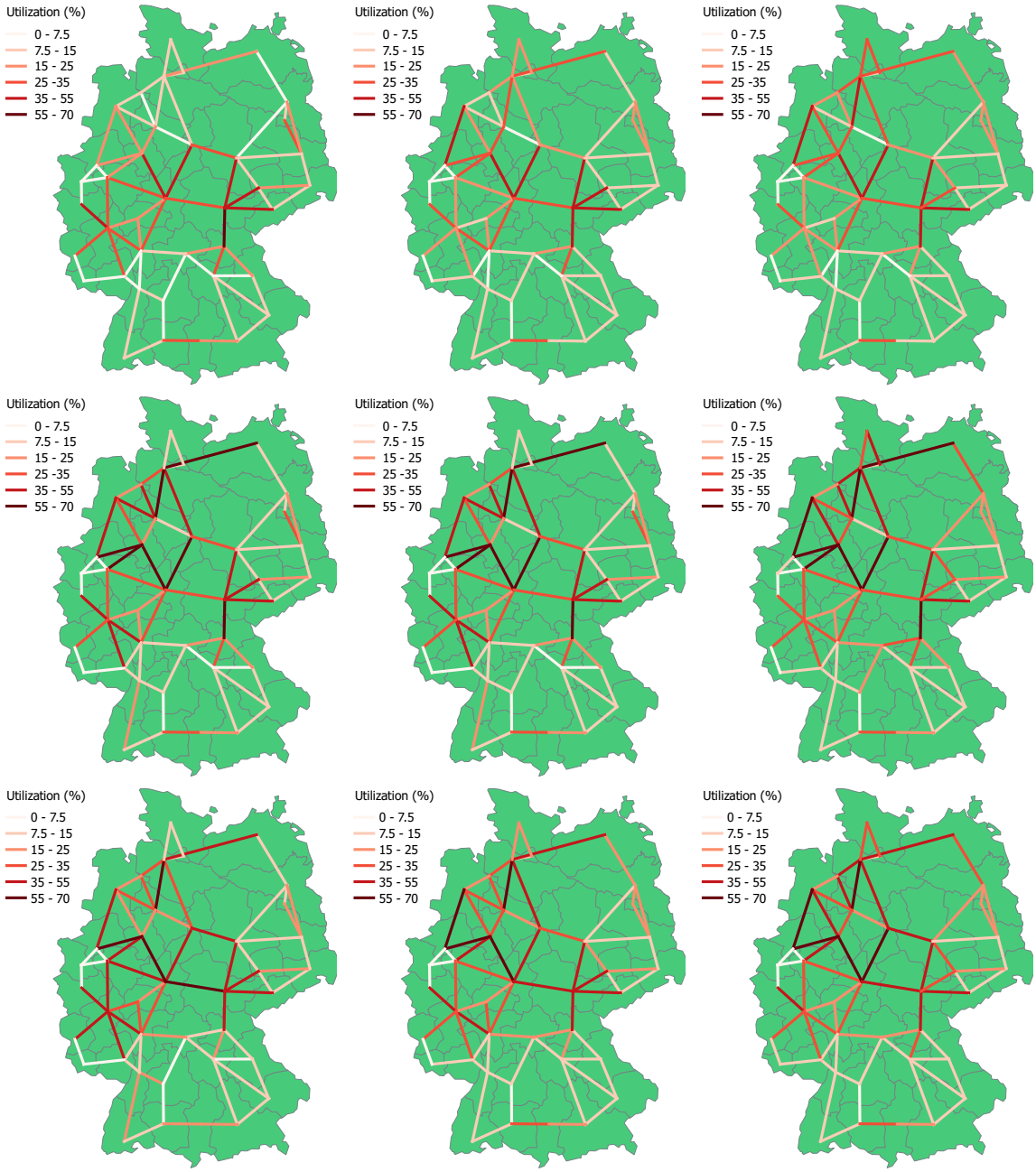

(a) 2015 (b) 2025 (c) 2035

Figure B.6: Grid utilizations for different grid flexibility scenarios in Germany. The scenarios are ordered vertically from top to bottom: 1. Base scenario, 2. Switching of AC lines to DC, 3. Inclusion of PSTs

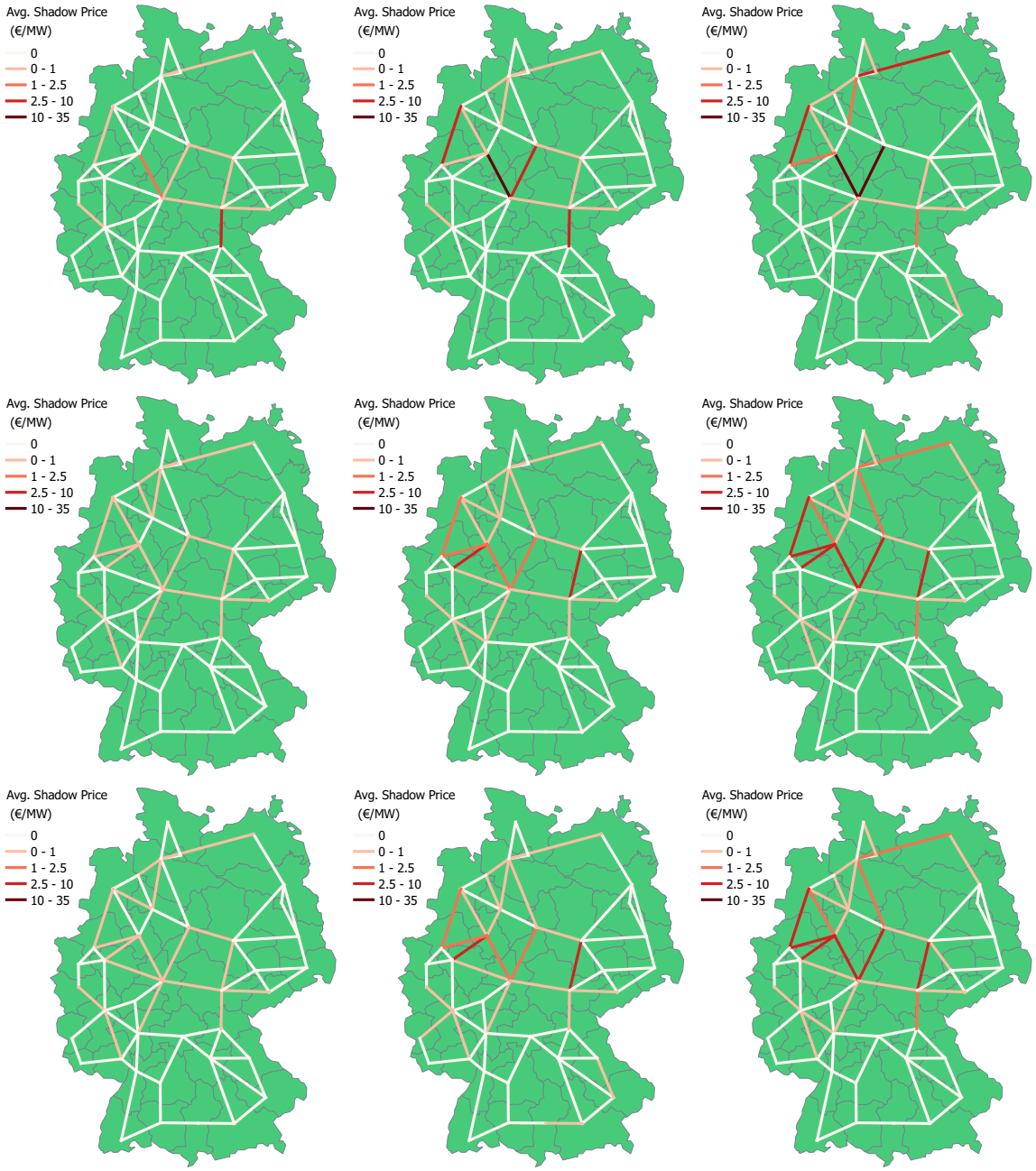

(a) 2015 (b) 2025 (c) 2035

Figure B.7: Shadow prices on line capacities for different grid flexibility scenarios in Germany. The scenarios are ordered vertically from top to bottom: 1. Base scenario, 2. Switching of AC lines to DC, 3. Inclusion of PSTs

Appendix C

Additional Results for the European System

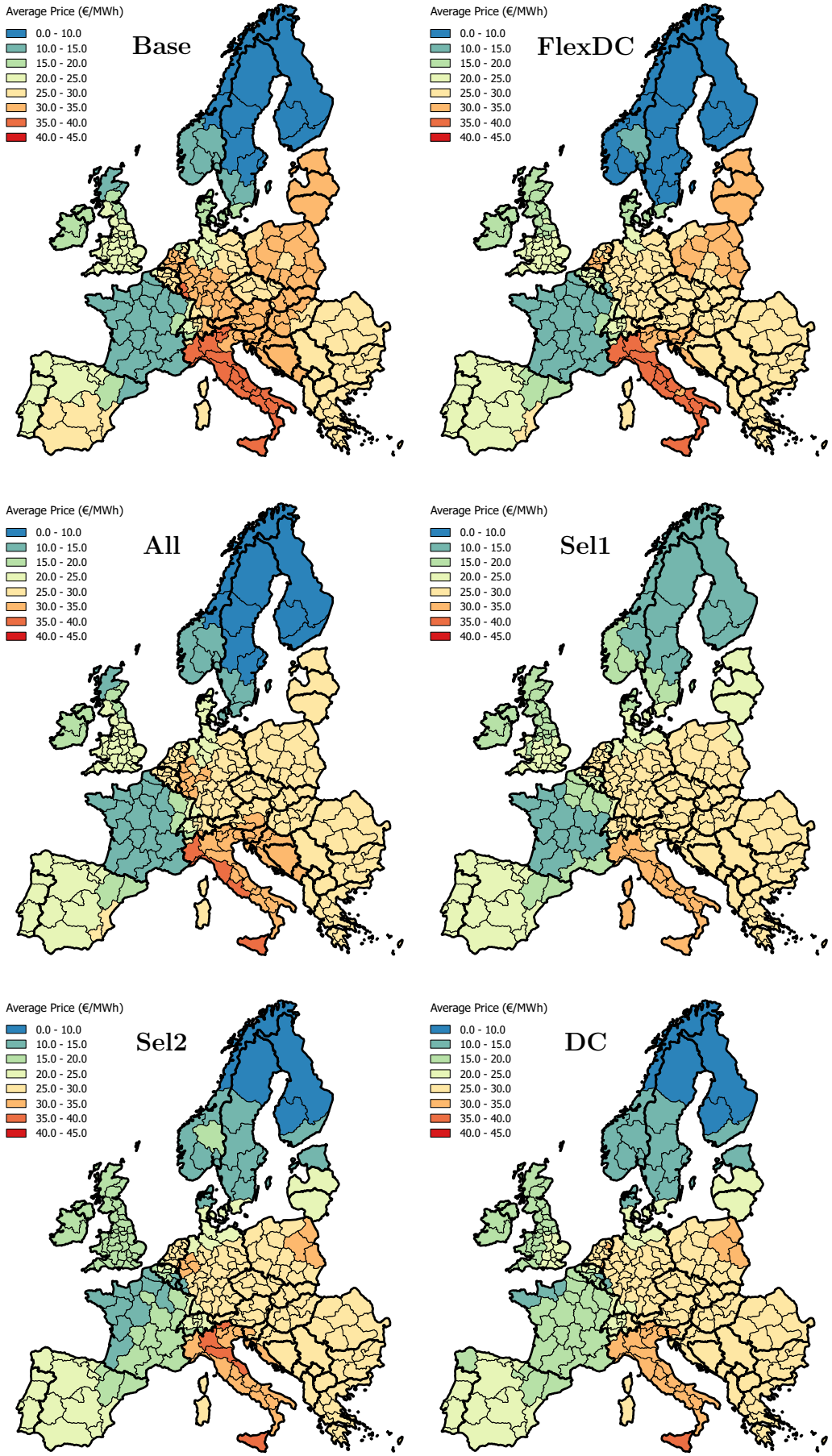

Figure C.1: Nodal prices for different grid flexibility and grid extension scenarios in Europe for the year 2035

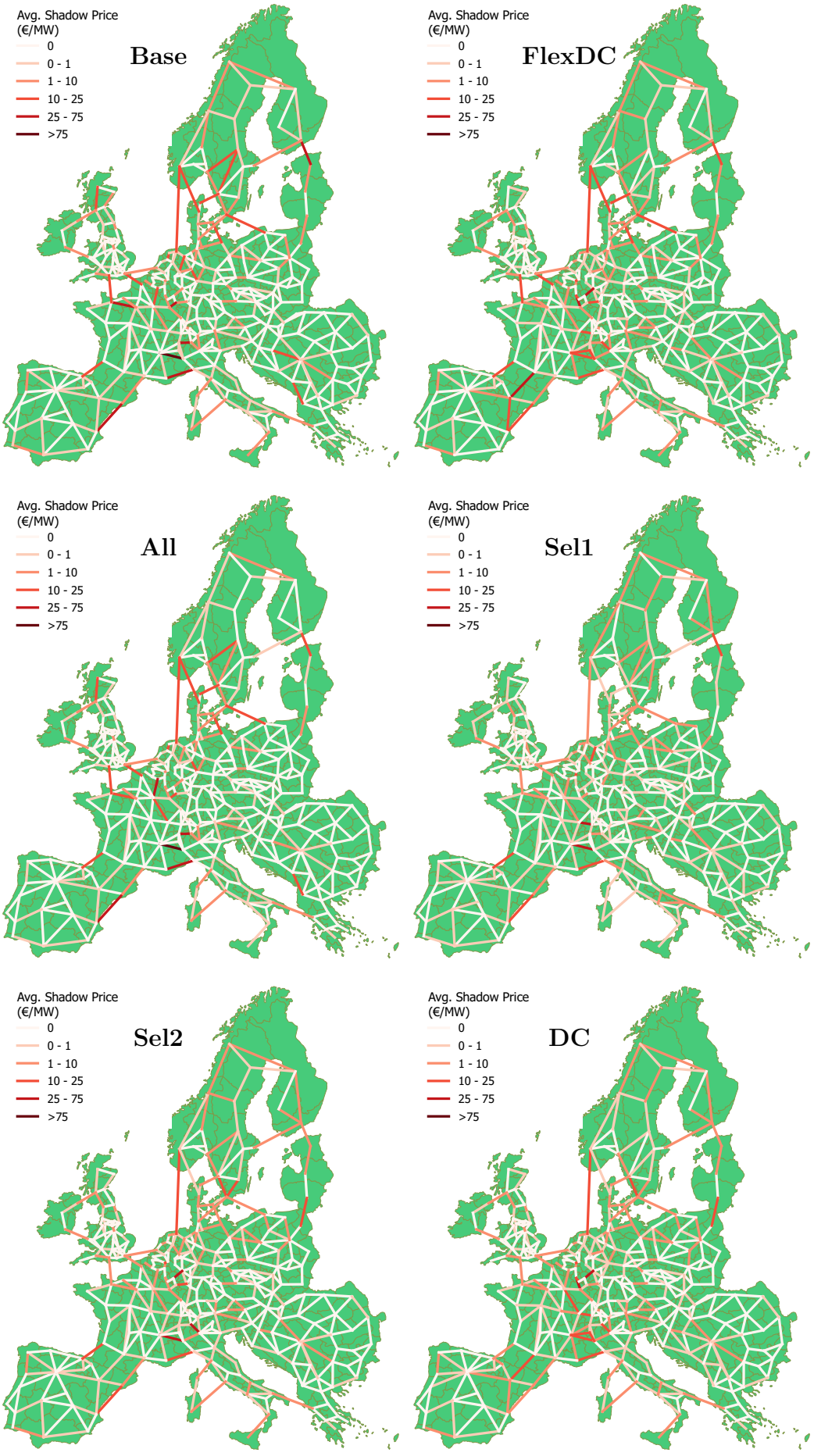

Figure C.2: Shadow prices on transmission lines for grid flexibility and grid extension scenarios in Europe for the year 2035

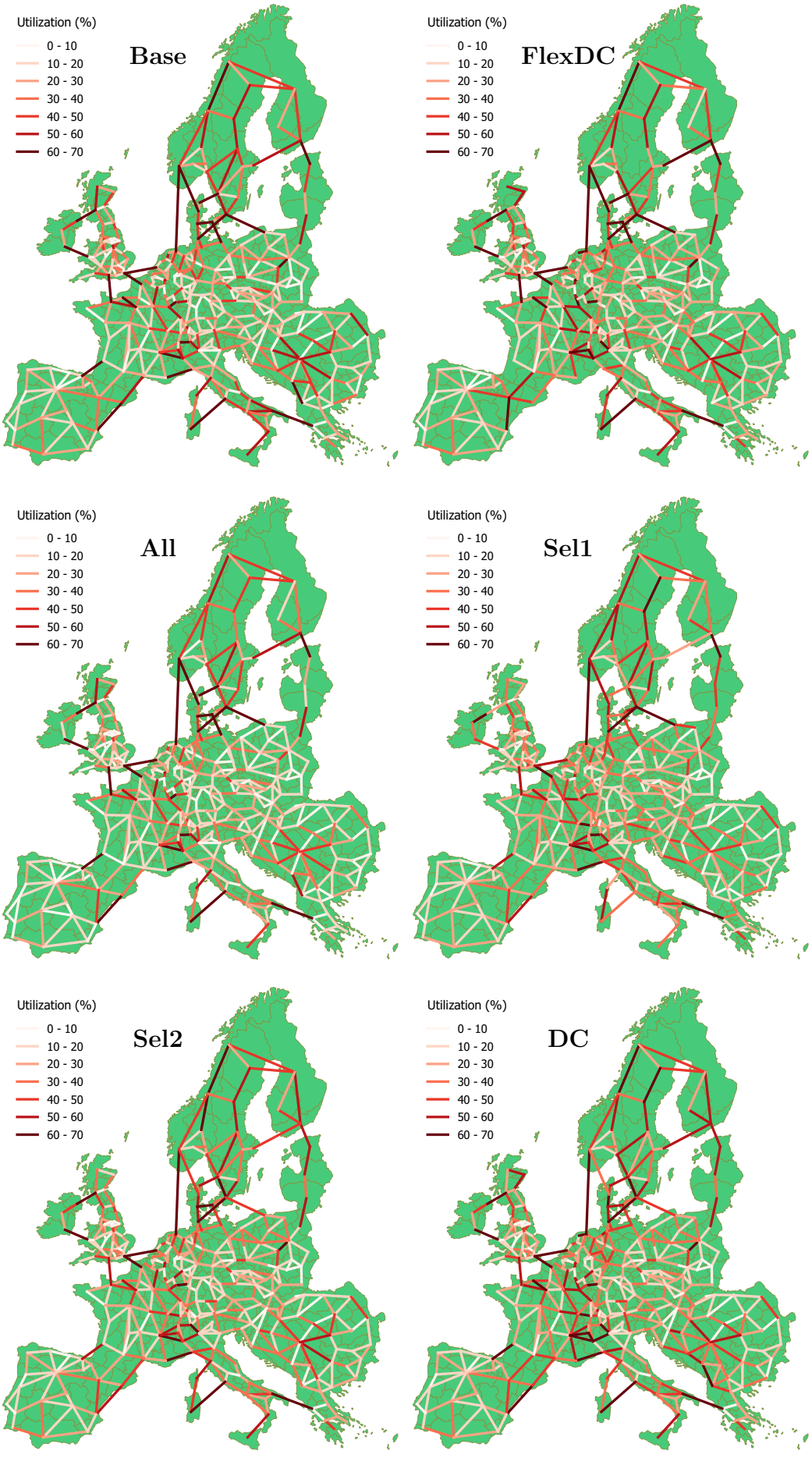

Figure C.3: Line utilization for grid flexibility and grid extension scenarios in Europe for the year for the year 2035

List of Figures

List of Tables

Nomenclature

Sets

Symbol	Description
$\mathcal{C}$	Segments of piecewise linear function, $\mathcal{C} = [1 .. C]$
$\mathcal{E}$	Start-up types, $\mathcal{E} = [1 .. E]$
$\mathcal{I}$	Generating units, $\mathcal{I} = [1 .. I]$
$\mathcal{I}_o$	Generating units in control area o, $\mathcal{I}_o = [1 .. I_o]$
$\mathcal{L}$	Lines in Graph/Network, $\mathcal{L} = [1 .. L]$
$\mathcal{N}$	Nodes in Graph/Network, $\mathcal{N} = [1 .. N]$
$\mathcal{N}_k$	Nodes in a specific country k, $\mathcal{N}_k = [1 .. N_k]$
$\mathcal{O}$	Control areas, $\mathcal{O} = [1 .. O]$
$\mathcal{R}$	Reserve types, $\mathcal{R}$={Primary, Secondary, Tertiary}
$\mathcal{R}^+$	Positive reserves
$\mathcal{R}^-$	Negative reserves
$\mathcal{S}$	Storage units, $\mathcal{S} = [1 .. S]$
$\mathcal{S}_o$	Storage units in control area o, $\mathcal{S}_o = [1 .. S_o]$
$\mathcal{T}$	Time steps, periods, $\mathcal{T} = [1 .. T]$
Ω	Set of scenarios in stochastic unit commitment

Indices

Symbol	Description
$c \in \mathcal{C}$	Segment of piecewise linear function
$e \in \mathcal{E}$	Start-up type
$i \in \mathcal{I}$	Power plant / unit
$m \in \mathcal{L}$	Transmission line
$a, b, n \in \mathcal{N}$	Node/Buse
$o \in \mathcal{O}$	Control area
$r \in \mathcal{R}$	Reserve type
$s \in \mathcal{S}$	Storage plant
$t \in \mathcal{T}$	Time step, period
$\omega \in \Omega$	Scenario
$l \in \mathbb{N}$	Look-back time, off-line time

Parameters

Symbol	Description	Unit
A_i	Fix production costs in on-line state	€
B_i	Variable production costs	€/MWh
$\mathrm{CF}_i(t)$	Capacity factor of VRE technology $i \in \{Wind, PV\}$	(-)
$CL^{t,\max}$	Maximal possible charging in period t	MW
$CT(t_a, t_p)$	Charging table for EVs arriving at t_a and parking t_p hours	MWh
D^t	Electricity demand	MW
DT_i	Minimum downtime	hour
$ES_s^{\max}$	Maximal storage content	MWh
$f_m^{L,\max}$	Maximal power flow over line $m \in \mathcal{L}$	MW
F_i	Fixed start-up costs	€
$H_i^{\max}$	Maximum possible heating energy	(-)
K_i^l	Start-up costs after l off-line periods	€
K_{tol}	Start-up costs approximation tolerance	(-)
$\mathrm{NL}(t)$	Net load in period t	MW
PD_i	Previous downtime of power plant	hour
P_i	Power output of renewable technology $i \in \{Wind, PV\}$	(-)
$P_i^{\max}$	Maximum power output	MW
$P_i^{\min}$	Minimum power output	MW
$PS_s^{\max}$	Maximim input/output of storage power plants (Pump/-Turbine)	MW
$PSA_m^{\max}$	Maximal phase shift angle on line m	(°)
$R_{o,r}^t$	Required reserve capacities in control area o	MW
RU_i	Maximum ramp-up speed	MW/min
RD_i	Maximum ramp-down speed	MW/min
SU_i	Maximum ramp-up at start-up	MW (/start)
SD_i	Maximum ramp-down at shut-down	MW (/start)
$SUT_i(l)$	Required start-up time after cooling	hour
$TH_i(l)$	Required heating after cooling	(-)
UT_i	Minimum uptime	hour
V_i	Variable start-up costs	€
$VRE_n^{t,\min}$	Minimal forecasted generation from VRE	MW
$VRE_n^{t,\max}$	Maximal forecasted generatoin from VRE	MW
$VRE_n^{t,\mathrm{nom}}$	Nominal forecasted generation from VRE	MW
PTDF	Power transfer distribution factors	(-)
DCDF	Direct current distribution factors	(-)
PSDF	Phase shift distribution factors	(-)
α	Share of VRE in electricity supply	(-)
β	Share of PV within the wind/PV mix	(-)
γ	Weight for scenario in stochastic optimization	(-)
$\Delta\mathrm{temp}_i^{\max}$	Maximum temperature difference during heating	(-)
ζ_i	Fix part of wear-and-tear costs	€

$\eta_i^{\max}$	Efficiency at maximum power output	(-)
$\eta_i^{\min}$	Efficiency at minimum power output	(-)
λ_i	Heat-loss coefficent, $\lambda_i \in (0,1)$	$^1/_{\text{hour}}$
π_ω	Probability of occurrence of scenario ω	(-)
ϕ_i	Variable part of wear-and-tear costs	€
ψ_n	Share of renewable capacity in region $n \in \mathcal{N}$	(-)

Variables

Symbol	Description	Unit
cl^t	Charging load for EVs	MW
v_i^t	State of power plant, $v_i^t \in \{0,1\}$	(-)
w_i^t	Hot state of power plant, $\text{w}_i^t \in \{0,1\}$	(-)
p_i^t	Power output	MW
ps_s^t	Power output of storage plant	MW
es_s^t	Energy content of storage plant	MWh
temp_i^t	Temperature, normalized to [0,1]	(-)
h_i^t	Heating, normalized to [0,1]	(-)
y_i^t	Start-up indicator, $y_i^t \in \{0,1\}$	(-)
z_i^t	Shut-down indicator, $z_i^t \in \{0,1\}$	(-)
$g_i^t(s)$	Start-up type indicator	(-)
cp_i^t	Production cost of power plant	€
cu_i^t	Start-up cost of power plant	€
cw_i^t	Wear-and-tear cost of power plant during start-up	€
f_a^N	Active power flow at node a	MW
$\boldsymbol{f}^N$	Active power flow for nodal balances, matrix form	MW
$f_{a,b}^L$	Active power flow from node a to b	MW
$\boldsymbol{f}^L$	Active power flow on lines in matrix form	MW
$q_{a,b}^L$	Reactive power flow from node a to b	var
psa_m	Phase shift angle on line m	(°)
$\boldsymbol{psa}$	Phase shift angle in vector form	(°)
$\text{rv}_i^{t,r}$	Reserve provision from power plants	MW
$\text{rvs}_s^{t,r}$	Reserve provision from power plants	MW
$vre_n^{t,\min}$	Minimal scheduled generation from VRE	MW
$vre_n^{t,\max}$	Maximal scheduled generation from VRE	MW
vre_n^t	Nominal scheduled generation from VRE	MW
$\text{rdp}_i^{t,\max}$	Reserve deployment for maximal VRE generation	MW
$\text{rdp}_i^{t,\min}$	Reserve deployment for minimal VRE generation	MW

Other (Non-Model Description)

Symbol	**Description**	**Unit**
B	Susceptance	$S(=\Omega^{-1})$
LA(length)	Loadability factor according to St.Clair	(-)
R	Resistance	Ω
SIL	Surge impedance loading	MW
V	Voltage	volts
X	Reactance	Ω
x	Specific reactance	Ω/m
δ	Phase angle	$^{\circ}$

Acronyms

Acronym	Description
AGC	Automatic generation control
AC	Alternating current
DC	Direct current
DSM	Demand side management
ED	Economic dispatch
EEX	European Energy Exchange
ENTSO-E	European Network of Transmission System Operators
EPEX	European Power Exchange
Eureletric	The Union of the Electricity Industry
FLHs	Full load hours
GAMS	General Algebraic Modeling System
GIS	Geographic information system
HVDC	High voltage direct current
IP	Integer programming
LP	Linear programming
MILP	Mixed-integer linear programing
MIP	Mixed-integer programming
NTC	Net transfer capacities
OTC	Over-the-counter
PST	Phase shift transformer
RMSE	Root-mean-square error
UC	Unit commitment
USA	United States of America
VRE	Variable renewable energy

Bibliography

[1] T. Aboumahboub. *Development and Application of a Global Electricity System Optimization Model with a Particular Focus on Fluctuating Renewable Energy Sources*. PhD Thesis, TU München, München, 2012. URL: https://mediatum.ub.tum.de/doc/1084602/1084602.pdf.

[2] T. Aboumahboub, K. Schaber, P. Tzscheutschler, and T. Hamacher. Optimal Configuration of a Renewable-based Electricity Supply Sector. In *WSEAS Transactions on Power Systems*, volume 5, pages 120–129, 2010. URL: http://www.wseas.us/e-library/transactions/power/2010/89-612.pdf.

[3] J. Abrell and F. Kunz. Integrating Intermittent Renewable Wind Generation: A Stochastic Multi-Market Electricity Model for the European Electricity Market. *Networks and Spatial Economics*, pages 1–30, 2013. doi:10.1007/s11067-014-9272-4.

[4] P. Ahlhaus and P. Stursberg. Transmission capacity expansion: An improved Transport Model. In *IEEE PES ISGT Europe 2013*, pages 1–5, Copenhagen, 2013. Ieee. doi:10.1109/ISGTEurope.2013.6695322.

[5] G. E. Andersson. Modelling and Analysis of Electric Power Systems, 2008. URL: http://www.eeh.ee.ethz.ch/uploads/tx_ethstudies/modelling_hs08_script_01.pdf.

[6] R. Baldick. The generalized unit commitment problem. *IEEE Transactions on Power Systems*, 10(1):465–475, 1995. doi:10.1109/59.373972.

[7] R. Baldick. Shift factors in ERCOT congestion pricing. 2003. URL: http://www.ksg.harvard.edu/hepg/Papers/baldick_shift.factors.ercot.cong_3-5-03.pdf.

[8] R. Baldick. Border flow rights and contracts for differences of differences: Models for electric transmission property rights. *IEEE Transactions on Power Systems*, 22(4):1495–1506, 2007. doi:10.1109/TPWRS.2007.907124.

[9] R. Baldick, U. Helman, B. F. Hobbs, and R. P. O'Neill. Design of Efficient Generation Markets. *Proceedings of the IEEE*, 93(11):1998–2012, 2005. doi:10.1109/JPROC.2005.857484.

[10] R. Barth, L. Söder, C. Weber, H. Brand, and D. J. Swider. Methodology of the Scenario Tree Tool. *Institute of Energy Economics and the Rational Use of Energy University of Stuttgart*, 2(January 2006):1–27, 2006. URL: http://www.wilmar.risoe.dk/Deliverables/Wilmard6_2_d_ScenarioTree_doc.pdf.

[11] C. Batlle, P. Mastropietro, and R. Gómez-Elvira. Toward a Fuller Integration of the EU Electricity Market: Physical or Financial Transmission Rights? *Electricity Journal*, 27(1):8–17, 2014. doi:10.1016/j.tej.2013.12.001.

[12] M. S. Bazaraa, J. J. Jarvis, and H. D. Sherali. *Linear Programming and Network Flows*. John Wiley & Sons, Hoboken, New Jersey, 2010. doi:dx.doi.org/10.1002/9780471703778.

[13] B. J. W. Beauchamp. Electricity Supply Tariffs and Methods of Charge. *Journal of the Institution of Electrical Engineers*, pages 152–155, 1930.

[14] S. Becker, R. Rodriguez, G. Andresen, S. Schramm, and M. Greiner. Transmission grid extensions during the build-up of a fully renewable pan-European electricity supply. *Energy*, 64:404–418, jan 2014. URL: http://linkinghub.elsevier.com/retrieve/pii/S0360544213008438, doi:10.1016/j.energy.2013.10.010.

[15] K. V. D. Bergh, J. Boury, and E. Delarue. The Flow-Based Market Coupling in Central Western Europe: Concepts and Definitions. KU Leuven Energy Institute, number WP EN2015-13 in TME Working Paper - Energy and Environment, 2015. doi:10.1016/j.tej.2015.12.004.

[16] K. V. D. Bergh and E. Delarue. Facilitating variable generation of renewables by conventional power plant cycling : costs and benefits. KU Leuven, number WP EN2014-9 in TME Working Paper - Energy and Environment, 2014.

[17] K. V. D. Bergh and E. Delarue. Cycling of conventional power plants: Technical limits and actual costs. *Energy Conversion and Management*, 97(March):70–77, 2015. doi:10.1016/j.enconman.2015.03.026.

[18] K. V. D. Bergh, E. Delarue, and W. D'haeseleer. DC power flow in unit commitment models. KU Leuven, number WP EN2014-12 in TME Working Paper - Energy and Environment, 2014.

[19] K. V. D. Bergh, C. Wijsen, E. Delarue, D. William, K. V. D. Bergh, C. Wijsen, E. Delarue, and D. William. The impact of bidding zone configurations on electricity market outcomes The impact of bidding zone configurations on electricity market outcomes. KU Leuven Energy Institute, number WP EN2016-1 in TMW Working Papre - Energy and Environment, 2016.

[20] D. Bertsimas, E. Litvinov, X. A. Sun, J. Zhao, and T. Zheng. Adaptive Robust Optimization for the Security Constrained Unit Commitment Problem. *IEEE Transactions on Power Systems*, 28(1):52–63, feb 2013. URL: http://

ieeexplore.ieee.org/lpdocs/epic03/wrapper.htm?arnumber=6248193, doi:10.1109/TPWRS.2012.2205021.

[21] J. R. Birge and F. Louveaux. *Introduction to Stochastic Programming*. Springer, second edi edition, 2011. doi:10.1007/978-1-4614-0237-4.

[22] J. Boucher and Y. Smeers. Towards a common European Electricity Market – Paths in the right direction ... still far from an effective design. *Competition and Regulation in Network Industries*, 3:375–425, 2002.

[23] BP. Statistical Review of World Energy, 2015. URL: http://www.bp.com/content/dam/bp/pdf/energy-economics/statistical-review-2015/bp-statistical-review-of-world-energy-2015-renewables-section.pdf.

[24] S. P. Bradley, T. L. Magnanti, and A. C. Hax. *Applied Mathematical Programming*. Addison Wesley, 1977. URL: http://web.mit.edu/15.053/www/AMP-Chapter-09.pdf, doi:10.1186/1471-2105-11-S11-S4.

[25] R. Brandenberg, M. Huber, and M. Silbernagl. The summed start-up costs in a unit commitment problem. *EURO Journal on Computational Optimization*, 2016. doi:10.1007/s13675-016-0062-2.

[26] R. Brandenberg and M. Silbernagl. Implementing a Unit Commitment Power Market Model in Implementing a Unit Commitment Power Market Model in FICO Xpress-Mosel. FICO Xpress Optimization Suite, FICO Xpress Optimization Suite whitepaper, 2014.

[27] W. Brauner, G; Bofinger, S; Glaunsinger, W; Pyc, I; Steinke, F; Schwing, U; Magin. Flexibility of thermal power generation for RES supply in Germany until 2020. In *CIGRE 2014*, pages 1–8, 2014.

[28] A. S. Brouwer, M. Van Den Broek, A. Seebregts, and A. Faaij. Impacts of Large-scale Intermittent Renewable Energy Sources on electricity systems, and how these can be modeled. *Renewable and Sustainable Energy Reviews*, 33:443–466, 2014. doi:10.1016/j.rser.2014.01.076.

[29] O. Brückl. *Wahrscheinlichkeitstheoretische Bestimmung des Regel- und Reserveleistungsbedarfs in der Elektrizitätswirtschaft*. PhD Thesis, TU München, 2006. URL: https://mediatum.ub.tum.de/doc/674473/document.pdf.

[30] M. A. Bucher, S. Delikaraoglou, K. Heussen, and P. Pinson. On Quantification of Flexibility in Power Systems. In *Powertech*, Eindhoven, 2015.

[31] M. A. Bucher, R. Wiget, G. Hidalgo-Barquero Pérez, and G. Andersson. Optimal Placement of Multi-Terminal HVDC interconnections for increased Operational Flexibility. In *IEEE PES ISGT Europe 2014*, Istanbul, Turkey, 2014.

[32] Bundesministerium für Wirtschaft und Energie. Zeitreihen zur Entwicklung der erneuerbaren Energien in Deutschland, 2015. URL: https://www.erneuerbare-energien.de/.

[33] Bundesnetzagentur. List of Power Plants, 2015. URL: http://www.bundesnetzagentur.de/cln_1412/DE/Sachgebiete/ElektrizitaetundGas/Unternehmen_Institutionen/Versorgungssicherheit/Erzeugungskapazitaeten/Kraftwerksliste/kraftwerksliste-node.html.

[34] D. W. Bunn. Forecasting loads and prices in competitive power markets. *Proceedings of the IEEE*, 88(2):163–169, 2000. doi:10.1109/5.823996.

[35] California ISO. What the duck curve tells us about managing a green grid, 2012. URL: https://www.caiso.com/Documents/FlexibleResourcesHelpRenewables_FastFacts.pdf.

[36] C. C. Carøe and R. Schultz. A Two-Stage Stochastic Program for Unit Commitment Under Uncertainty in a Hydro-Thermal Power System. Konrad-Zuse-Zentrum fur Informationstechnik, number PREPRINT SC 98-11, 1998. URL: http://citeseerx.ist.psu.edu/viewdoc/summary?doi=10.1.1.28.7817.

[37] M. Carrión and J. M. Arroyo. A Computationally Efficient Mixed-Integer and Linear Formulation and for the Thermal and Unit. In *IEEE Transaction on Power Systems, Vol. 21, No. 3, August*. IEEE, 2006.

[38] S. Chatzivasileiadis, D. Ernst, and G. Andersson. The Global Grid. *Renewable Energy*, 57:372–383, sep 2013. doi:10.1016/j.renene.2013.01.032.

[39] S. Chatzivasileiadis, S. Member, and T. Krause. HVDC Line Placement for Maximizing Social Welfare — An Analytical Approach. In *IEEE Powertech*, pages 1–6, 2013. doi:10.1109/PTC.2013.6652474.

[40] Y. C. Chen, A. D. Dominguez-Garcia, and P. W. Sauer. Online computation of power system linear sensitivity distribution factors. *Proceedings of IREP Symposium: Bulk Power System Dynamics and Control - IX Optimization, Security and Control of the Emerging Power Grid, IREP 2013*, 2013. doi:10.1109/IREP.2013.6629394.

[41] CIA. The World Factbook. https://www.cia.gov/library/publications/the-world-factbook/rankorder/2236rank.html, 2016.

[42] H. S. Clair. Practical Concepts in Capability and Performance of Transmission Lines. *Transactions of the American Institute of Electrical Engineers. Part III: Power Apparatus and Systems*, pages 1152–1157, 1953. doi:10.1109/AIEEPAS.1953.4498751.

[43] A. Clerici and L. Paris. HVDC conversion of HVAC lines to provide substantial power upgrading. *IEEE Trans. Power Delivery*, 6(1):324–333, 1991. doi:10.1109/61.103755.

[44] M. Conforti, G. Cornuéjols, and G. Zambelli. *Integer Programming*, volume 271. Springer, Heidelberg, New York, London, 2014. doi:10.1007/978-3-319-11008-0.

[45] J. Contreras, O. Candiles, J. I. de la Fuente, and T. Gomez. Auction Design in Day-Ahead Electricity Markets. *IEEE Power Engineering Review*, 21(2):54–55, 2001. doi:10.1109/MPER.2001.4311283.

[46] P. Cramton, A. Ockenfels, and S. Stoft. Capacity Market Fundamentals. 2013. URL: http://dx.doi.org/10.5547/2160-5890.2.2.2.

[47] J. Ćwiek-Karpowicz, A. Gawlikowska-Fyk, and K. Westphal. German and Polish Energy Policies : Is Cooperation Possible? Technical Report 1, The Polish Institute of International Affairs, 2013. URL: https://www.pism.pl/files/?id_plik=12692.

[48] G. Czisch. *Szenarien zur zukünftigen Stromversorgung*. PhD Thesis, Universität Kassel, 2005.

[49] C. Davis, A. Chmieliauskas, G. Dijkema, and I. Nikolic. Enipedia, 2015. URL: http://enipedia.tudelft.nl.

[50] J. P. Deane, G. Drayton, and B. P. Ó. Gallachóir. The impact of sub-hourly modelling in power systems with significant levels of renewable generation. *Applied Energy*, 113:152–158, 2014. doi:10.1016/j.apenergy.2013.07.027.

[51] E. Denny and M. O'Malley. The impact of carbon prices on generation-cycling costs. *Energy Policy*, 37(4):1204–1212, 2009. doi:10.1016/j.enpol.2008.10.050.

[52] D. Dentcheva and W. Römisch. Optimal Power Generation under Uncertainty via Stochastic Programming. In *Stochastic Programming Methods and Technical Applications*, pages 22–56. Springer, 1997. doi:10.1007/978-3-642-45767-8_2.

[53] T. N. Dos Santos and A. L. Diniz. A dynamic piecewise linear model for DC transmission losses in optimal scheduling problems. *IEEE Transactions on Power Systems*, 26(2):508–519, 2011. doi:10.1109/TPWRS.2010.2057263.

[54] C. Duthaler, G. Andersson, M. Emery, and M. Kurzidem. Analysis of the Use of PTDF in the UCTE Transmission Grid. In *Power Systems Computation Conference*, Glasgow, 2008. URL: https://www.researchgate.net/publication/228371289_Analysis_of_the_use_of_PTDF_in_the_UCTE_Transmission_Grid.

[55] C. L. Duthaler. *Power Transfer Distribution Factors: Analyse der Anwendung im UCTE-Netz*. Master thesis, ETH Zürich, 2007. URL: https://www.eeh.ee.ethz.ch/uploads/tx_ethpublications/ma_duthaler.pdf.

[56] J. Egerer, C. Gerbaulet, R. Ihlenburg, F. Kunz, B. Reinhard, C. V. Hirschhausen, A. Weber, and J. Weibezahn. Data Documentation - Electricity Sector Data for Policy-Relevant Modeling. DIW, 2014. URL: https://www.diw.de/documents/publikationen/73/diw_01.c.440963.de/diw_datadoc_2014-072.pdf.

[57] J. Egerer, C. V. Hirschhausen, J. Weibezahn, and C. Kemfert. Energiewende und Strommarktdesign : Zwei Preiszonen für Deutschland sind keine Lösung. Number 9 in DIW Wochenbericht, 2015.

[58] EIRGRID. Wind generation. Last accessed: October 30, 2013. URL: www.eirgrid.com.

[59] E. Ela, M. Milligan, and B. Kirby. Operating Reserves and Variable Generation Operating Reserves and Variable Generation. (August), 2011. URL: http://www.nrel.gov/docs/fy11osti/51978.pdf.

[60] ENTSO-E European Network of Transmission System Operators for Electricity. Monthly Consumption 2014. URL: https://www.entsoe.eu/db-query/consumption/monthly-consumption-of-all-countries-for-a-specific-year.

[61] ENTSO-E European Network of Transmission System Operators for Electricity. Deterministic frequency deviations – root causes and proposals for potential solutions. Technical Report December, Brussels, 2011.

[62] ENTSO-E European Network of Transmission System Operators for Electricity. Hourly Consumption Profiles 2011, 2011. URL: https://www.entsoe.eu/data/data-portal/consumption/.

[63] ENTSO-E European Network of Transmission System Operators for Electricity. Monthly Statistics on Hydro Generation, 2011. URL: https://www.entsoe.eu/db-query/production/monthly-production-for-a-specific-year.

[64] ENTSO-E European Network of Transmission System Operators for Electricity. Grid Map, 2012. URL: www.entsoe.eu.

[65] ETG-Task Force Flexibilisierung des Kraftwerksparks. Erneuerbare Energie braucht flexible Kraftwerke – Szenarien bis 2020. Technical report, VDE Verband der Elektrotechnik Elektronik Informationstechnik e.V., 2012.

[66] Eurelectric. Efficiency in Electricity Generation. 2003.

[67] Eurelectric. Hydro in Europe : Powering Renewables. Technical report, 2010. URL: http://www.eurelectric.org/media/26690/hydro_report_final-2011-160-0011-01-e.pdf.

[68] Eurelectric. Flexible Generation : Backing up Renewables. Technical report, 2011. URL: http://www.eurelectric.org/media/61388/flexibility_report_final-2011-102-0003-01-e.pdf.

[69] European Commision. EU Energy, Transport and GHG Emissions Trends to 2050. Reference Scenario 2013. Technical report, 2013. doi:10.2833/17897.

[70] European Photovoltaic Industry Association. Global Market Outlook For Photovoltaics 2014-2018, 2014. URL: http://www.cleanenergybusinesscouncil.com/global-market-outlook-for-photovoltaics-2014-2018-epia-2014.

[71] Eurostat. Glossary:Nomenclature of territorial units for statistics (NUTS). URL: http://ec.europa.eu/eurostat/statistics-explained/index.php/Glossary:NUTS.

[72] Eurostat. Population 2013. URL: http://ec.europa.eu/eurostat/de/data/database.

[73] Eurostat. Regional Economic Accounts 2013, 2013. URL: http://ec.europa.eu/eurostat/de/data/database.

[74] P. Finn and C. Fitzpatrick. Demand side management of industrial electricity consumption: Promoting the use of renewable energy through real-time pricing. *Applied Energy*, 113:11–21, jan 2014. URL: http://linkinghub.elsevier.com/retrieve/pii/S0306261913005692, doi:10.1016/j.apenergy.2013.07.003.

[75] T. Foley, K. Thornton, R. Hinrichs-rahlwes, S. Sawyer, M. Sander, R. Taylor, S. Teske, H. Lehmann, M. Alers, and D. Hales. Renewables 2015 - Global Status Report. Technical report, REN21 - Renewable Energy Policy Network for the 21st Century, 2015.

[76] A. Frangioni, C. Gentile, and F. Lacalandra. Tighter Approximated MILP Formulations for Unit Commitment Problems. *IEEE Transactions on Power Systems*, 24(1):105–113, feb 2009. URL: http://ieeexplore.ieee.org/lpdocs/epic03/wrapper.htm?arnumber=4682641, doi:10.1109/TPWRS.2008.2004744.

[77] GAMS Development Corporations. GAMS — The Solver Manuals. Technical Report March, Washington DC, 2016.

[78] L. L. Garver. Power Generation Scheduling by Integer Programming–Development of Theory. *Transactions of the American Institute of Electrical Engineers. Part III: Power Apparatus and Systems*, 81(3):730–734, 1962. URL: http://ieeexplore.ieee.org/lpdocs/epic03/wrapper.htm?arnumber=4501405, doi:10.1109/AIEEPAS.1962.4501405.

[79] German Transmission System Operators. Wind and PV power feed-in. URL: www.amprion.net,www.50hertz.com,www.tennettso.de,www.transnetbw.de.

[80] German Transmission System Operators. Netzentwicklungsplan Strom 2025, Erster Entwurf der Übertragungsnetzbetreiber, 2015.

[81] Germany Trade & Invest. The energy storage market in Germany. Technical report, www.gtai.com, 2015.

[82] B. Gohla-Neudecker, P. Wimmer, M. Huber, and T. Hamacher. Energy Economic Assessment of Range Extension Technologies for BEVs in 2020. In *Conference on Future Automotive Technology Focus Electromobility*, Munich, 2013. URL: https://mediatum.ub.tum.de/doc/1198220/1198220.pdf.

[83] R. Gomory. Outline of an Algorithm for Integer Solutions to Linear Programs. *Bulletin of the American Mathematical Society*, 64:275–278, 1958.

[84] P. Guha Thakurta, J. Maeght, R. Belmans, and D. Van Hertem. Increasing Transmission Grid Flexibility by TSO Coordination to Integrate More Wind Energy Sources while Maintaining System Security. *IEEE Transactions on Sustainable Energy*, 6(3):1122–1130, 2015. doi:10.1109/TSTE.2014.2341640.

[85] S. Hagspiel, D. Lindenberger, T. Brown, S. Cherevatskiy, and E. Tr. Cost-Optimal Power System Extension under Flow-based Market Coupling. *Energy*, 66:654–666, 2014. doi:doi:10.1016/j.energy.2014.01.025.

[86] T. Hamacher, T. Hartmann, K. Siala, M. Huber, P. Kuhn, and L. Stolle. Gesicherte Stromversorgung in Bayern. Technical Report April, Technische Universität München, München, 2016. URL: https://www.energie-innovativ.de/fileadmin/user_upload/energie_innovativ/Bilder/Publikationen/2016-07-26-TFN_-_Gesicherte_Stromversorgung_in_Bayern.pdf.

[87] T. Hamacher, M. Huber, J. Dorfner, K. Schaber, and A. M. Bradshaw. Nuclear fusion and renewable energy forms: Are they compatible? *Fusion Engineering and Design*, 88(6-8):657–660, 2013. doi:10.1016/j.fusengdes.2013.01.074.

[88] B. Hasche. *Operational impacts of large-scale wind power generation in the German power system and effects of integration measures*. PhD Thesis, Universität Stuttgarrt, 2012. URL: http://elib.uni-stuttgart.de/opus/volltexte/2013/8050/pdf/Dissertation_Hasche_2012.pdf.

[89] K. Hedegaard, B. V. Mathiesen, H. Lund, and P. Heiselberg. Wind power integration using individual heat pumps – Analysis of different heat storage options. *Energy*, 47(1):284–293, nov 2012. URL: http://linkinghub.elsevier.com/retrieve/pii/S0360544212007086, doi:10.1016/j.energy.2012.09.030.

[90] D. Heide, M. Greiner, L. von Bremen, C. Hoffmann, and L. V. Bremen. Reduced storage and balancing needs in a fully renewable European power system with excess wind and solar power generation. *Renewable Energy*, 36(9):2515–2523, sep 2011. doi:10.1016/j.renene.2011.02.009.

[91] D. Heide, L. von Bremen, M. Greiner, C. Hoffmann, M. Speckmann, S. Bofinger, and L. V. Bremen. Seasonal optimal mix of wind and solar power in a future, highly renewable Europe. *Renewable Energy*, 35(11):2483–2489, nov 2010. doi:10.1016/j.renene.2010.03.012.

[92] C. Henderson. Increasing the flexibility of coal fired power plants. Technical Report 12, IEA Clean Coal Centre, London, 2014. URL: https://www.usea.org/sites/default/files/092014_Increasingtheflexibilityofcoal-firedpowerplants_ccc242.pdf.

[93] C. Hernandez-Aramburo, T. Green, and N. Mugniot. Fuel Consumption Minimization of a Microgrid. *IEEE Transactions on Industry Applications*, 41(3):673–681, may 2005. doi:10.1109/TIA.2005.847277.

[94] D. V. Hertem, J. Verboomen, K. Purchala, R. Belmans, and W. L. Kling. Usefulness of DC Power Flow for Active Power Flow Analysis with Flow Controlling Devices. *IEEE Power Engineering Society General Meeting 2005*, 1:2457–2462, 2005. URL: http://ieeexplore.ieee.org/lpdocs/epic03/wrapper.htm?arnumber=1489581.

[95] C. Hewicker, M. Hogan, A. Mogren, and Roadmap 2050. Power Perspectives 2030 On the road to a decarbonised power sector. Technical report, 2011. URL: http://www.roadmap2050.eu/attachments/files/PowerPerspectives2030_FullReport.pdf.

[96] L. Hirth and I. Ziegenhagen. Balancing power and variable renewables: Three links. *Renewable and Sustainable Energy Reviews*, 50:1035–1051, 2015. URL: http://linkinghub.elsevier.com/retrieve/pii/S1364032115004530, doi:10.1016/j.rser.2015.04.180.

[97] B.-M. Hodge and M. Milligan. Wind Power Forecasting Error Distributions over Multiple Timescales Preprint. In *IEEE Power & Energy Society General Meeting*, 2011. URL: http://www.nrel.gov/docs/fy11osti/50614.pdf.

[98] W. Hogan. Independent System Operator: Pricing and Flexibility in a Competitive Electricity Market. Center for Business and Government, JF Kennedy School of Government, Harvard University, MA., 1998.

[99] W. Hogan. Transmission Congestion : The Nodal-Zonal Debate Revisited. Center for Business and Government, JF Kennedy School of Government, Harvard University, MA., 1999. URL: https://www.hks.harvard.edu/fs/whogan/nezn0227.pdf.

[100] H. Holttinen. The impact of large scale wind. VTT Publications, number 554, 2004. URL: http://www.vtt.fi/inf/pdf/publications/2004/P554.pdf.

[101] H. Holttinen, J. Kiviluoma, A. Estanqueiro, E. Gómez-lázaro, B. Rawn, P. Meibom, E. Lannoye, T. Aigner, Y. H. Wan, and M. Milligan. Variability of load and net load in case of large scale distributed wind power. 2012.

[102] K. E. V. Horn. A Network-Inclusive , Optimization-Based Approach to Power System Flexibility Evaluation. In *North American Power Symposium (NAPS)*, 2014. doi:10.1109/NAPS.2014.6965382.

[103] M. Hotz, S. Member, W. Utschick, and S. Member. A Hybrid Tranmssion Grid Architectur Enabling Efficient Optimal Power Flow. *IEEE Transaction on Power Systems*, (99):1–13, 2016. doi:10.1109/TPWRS.2015.2507639.

[104] B. Hua and R. Baldick. A Convex Primal Formulation for Convex Hull Pricing. 2016. URL: http://arxiv.org/abs/1605.05002, arXiv:1605.05002.

[105] M. Huber, D. Dimkova, and T. Hamacher. Integration of wind and solar power in Europe: Assessment of flexibility requirements. *Energy*, 69:236–246, may 2014. URL: http://linkinghub.elsevier.com/retrieve/pii/S0360544214002680, doi:10.1016/j.energy.2014.02.109.

[106] M. Huber, J. Dorfner, and T. Hamacher. Electricity system optimization in the EUMENA region. Technical report, Dii GmbH, jan 2012. URL: http://mediatum.ub.tum.de/node?id=1171502, doi:http://dx.doi.org/10.14459/2013md1171502.

[107] M. Huber, S. Florian, and T. Hamacher. Coordinating Smart Homes in Microgrids: A Quantification of Benefits. In *IEEE PES Innovative Smart Grid Technologies Europe (ISGT Europe)*, Copenhagen, 2013. doi:10.1109/ISGTEurope.2013.6695357.

[108] M. Huber, T. Hamacher, C. Ziems, and H. Weber. Combining LP and MIP approaches to model the impacts of renewable energy generation on individual thermal power plant operation. In *IEEE Power and Energy Society General Meeting*, Vancouver, 2013. doi:10.1109/PESMG.2013.6672804.

[109] M. Huber, A. Roger, and T. Hamacher. Optimizing long-term investments for a sustainable development of the ASEAN power system. *Energy*, 88:180–193, 2015. URL: http://dx.doi.org/10.1016/j.energy.2015.04.065, doi:10.1016/j.energy.2015.04.065.

[110] M. Huber and F. Sänger. Das „ Post-EEG “ - Potenzial von Photovoltaik im privaten Strom- und Wärmesektor. *Energiewirtschaftliche Tagesfragen*, pages 57–61, 2013.

[111] M. Huber and M. Silbernagl. Modeling start-up times in unit commitment by limiting temperature increase and heating. In *International Conference on the European Energy Market, EEM*, volume 2015-Augus, 2015. doi:10.1109/EEM.2015.7216755.

[112] M. Huber, A. Trippe, P. Kuhn, and T. Hamacher. Effects of large scale EV and PV integration on power supply systems in the context of Singapore. *2012 3rd IEEE PES Innovative Smart Grid Technologies Europe (ISGT Europe)*, pages 1–8, oct 2012. URL: http://ieeexplore.ieee.org/lpdocs/epic03/wrapper.htm?arnumber=6465831, doi:10.1109/ISGTEurope.2012.6465831.

[113] M. Huber and C. Weissbart. On the optimal mix of wind and solar generation in the future Chinese power system. *Energy*, 90:235–243, 2015. URL: http://dx.doi.org/10.1016/j.energy.2015.05.146, doi:10.1016/j.energy.2015.05.146.

[114] Hughes. *Networks of Power - Electrification in Western Society, 1880-1930*. The Johns Hopkins University Press, Baltimore, Maryland, 1983.

[115] International Energy Agency. Harnessing Variable Renewables - A Guide to the Balancing Challenge. Technical report, Paris, 2011. URL: https://www.iea.org/publications/freepublications/publication/Harnessing_Variable_Renewables2011.pdf.

[116] K. A. Janker. *Aufbau und Bewertung einer für die Energiemodellierung verwendbaren Datenbasis an Zeitreihen erneuerbarer Erzeugung und sonstiger Daten*. PhD Thesis, TU München, 2014. URL: https://mediatum.ub.tum.de/doc/1207265/1207265.pdf.

[117] A. Jokic. *Price-based Optimal Control of Electrical Power Systems*. PhD Thesis, Technische Universtität Eindhoven, 2007. URL: https://pure.tue.nl/ws/files/2136716/200711654.pdf.

[118] P. Keatley, A. Shibli, and N. J. Hewitt. Estimating power plant start costs in cyclic operation. *Applied Energy*, 111:550–557, nov 2013. doi:10.1016/j.apenergy.2013.05.033.

[119] M. Kefayati. *Harnessing Demand Flexibility to Minimize Cost , Facilitate Renewable Integration , and Provide Ancillary Services*. PhD Thesis, University of Texas, Austin, 2014.

[120] W. Kempton and J. Tomić. Vehicle-to-grid power fundamentals: Calculating capacity and net revenue. *Journal of Power Sources*, 144(1):268–279, 2005. doi:10.1016/j.jpowsour.2004.12.025.

[121] J. King, B. Kirby, and M. Milligan. Flexibility Reserve Reductions from an Energy Imbalance Market with High Levels of Wind Energy in the Western Interconnection Flexibility Reserve Reductions from an Energy Imbalance Market with High Levels of Wind Energy in the Western Interconnection. Technical Report October, NREL, 2011. URL: http://www.nrel.gov/docs/fy12osti/52330.pdf.

[122] D. Kirschen and G. Strbac. *Fundamentals of Power System Economics*. John Wiley & Sons, Chichester, West Sussex, 2004.

[123] G. Klingenberg. Electricity Supply of Large Cities. *Journal of the Institution of Electrical Engineers*, 52(225):123–141, 1914.

[124] M. Koch, D. Bauknecht, C. Heinemann, D. Ritter, M. Vogel, and E. Tröster. Modellgestützte Bewertung von Netzausbau im europäischen Netzverbund und Flexibilitätsoptionen im deutschen Stromsystem im Zeitraum 2020–2050.

Zeitschrift für Energiewirtschaft, 2015. URL: http://link.springer.com/10.1007/s12398-015-0147-2, doi:10.1007/s12398-015-0147-2.

[125] P. Kuhn. *Iteratives Modell zur Optimierung von Speicherausbau und -betrieb in einem Stromsystem mit zunehmend fluktuierender Erzeugung*. PhD Thesis, TU Munich, 2011. URL: http://d-nb.info/1031075666/34.

[126] P. Kuhn, M. Huber, J. Dorfner, and T. Hamacher. Challenges and opportunities of power systems from smart homes to super-grids. *Ambio*, 45(1):50–62, 2016. doi:10.1007/s13280-015-0733-x.

[127] M. Kühne. *Drivers of energy storage demand in the German power system : an analysis of the influence of methodology and parameters on modelling results*. PhD Thesis, TU Munich, 2016.

[128] N. Kumar, P. Besuner, S. Lefton, D. Agan, and D. Hilleman. Power Plant Cycling Costs. Technical Report July, NREL, Golden, Colorado, 2012. URL: http://wind.nrel.gov/public/wwis/aptechfinalv2.pdf.

[129] P. Kundur. *Power System Stability and Control*. McGraw-Hill, 1993.

[130] E. Lannoye, D. Flynn, and M. O. Malley. Evaluation of Power System Flexibility. *IEEE Transactions on Power Systems*, 27(2):922–931, 2012. doi:10.1109/TPWRS.2011.2177280.

[131] E. Lannoye, D. Flynn, and M. O. Malley. Power System Flexibility Assessment - State of the Art. In *Power and Energy Society General Meeting, 2012 IEEE*, Vancouver, 2012. doi:10.1109/PESGM.2012.6345375.

[132] E. Lannoye, S. M. Ieee, D. Flynn, M. Ieee, M. O. Malley, F. Ieee, M. O'Malley, and O. Malley. The Role of Power System Flexibility in Generation Planning. *2011 IEEE Power and Energy Society General Meeting*, pages 1–6, jul 2011. doi:10.1109/PES.2011.6039009.

[133] D. M. Larruskain, I. Zamora, O. Abarrategui, A. Iraolagoitia, M. D. Gutiérrez, E. Loroño, and F. D. Bodega. Power transmission capacity upgrade of overhead lines. In *Int. Conf. Renewable Energies and Power Quality*, 2006. URL: http://www.icrepq.com/icrepq06/296_Larruskain.pdf.

[134] D. Lee, S. Member, J. Lee, and R. Baldick. Wind Power Scenario Generation for Stochastic Wind Power Generation and Transmission Expansion Planning. In *IEEE PES General Meeting*, pages 1–5, National Harbor, MD, 2014. doi:10.1109/PESGM.2014.6939930.

[135] J. Lee, J. Leung, and F. Margot. Min-up/min-down polytopes. *Discrete Optimization*, 1(1):77–85, jun 2004. URL: http://linkinghub.elsevier.com/retrieve/pii/S1572528604000064, doi:10.1016/j.disopt.2003.12.001.

[136] V. Lenzi, A. Ulbig, and G. Andersson. Impacts of forecast accuracy on grid integration of renewable energy sources. *2013 IEEE Grenoble Conference*, pages 1–6, 2013. URL: `http://ieeexplore.ieee.org/xpls/abs_all.jsp?arnumber=6652486`, `doi:10.1109/PTC.2013.6652486`.

[137] London Economics and Global Energy Decisions. Structure and Performance of Six European Wholesale Electricity Markets in 2003, 2004, and 2005. Technical Report February, London, 2007.

[138] C. Loutan and D. Hawkins. Integration of renewable resources. Technical Report November, 2007. URL: `http://www.caiso.com/Documents/Integration-RenewableResourcesReport.pdf`.

[139] F. L. F. Lu and H. Gan. National Electricity Market of Singapore. In *2005 International Power Engineering Conference*, volume 1, pages 16–19, Singapore, 2004. `doi:10.1109/IPEC.2005.207055`.

[140] J. Ma, V. Silva, R. Belhomme, D. S. Kirschen, and L. F. Ochoa. Evaluating and Planning Flexibility in Sustainable Power Systems. In *IEEE Power & Energy Society General Meeting*, volume 4, pages 200–209, Vancouver, 2013.

[141] R. Madlener and M. Kaufmann. Power exchange spot market trading in Europe: theoretical considerations and empirical evidence. Technical report, OSCOGEN: Optimization of Cogeneration Systems in a Competitive Market Environment, 2002.

[142] D. Madzharov, E. Delarue, and W. D'haeseleer. Integrating electric vehicles as flexible load in unit commitment modeling. *Energy*, 65:285–294, 2014. `doi:10.1016/j.energy.2013.12.009`.

[143] H. Mangesius, M. Huber, S. Hirche, and T. Hamacher. A Framework to Quantify Technical Flexibility in Power Systems Based on Reliability Certificates. In *IEEE PES Innovative Smart Grid Technologies Europe (ISGT Europe)*, Copenhagen, 2013. `doi:10.1109/ISGTEurope.2013.6695460`.

[144] P. Meibom, R. X. F. D. Barth, B. Hasche, H. Brand, C. Weber, and M. O'Malley. Stochastic Optimization Model to Study the Operational Impacts of High Wind Penetrations in Ireland. *IEEE Transactions on Power Systems*, 26(3):1367–1379, 2011. `doi:10.1109/TPWRS.2010.2070848`.

[145] A. Mills and R. Wiser. Implications of Wide-Area Geographic Diversity for Short-Term Variability of Solar Power. Technical Report September, Ernest Orlando Lawrance Berkeley National Laboratory, 2010. URL: `http://eetd.lbl.gov/ea/ems/reports/lbnl-3884e.pdf`.

[146] G. Morales-Espana. *Unit Commitment - Computational Performance, System Representation and Wind Uncertainty Management*. PhD Thesis, Uinversidad Pontificia Comillas Madrid, Madrid, 2014.

[147] G. Morales-España, R. Baldick, J. García-González, and A. Ramos. Power-Capacity and Ramp-Capability Reserves for Wind Integration in Power-Based UC. *IEEE Transactions of Sustainable Energy*, pages 1–8, 2015. doi:10.1109/TSTE.2015.2498399.

[148] G. Morales-España, J. M. Latorre, J. Garciía-Gonzales, and A. Ramos. Talk on Tight and Compact MILP Formulations for Unit Commitment Problems. In *FERC Technical Conference*, Washington DC, 2013.

[149] G. Morales-España, J. M. Latorre, and A. Ramos. Tight and Compact MILP Formulation of Start-Up and Shut-Down Ramping in Unit Commitment. *IEEE Transactions on Power Systems*, pages 1–1, 2012. URL: http://ieeexplore.ieee.org/lpdocs/epic03/wrapper.htm?arnumber=6365287, doi:10.1109/TPWRS.2012.2222938.

[150] G. Morales-España, J. M. Latorre, and A. Ramos. Tight and Compact MILP Formulation for the Thermal Unit Commitment Problem. *IEEE Transactions on Power Systems*, 28(4):4897–4908, 2013. doi:10.1109/TPWRS.2013.2251373.

[151] G. Morales-España, A. Ramos, and J. García-González. An MIP Formulation for Joint Market-Clearing of Energy and Reserves Based on Ramp Scheduling. *IEEE Transaction on Power Systems*, 29(1):476–488, 2014.

[152] E. K. Morlok and D. J. Chang. Measuring capacity flexibility of a transportation system. *Transportation Research Part A*, 38:405–420, 2004. doi:10.1016/j.tra.2004.03.001.

[153] J. a. Muckstadt and R. C. Wilson. An Application of Mixed-Integer Programming Duality to Scheduling Thermal Generating Systems. *IEEE Transactions on Power Apparatus and Systems*, PAS-87(12):1968–1978, 1968. URL: http://ieeexplore.ieee.org/lpdocs/epic03/wrapper.htm?arnumber=4073484, doi:10.1109/TPAS.1968.292156.

[154] Museum of Vertebrate Zoology University of Berkley. GADM Database of Global Administrative Areas, 2013. URL: www.gadm.org/home.

[155] F. Müsgens, A. Ockenfels, and M. Peek. Economics and design of balancing power markets in Germany. *International Journal of Electrical Power and Energy Systems*, 55:392–401, 2014. URL: http://dx.doi.org/10.1016/j.ijepes.2013.09.020, doi:10.1016/j.ijepes.2013.09.020.

[156] D. Newbery, G. Strbac, and V. Ivan. The benefits of integrating European electricity markets. Faculty of Economics, University of Cambridge, number 1504, 2015. doi:http://www.eprg.group.cam.ac.uk/wp-content/uploads/2015/02/EPRG-WP-1504.pdf.

[157] H. Nosair, S. Member, F. Bouffard, and S. Member. Flexibility Envelopes for Power System Operational Planning. *IEEE Transactions of Sustainable Energy*, pages 1–10, 2015. doi:10.1109/TSTE.2015.2410760.

[158] M. P. Nowak and W. Römisch. Stochastic Lagrangian Relaxation Applied to Power Scheduling in a Hydro-Thermal System under Uncertainty. *Annals of Operations Research*, 100(1–4):251–272, 2000. doi:10.1023/A:1019248506301.

[159] J. Ostrowski, M. F. Anjos, and A. Vannelli. Tight Mixed Integer Linear Programming Formulations for the Unit Commitment Problem. *IEEE Transactions on Power Systems*, 27(1):39–46, 2012. doi:10.1109/TPWRS.2011.2162008.

[160] A. L. Ott. Evolution of computing requirements in the PJM market: Past and future. In *IEEE PES General Meeting, PES 2010*, pages 1–4, 2010. doi:10.1109/PES.2010.5589842.

[161] N. Padhy. Unit Commitment—A Bibliographical Survey. *IEEE Transactions on Power Systems*, 19(2):1196–1205, 2004. doi:10.1109/TPWRS.2003.821611.

[162] A. Papavasiliou, U. C. Berkeley, S. S. Oren, and R. P. O. Neill. Reserve Requirements for Wind Power Integration : A Stochastic Programming Framework. *Operations Research*, 26(4):2197–2206, 2010. doi:10.1109/TPWRS.2011.2121095.

[163] R. H. Parsons. *The Early Days of the Power Station Industry*. Cambridge University Press, 1940.

[164] PCR Price Coupling of Regions. EUPHEMIA Public Description - PCR Market Coupling Algorithm. Technical report, 2016. URL: https://www.epexspot.com/document/34460/Euphemia:Publicdocumentation-January2016.

[165] P. Pedroso, M. Kubo, and A. Viana. Unit commitment with valve-point loading effect Unit commitment with valve-point loading effect. Technical Report Series: DCC-2014-05, 2014. arXiv:1404.4944.

[166] P. Pinson. *Estimation of the Uncertainty in Wind Power Forecasting*. PhD Thesis, Ecole Mines de Paris, 2006.

[167] P. Pinson, H. Madsen, G. Papaefthymiou, and B. Klöckl. From Probabilistic Forecasts to Wind Power Production. *Wind Energy*, 12(1):51–62, 2009. doi:10.1002/we.284.

[168] PLATTS. Powervision Package, 2014.

[169] W. Powell. Clearing the Jungle of Stochastic Optimization. *Informs TutORials*, (c):1–37, 2014. URL: http://www.castlelab.princeton.edu/Papers/Powell-ClearingJungleStochasticOptimization_OR_TutORialsJune2014.pdf.

[170] W. B. Powell and S. Meisel. Tutorial on Stochastic Optimization in Energy-Part I: Modeling and Policies. *IEEE Transactions on Power Systems*, pages 1–9, 2015. doi:10.1109/TPWRS.2015.2424974.

[171] W. B. Powell and S. Meisel. Tutorial on Stochastic Optimization in Energy-Part II: An Energy Storage Illustration. *IEEE Transactions on Power Systems*, pages 1–8, 2015. doi:10.1109/TPWRS.2015.2424980.

[172] S. Pryor and R. Barthelmie. Climate change impacts on wind energy: A review. *Renewable and Sustainable Energy Reviews*, 14(1):430–437, jan 2010. doi:10.1016/j.rser.2009.07.028.

[173] H. V. Pugh. The Generation of Electricity in the London Area. *Journal of the Institution of Electrical Engineers*, (2445):484–497, 1957. doi:10.1049/pi-a.1958.0089.

[174] L. Puka and K. Szulecki. Beyond the "Grid-Lock" in Electricity Interconnectors. DIW, Discussion Papers, 2014. URL: https://www.diw.de/documents/publikationen/73/diw_01.c.463023.de/dp1378.pdf.

[175] D. Rajan, S. Takriti, and Y. Heights. Minimum Up / Down Polytopes of the Unit Commitment Problem with Start-Up Costs, 2005.

[176] Y. Rebours and D. S. Kirschen. A Survey of Definitions and Specifications of Reserve Services. *Report, University of Manchester*, pages 1–38, 2005. URL: http://www.ee.washington.edu/research/real/Library/Reports/Survey_of_Reserve_Services.pdf.

[177] E. Rienecker, M. M.; Suarez, M. J.; Gelaro, R.; Todling, R.; Bacmeister, J.; Liu, J. C. Bosilovich, M. G.; Schubert, S. D.; Takacs, L.; Kim, G.; Bloom, S.; Chen, R. lins, D.; Conaty, A.; da Silva, A.; Gu, W.; Joiner, J.; Koster, R. D.; Lucchesi, C. R. R. Molod, A.; Owens, T.; Pawson, S.; Pegion, P.; Redder, and J. Rolf; Robertson, Franklin R.; Ruddick, Albert G.; Sienkiewicz, M.; Woollen. MERRA: NASA's Modern-Era Retrospective Analysis for Research and Applications. *Journal of Climate*, 24(14):3624–3648, jul 2011. doi:10.1175/jcli-d-11-00015.1.

[178] S. Roon and M. Huber. Modeling Spot Market Pricing with the Residual Load. In *Enerday: 5th Conference on Energy Economics and Technology*, Dresden, 2010. URL: https://www.ffe.de/download/wissen/297_Enerday/20100416_FfE_von_Roon-Huber_paper.pdf.

[179] S. V. Roon. *Auswirkungen von Prognosefehlern auf die Vermarktung von Windstrom*. PhD Thesis, Technische Universität München, 2012. URL: https://www.ffe.de/download/article/463/20120228_Dissertation_von_Roon.pdf.

[180] K. Schaber. *Integration of Variable Renewable Energies in the European power system: a model-based analysis of transmission grid extensions and energy sector*

coupling. PhD Thesis, Technische Universität München, 2013. URL: https://mediatum.ub.tum.de/doc/1163646/1163646.pdf.

[181] K. Schaber, F. Steinke, and T. Hamacher. Transmission grid extensions for the integration of variable renewable energies in Europe: Who benefits where? *Energy Policy*, 43(0):123–135, 2012. doi:10.1016/j.enpol.2011.12.040.

[182] K. Schaber, F. Steinke, P. Mühlich, and T. Hamacher. Parametric study of variable renewable energy integration in Europe: Advantages and costs of transmission grid extensions. *Energy Policy*, 42:498–508, mar 2012. URL: http://linkinghub.elsevier.com/retrieve/pii/S0301421511010081, doi:10.1016/j.enpol.2011.12.016.

[183] A. Schröder, F. Kunz, J. Meiss, R. Mendelevitch, and C. von Hirschhausen. Data Documentation: Current and Prospective Costs of Electricity Generation until 2050. DIW, 2013. URL: http://www.diw.de/documents/publikationen/73/diw_01.c.424566.de/diw_datadoc_2013-068.pdf.

[184] G. B. Sheble and G. N. Fahd. Unit commitment literature synopsis. *IEEE Transactions on Power Systems*, 9(1):128–135, 1994. doi:10.1109/59.317549.

[185] M. Silbernagl, M. Huber, and R. Brandenberg. Improving Accuracy and Efficiency of Start-Up Cost Formulations in MIP Unit Commitment by Modeling Power Plant Temperatures. *IEEE Transactions on Power Systems*, pages 1–9, 2015. doi:10.1109/TPWRS.2015.2450776.

[186] C. K. Simoglou, P. N. Biskas, and A. G. Bakirtzis. Optimal Self-Scheduling of a Thermal Producer in Short-Term Electricity Markets by MILP. *IEEE Transaction on Power Systems*, 25(4):1965–1977, 2010. doi:10.1109/TPWRS.2010.2050011.

[187] A. B. Skånlund, A. von Schmede, B. Tennbakk, G. Gravdehaug, and R. Grøndahl. Loop flows – Final advice - Prepared for The European Commission. Technical Report October, Thema Consulting Group, 2013.

[188] H. Spliethoff. *Power Generation from Solid Fuels*. Springer, 2010.

[189] N. Stadlmair and T. Sattelmayer. Measurement and Analysis of Flame Transfer Functions in a Lean-Premixed, Swirl-Stabilized Combustor with Water Injection. In *54th AIAA Aerospace Sciences Meeting*, San Diego, California, USA, 2016.

[190] F. Steinke, P. Wolfrum, and C. Hoffmann. Grid vs storage in a 100% renewable Europe. *Renewable Energy*, 50:826–832, 2013. doi:10.1016/j.renene.2012.07.044.

[191] J. Stich, M. Mannhart, T. Zipperle, T. Massier, M. Huber, and T. Hamacher. Modelling a Low-Carbon Power System for Indonesia, Malaysia and Singapore. In *33rd IEW International Energy Workshop*, pages 1–11, Beijing, 2014. URL: https://mediatum.ub.tum.de/doc/1233948/160250.pdf.

[192] B. Stott, J. Jardim, and O. Alsac. DC Power Flow Revisited. *IEEE Transactions on Power Systems*, 24(3):1290–1300, 2009. doi:10.1109/TPWRS.2009.2021235.

[193] M. Stötzer, I. Hauer, M. Richter, and Z. A. Styczynski. Potential of demand side integration to maximize use of renewable energy sources in Germany. *Applied Energy*, 146:344–352, 2015. doi:10.1016/j.apenergy.2015.02.015.

[194] G. Strbac. Demand side management: Benefits and challenges. *Energy Policy*, 36(12):4419–4426, 2008. doi:10.1016/j.enpol.2008.09.030.

[195] D. Streiffert, R. Philbrick, and A. Ott. A mixed integer programming solution for market clearing and reliability analysis. In *IEEE Power Engineering Society General Meeting, 2005*, pages 1–8, 2005. doi:10.1109/PES.2005.1489108.

[196] S. Takriti, J. Birge, and E. Long. A stochastic model for the unit commitment problem. *IEEE Transactions on Power Systems*, 11(3):1497–1508, 1996. doi:10.1109/59.535691.

[197] K. Trepper, M. Bucksteeg, and C. Weber. Market splitting in Germany - New evidence from a three-stage numerical model of Europe. *Energy Policy*, 87:199–215, 2015. URL: http://dx.doi.org/10.1016/j.enpol.2015.08.016, doi:10.1016/j.enpol.2015.08.016.

[198] N. Troy. *Generator Cycling due to High Penetrations of Wind Power*. PhD Thesis, University College Dublin, 2011.

[199] M. Tuffaha and J. T. Gravdahl. Mixed-integer formulation of unit commitment problem for power systems: Focus on start-up cost. In *IECON Proceedings (Industrial Electronics Conference)*, pages 8160–8165, 2013. doi:10.1109/IECON.2013.6700498.

[200] A. Tuohy, P. Meibom, E. Denny, and M. O'Malley. Unit commitment for systems with significant wind penetration. *IEEE Transactions on Power Systems*, 24(2):592–601, 2009. doi:10.1109/TPWRS.2009.2016470.

[201] A. Ulbig. *Operational Flexibility in Electric Power Systems*. PhD Thesis, ETH Zurich, 2014. doi:10.3929/ethz-a-010337152.

[202] A. Ulbig, S. Member, and G. Andersson. On Operational Flexibility in Power Systems. In *IEEE Power and Energy Society General Meeting*, page 9, 2012. doi:10.1109/PESGM.2012.6344676.

[203] D. Van Hertem, J. Rimez, and R. Belmans. Power flow controlling devices as a smart and independent grid investment for flexible grid operations: Belgian case study. *IEEE Transactions on Smart Grid*, 4(3):1656–1664, 2013. doi:10.1109/TSG.2013.2249597.

[204] J. Verboomen, D. Van Hertem, P. Schavemaker, W. Kling, and R. Belmans. Phase shifting transformers: principles and applications. In *2005 International Conference on Future Power Systems*, number February 2016, pages 6 pp.–6, 2005. doi:10.1109/FPS.2005.204302.

[205] A. Viana and J. P. Pedroso. A new MILP-based approach for unit commitment in power production planning. *International Journal of Electrical Power & Energy Systems*, 44(1):997–1005, jan 2013. doi:10.1016/j.ijepes.2012.08.046.

[206] M. Vrakopoulou. *Optimal decision making for secure and economic operation of power systems*. PhD Thesis, ETH Zurich, 2013. doi:http://dx.doi.org/10.3929/ethz-a-010164368.

[207] T. Weißbach and E. Welfonder. High Frequency Deviations within the European Power System – Origins and Proposals for Improvement. *VGB Power Tech*, (6):1–6, 2009.

[208] Wikimedia Commons. The synchronous grids of Europe, 2006. URL: https://commons.wikimedia.org/wiki/File:ElectricityUCTE.svg.

[209] Wikipedia. List of Power Stations. URL: https://en.wikipedia.org/wiki/List_of_power_stations.

[210] R. Wilson. Architecture of Power Markets. *Econometrica*, 70:1299–1340, 2002.

[211] A. J. Wood, B. F. Wollenberg, and G. B. Sheble. *Power Generation, Operation and Control*. Wiley, 2013.

[212] L. Wu. A tighter piecewise linear approximation of quadratic cost curves for unit commitment problems. *IEEE Transactions on Power Systems*, 26(4):2581–2583, 2011. doi:10.1109/TPWRS.2011.2148370.

[213] C. Ziems, S. Meinke, J. Nocke, H. Weber, and E. Hassel. Kraftwerksbetrieb bei Einspeisung von Windparks und Photovoltaikanlagen. Technical report, Universität Rostock, Rostock, 2012. URL: https://www.vgb.org/vgbmultimedia/333_Abschlussbericht-p-5968.pdf.

[214] G. Zoettl. Investment decisions in Liberalized Electricity Markets : A framework of Peak Load Pricing with strategic firms. CORE - Université Catholique de Louvain, 2008. URL: https://www.hks.harvard.edu/hepg/PeakLoadPricingZoettl.pdf.